Investigation of the early immune events in African trypanosome infections

Olumide Ajibola

B.Sc. M.Sc. M.Res.

Submitted in fulfilment of the requirements for the Degree of Doctor of Philosophy

The Institute of Infection, Immunity and Inflammation
College of Medical, Veterinary and Life Sciences
University of Glasgow

September 2015

Abstract

African trypanosomes, the causative agent of sleeping sickness in humans, and nagana in cattle, are typically transmitted by the bite of an infected tsetse fly. The nature of the mammalian innate immune response during and immediately after the bite of an infected tsetse fly remains poorly understood. Previous studies characterising the events occurring in the skin post-infected tsetse fly bite have mainly focussed on the development of the chancre, which occurs from day 5 post-infection. Additionally, most immunopathological studies on trypanosomes have used intravenous or intraperitoneal injections of blood stage parasites, therefore bypassing relevant inoculation routes (tsetse fly), site (skin), and parasite life cycle stages (metacyclics). It is known that following tsetse fly bites, trypanosomes leave the skin via the host lymphatic system in order to initiate a blood stage infection. However, how the host responds to this challenge and how the parasite negotiates the anatomy of the host immune system remains unclear. In the present study, I have built on existing intravital microscopy tools to visualise *T. b. brucei* infections in the dermis and lymphatics of an infected mouse ear after transmission. I have also characterised by flow cytometry, taqman low density arrays and depletion studies the magnitude and kinetics of the early innate immune response in the skin, as well as the functional role of neutrophils, by examining infections in the context of the natural route of infection- the bite of a tsetse fly. Neutrophils were identified to be the predominant responders at the bite site, the neutrophil response was rapid, and they were recruited independent of the infection status of the tsetse flies. Taqman low-density arrays, which measured expression levels of inflammation-associated genes, suggested that neutrophil recruitment was mediated by CXCL1/CXCL2 release in the skin following mechanical trauma by the tsetse fly, in addition to the release of pro-inflammatory cytokines- IL-1ß and IL-6. Following the identification of neutrophils by flow cytometry, I then applied intravital microscopy to visualise influx of neutrophils, which was rapid, directed at the bite site, and did not form dynamic clusters. To further test the functional role of neutrophils very early in infection, neutrophils were depleted using a monoclonal antibody and mice infected via tsetse fly bites. Neutrophil depleted mice had no effect on pathogenesis in vivo. Using Prox-1 mOrange reporter mice, I also examined the interaction of bloodstream trypanosomes with lymphatic vessels in the skin in the period immediately following

inoculation using intravital imaging. I imaged metacyclic trypanosomes in situ and demonstrated that they had significantly higher velocity in the extravascular matrix compared to bloodstream forms. Additionally, my data showed bloodstream parasites actively migrating towards lymphatic vessels, and intra-lymphatic *T. b. brucei* were also observed, enabling comparison of trypanosome motility in the extravascular matrix and lymphatic vessels; in lymph vessels trypanosomes were moving in a more directional and rapid manner. This work revealed the early cellular and molecular responses to *T. b. brucei* infection and investigated interactions of parasites with the anatomy and cells of the host immune system. These studies demonstrate that furthering our understanding of the very early events in trypanosome infections is essential to understand how a systemic trypanosome infection is established.

Table of Contents

List of Tables

List of Figures

Acknowledgements

I would like to appreciate my supervisor Prof Jim Brewer, for being very patient with me during my thesis writing and your invaluable inputs during the experimental phase of my project. Also, my secondary supervisor Dr. Liam Morrison you have been an immense source of support especially during the parasitology aspects of this project, your help with the in vitro and in vivo aspects of my work, your critiquing of my ideas and writing have made me better. I also want to thank Prof Paul Garside for challenging me to learn and read more about immunology, those one to one meetings challenged me and would not be forgotten. Special thanks also goes to Prof Dave Barry for accepting me into his lab, and starting this project with me before his retirement. I am very grateful to the Wellcome Trust for funding my research, there is no way on earth I would have been able to afford it! To the Wellcome Trust 4 yr PhD program directors- Darren Monckton and Olwyn Byron, you guys are amazing!

I also want to say a special and big thank you to uncle Bob, I never would have been able to perform any of the immunology experiments without your help at the start of my PhD, your patience and understanding will always remain with me. Thank you also for the time you spared to chat me up about my project and make me think critically about it, for finding time to attend my meetings, I am very grateful. I also want to appreciate every member of the GBM group and students in the level 5 office, for their love and support towards my family.

I am grateful to staff at the JRF- David Gormal, Colin Chapman, you amaze me with your keen interest to help even when its not convenient for you. Thanks to Craig Lapsley, for your help with the pupae orders, tsetse infections and Anne Donachie for teaching me how to carry out injections in mice and stabilate preparation.

To every worker in my church, RCCG FOL Glasgow, I say thank you. Special thanks to Pastor and Pastor (Mrs) Makun for all your prayers that have been answered in my life, Pastor Segun Ibigbemi, his wife my HOD, and son Seyi, for their concern, care, and love towards my progress and support towards my

family. Also, I want to appreciate Pastor Bola Owati for his prayers and constant love towards me, and my family-thank you sir.

Finally, I want to appreciate, my late father-Caleb Olufisayo Ajibola, that taught me the meaning of hard work through his life style, you left at the start of my PhD but I know you will be proud of me now, my mother (Mama Voma) without your prayers, I know I won't be where I am today, my parents-in-love for their support and prayers, my siblings- late Mrs. Omolola Adesina, Kemi, Biodun and my siblings-in-love. Thanks to Mummy Arewa, Yinka Arewa and his siblings, Bode Bankole and his family, Akinbami Adenugba for the prayer meetings and discussions, you have all been a great source of strength to my family during all the trying times we went through in the last 4 years- only God can reward you. To my inestimable jewel, my wife, you have been very patient with me during the thesis-writing period, I am very grateful and I love you. To my daughter Oluwadamilola Esther Jesutofunmi, you came into our world at the best time, and you are part of the wonderful history we have made as a family, I love you and thank you.

Above all, I say thank you to the one that promises and fulfils, the God of Abraham, Isaac and Jacob- thank you for the fulfilment of your Word in my life.

To God alone be all the glory.

Author's Declaration

I declare that this thesis and the results in it are the outcome of my own work except where otherwise stated. No part of this thesis has been previously submitted at any university for the award of a degree.

Olumide Ajibola

Abbreviations

AAT	Animal African Trypanosomiasis
APC	Antigen presenting cells
CATT	Card agglutination test for trypanosomes
CCCD	Cooled charge-coupled device
CD	Cluster of differentiation
CNS	Central nervous system
DAMP	Danger associated molecular patterns
DC	Dendritic cells
DDC	Dermal dendritic cells
dLN	Draining lymph node
DNA	Deoxyribonucleic acid
EpCAM	Epithelial adhesion molecules
ESAG	Expression site associated gene
GFP	Green fluorescent protein
GPI-PLC	Glycophosphatidyl inositol phospholipase C
HAT	Human African Trypanosomiasis
H & E	Hematoxylin and Eosin
HEV	High endothelial venules
IFN	Interferon
Ig	Immunoglobulin
IL	Interleukin
iNOS	Inducible nitric oxide synthase
i.p.	Intraperitoneal
i.v.	Intravenous
LN	Lymph node
LPS	Lipopolysaccharide
LTB4	Leukotriene B4
MFI	Mean fluorescent intensity
MHC	Major histocompatibility complex
MPLSM	Multiphoton laser scanning microscopy
MVSG	Metacyclic variant surface glycoprotein
NAG	N-acetyl glucosamine
NET	Neutrophil extracellular trap

NLR	NOD like receptor
NO	Nitric oxide
PAMP	Pathogen associated molecular pattern
PBS	Phosphate buffered saline
PCR	Polymerase chain reaction
PFR	Paraflagellar rod
PRR	Pattern recognition receptors
RIN	RNA integrity number
RLR	Retinoic- acid-inducible gene-I-like receptors
RNA	Ribonucleic acid
Th	T helper
TLDA	Taqman low density array
TLR	Toll like receptor
TNF	Tumor necrosis factor
VSG	Variant surface glycoprotein

1 General Introduction

1.1 Introduction to African trypanosomes

African trypanosomes belong to the family *Trypanosomatidae*, order *Kinetoplastida*, they live and multiply extracellularly in the blood and tissue fluids of mammals [1, 2]. The main species of African trypanosomes that cause human and animal disease are *Trypanosoma congolense, Trypanosoma vivax,* and *Trypanosoma brucei*. *T. congolense* and *T. vivax* infect a range of livestock in which they cause nagana or African Animal Trypanosomiasis (AAT). Other pathogenic species of African trypanosomes of agricultural importance are *T. equiperdum* and *T. evansi*. Two subspecies of *T. brucei*, *T. b. gambiense* and *T. b. rhodesiense*, also infect humans and cause Human African Trypanosomiasis (HAT), also known as sleeping sickness [3, 4]. AAT and HAT are transmitted by the bite of infected tsetse flies. Consequently, the distribution of tsetse flies across much of sub-Saharan Africa renders swathes of land unavailable for the productive raising of cattle, and a large human population vulnerable to infection.

AAT is endemic to 37 sub-Saharan countries with over 46 million cattle at risk, over an estimated 8.7 million km^2 [5, 6]. Currently, it is estimated that fewer than 12 000 HAT cases are reported per year. HAT is a disease of the poor, affecting remote and poor parts of Africa. Disease is transmitted in areas of Africa where the people thrive on farming, hunting, fishing, or live and carry out their activities near streams [3]. Direct economic losses from AAT in cattle has been estimated to be approximately US $2.5 billion in east Africa alone [7]. Further studies estimated that the economic cost of trypanosomiasis in Africa was about US $4.5 billion. In addition to economic losses from contracting AAT, it also has indirect impact on crop agriculture, human welfare and economic development in afflicted areas [6].

1.1.1 Life cycle of *Trypanosoma brucei*

African trypanosomes have a complex digenetic lifecycle (Figure 1.1), occurring in mammalian and tsetse fly hosts [8]. In each host, *T. brucei* undergoes specific developmental stages, involving proliferation, expression of specific proteins on

their surface, and distinct morphologies in order to adapt to different environments.

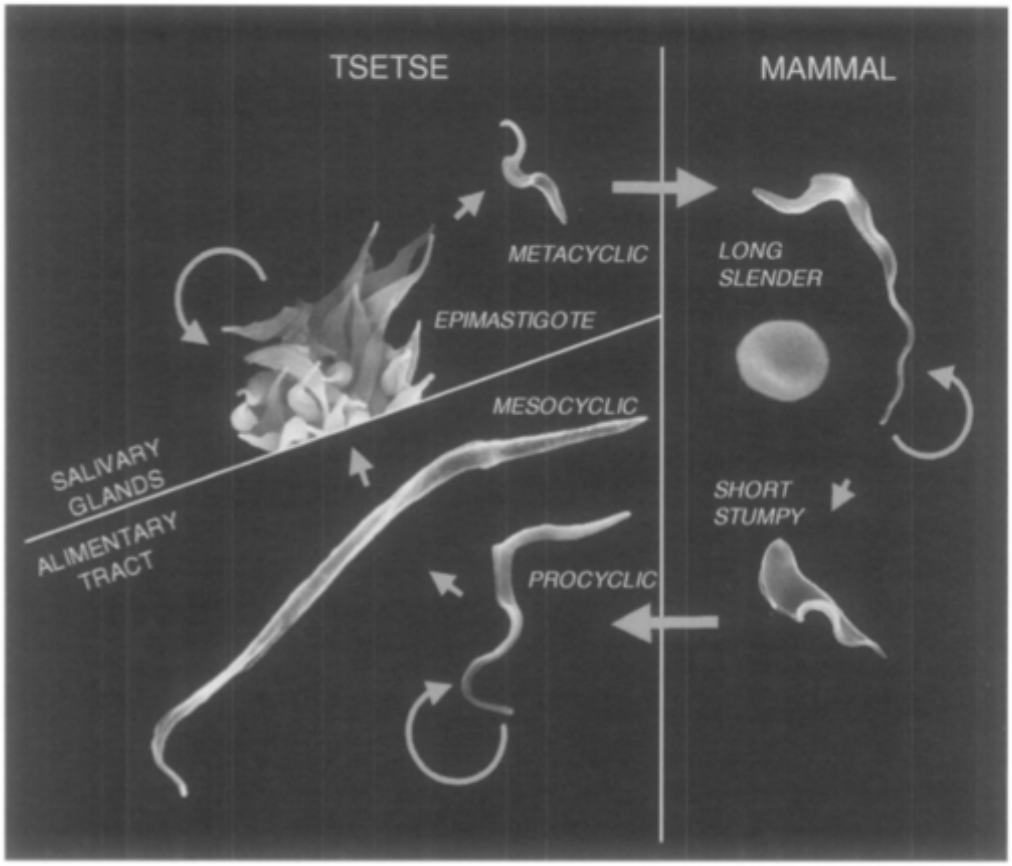

Figure 1-1 Life cycle of *Trypanosoma brucei*.
The different life cycle stages of *T. brucei* in the tsetse fly and mammalian hosts are shown by scanning electron micrographs. The circular arrows indicate the stages that are capable of cell division. Mammalian hosts are infected through the deposition of metacyclic stage trypanosomes in the skin. Metacyclic stage parasites differentiate into long slender forms also known as bloodstream stage. For tsetse fly transmission to occur, the blood stream form parasites differentiate into stumpy forms, which are then taken up during a tsetse fly feed. Figure adapted from [9].

The *T. brucei* lifecycle in mammals starts through the bite of its vector, the tsetse fly, which deposits metacyclic stage trypanosomes in the skin [10]. In cattle and humans, deposition of trypanosomes in the skin is followed by the development of a skin lesion called the chancre at the site of inoculation, its diameter varying in size from a few millimetres to several centimeters appearing as from day 5 post infection [11]. The chancre is characterised by an intense host inflammatory reaction, more frequent in *T. b. rhodesiense* HAT and disappearing within two to three weeks [12]. However, chancre appears to be absent in rodents challenged with infected tsetse flies [13]. The chancre was also found to serve as a site for proliferation and establishment of trypanosomes

in the skin, and also represents the parasitic invasion phase of the lymphatic organs in stage 1 HAT. Following the deposition of the metacyclic stage trypanosomes, they differentiate into the bloodstream forms, that swim freely in the blood and tissue fluids of mammals [14]. Bloodstream trypanosomes express variant surface glycoproteins (VSG) on their cell surface in order to survive the host immune assault and continue to thrive in its host (see section 1.12.1 for further details) [9, 15, 16]. At peak parasitemia, most of the surviving trypanosomes undergo terminal differentiation to a stage of the parasite that can survive in the tsetse fly when it takes a blood meal. These terminally differentiated trypanosomes are described as short stumpy form trypanosomes, which are adapted for survival in the tsetse fly [17]. Some of the changes include a switch in the parasites metabolic requirement from a glucose rich environment in the bloodstream of mammals, to the proline rich environment in the tsetse fly midgut [18], other biochemical and morphological changes also occur in the parasites [2, 19]. Despite the changes the bloodstream form parasites undergo in order to survive in the tsetse fly, about 99% of the ingested parasites do not survive the initial phase of development, including stumpy forms [20], although pre-adapted for life in the tsetse fly [18].

Once the parasites arrive in the midgut of the tsetse, the stumpy trypanosomes differentiate into procyclic trypanosomes. The procyclic trypanosomes change expression of their surface coat from the VSG to a less dense coat comprised of the surface antigens, EP (characterised by an internal repeat of glutamic acid E and proline P) and GPEET (characterised by an internal repeat of glycine G, proline P, glutamic acid E, and Threonine T) procyclin [21]. Colonization of the midgut of the tsetse fly is accompanied by an expansion of procyclic trypanosomes in the ectoperitrophic space of the midgut and parasite elongation, progressing from the posterior to the anterior ends. Long trypomastigote forms found in the anterior position of the midgut, in the ectoperitrophic space of the tsetse fly near the proventriculus, are called the mesocyclic forms [18]. The mesocyclic forms have undergone a cell cycle arrest and are at the G0/G1 phase of development, which represents the endpoint in parasite establishment in the midgut. The transformation into mesocylic stage parasites is also crucial for migration into the lumen of the proventriculus, and subsequently to travel into the foregut and proboscis, where they undergo the

next stage of differentiation into epimastigote forms. The incoming mesocyclic cells produce two types of morphologically identical epimastigote forms during asymmetric division; long and short epimastigotes, and both types have diploid DNA contents [22]. The short epimastigote forms have reduced motility due to a short flagellum, and heteronuclear kinetoplast, resembling the attached epimastigote stage in the salivary gland. In order for the parasites to swim from the proboscis through the hypopharynx and reach the salivary glands, only the highly asymmetrical, highly motile and dividing epimastigote parasites succeed in migrating [20]. Once they succeed in migrating, the short epimastigote forms are now in a convenient location for attachment with their flagellum. The series of differentiation the parasites undergo at this phase are irreversible. In the salivary gland of the tsetse fly, the parasites attach to epithelial surfaces as epimastigote forms [23]. The epimastigote forms are proliferative and eventually generate the non-proliferative metacyclic trypanosomes, which have reacquired the VSG coat, which can then be transmitted into its new mammalian host during a tsetse feed/probe [18, 19, 23, 24]. The post-mesocyclic forms represents an essential bridge between the procyclic and metacyclic production phase in the salivary glands [20].

1.2 Clinical features of Trypanosomiasis

1.2.1 Animal African Trypanosomiasis

Livestock affected by AAT show extensive immune mediated pathology, cardiac involvement and severe anemia [25], and are weak and unproductive particularly in the chronic stage of disease. Animals show intermittent fever, weight loss and lymphadenopathy. They also exhibit reduced milk production, herd size, growth and work output. Deaths are common in chronically infected animals, and animals that recover may relapse when stressed. This loss in animal productivity has important socio economic implications for people whose livelihood depends on these animals [26]. Anemia is a consistent observation in HAT patients [27] and AAT affected animals [28]. Anemia is present in the acute and chronic stages of infection in animals. During the acute phase of infection, anemia has been associated with the immune response of the host, due to binding of immune complexes to erythrocytes [25]. While during the chronic phase when the

animals are immunosuppressed multiple factors are involved such as splenomegaly, sensitisation of erythrocytes by immune complexes, and haemodilution [25].

1.2.2 Human African Trypanosomiasis

HAT or sleeping sickness is caused by two subspecies of *T. brucei, T. b. rhodesiense and T. b. gambiense* (Figure 1.2 for distribution).

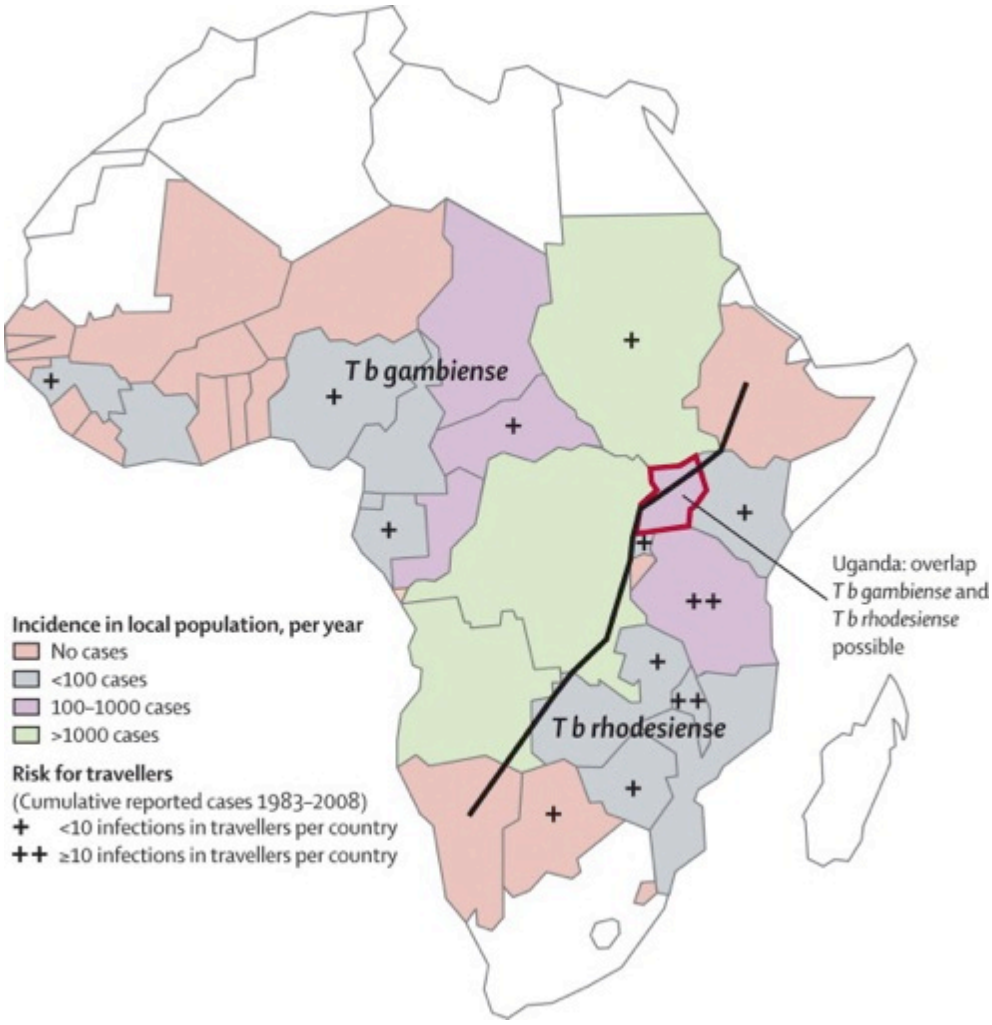

Figure 1-2 Human African Trypanosomiasis
Diagram adapted from http://www.who.int/csr/resources/publications/CSR_ISR_2000_1tryps/en/. The map of Africa depicting the cases of HAT in Africa and areas of Africa that are free from HAT. Cases of HAT above 100 persons are predominantly located in West Africa.

The course of infection of HAT is dependent on the sub-species infecting humans. *T. b. rhodesiense* is found in eastern and southern parts of Africa and results in an acute form of infection (weeks-months) whereas *T. b. gambiense,* found in west and central Africa, causes more chronic infections (months-years).

1.2.2.1 Clinical features

HAT appears in two stages, the first is the haemolymphatic stage, characterised by restriction of the parasites to the blood and lymph, and Stage 2, the meningoencephalitic stage characterised by the invasion of the central nervous system (CNS). Trypanosomes are thought to penetrate the blood brain barrier and enter the CNS in an active manner, at or near intracellular junctions of the endothelia [29]. The resulting encephalitis from Stage 2 disease produces the symptoms of sleeping sickness and is the major cause of death in patients infected with both sub-species of *T. brucei*. Death from *T. b. rhodesiense* usually occurs within weeks or months of infection due to its acute nature [30].

During infection with *T. b. rhodesiense* there can be the appearance of a chancre at the tsetse fly bite site, which is a persistent swelling found in about 19% of patients and disappears in about two to three weeks [12], whereas chancres are rarely seen in *T. b. gambiense* infections [3]. In addition, clinical signs associated with Stage 1 HAT include chronic and intermittent fever, headache, lymphadenopathy, joint pains and itching. Fevers in stage 1 HAT may last from a day to a week, separated by intervals of a few days to a month or longer, and are rarely present in Stage 2 disease [31, 32].

The leading symptom of stage 2 of disease is the sleep disorder experienced by patients. At this stage, infection causes a dysregulation of the circadian rhythm controlling the host's sleep/wake cycle, and consequently fragmentation of the sleep pattern. The degree of disruption of the 24 hrs sleep/wake cycle of patients is proportional to the severity of clinical symptoms. Patients also experience neurological symptoms such as tremor, general motor weakness, hemiparesis, limb paralysis, abnormal movements and ultimately death if untreated [33, 34].

1.2.3 Diagnosis

Different approaches are used in diagnosis of *T. b. gambiense* and *T. b. rhodesiense* infection. The reasons for these differences are that firstly, there is no serological test available for *T. b. rhodesiense*. Secondly, there is the presence of permanent parasitemia in *T. b. rhodesiense* compared to *T. b.*

gambiense where there are few parasites in peripheral circulation, except at periods of chronic disease [35]. Therefore, thin or thick blood smears are usually sufficient to diagnose *T. b. rhodesiense* (Figure 1.3).

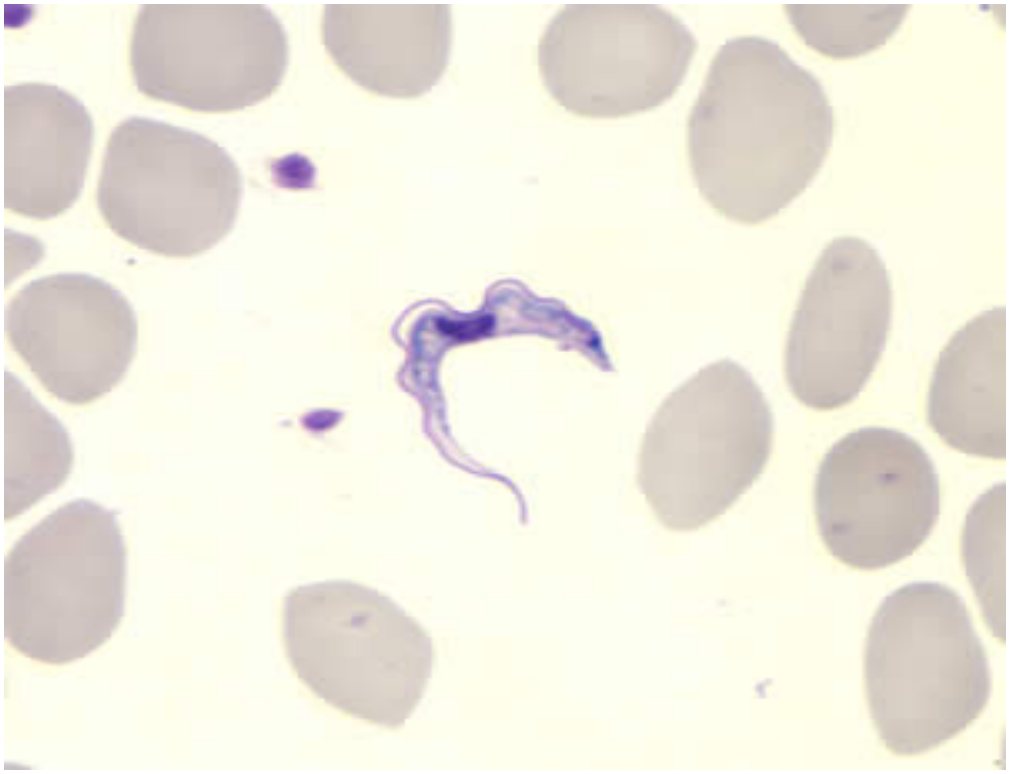

Figure 1-3 Photomicrograph of a Giemsa stained *Trypanosoma brucei*
Diagram adapted from http://www.cdc.gov/parasites/sleepingsickness/epi.html. A thin blood smear (x1000 magnification) of *Trypanosoma brucei spp.* Image approved for reproduction by the Centres for Disease Control and Prevention.

Currently, the card agglutination test for trypanosomes (CATT) which can be performed on serum, blood from impregnated filter papers, or blood obtained from finger pricks using a blood lancet is commonly used in *T. b. gambiense* diagnosis [20, 36, 37]. The CATT test is a rapid test that can be used to screen hundreds of individuals daily, and is the most efficient screening method available to date. CATT has also been reported to have a sensitivity of about 87-98% and specificity of 93-95% [38, 39]. In non-endemic countries, other serological tests such as immunofluorescence assay, or enzyme linked immunosorbent assays detecting parasite-specific IgG subclasses (IgG1 and IgG3) and IgM isotypes in serum and cerebrospinal fluid of individuals with suggestive clinical features of HAT are carried out [39-43]. Serological tests are not 100% sensitive in the detection of HAT, because of the high capacity for the parasite to switch its VSGs, which are the antigens used in serological tests [44, 45].

Consequently, microscopic examination is still employed in addition to other diagnostic methods to search for trypanosomes in individuals that have chancre or symptoms of HAT [39, 40]. Microscopic confirmation of parasites in lymph node aspirates, cerebrospinal fluid (CSF) or blood remains the gold standard for parasitological confirmation [3].

Staging of HAT patients is important because of substantial differences in the drugs administered in the two stages of HAT. According to the World Health Organisation (WHO) recommendations, the presence of more than five white blood cells per µl in the CSF or increased protein content (>370 mg/L) confirms the second stage of the disease [37, 46, 47]. Some researchers have suggested that there may be an intermediate stage of infection with a CSF WBC of < 20/µl, where the parasites penetrate the blood brain barrier and are treated with early stage drugs. The notion of an intermediate stage requires caution in its approach [35, 48]. Research is currently on-going through the organisation, Foundation for Innovative New Diagnostics (FIND) to improve the diagnosis and staging of HAT, including using recombinant trypanosome native antigens for development of rapid diagnostic tests [49]. These new diagnostic tests could be used for screening populations that are at risk of infection. Improved methods of confirming cases of HAT, using a LED fluorescence microscope and evaluation of a molecular test based on Loop-Mediated Isothermal Amplification of DNA (LAMP) are also in development [50].

1.3 Prevention and control of Animal and Human African Trypanosomiasis

The prevalence of animal and human African trypanosomiasis could be controlled via approaches targeted at the vector, parasite and the host described below.

1.3.1 Host

Genetic resistance to African trypanosomes has been identified in certain breeds of livestock, and these animals are described as trypanotolerant. Exploiting the inherent genetic properties of the host to control disease has been applied in AAT, where some breeds of cattle such as N'dama and Muturu remain infected

with trypanosomes, but do not suffer the severe clinical signs of susceptible counterparts [51]. The ability of N'dama cattle to limit anemia has been linked to the presence of hematopoietic tissue of trypanotolerant origin. T cells and antibodies were described not to contribute to trypanotolerance, hence a role for erythropoiesis was proposed [52]. In some trypanosome endemic areas, it has been advised to selectively breed from trypanotolerant cattle in order to maintain productivity in the face of infection [53, 54]. In the past, wild game that served as reservoirs for trypanosomes, have also been targeted by culling, in order to reduce the overall prevalence of the parasite and reduce the ratio of infected tsetse flies in such areas. This approach is no longer considered acceptable and no longer in practice. More recently, the expression of a trypanosome resistance gene, *APOL1*, in transgenic livestock is currently been investigated with the aim of reducing susceptibility of animal reservoirs. The presence of the primate APOL1 is sufficient to confer resistance in these animals, as observed in transgenic mice expressing human APOL1 [55]. So it is expected that expression of baboon APOL1 in transgenic cattle would also confer resistance against *T. b. brucei* and *T. b. rhodesiense*. These studies are currently ongoing and it is hoped that these would provide a new avenue to control African trypanosomes [56].

1.3.2 Vector

Approaches targeted at the vector are aimed either at indirectly reducing the available habitat for the tsetse fly to thrive, or directly by reducing the tsetse population in such areas. Traditional methods employed include bush clearing and application of insecticides. However, insecticides are clearly indiscriminate and kill both the tsetse fly and other insects in the ecosystem, in addition to other undesirable effects the insecticides may have. Currently, the use of traps is more acceptable because its more environmentally friendly and does not kill other insects in the population. The pan African Tsetse and Trypanosomiasis Eradication Campaign (PATTEC), has in addition to the use of traditional methods of control of tsetse flies, also included the use of sterile insect technique in tsetse fly control. The sterile insect technique involves the release of sterile males, which mate unproductively with females, and has been

effective in contributing to the elimination of *Glossina austeni* from the island of Unguja in Zanzibar [57, 58].

1.3.3 Parasite

The sole method of control available at the parasite level currently is limited to chemotherapy. The drugs for treatment of both AAT and HAT are currently limited and few new drugs have been formulated over recent decades, largely because of a combination of the cost of developing new drugs and the fact that trypanosomiasis occurs in a region of the world that does not represent a sufficiently profitable market [59]. The drugs currently in use for treatment of HAT are donated by pharmaceutical companies to the World Health Organisation.

1.3.4 Drugs for treatment of Human African Trypanosomiasis

For Stage 1 or the haemolymphatic stage of HAT, there are only two licensed drugs, pentamidine and suramin for treatment of *T. b. gambiense* and *T. b. rhodesiense* infections, respectively. For Stage 2 disease, melarsorprol and difluoromethlyornithine, Ornidyl ® (DFMO), and nifurtimox-eflornithine combination therapy (NECT) are the drugs currently in use [60-63]. In addition to the drugs currently in use, new drug candidates are also been investigated in the treatment of HAT. One of such novel drugs with great potential is nitroimidazole, an analogue of fexinidazole rediscovered by Drugs for Neglected Diseases Initiative (DNDi) [64]. This drug has been shown to have potential against both strains of HAT in the two stages, and it is administered orally. Other promising candidates in development include the oxaboroles [65] administered orally, and DB75 (Furamidine), a diamidine analogue of pentamidine [59]. Some other trypanocidal drugs currently used in anti-cancer therapies are also been tested but are yet to undergo full scale clinical trials, and examples include cordycepin, deoxycoformycin and lodamine, a known oral anti-cancer agent [65]. The main drugs currently in use are described below.

1.3.4.1 Pentamidine

Pentamidine is the drug of choice for treatment of *T. b. gambiense* for patients in the first stage of disease. Resistance to pentamidine has been unreported since the introduction of the drug in 1940 and it has remained the first line treatment drug for *T. b. gambiense* sleeping sickness for more than 60 years. Treatment failures from pentamidine are uncommon, and believed to be due to misdiagnosis of the stage of disease. The mode of action of pentamidine has been linked to the high accumulation of the drug by the parasite, while its likely mode of resistance based on work carried out on laboratory selected isolates is linked to efflux of the drug or decreased uptake [66].

1.3.4.2 Suramin

Suramin can also be used for treatment of Stage 1 *T. b. rhodesiense* and *gambiense*, although it is not used against *T. b. gambiense* in western and central Africa. Suramin is not used in second stage treatment of HAT because it does not cross the blood-brain barrier. The use of suramin in west and central Africa is avoided due to the presence of *Onchocerca spp.* in these areas, as the activity of suramin against *Onchocerca spp.* can increase the risk of allergic reactions. Suramin presents with toxic side effects such as nephrotoxicity, peripheral neuropathy, bone marrow toxicity with agranulocytosis and thrombocytopenia. Suramin is a large polyanion and exerts inhibitory properties on a wide spectrum of enzymes such as fumarase, dihydrofolate reductase, hexokinase, thymidine kinase, trypsin and dehydrogenase [67, 68].

1.3.4.3 Melarsoprol

Melarsorprol was introduced in 1950 to replace earlier organo-arsenics that were ineffective. This remains the drug of choice in the treatment of second stage HAT caused by *T. b. gambiense*, especially in poor countries where eflornithine is not available. Second stage HAT caused by *T. b. rhodesiense* is only treated with melarsorprol. Adverse reaction to melarsoprol is frequent and is often life threatening, with between 4% and 12% of patients who receive melarsoprol dying from side effects associated with the drug [69, 70]. Treatment failures and

resistance to melarsorprol have also been on the increase in the last decade in endemic areas such as southern Sudan, Congo and Angola [3, 71].

1.3.4.4 Eflornithine

In the last 50 yrs, Eflornithine also known as DFMO is the only new molecule that has been introduced for the treatment of HAT. Eflornithine has been demonstrated to show reduced mortality in the treatment of second stage HAT more than melarsoprol. Eflornithine is recommended as first line drug in the treatment of *T. b. gambiense* disease, but is not recommended in the treatment of *T. b. rhodesiense*, which is less innately susceptible to eflornithine [72, 73].

1.3.5 Drugs used for Animal African trypanosomiasis (AAT)

Chemotherapy of AAT faces similar challenges to those in treatment of HAT. These challenges include the limited availability of drugs due to reluctance of the pharmaceutical companies to invest in research and development of new drugs for a neglected disease, in addition to resistance development against the drugs by the parasite. The drugs currently used in the treatment of AAT in cattle; diminazene aceturate (Berenil®), ethidium bromide and isometamidium chloride (Samorin®, Trypamidium®), while cymelarsan is used for treating *T. evansi* infection in camels. Diminazene aceturate and isometamidium chloride have been widely used as therapeutic and prophylactic trypanocides, respectively. However, cases of resistance by trypanosomes against these drugs have been reported [74-77].

1.3.6 Drug resistance

The control of human and animal African trypanosomiasis principally relies on chemotherapy, owing to the absence of vaccines and effective vector control strategies. Resistance to commonly used animal trypanocides such as suramin, the preferred drug for treatment of camel trypanosomiasis, diminazene aceturate, cymelarsan, homidium and isometamidium chloride has been reported in the field [78, 79]. More recently, mutations in *T. b. gambiense* aquaglyceroporin gene in field isolates were demonstrated to be responsible for resistance to melarsoprol and pentamidine [80]. Also, some researchers have

recently carried out genome scale RNA interference target sequencing (RIT-seq) screens on all five known HAT drugs to identify transporters, metabolic pathways and enzymes in *T. brucei* that function to enable antitrypanosomal drug action. Furthermore the use of RIT-seq analysis also revealed over 50 genes that enhance drug susceptibility. This study further corroborated the role of aquaglyceroporin in pentamidine and melarsoprol cross resistance [81]

1.4 The Tsetse fly: Vector of African trypanosomes

The tsetse fly (Figure 1.4) belongs to the genus *Glossina,* family *Glossinidae* and order *Diptera*; there are 22 different species currently recognised, and their distribution is restricted to sub-Saharan Africa. Tsetse flies are classified into three main groups, the Morsitans, the Palpalis and the Fusca groups. Both male and female tsetse flies are capable of transmitting trypanosomes.

Figure 1-4 Photomicrograph of a tsetse fly
Diagram adapted from http://www.cdc.gov/parasites/sleepingsickness/epi.html. A recently fed tsetsefly with an engorged abdomen..

1.4.1 Distribution of Tsetses

The three main groups of tsetse differ in their distribution according to the availability of their preferred type of vegetation. The distribution of tsetse flies in Africa is described using the map below (Figure 1.5).

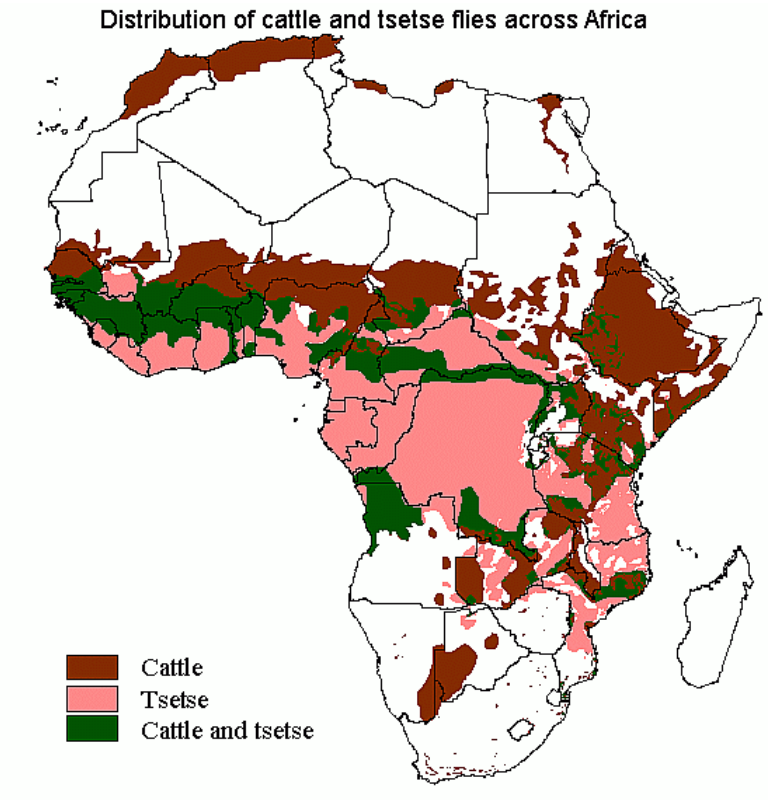

Figure 1-5 Tsetse fly distribution in Africa
Image from http://www.genomics.liv.ac.uk/tryps/images/africamap3.gif. The distribution of tsetse flies and cattle in Africa, and areas that are susceptible to cattle infection by tsetse flies are shown in the map.

1.4.1.1 Morsitans group

Morsitans group species are found in the savannah regions of Africa, and are not present in rain forests or swampy areas. The distribution of Morsitans species is also limited by colder climatic conditions in southern Africa, hot and dry conditions in the north-west and central Africa. In this group, *G. morsitans morsitans* is the most widespread; other members of importance to transmitting trypanosomes include *G. m. centralis, G. pallidipes, G. longipalis.*

1.4.1.2 Palpalis group

This group of tsetse flies are present in humid areas of Africa, including mangrove swamps, rain forest, lakeshores and along rivers. Members of this group important in transmitting trypanosomes include *G. palpalis, G. fuscipes,*

G. tachinoides, *G. caliginea* and *G. pallicera*. *G. caliginea* and *G. pallicera*, and are mainly limited to areas of West Africa.

1.4.1.3 Fusca group

There are three main types of the Fusca group, which differ in their distribution. *Glossina longipennis* is found in rather dry countries such as Sudan (south east corner), Ethiopia (southern border), Somalia, Kenya, and northeastern Tanzania. The second group *Glossina brevipalpalis* is scattered through the eastern parts of Africa e.g. Ethiopia and Somalia. The last group is limited to more thickly forested areas of Africa, with similar distribution to *G. papalis*/*G. fuscipes*.

1.5 The skin

The skin is a highly complex organ composed of the epidermis, dermis and subcutaneous fatty layers. These layers accommodate various structures such as hair follicles, sweat glands in humans (absent in mice), blood vessels and lymphatics. The layers of the skin are populated by cells involved in immune surveillance and innate immune responses to infection. The skin serves as protective interface against environmental toxins, and physical stresses [82]. The cellular components of the skin, the layers that cells are present are described in section 1.7, and the description of the lymphatic system is given in section 1.12.

1.6 The Innate Immune system

Skin and mucosal surfaces provide a barrier function to protect the host from infection through contact with pathogens. However on breach of this barrier, the ability to fight these pathogens relies on the efficacy of the immune system. The immune system can be divided into the innate and adaptive arms. The adaptive arm of immunity is specific and slow to develop on first encounter with pathogens. The innate arm of immunity on the other hand is very critical during the first few hours of pathogen encounter, and plays an important role in initiating and shaping the subsequent adaptive immune response that provides long lasting immunity.

Innate immune responses are relatively non-specific for pathogens, and rely on germ-line encoded receptors expressed on immune cells that recognise certain Pathogen Associated Molecular Patterns (PAMPs). The innate arm of immunity can also be triggered by various physical or metabolic insults, which produce soluble mediators of inflammation known as Danger Associated Molecular Patterns (DAMPs). The inflammatory responses produced mostly resolve once the source of inflammation has been eliminated, though in some instances this can persist or there can be aberrant resolution of the inflammatory response [83, 84]. Preformed, soluble components of the innate immune system include the complement system, the coagulant and fibrinolytic cascades and antimicrobial peptides [85, 86]. Innate immune cells include resident cells, such as macrophages, dermal dendritic cells, mast cells and Langerhans cells, and also recruited cells, such as eosinophils, basophils, neutrophils and monocytes. These innate immune cells respond to PAMPs as well as host derived DAMPS, and products of the complement cascade [87]. This activates innate cells with the concomitant release of pro-inflammatory cytokines/chemokines, which initiate inflammation and recruitment of immune cells to the site of injury. The skin also serves as the main interface for encounter with pathogens, through Pattern Recognition Receptors (PRRs). The crucial role PRRs play in recognition of PAMPs and DAMPs, activation/recruitment of cells in the skin, and the complement system has been detailed.

1.6.1 Pattern recognition receptors (PRRs)

PRRs are germ-line encoded and play a crucial role in sensing the presence of foreign objects via PAMPs and also endogenous molecules released from damaged cells (DAMPS) in the body. There are four families of PRRs that have been identified to date. These families include transmembrane proteins like Toll-like receptors (TLRs) and C-type lectin receptors (CLRs), cytoplasmic proteins such as retinoic acid-inducible gene (RIG)-I-like receptors (RLRs) and the NOD-like receptors (NLRs). PRRs are expressed on professional (macrophages and dendritic cells) and non-professional immune cells such as epithelial cells, fibroblasts and endothelial cells [84]. The sensing of PAMPs by PRRs results in the upregulation of gene transcripts involved in inflammation.

Table 1-1 PRRs, their ligands and pathogens that express them

PRRs	Localisation	Origin of the Ligand
TLR		
TLR1	Plasma membrane	Bacterial triacyl lipoprotein
TLR2	Plasma membrane	Lipoprotein e.g. bacteria, parasites, viruses
TLR3	Endolysosome	Viral dsRNA
TLR4	Plasma membrane	LPS e.g. bacteria
TLR5	Plasma membrane	Bacterial flagellin
TLR6	Plasma membrane	Bacteria and viral diacyl lipoprotein
TLR7	Endolysosome	ssRNA e.g. virus and bacteria
TLR9	Endolysosome	CpG DNA e.g. protozoa, and bacteria
TLR10	Endolysosome	Unknown
TLR11	Plasma membrane	Protozoa profilin-like molecule
RLR		
RIG-I	Cytoplasm	Short dsRNA e.g. RNA viruses
MDA5	Cytoplasm	Long dsRNA e.g. RNA viruses
LGP2	Cytoplasm	RNA viruses, ligands unknown
NLR		
NOD1	Cytoplasm	iE-DAP from bacteria

NOD2	Cytoplasm	MDP from bacteria
CLR		
Dectin-1	Plasma membrane	ß-Glucan e.g. Fungi
Dectin-2	Plasma membrane	ß-Glucan e.g. Fungi
MINCLE	Plasma membrane	SAP130 e.g. Fungi

TLRs are the most studied PRRs and are involved in the sensing of pathogens outside the cell, and in the intracellular endosomes and lysosomes of phagocytes. They have a vital role in triggering innate immunity and orchestrating the adaptive immune response. Table 1.1 gives a summary of the families of PRRs and the PAMP ligands they recognise.

1.6.2 Complement

In addition to the cells of the innate response, the complement system is one of the major effector mechanisms of the innate immune system [88]. Its name was derived by its ability to 'complement' the antibacterial properties of antibodies in the heat stable fraction of the serum. Complement is made up of more than 30 proteins that constitute approximately 15% of the globular fraction of plasma and can respond efficiently, and produce tightly regulated inflammatory and cytolytic immune responses to pathogens. Activation of the complement system occurs via three main pathways; classical, lectin and alternative pathways [85, 86]. The initiation, activation and termination of the three main pathways is summarised in figure 1.6. Although the proteins involved in the initiation of complement activation are different, the three pathways converge with the generation of C3 convertase. The classical pathway is immunoglobulin dependent as it involves the binding of the C1 complex (C1q in complex with C1r and C1s serine proteases) to the Fc region of complement fixing antibodies [88]. The lectin pathway, though similar to the classical pathway, is immunoglobulin independent in its mechanism of action.

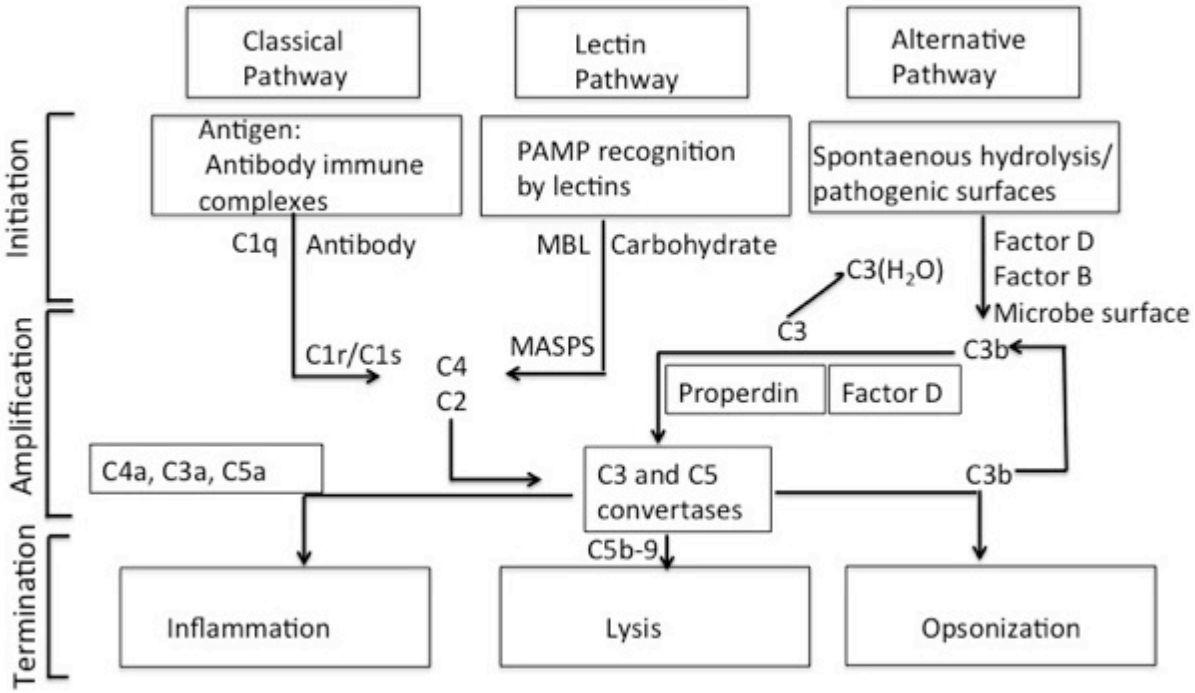

Figure 1-6 The Complement pathway
Complement can be activated through three ways: classical, lectin and alternative pathways. Complement activation through the classical pathway is initiated when C1q binds to antibody attached to an antigen, which then activates C1r and C1s, which then cleaves C4 and C2. In the lectin pathway, activation begins when mannose- binding lectin (MBL) comes in contact with conserved pathogenic motifs, which then proceeds through C4 and C2 which produce activated complement proteins further down the cascade. In contrast to the classical pathway, the lectin pathway does not recognize antibody bound to antigen. The alternative pathway is activated through spontaneous hydrolysis of C3, which forms the initial products of the alternate pathway, C3 convertase, (C3(H_20)Bb. Formation of C3 convertase allows the binding of plasma proteins Factor B and Factor D, to cleave to Ba and Bb and formation of C3bBb and C5 convertase C3bBbC3b. The three complement pathways ultimately result in the formation of convertases, which generate the major effectors of the complement system such as anaphylatoxins, the membrane attack complex (MAC), and opsonins. Figure adapted from [88].

The lectin pathway employs PRRs, mannose binding lectin (MBL) and ficolins, for nonself recognition. The lectin pathways uses these PRRs to recognise PAMPs associated with microorganisms [89, 90]. The alternative pathway on the other hand is distinct from both the classical and lectin pathways. It is initiated by spontaneous hydrolysis of C3, which is abundant in blood plasma. Hydrolysis of C3 to the C3b analog, C3(H_2O) enables binding to Factor B, in turn allowing cleavage of Factor B into its two components Bb and Ba by factor D. This forms the initial alternative pathway C3 convertase, which then forms the basis of the amplification loop at later stages of the cascade. In summary, irrespective of the pathway of complement activation, it basically serves to carry out the following broad effector functions; These functions include the direct lysis of targeted

surfaces, generating a potent proinflammatory reaction through anaphylatoxins, opsonisation and phagocytosis of targeted surfaces through the engagement of complement receptors on phagocytic cells such as macrophages and neutrophils [85, 86, 88].

1.7 Immunity in the skin

The skin is arguably the largest organ of the human body, composed of 1.8 m^2 of diverse habitats, consisting of folds, invaginations and specific niches that support a wide range of microorganisms. The skin serves as a physical barrier to protect the human body from the assault of foreign organisms or toxic substances. The skin also serves as an interface between the body and the outside environment. It is therefore very important in interactions involving pathogenic organisms that rely on the skin as a route of entry for establishment and dissemination throughout the body. Pathogenic protozoa that enter via the skin include the vector-borne protozoa *T. brucei*, *Plasmodium* spp., and *Leishmania* spp. The skin also consists of a plethora of cell types that are resident, together with other structures, such as sweat glands (absent in mice), nerves, blood vessels, and lymphatics [82]. These small organs contribute to functions such as temperature regulation, barrier maintenance and immunity. The skin is composed of the epidermis and the dermis (Figure 1.7). The epidermis is attached to the basement membrane, beneath which lie the dermis and a subcutaneous fatty region. Structurally, the epidermis comprises several layers of keratinocytes. During physical damage to the skin such as vector bite, or needle, keratinocytes can become activated via the TLR pathway where they release IL-1α [91, 92].

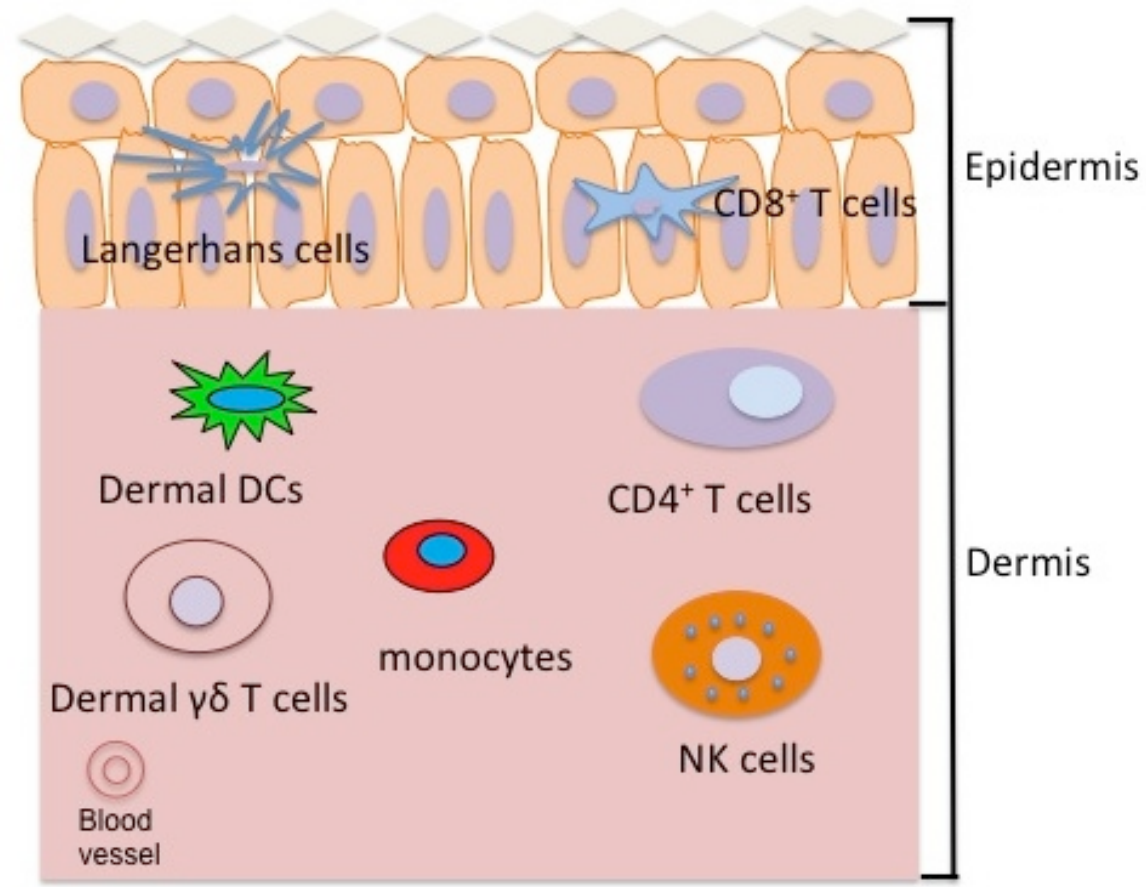

Figure 1-7 Mouse skin resident immune cells
The epidermis is made up of Langerhans cells, and resident memory CD8+ T cells. The dermis comprises CD4+ T cells (effector and memory), γδ T cells, NKT cells, dermal DCs and macrophages. Figure adapted from [82].

As well as responding to physical trauma, the ability of keratinocytes to recognise various pathogen molecules and activate the TLR pathway makes them a formidable force for frontline protection against pathogen invasions. Keratinocytes may also produce cytokines such as interleukin 22 (IL-22), IL-1α and IL-1ß, IL-6, IL-10, IL-18 and IL-33, chemokines including CXCL9, 10, 11 and CCL20, or antimicrobial peptides such as ß-defensins [93, 94]. The epidermis also contains Langerhans cells (epidermal dendritic cells), and $CD8^+$ T cells.

Beneath the epidermis is the dermis composed of elastin fibres, collagen and other extracellular matrix proteins produced by fibroblasts. The dermis also contains blood vessels, and draining lymphatics begin in the dermis and penetrate deeper into the skin to access the lymph nodes. Immunologically important cells of the dermis include the mast cells, dermal DCs (DDCs), macrophages, γδT cells, and NK cells. DDCs are evenly dispersed across the dermis and can be distinguished from Langerhans cells through lack of expression of epithelial cell adhesion molecule (EpCAM) [95]. A certain group of T cells

referred to as unconventional or innate like T cells (γδT and NK cells) are also present in the epidermis and dermis, and perform immunosurveillance roles.

1.7.1 Skin resident immune cells

1.7.1.1 Dendritic cells

Langerhans cells are positioned in the epidermis above the basal keratinocytes and are found in both humans and mice. The role of Langerhans cells has been extensively studied, and recent evidence suggests that they contribute to priming adaptive immunity to skin pathogens such as *Candida albicans*, and bacteria such as *Staphylococcus aureus* [96, 97]. During infection or topical application of allergens, LCs can transit from the epidermis via afferent lymphatics to the LN, and can be distinguished from other cutaneous DCs based on high surface expression of EpCAM [98]. Langerhans cells can also sample bacterial toxins in order to generate humoral immunity, and have also been demonstrated to possess immunosuppressive effects, either through induction of T cell deletion or activation of regulatory T cells that dampen skin responses [99, 100].

$CD103^+$ dermal DCs have a well-defined role in immunity, particularly in anti-viral immunity [98, 101, 102]. $CD103^+$ dermal DCs have also been shown to efficiently cross present self-antigens to $CD8^+$ T cells, which suggest a potential role in self-tolerance in the steady state. $CD11b^+$ DCs are also present in the skin and represent a highly heterogeneous group of DCs. $CD11b^+$ migratory DCs in the mouse skin have been linked to T_H17 cell-mediated immunity [103]. In addition, intradermal injection of *Leishmania spp*. has revealed an important role for $CD11b^+$ DCs in antigen presentation [104].

1.7.1.2 Macrophages

Macrophages are a highly plastic and heterogeneous population of professional phagocytes involved in tissue homeostasis through clearance of senescent cells and tissue repair after inflammation [105, 106]. Macrophages are present in the normal skin at a low density of 1-2 per mm^2. Tissue resident macrophages are well known for their role as immune sentinels, and also for being amongst the

cells that participate early in the immune response. They engulf apoptotic cells and pathogens and release immune effector molecules, and can also present antigens. Resident tissue macrophages have been implicated to have a role in tissue repair and remodelling [107]. Resident skin macrophages are thought to scan the skin and participate in the early detection of, and response to pathogens entering the body through the skin. After an initial recognition of microbial challenge, resident macrophages, alongside other resident cells, release inflammatory mediators to drive recruitment of innate cells, initially neutrophils within a few minutes, followed by monocytes as early as six hours.

During tissue repair following an insult, the tissue formation phase, which is the mid stage in the restoration of skin integrity and homeostasis post injury, requires the presence of macrophages. The other two stages involved in wound repair are inflammation and maturation phases. Depletion of macrophages during the tissue formation phase leads to haemorrhage, failure of wound closure, and transition to the tissue maturation phase [106, 108-113]. The pro-inflammatory role of resident macrophages has been described in studies in which depletion of macrophages impacted chemokine production and neutrophil influx [114-116]. Depletion of resident macrophages through clodronate liposomes led to a reduction in host protection to infection, loss of inflammatory mediators such as chemokines, cytokines and altered inflammatory cell recruitment [115-117].

In summary, dermal macrophages lack migratory capabilities to the draining lymph node, poor antigen presentation properties, involved in maintaining tissue homeostasis, repair and might have an immunosurveillance role in the skin in sensing foreign invaders [106].

1.7.1.3 Skin resident T cells

The normal human skin contains more than 2×10^{10} skin-resident T cells, which is more than twice the total number of T cells in the blood [118]. In the epidermis, T cells are mostly $CD8^+$ αß T cells that are distributed in the basal and suprabasal keratinocyte layer, in close proximity to Langerhans cells. In the dermis, T cells are often clustered around postcapillary venules and the proportion of $CD4^+$ and $CD8^+$ T cells are almost the same, with most of the T

cells displaying a memory phenotype and expressing cutaneous lymphocyte associated antigen (CLA), CCR4 and CCR6 skin homing addressins that interact with E-selectin [118]. Specifically, CLA is thought to be a ligand for E-selectin, while other vascular addressins CCR4 and CCR6 contribute to selective trafficking from circulation into the skin. Most of the skin resident T cells have a Th1 effector memory phenotype, although T regulatory and central memory cells are also present [118]. T cells present in the skin (~80%), lacked expression of CCR7 and CCR4, while those that were present in the skin and expressed CCR7 and L-selectin, but also had expression of CLA have been identified as an intermediate phenotype capable of accessing the skin and secondary lymphoid organs [118]. Most of the CLA^+ T cells (~80%) are resident in the skin even in the absence of inflammation.

Until recently skin resident T cells have received less attention than those T cells that migrate between the skin draining lymph node and the peripheral tissue. The preferential accumulation of CLA^+ effector memory T cells in the skin highlights their importance in cutaneous immunosurveillance in the skin, and also in responding immediately to antigenic challenges. Skin resident T cells form a large pool of cells capable of interacting with dermal DCs for prompt response against microbial invasion, although it could contribute to the perpetuation of inflammatory diseases [119].

In addition to the presence of conventional T cells resident in the skin, there is also another group of T cells described as unconventional or innate-like T cells [120, 121]. Invariant NKT cells (iNKT) in the skin have been demonstrated to recognise bacterial glycolipids, hence play a protective role as antimicrobial immune sentinels [121]. In summary, T cells in the skin have a diverse repertoire, are Th1 biased, comprised primarily of effector memory cells, and subpopulations of central memory and T regulatory cells are also present.

1.8 Cytokines in inflammation

Cytokines are small-secreted proteins that have specific effects on interactions and communication of cells of the immune system. The name cytokine is a general name, which includes lymphokine (cytokines made by lymphocytes),

monokine (cytokines made by monocytes), chemokines (cytokines with chemotactic activities, described in section 1.9), interleukins (cytokines made by one leukocyte acting on other leukocytes). Cytokines carry out their action by acting directly on cells that secrete them (autocrine), on nearby cells (paracrine), or at cells at a distance from where they are released (endocrine) [122, 123]. Cytokines exhibit redundancy in their activity, that is one or more cytokines may carry out the same function, and they may act synergistically or antagonistically. Cytokines are mostly produced by helper T cells (Th) and macrophages, although other cell populations may also produce cytokines. During inflammation, cytokines released may play a pro or anti-inflammatory role in tissues [122].

Proinflammatory cytokines are produced by activated macrophages, and other immune cells such as fibroblasts and endothelial cells during tissue injury, infection, invasion and inflammation. This class of cytokines include IL-1ß, Il-6, TNF-α, IL-15, and Il-18. Their classification as proinflammatory is based on the observation that this class of molecules are upregulated during inflammation [123]. For example during inflammation, IL-1 and TNF-α are upregulated, which are inducers of endothelial adhesion molecules, which is essential for leukocyte adhesion to endothelial surfaces prior to extravasation into tissues [123]. In the intracellular parasite *Trypanosoma cruzi* that is capable of replicating in a variety of host cells including macrophages, efficient control of *T. cruzi* during the first few weeks of infection was found to depend on macrophage activation by cytokines. In vitro data available suggests that treatment of macrophages with IFN-γ [124, 125] and/or TNF-α [126, 127], resulted in more efficient parasite killing. In vivo experiments further suggested that injection of IFN-γ into mice resulted in increased resistance [128], consistent with in vitro data. In malaria, studies in mice suggested that mice treated with anti-TNF-α, took longer to clear infection, suggesting that TNF-α was important early in infection [129]. Similar results have also been obtained when *P. chaubaudi chaubaudi* was injected into mice to investigate the role of IFN-γ, suggesting their importance in protection during infection [130]. In humans and animal trypanosomiasis, studies in mouse models have revealed that TNF-α was found to be crucial for parasite control through its trypanolytic effects on *T. b. brucei* and *T. b. gambiense* [131]. In *T. b. rhodesiense* and *T. congolense*, a role has been

proposed for TNF-α to carry out its trypanolytic activity in conjunction with IFNγ and NO. Studies in IFNγ knock out (KO) mice has also revealed a role for this cytokine in clearing infection, with these KO mice infected with *T. brucei* experiencing early mortality due to excessive parasitemia. Hence, TNF-α and IFNγ have been described to be involved in controlling parasitemia early in infection, but also involved in infection associated inflammatory complications [132].

1.9 Chemokines and their receptors

Chemokines, also known as chemotactic cytokines, are a group of over 50 proteins with a molecular weight of about 8-10 kDa. Chemokines play a principal role in the recruitment and guidance of cells in development, homeostasis and inflammation. This group of proteins have about 20-70% homology at the amino acid sequence level, and are subdivided into four families based on the relative position of their cysteine residues. The cysteine residues in chemokines are important for maintaining their structural integrity.

1.9.1 Nomenclature and classification of chemokines

The chemokine sequences are characterized by having four conserved cysteine residues, and are classified based on the position of the first two cysteines. They are divided into four subfamilies; α (CXC), ß (CC), γ (C), CX3C (δ). Chemokines bind to their receptors, which are G-coupled seven transmembrane domain receptors. Chemokine receptors have been named based on the chemokine class i.e. CXCR1, 2, 3, 4, and 5 (bind CXC chemokines); CCR1-9 (bind CC chemokines), XCR1 (binds C chemokine), and CX3CR1 (binds CX3C chemokine, fractalkine) [133, 134]. When chemokines are secreted, cells respond in a rapid and transient manner. Some chemokines do not partake in the recruitment of cells, for example the promiscuous chemokine receptor D6 and the duffy antigen-related chemokine receptor (DARC) but rather scavenge chemokines [135].

1.9.2 Homeostatic and Inflammatory chemokines

Chemokines, in addition to being classified based on structure, can also be classified based on function. A group of chemokines known as inflammatory chemokines control the recruitment of effector leucocytes in infection, inflammation, tissue injury, and tumours. Inflammatory chemokines have a broad spectrum of activity and play a significant role in the innate immune system, through attraction of neutrophils, monocytes, macrophages, dendritic cells and natural killer cells [136]. A second group of chemokines that has been described are the homeostatic chemokines that help navigate leukocytes during hematopoiesis in the bone marrow, thymus, and during the initiation of an adaptive immune responses in secondary lymphoid organs such as the spleen and lymph nodes. Homeostatic chemokines are also involved in immune surveillance functions of healthy peripheral tissues [135].

1.9.2.1 Homeostatic chemokines

Homeostatic chemokines also known as constitutively expressed chemokines are also important for migration of antigen presenting cells (APCs) and lymphocytes to lymphoid organs, and can also be expressed under inflammatory conditions [137, 138]. For example, CCL17 and 27 are involved in skin homing, while CCL21 which is expressed on the luminal side of high endothelial venules is involved in homing of T and B cells to the lymphoid organs. However, under inflammatory stimuli, CCL21 could be induced in the afferent lymphatics, hence boosting the numbers of DCs that arrive at the lymph node [139]. Homeostatic chemokines are important for regulation of basal leukocyte trafficking and regulate immune surveillance processes in the tissues such as homing of DC to the draining lymph node (dLN) [140-142]. In sum, homeostatic chemokines have a more monogamous receptor usage compared to inflammatory chemokines.

1.9.2.2 Inflammatory chemokines in innate immunity

Initiation of the innate immune system through the recognition of PAMPS or DAMPS by PRR results in production of inflammatory cytokines such as IL-1, interferons, IL-4, 5, 6, 13, 17 and chemokines. [143, 144]. Phagocytic cells such as neutrophils, monocyte/macrophages are recruited in the inflammatory

response through expression of chemokine receptors and respond to different chemoattractants (Figure 1.8).

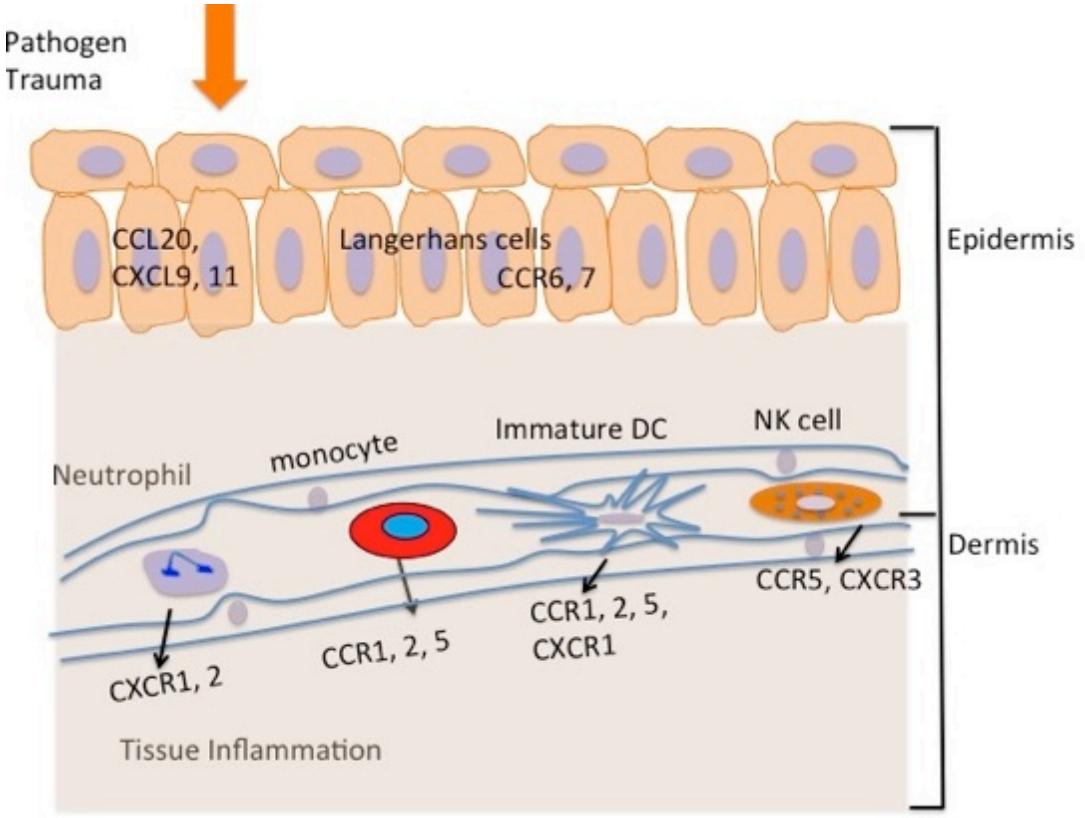

Figure 1-8 The role of chemokines in innate cell recruitment in the skin
Chemokines orchestrate events that impact on cellular recruitment during the early phase of a microbial challenge or trauma to the skin. This results in the release of inflammatory cytokines or chemokines, which activates the endothelium, followed by the recruitment and activation of leukocytes critical for the innate immune responses such as neutrophils, monocytes, DCs, and NK cells. Some chemokines may also act directly on the pathogens as antimicrobial peptides e.g. CCL20, CXCL9, 11. Figure adapted from [144].

Neutrophils, which are the cells that arrive first at inflammation sites, respond to CXC ligands such as CXCL1, 5 and 8 via their expression of CXCR1 and CXCR2 receptors. On the other hand, monocytes and other mononuclear cells express CCR1, CCR2, and CCR5 receptors and respond to their chemokine ligands CCL2, 3 and 5 and arrive at sites of inflammation at later time points [137].

1.10 Cell recruitment during inflammation

During tissue damage and inflammation, leukocytes are recruited from the blood, by mechanisms that involve selective leukocyte endothelial cell

recognition. This process is highly specific for the inflammatory stimuli, the stage of the inflammatory response and the tissue site involved. Examples include the specific recruitment of neutrophils during acute inflammation, and tissue selective interaction of lymphocyte subsets with high endothelial venules. Hence, activation of the endothelium plays an important role during leukocyte recruitment. This process has been demonstrated to occur both in vivo and in vitro [145], and in mouse models leukocyte accumulation is influenced by the endothelial stimulus [146]. Activation of the endothelium occurs through signals, delivered by receptors that recognize inflammatory, traumatic stimuli or oxidants. The vascular endothelium is diversified at different levels, consisting of large vessels, which differ from small vessels and capillaries, while the venular endothelium also differs from the arterial endothelium [147]. Leukocytes preferentially migrate through postcapillary venules due to lower shear stress, which is more favourable for leukocyte attachment than in capillaries or arterioles. Also the abundance of selectins such as P –selectin, induction of E-selectin and vascular adhesion molecule-1 (VCAM-1), which are much more expressed during inflammation on postcapillary venules makes them preferred by leukocytes [148, 149]. The display of these selectins following activation of the endothelium mediates the other stages of leukocyte extravasation; capture, tethering and rolling.

A summary of some of the leukocyte adhesion receptors and the ligands they bind to on activated endothelial cells are provided in table 1.2. The subsequent sections then give a description of the cells that are recruited in inflammation and their functions.

Table 1-2 Leukocyte adhesion receptors and their ligands on activated endothelial cells

Leukocyte adhesion receptor	Endothelial ligand	Function(s)
PSGL-1	P-selectin	Capture, Rolling
L-selectin	P-selectin, E-selectin,	Capture

$\alpha_4\beta_7$ (unactivated)	MadCAM-1	Rolling
$\alpha_4\beta_7$ (activated)	VCAM-1/MAdCAM-1	Firm adhesion
$\alpha_4\beta_1$ (unactivated)	VCAM-1	Rolling
PECAM-1	PECAM-1	Emigration
CD11a/CD18 (LFA-1)	ICAM-1, ICAM-2	Firm adhesion, Emigration

1.10.1 Neutrophils

Neutrophils are the first line of defense and play a key role in the elimination of pathogens [150]. In addition to their microbicidal role, neutrophils are also crucial in wound healing and tissue repair [151, 152]. As a key component of the inflammatory response, neutrophils play an important role in recruitment, activation and interaction with APCs. Neutrophils also release chemotactic signals to attract monocytes and DCs, and influence the differentiation of macrophages either to a pro or anti-inflammatory state. Neutrophils follow chemotactic gradients produced by host (IL-8) and pathogens (e.g. fMLP; N-Formylmethionyl leucyl-phenylalanine) in order to reach sites of infection [151]. Neutrophils have also been implicated in immune regulation, as a source of cytokines, such as IL-12, IL-10, IFNg and TNF-α, suggesting that they help bridge the innate and adaptive immune system [153]. Neutrophils are known to express PRRs e.g. FPR1 (Formyl peptide receptor 1), which is a seven transmembrane G-coupled receptor that helps in neutrophil chemotaxis to sites of tissue damage and recognition of microbial moieties. Other PRRs expressed by neutrophils include all members of the TLR family, excluding TLR3, C-type lectin receptors dectin 1 (CLEC7A), CLEC2 (absent in mouse neutrophils), and cytoplasmic sensors of ribonucleic acids (RIG-1 and MDA5). These PRRs expressed by neutrophils are essential together with other lymphoid cell-derived signals to sense tissue damage and pathogens, which then activates the effector functions of neutrophils.

Neutrophils carry out their killing functions either through intra or extracellular means. When neutrophils encounter pathogens, they can phagocytose them, and the pathogens become encapsulated in the phagosomes. Following encapsulation, the pathogens are then killed using reactive oxygen species or antibacterial proteins such as cathepsins, defensins, lactoferrin and lysozyme [154, 155]. These antibacterial proteins are released from neutrophil granules either into phagosomes or the extracellular milieu. Hence, they can act both on intracellular or extracellular pathogens. In some infections, neutrophils can become highly activated and eliminate extracellular microorganisms through the formation of neutrophil extracellular traps (NETs) [156]. NETs are composed of core DNA elements bound to histones, proteins and enzymes such as myeloperoxidase and neutrophil elastase. NETs can trap pathogens, preventing their spread and subsequently exact a direct killing effect through antimicrobial histones and proteases [157]. NETs have been described to be formed in *Staphylococcus aureus* [158], *Candida albicans* [159], and *Leishmania* infections [160].

In addition to their innate immune functions, individuals with insufficient neutrophils (neutropenia) have been shown to have wounds that heal poorly or with lethal outcomes [161], and total absence of neutrophils could lead to death. Inherited neutrophil defects such as severe congenital neutropenia (SCN), chronic granulomatous disease (CGD) and myeloperoxidase (MPO) deficiency exemplify the importance of neutrophils in various infectious and non-infectious conditions. For example in CGD caused by mutations in the genes encoding the subunits of NADPH oxidase complex, has an incidence around 1/200, 000 [162]. These individuals have phagocytes that are fail to kill ingested pathogens, due to inability to effectively produce superoxide, leading to severe infections mainly by *Aspergillus* and *Staphylococcus* species [162, 163]. CGD patients also exhibit a state of chronic immune activation, making them more prone to autoimmune disorders such as rheumatoid arthritis, and systemic lupus erythematous [163, 164].

In intracellular parasitic infections such as *Leishmania major* in mouse models, neutrophils recruited to sites of infection have been described to enhance pathogenesis. Depletion of neutrophils in vivo using a monoclonal antibody (anti-Ly6G), appeared to decrease the parasitemia in mouse models of *Leishmania*

major infections **[165, 166]**. This suggested that despite the fact that the primary role of neutrophils was killing foreign substances, and they were the first cells to be recruited during tissue injury, inflammation, or infection, some parasites have evolved mechanisms to by-pass neutrophil killing functions and use them to thrive in its host.

1.10.2 Monocytes

Monocytes are mononuclear leukocytes with a bilobed nucleus, which are bone marrow derived and along with other cells such as neutrophils, eosinophils, mast cells and natural killer cells, are part of the innate immune system. In addition to the bone marrow, the spleen also serves as an important reservoir of monocytes, and in myocardial infarctions, the spleen and not the bone marrow is the source of monocytes [167-170]. Monocytes can also migrate to other tissues of the body such as the lungs, spleen, lymph nodes, liver, subcutaneous tissue and peritoneal cavity [168, 171]. Recruited, inflammatory monocytes may also support dendritic cells in the transport of antigens to the draining lymph nodes [172]. In mice, monocytes express the lineage markers CD11b, F4/80 and in humans CD11b, CD14, and CD11c [167]. Monocytes express MHC class I and II and can also present antigen to T cells in infection [170]. The plasticity of monocytes has been shown by their ability to produce different subsets of inflammatory DCs such as Tumour necrosis factor and Inducible nitric oxide synthase (iNOS)-Producing (Tip)-DCs, and $Ly6C^{hi}$ DCs [171]. Two monocyte subsets have been characterized in mice using adoptive transfer technology, based on their expression of the lineage marker GR1 (Ly6C and Ly6G), CCR2 and the fractalkine receptor (CX_3CR1). These two classes of monocytes in mice were similar to those identified in human blood, and are summarised in table 1.3 with the phenotypic markers they express. Inflammatory monocytes in mice, which home to sites to injury, have the classical expression $Ly6C^{hi}$ $CCR2^{+}$ CX_3CR1^{lo}, which is similar to $CD14^{+}$ monocytes in humans.

Table 1-3 Monocyte subsets in Mouse and human blood

	Mouse monocyte subsets	Human monocyte subsets
Subsets		

Inflammatory	$CD11b^{+}Ly6C^{hi}$ $CCR2^{+}$ CX_3CR1^{-}	$CD14^{++}$ $CD16^{-}$
Resident/ patrolling	$CD11b^{+}Ly6C^{lo}$ $CCR2^{-}$ CX_3CR1^{+}	$CD14^{dim}$ $CD16^{+}$
Percentage of cells		
Inflammatory monocytes	50%	90%
Resident monocytes	50%	10%
Morphology and size		
Inflammatory monocytes	Granular, 10-14 μm	Granular, ~18 μm
Resident monocytes	Less granular, 8-12 μm	Less granular,~14μm

Non-classical or resident murine monocytes have the expression $Ly6C^{lo}$ $CCR2^{-}$ $CX_3CR1^{hi,}$ similar to $CD14^{dim}$ $CD16^{+}$ human monocytes. Patrolling or non-classical monocytes are involved in tissue surveillance roles in the absence of inflammation, and they detect infection or injury [173]. In protozoan infections such as orally transmitted toxoplasmosis, rapid influx of inflammatory monocytes to the gastrointestinal tract acts as the first line of defence in infection (see table 1.4 for summary). Mice that were $CCR2^{-}$ deficient were more susceptible to infection by *T. gondii,* which further supports the evidence that CCR2 was crucial for emigration of inflammatory monocytes to sites of infection [174]. In African trypanosomiasis, inflammatory monocytes appeared to have a pathogenic role. Inflammatory monocytes were observed to accumulate in the liver, spleen, and lymph nodes of infected mice [175].

Table 1-4 The role of monocytes during protozoan infections

Protozoan parasite	Localisation in host cells	Disease caused	Site of infection	Role of monocytes
T.	Extracellula	African	Liver	Tip-DCs

brucei[176]	r	trypanosomiasis		
P. chaubaudi [177]	Intracellular	Malaria	Spleen	TNF and iNOS producing monocytes
L. major[178]	Intracellular	Cutaneous leishmaniasis	Skin	Effector monocytes/ iNOS producing DCs
Toxoplasma gondii[179]	Intracellular	Oral toxoplasmosis	Peritoneum	Inflammatory macrophages and DCs, TNF and iNOS producing monocytes

Adapted from [175-180]

During trypanosomiasis, the presence of Tip DCs in the liver caused necrosis and apoptosis, which resulted in the exacerbation of disease and reduced survival of infected mice. In the absence of CCR2, there was reduced pathology in infected mice, due to lower numbers of Tip DCs, which was related to an increase in the number of inflammatory monocytes in the bone marrow and decrease in the liver [181]. The role of inflammatory monocytes in other parasitic infections such as, *Plasmodium chaubaudi*, visceral, and cutaneous leishmaniasis have also been studied in vivo using mice models [177, 182].

1.11 Host parasite interactions in the skin

Studies with a number of pathogen models have identified that pathogenesis is critically influenced by the earliest interactions between host and pathogen. This has been particularly true in experimental *Plasmodium* infections, where analysis of the initiation of infection and the associated host response has provided novel and fundamental biological insights challenging existing dogma. Imaging mosquito delivered, *Plasmodium berghei* infections in mice has revealed that sporozoites are initially deposited in skin and subsequently find and invade blood vessels through their ‘gliding’ behaviour [183]. These studies also reveal

the surprising quantity of sporozoites that progress to the lymphatic system where they can undergo extra-hepatic transformation to merozoites [184], and have identified the skin draining lymph node as the site where the host's adaptive immune response is initiated [185].

1.11.1 Current knowledge about events in the skin following African trypanosome deposition

In African trypanosomes, very little is known about the key events at the bite site following the bite of an infected tsetse fly. Most research on trypanosome infections have used intravenous or intraperitoneal injections of the bloodstream stage of the parasite into mice, which is not the route of infection in nature, and also not the appropriate infective stage of the parasite. These studies have also focussed on what happens when the parasite is in the blood, hence information that we have in abundance about the immune response is mostly on adaptive immunity.

Following the bite of an infected tsetse fly, metacyclic stage trypanosomes are released into the dermis of the skin, along with the saliva of the tsetse fly that contains immunomodulatory factors and anticoagulants, which are important in tsetse feeding and infection of its host [186, 187]. Data suggests that the tsetse saliva biases the host immune system towards a Th2 associated cytokine response (IL-4, and IL-10), inhibiting proinflammatory cytokines (TNF-α, IL-6, IL-12) that have trypanocidal effects in vivo [188]. While the infective metacyclic trypanosomes are in the dermis of the skin, they proliferate and become established. A local skin reaction about 2-3 mm in diameter, described as a chancre develops within 5-7 days following infected tsetse bites in humans and ruminants. The chancre also serves as a focal point for interactions between trypanosomes and host immune cells, as evidenced by the presence of neutrophils, macrophages, lymphocytes and trypanosomes in the chancre of infected mammals [13].

Previous reports on the cellular infiltrate in the skin following infected tsetse bite have observed the cellular events in the skin after the onset of the chancre (from day 5). In experiments that have been carried out in large animals such as

goats, *T. congolense* was still present in the dermis of the skin at day 8 post tsetse bite, with parasites occasionally found between hair follicles [189]. During day 8 post infected tsetse bite, histological characterisation reveals the cellular infiltrate in the skin to comprise of small lymphocytes, numerous neutrophils, but few macrophages and very few trypanosomes. At day 11 post infection, aspirates taken reveal the presence of predominantly large lymphocytes, lymphoblasts, numerous macrophages, trypanosomes and few neutrophils [11, 190]. To date, the information we have on the events in the skin following interactions of the parasite with the host mostly relates to events that coincide with the appearance of the parasites in the blood. Therefore information is lacking on the very initial interactions of parasites, and host cells at the bite site.

1.11.2 How do African trypanosomes get into the bloodstream?

Following the deposition of the metacyclic trypanosomes in the skin and proliferation in the skin, trypanosomes begin to appear in large numbers in the lymph, 2-3 days before detectable parasitemia. Cannulation of afferent and efferent lymphatics in large animals such as goats has been able to establish the importance of the lymphatics in parasite dissemination into the blood stream from the site of inoculation. These observations of parasites in the lymph before detection in the blood have been demonstrated using *T. congolense* and *T. b. brucei* infected tsetse flies [11, 189, 191, 192]. Hence, the lymphatic system has been postulated to be a principal route of parasite entry into the bloodstream when establishing infections with cyclically transmitted parasites.

1.12 Lymphatic system

The lymphatic system is a uni-directional system of conduits that helps in draining excess fluids in the interstitial, and also serves immunological functions. The draining function of the lymphatic system helps to regulate tissue fluid balance, which then complements the functions of the blood vascular system. Although there is an interdependence of the blood and lymphatic vasculatures for maintenance of tissue homeostasis, they are structurally and

functionally distinct entities. Lymphatic vessels help direct leukocytes and antigens in tissues to the lymph nodes, which is critical for the initiation of an immune response [193]. However, we now know that the diverse structure of lymphatic capillaries may explain some of the differences observed between the migratory patterns of cells.

1.12.1 How the structure of lymphatic capillaries relates to its function

Lymphatic capillaries are blind ended vessels, bounded by an endothelial cell layer and optimised for uptake of fluid, macromolecules, and cells [194]. Compared with blood capillaries, lymphatic capillaries have a more irregular morphology with a very narrow endothelium (Figure 1.9), and an incomplete basement membrane with sparsely populated pericytes. A distinguishing trait of lymphatic capillaries is their overlapping junctions or button-like junctions, formed by the superimposition of adjacent lymphatic endothelial cells.

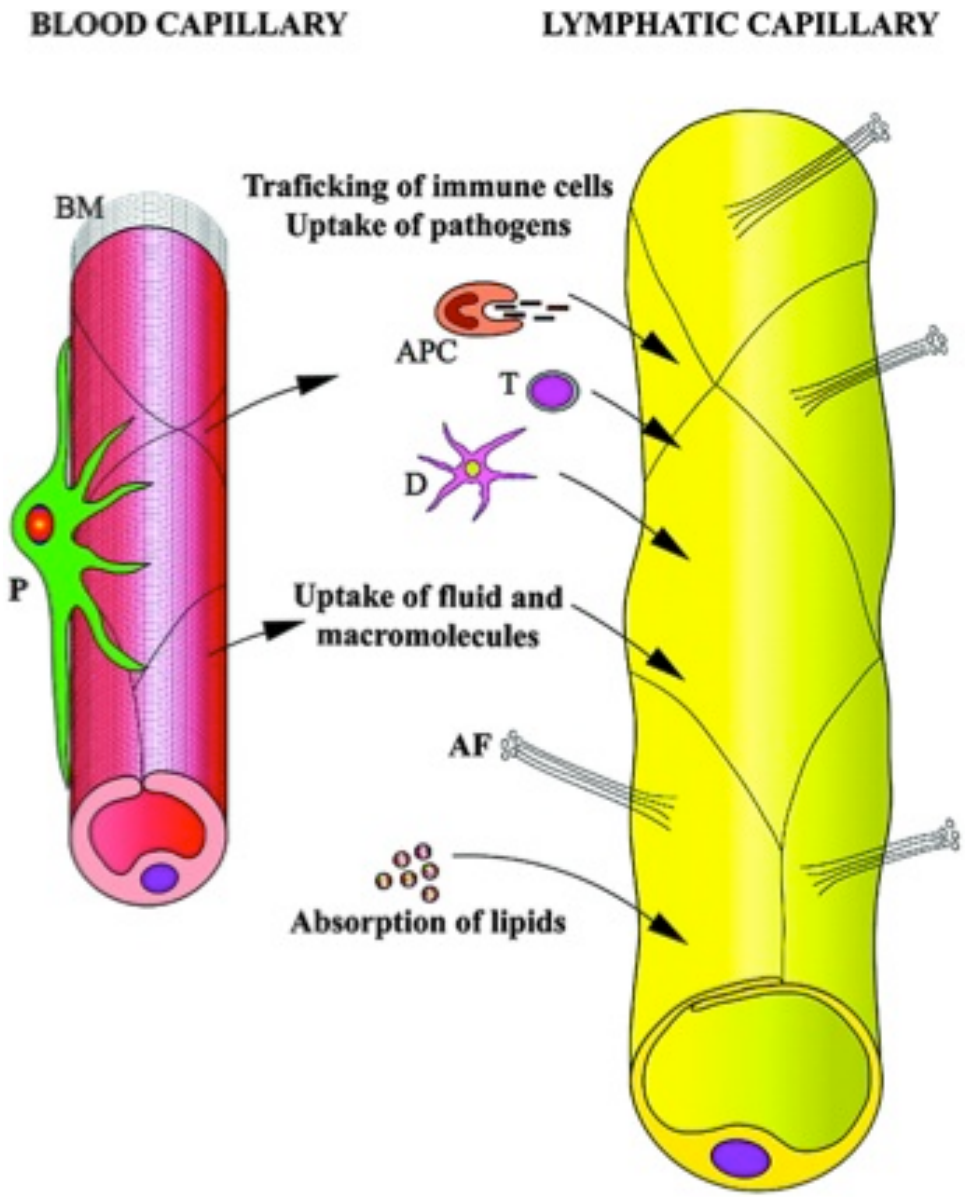

Figure 1-9 Comparison of the structure and function of lymphatic vessels
Comparison of the structure of the blood vessel to the lymphatic vessel reveals that the basement membrane (BM) of lymphatics is incomplete with few pericytes (P). APC, antigen presenting cell; T, T cell; D, dendritic cell, AF; anchoring filaments. Adapted from [194].

These button-like junctions can open due to increases in interstitial fluid, thereby permitting the passage of fluid and particles into the vessels. Once fluid enters the vessels, the pressure in the vessel decreases, the junctions close and this prevents a back flow of the fluid into the interstitium [195, 196].

1.12.2 Leukocyte migration through lymphatic vessels

The cells that migrate through the lymphatics to the lymph node include T cells and myeloid cells [197-199], the majority of which are DCs. Due to their importance in the initiation of adaptive immunity, DC trafficking towards the

lymph node has been extensively studied [200]. Under steady state, epidermal resident $CD206^{+}$ Langerhans cells, as well as dermal resident DCs continuously migrate to the LN at modest intensities.

During inflammation, migration of DCs to lymphatics is significantly increased in response to chemotactic signals induced by the products of inflammation [201]. The migration of DCs to the lymphatic vessels is largely driven by CCR7, and the expression of its ligand, CCL21 on lymphatic vessels is strongly upregulated in the presence of pro-inflammatory cytokines such as TNF-α [202]. There is also experimental evidence to suggest that as lymph flow increases during inflammation, there is also a concomitant increase in CCL21 expression [202]. The ingress of DCs into the lymphatic vessels occurs through the basement membrane of initial lymphatics in close proximity to CCL21 depots. Inside the lymphatics, DCs crawl directionally on the luminal side of the capillary [203]. These data provide a strong correlation with DC migration along areas of dense CCL21 depots on lymphatic vessels [204].

1.13 Host- trypanosome interactions

African trypanosomes spend a large part of their life in the mammalian bloodstream [205], being extracellular parasites and interact with the host immune system. In HAT caused by *T. b. rhodesiense* and *T. b. gambiense*, the parasites are able to evade lysis by human serum apolipoprotein (APOL1), which is crucial in innate immunity against African trypanosomes. APOL1 resides in two fractions, trypanolytic factors 1 (TLF-1) and 2 (TLF-2) [206]. APOL1 kills trypanosomes after insertion into lysosomal membrane. TLF-1 binds to the parasite through interaction with the haptoglobin-related protein (HPR) and the haptoglobin haemoglobin receptor (HpHbR) in the flagellar pocket of the parasite, while TLF-2 interacts with HpHbR through an alternative route [207, 208]. *T. b. rhodesiense* evades killing in human serum through interaction of serum resistance associated gene (SRA) with APOL1 in the lysosome preventing lysis [60]. While in *T. b. gambiense*, resistance to TLFs is via a hydrophobic ß sheet of the *T. b. gambiense* specific glycoprotein (TgsGP), which prevents APOL1 toxicity and induces the stiffening of the membranes [209]. In AAT caused by *T. b. brucei* and most trypanosomes, these paraistes are susceptible to serum

killing by APOL1. The section below highlights some of the mechanisms employed by *T. brucei* in evading the immune response.

1.13.1 Variant Surface Glycoprotein Coat

As a result of being exposed, a trypanosome's cell surface serves as the primary target against immune responses from the host. African trypanosomes are completely covered with a monomolecular layer of a single species of a glycoprotein coat [210]. Trypanosomes are able to persist in the bloodstream of mammals by replacing this monolayer of VSG coat that shields it from the immune effectors of the host [211, 212]. The switching of their VSG coat is a mechanism that has been employed in order to thrive for long-lasting periods, enhancing transmission to the tsetse fly, although also resulting in pathological manifestations. Trypanosomes undergo VSG switching, up to 10^{-3} switches per cell division, allowing it to produce unique VSGs that the immune system cannot recognise when antibodies against the currently expressed VSGs are produced [213]. The high switch rate of the VSG coat has also made it difficult to develop effective vaccines against human and African animal trypanosomiasis.

1.13.2 Immune suppression in African trypanosomes

Immunosuppression has been observed in humans and mammals, although most of our understanding of immunosuppression comes from experimental data in mice. African trypanosomiasis, whether in humans or experimental inoculations in animals, presents with numerous alterations in the normal functioning of T and B cells. Immune suppression in African trypanosome infected livestock results in a reduced ability to mount an effective humoral response against non-trypanosome antigens, depressed T cell proliferation, reduced cytokine production, most notably IL-2 and phenotypic changes to monocyte effector functions [214, 215]. Also, immune suppression in African trypanosome infected mice is also responsible for the inefficacy of other administered vaccines such as diphtheria, tetanus and pertussis. Failure to control parasitemia levels and ineffective vaccination regimes against other infections are hallmarks of immune suppression in African animal trypanosomiasis [216].

1.14 African Trypanosomes are highly motile

African trypanosomes derived the name of their genus *Trypanosoma* from two Greek words Trypanon and soma, meaning auger and body, respectively. The name was based on the observation of their corkscrew motion in mammalian blood. Trypanosomes have an undulating membrane, which is the flagellum and their motility has been the subject of interest over the years [19, 217-219]. The flagellum of *T. brucei* has the canonical '9+2' axoneme, which serves as the platform for the assembly of dynein motors that regulate the flagellar beat [220]. Motility of African trypanosomes is driven by the flagellar wave that is initiated at the tip of the flagella towards the base of the flagellum [221]. The importance of motility for parasite transmission has also been recently demonstrated in *T. brucei,* where the propulsive motility of the parasite is essential for infection of the tsetse fly [22]. Owing to the fact that the flagellum is an essential organelle, which has also been directly linked to parasite pathogenesis, chemotherapeutic approaches have also begun to investigate the possibility of the flagellum as a drug target [220, 222-224]. Trypanosomes move through the propagation of the flagellar wave along the cell, allowing the cell to move in the surrounding fluid through the beat propagation of the flagellum in the opposite direction. Thus, three classic descriptions of trypanosome motility have been described, which presumably confer advantages to the parasite in particular scenarios. However the exact mechanisms guiding motility has yet to be understood. In the first model, using state of the art high-speed microscopy imaging, analyses of the movement of bloodstream form *T. brucei* parasites were carried out in liquid cultures, and by simulating the bloodstream environment. In their experiments, it was shown that the tip of the flagellum moves faster than the posterior of the cell [225, 226]. In the second model, mathematical models were used to propose a plane rotational model of motility in African trypanosomes. This was based on the observation that the cell body rotates as it moves forward, with the rotation of the cell body occurring uniformly in an anticlockwise direction. The plane rotational model suggests that the flagellum beats in a planar fashion, and the beats become helical as it moves forward due to physical constraints from the attached cell body [227]. This proposition of a planar model contrasts previous reports of a helical model for *T. brucei* and other flagellated protists [226]. The third model for trypanosome

motility was described as a bihelical model. In this model, the flagellar waveform alternates between left-handed and right-handed helical waves, which cause the trypanosome body to alternate in anti-clockwise, and clockwise directions [226]. Bihelical motility has also been observed in the bacterium *Spiroplasma melliferum* and *Plasmodium berghei* [228, 229].

1.14.1 The role of motility in African Trypanosomes pathogenesis

In the tsetse fly, trypanosomes have to traverse between different environments, e.g. from the midgut to the salivary gland [18]. In order to arrive at the salivary gland from the alimentary canal, parasites travel a distance that is estimated to equal the entire body length of the tsetse fly, and must penetrate the proventriculus and peritrophic membranes. Available data suggests that some of the crossing events in the tsetse fly require active parasite motility [230]. In the mammalian host, following the deposition of motile metacyclic parasites into the skin, the parasites need to navigate their way through the crowded environment of the skin [226, 231]. The role of the flagellum very early on is yet unclear, but might be crucial for entry into the lymphatic vessels. Despite the potential role of the flagellum in pathogenesis, only one study to date has directly investigated the contribution of motility mutants in establishing infection [232].

One major challenge in studying the role of motility mutants in trypanosome infections has been the inability to generate viable mutants. However, using loss of function point mutants, instead of depleting proteins through RNAi, a mutant with a defect in motility was generated. This technique allowed the generation of bloodstream form mutants that had its outer dynein structure intact and viable. Using this mutant, it was demonstrated that mutants that had their motility fundamentally altered, showed no difference in patency, gross pathology, and lethality between motility mutants and wild type blood stream form *T. b. brucei* 427 strain. However, a major limitation of this study was that infection was carried out using the intraperitoneal route of injection; secondly the mutants still retained some residual motility, which may be sufficient for the parasites to establish infection [232]. Despite these findings, trypanosome

motility is generally agreed to be essential for penetration of the blood brain barrier, and invasion of the central nervous system (CNS) [233-237]. Also, parasite uptake by the tsetse fly may require motility, in addition to migration through the tsetse fly in order to establish mature infections in the salivary gland [22, 238, 239].

In addition, through the flagellar pocket and endosomal system, *T. brucei* has optimised endocytosis and recycling of VSGs as an adaptation to its unique lifestyle. During infection in the blood stream, anti-VSG antibodies bind the surface of the parasite, which can effectively kill the parasite via complement-mediated lysis. Parasites can use the hydrodynamic forces generated by the flagella to sweep anti-VSG antibodies to the posterior of the cell into the flagellar pocket where they are endocytosed [240]. Anti-VSG complexes are then degraded and intact VSGs recycled back to the surface via RAB11b recycling endosomes [241, 242]. In bloodstream form *T. brucei,* the parasites are able to turn over back to the parasite's surface the entire VSG pool in approximately 12. 5 mins [243].

1.14.2 Flagellar pocket and host-parasite interactions

The flagellar pocket is the site of exchange of macromolecules between the parasite and its environment. For example, the parasite takes up host transferrin as a source of iron, but can also take up trypanolytic factors that are present in the host serum [207, 244, 245]. The flagellum also releases proteins that modulate virulence in the mammalian host. For example, glycophosphatidylinositol-phospholipase C (GPI-PLC) is required for virulence in pleomorphic trypanosomes (parasites that can differentiate from the bloodstream form and complete its life cycle in the tsetse fly). The role of GPI-PLC in virulence was demonstrated in mice infected with parasites lacking GPI-PLC, which survived longer and gave lower parasitemia [246]. GPI-PLC also facilitates differentiation of parasites from blood stream form to the tsetse procyclic stage [247]. Other flagellar proteins, which also serve as virulence factors, such as calflagins, metacaspase 4, and the expression site associated gene 4 (ESAG4) have further shed light on flagellar and host-parasite interactions [248-250].

1.15 Imaging host-parasite interactions in vivo

Advances in molecular biology through the use of fluorescent protein reporter genes coupled with advances in microscopy, have facilitated further understanding of parasite behaviour in vivo and in vitro. The availability of transgenic mice expressing cell specific fluorescent reporters have also helped in understanding the interaction of parasites with host cells in vivo [251]. These approaches are important in identifying new strategies to solve the disease burden posed by protozoan parasites such as *Leishmania* spp., *Plasmodium* spp., and *Trypanosoma* spp. Conventional approaches for immunological studies, such as immunohistochemistry and flow cytometry, only give a snap shot of the events that occur and are unable to give exact spatiotemporal information. Microscopy provides tools to enable dynamic analysis of the cellular events that take place; in the case of a vector bite, specifically providing the ability to analyse aspects such as parasite entry into the skin and egress from the bite site, and similarly, location and dynamics of interactions with host immune cell populations.

1.15.1 Bioluminescence imaging

Bioluminescent imaging has been applied in testing drug efficacy and drug discovery for African trypanosomiasis and Leishmaniasis. Introducing firefly luciferase into protozoan parasites has made it possible to assess their localisation in their hosts, their proliferation over time and clearance when drugs are administered. The reaction of the luciferase enzyme with its substrate luciferin culminates in the release of photons, which is then detected by a high sensitivity cooled charge-coupled device (CCCD) camera. This approach is sensitive enough to allow whole body imaging of mice and localisation of the signal in specific tissues and organs. For example, testing efficacy of drugs in models of Stage 2 African trypanosomiasis takes approximately 180 days, but with in vivo bioluminescent imaging, the time can be reduced to 30 days [252]. In addition, novel information has been gained through these approaches on the dissemination of African trypanosomes and the location and dynamics of recrudescence after incomplete drug therapy [237, 252, 253]. In vivo fluorescence imaging has also been applied in similar ways to perform drug

screening, using GFP expressing *L. major* or *L. donovani*, and EGFP expressing *L. amazonensis* [254, 255]. Bioluminescent imaging has also been applied in understanding the development of *Leishmania* through its sand fly host using RFP-expressing *L. major* parasites [256, 257]. The introduction of red-shifted luciferase and fluorescent proteins has also helped in reducing loss of signal due to tissue absorption [258, 259]. The inability to image deeper into tissues with this technique, and the lack of resolution to visualise interactions at the cellular level, means that to address both of these issues necessitates the use of an optimised fluorescent microscopy approach such as multiphoton laser scanning microscopy (MPLSM).

1.15.2 Fluorescence microscopy

In order to overcome the challenges posed using bioluminescent approaches in imaging, fluorescence microscopy has provided a viable alternative. In contrast to bioluminescence approaches that require the availability of a substrate to execute the enzymatic reaction resulting in photon emission, fluorescent microscopy uses a single wavelength to excite a fluorescent molecule, and then as the excited electrons decay back to their ground state, detects emitted photons at a specific wavelength.

1.15.3 Epi-fluorescent microscopy

Epifluorescence microscopy allows the visualisation of cells or parasites using a broad excitation and detection system to capture fluorescence emission from samples. However this approach also collects out of focus light emitted above and below the focal plane, making quantitative cell tracking impossible. While software deconvolution does allow some correction for out of focus light this is very difficult to apply in complex 3- dimensional (D) specimens and is prone to artefact generation [260, 261]. This limits its use for investigating in vivo parasite host interactions for immunological studies.

1.15.4 Confocal microscopy

Confocal microscopy allows the visualisation of interactions both in 3 and 4 dimensions, that is, in space and time. This approach relies on high power (laser)

illumination of the specimen, and uses a pinhole to reject out of focus light emitted from the sample [262]. While laser scanning microscopy and subsequently high-speed spinning disk confocal microscopy have been used for in vivo imaging of host/parasite interactions [183], the high energy excitation light required due to the low efficiency recovery of light due to the pinhole causes cell damage and is limited in depth to 50 microns below the tissue surface [262].

1.15.5 Multiphoton laser scanning microscopy (MPLSM)

The development of MPLSM has been an important tool, which allows long term in vivo imaging, at deeper penetration depths, without the issue of phototoxicity associated with other single photon imaging approaches. MPLSM employs the physical property of a fluorochrome to be excited by near simultaneous absorption of two lower energy, longer wavelength photons [263]. The only place that the sample photon density is sufficient to achieve this process is at the focal point of the objective lens. This allows the MPLSM to recover all of the emitted light from the sample, with the knowledge that it was emitted from a single point in space, negating the requirement for a pinhole. Furthermore, longer wavelength, infra red light penetrates tissue more effectively allowing imaging depths of hundreds of microns into tissue, with minimal tissue damage [264]. As with other in vivo microscopy approaches, MPLSM also requires surgical exposure of the tissue of interest. MPLSM has helped in understanding of the anatomy and architecture of the immune system, and the role that the immune architecture may play in infectious diseases. MPLSM has been applied in visualising cellular interactions in *Leishmania, Plasmodium*, as well as viral and bacterial infections. Conventional techniques such as flow cytometry and immunohistochemistry have revealed the identity of inflammatory cells, but MPLSM has been able to reveal the spatial and temporal nature of single cells in vivo. For example, MPLSM studies in *Leishmania* have demonstrated that neutrophils were rapidly recruited to the bite site, where they formed a plug to close the sand fly bite, irrespective of the infection status of the sand fly, [165, 265]. With the MPLSM, the role of LCs and DDCs were investigated in a bacteria model of infection in the skin, using CD11cYFP transgenic mice. It was demonstrated that LCs were static, but carry out immunosurveillance functions

with their dendrites, and that DDCs migrate and respond to infection through its tissue surveillance activities [266].

1.16 Project aims

As already discussed, the very early immunological events following tsetse deposition of trypanosomes in skin have yet to be investigated in detail. In addition, the host parasite interactions that occur in the skin and cell to cell interactions/migration of the parasites through the lymphatic vessels as a result of the deposition of trypanosomes remains unknown. Understanding these interactions/events is important in designing new therapeutic approaches and also gaining an in-depth understanding of how trypanosomes disseminate into the bloodstream. In order to illuminate these grey areas, I hypothesised that 'mammals mount a potentially effective innate immune response against trypanosomes at the site of tsetse bite, and understanding these events would help promote our understanding of parasite dissemination. To test this hypothesis, the following aims were set out:

1. To establish a model for infecting tsetse in vitro and demonstrate that the ear pinna is a valid route of infection in mouse models. Following the establishment of the model, I set out to quantify parasite dissemination from the bite site to the draining lymph node prior to systemic infection. The results from these experiments are discussed in chapter 3.

2. To evaluate the inflammatory profile in the skin, characterising the mediators of inflammation and the cells that are recruited following tsetse fly bites. The results are described in chapter 4.

3. To visualise the parasites in the skin, examine their interactions with lymphatic vessels to attempt to understand the mechanisms of entry into the lymphatics in vivo. The results are described in chapter 5.

4. To reveal functional importance of the cells identified in aim 2 through depletion studies. The results are described in chapter 4.

2 Materials and Methods

2.1 Mice

For all immunological studies, female C57Bl/6 6-10 weeks old mice were obtained from Harlan laboratories (Bicester, UK). For obtaining infected mouse blood for tsetse fly feeds, female ICR or BALB/c mice aged 6-10 weeks purchased from Harlan were used. Mice were given one week to acclimatise in either the Joint Research Facility or Central Research Facility of the University of Glasgow and kept in conventional cages. LysM-GFP [267] and Prox-1 mOrange mice [268, 269] used for intravital microscopy were bred in house. Transgenic mice (Prox-1 mOrange, and LysM-GFP) used in these study had constitutive expression of the fluorescent reporters. All procedures were carried out in accordance with the United Kingdom Home Office regulations under the authority of the appropriate project and personal licenses. This study complied with the Animal Research: Reporting of In vivo Experiments (ARRIVE) guidelines [270]

2.2 Trypanosome strains and culture

2.2.1 Trypanosome strains

Pleomorphic *T. b. brucei* strains STIB247 (hereafter referred to as 'STIB247'), isolated in 1971 in the Serengeti national park (Tanzania) from a hartebeest (*Alcelaphus buselaphus*), and GVR35 were both used in this study [271, 272]. GVR35 was isolated from a wildebeest also in Serengetei in 1966, and this stabilate produces chronic infection in mice, and has been used to test the trypanocidal effects of drugs on trypanosomes in the CNS [272, 273]. Transgenic 247 and GVR35 expressing mCherry [234, 252] were supplied as a kind gift from Dr Elmarie Myburgh and Prof Jeremy Mottram, Wellcome Trust Centre for Molecular Parasitology (WTCMP), University of Glasgow.

2.2.2 Culturing bloodstream (BSF) *T. b. brucei*

In vitro culture of bloodstream form *T. b. brucei* 247 was carried out at 37 °C in a humidified 5% CO_2 incubator using modified HMI-9 medium [274] (see appendix I for details of media and general solutions) supplemented with 20% Serum Plus

(Sigma-Aldrich, Dorset, UK), 20% FBS gold (PAA Laboratories, Buckinghamshire, UK), and *T. b. brucei* 247 mCherry were maintained in culture media in the presence of puromycin (0.15 µg/ml). Parasites were allowed to grow to a cell density of 1-2 x 10^6, at which point the parasites were sub-passaged by adding 1-2 x 10^5 trypanosomes to 5 ml of fresh culture media. Blood stream form (BSF) cell density was determined microscopically using a bright line haemocytometer (Hausser Scientific, Horsham, USA). The number of parasites in a 10 µl aliquot of culture was determined by counting the parasites under a 1 mm square area and multiplying by 10^4 to obtain the number of cells per ml.

2.2.3 Trypanosome stabilate preparation

For long-term storage of trypanosomes, stabilates were prepared by addition of 10% w/v sterile glycerol to culture with a cell density of approximately 2 x 10^6 cells /ml. One ml aliquots were then placed in 1.2 ml cryotubes (Nunc, Paisley, UK), wrapped in cotton wool, frozen at -80 °C overnight and then transferred to liquid nitrogen. Records were entered with the appropriate stabilate numbers in the stabilate database. For stabilate retrieval from liquid nitrogen, frozen cells were defrosted at 37 °C, and placed in 5 ml modified HMI-9 culture media for 3-4 days before continuous passage as described above.

2.3 Maintenance and infection of Tsetse flies

2.3.1 Tsetse Flies (*Glossina morsitans morsitans*)

Tsetse fly- *Glossina morsitans morsitans* pupae were purchased from the Institute of Zoology, Slovak Academy of sciences, Slovakia (the contact person was Dr Peter Takac; Peter.Takac@savba.sk). Pupae were dispatched wrapped in cotton wool and placed in a sealed petri dish with holes on the lid to allow breathing. When pupae arrived, usually in batches of 400, approximately 50 pupae per meshed cage were kept at 25 °C and 70% relative humidity until eclosion. Newly emerged tsetse flies were then fed with blood meals (uninfected or infected with *T. b. brucei*).

2.3.2 Membrane feeding of tsetse flies

The membrane feeding system for tsetse flies used in this project has been previously described [275] (Figure 2.2). Newly hatched flies were fed within 24-48 hrs with the first infected blood meal. Two – three ml of fresh infected blood or thawed cryostabilates containing a majority of short stumpy stage trypanosomes was mixed with 18 ml of defibrinated horse blood (TCS Biosciences, Buckingham, UK) to feed 6 cages containing 50 tsetse flies each. Trypanosome infected blood meals were repeated thrice at one-day intervals, using a mixture of fresh infected blood and frozen fly feeds.

2.3.3 Maintenance of tsetse flies

The tsetse fly room (Figure 2.1) was maintained at a temperature of 25 °C, relative humidity 65%. The lights in the room are on 12 hours on/12 hours off cycle. Following the *T. b. brucei* infected feeds, tsetse flies were then maintained on defibrinated sterile horse blood by feeding 3 times a week (Mondays, Wednesdays and Fridays). This was carried out by pouring the defibrinated horse blood on a pre-sterilised metal tray on a hot plate pre-heated to 37 °C, covering with a silicone membrane, and tsetse flies in meshed drum cages were then fed [276].

Figure 2-1 Tsetse fly facility
Tsetse flies are kept in meshed drum cages, and placed in trays within a confined room at 65% relative humidity, 25 °C.

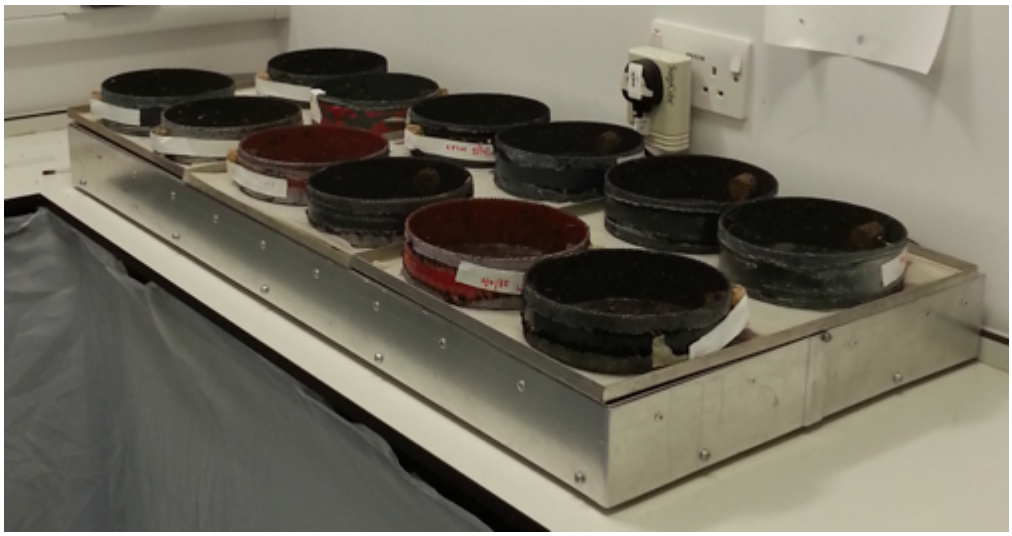

Figure 2-2 Tsetse fly feeds.
In order to feed the tsetse flies routinely post infected blood feeds, a hot plate was pre-heated to 37 °C, trays sterilised, and 20 ml defibrinated horse blood poured on each tray, covered with silicone membrane and tsetse flies in drum cages placed on the trays for feeds.

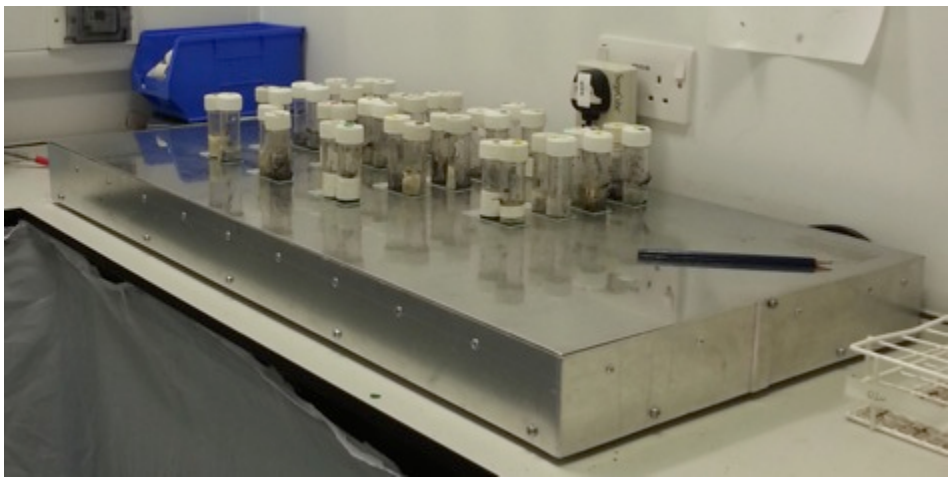

Figure 2-3 Tsetse fly screening for infection
Following 27 days post-infected feeds, tsetse flies were separated into universal tubes by cooling down at 4 °C for 5 mins in a refrigerator, and tsetses allowed to recover in the universal tubes at room temperature. Tsetse flies were then fed the day after separation into universal tubes with defibrinated horse blood. Two days post separation, tsetses were made to probe for approximately 10 mins on a warm glass slide, on a hot plate pre-heated to 37 °C, so that tsetse flies may extrude their saliva on the glass slide. Saliva containing extruded saliva was then viewed under the brightfield microscope.

Tsetse flies were maintained for 27 days for infections to mature before screening commenced. Once the 27 day period of maturation of parasites was over, tsetse flies were fed a day before, then cooled at 4 °C for 5 mins, and separated into universal tubes using forceps. Twenty-four hours post separation into universal tubes, tsetse flies were fed again with sterile defibrinated horse blood, and feeding of tsetse flies was increased to daily intervals, because tsetse flies were inclined to feed less when in individual tubes. Additionally, leaving

the tsetse flies in individual tubes for at least 10 mins on the hot plate greatly increased the number of tsetse flies that successfully fed as opposed to leaving for a shorter period of 5 mins.

2.3.4 Screening tsetse flies for Trypanosome infections

On days 28-30 the tsetses were induced to probe on microscope slides warmed on a hot plate pre-heated to 37 $^{\circ}$C (Figure 2.3). The saliva that was expelled onto the slides was checked under a brightfield microscope at x20 magnification for the presence of metacyclic trypanosomes. Some of the tsetse flies also regurgitated the proventicular (PV) stage in the saliva when screened. These PV trypanosomes are recognisably morphologically distinct from metacyclics, being significantly longer. For tsetse flies infected with mCherry-expressing trypanosomes, warm modified HMI9 culturing media (100 µl) was added to warm slides, and after tsetse flies made to probe, a coverslip was sealed over the area and examined under the Zeiss Axioskope using epifluorescent illumination for identification of fluorescent trypanosomes under the x63 oil immersion objective excitation/emission at 450nm and 550 nm respectively. Pictures were taken using a x63 oil immersion objective.

2.4 Infection of mice with Trypanosomes

2.4.1 Inoculation and monitoring mice infections

Mice were inoculated through the intraperitoneal route using blood straw stabilates resuspended in 200 µl phosphate buffered saline (PBS) (Sigma-Aldrich, Dorset, UK). Mice infections were maintained until they reached about 10^8 parasites within 10 days using the matching method [276], and then euthanised and blood collected by cardiac puncture method in a syringe containing 100 µl CBSS/heparin. Blood collected was used for either tsetse fly feeds or for preparation of blood straw stabilates.

2.4.2 Enumeration of parasite burden

To determine parasitemia for preparation of tsetse feeds, tail tips of mice were pricked with blood lancets and blood was collected using a 100 µl pipette (Gilson, Bedfordshire, UK). A drop of blood was then transferred to glass slides and sealed with a cover slip to estimate parasitemia using the matching method [276]. The matching method approach was used during preparation of tsetse feeds, and blood stabilate preparation. For a more precise determination of parasite burden post infected tsetse exposure, ten microliter of blood was lysed in equal volume of 0.8% ammonium chloride in PBS, and parasites counted using a haemocytometer (Hausser scientific, Pensylvannia, USA) as described in section 2.2.2.

2.4.3 Preparation of tsetse fly feeds from mice

Female ICR or BALB/c mice were infected with the STIB247 *T. b. brucei* to be used to infect the tsetse flies approximately 10 days before the estimated hatch date of the tsetse flies. Mice were inoculated and parasitaemia was measured as described in sections 2.4.1 and 2.4.2. In the cases where the parasitemia of the mice became patent and there were sufficient short stumpy *T. b. brucei* to make tsetse fly feeds (approximately 70%), but the tsetse flies were yet to hatch, cryostabilates were made by adding 10% glycerol to the volume of infected blood that could be extracted from the mouse after euthanasia and cryostabilated as described in section 2.2.3.

2.5 Nucleic acid analysis

2.5.1 DNA extraction from trypanosome culture

Trypanosome cultures at approximately 1 x 10^6 cells/ml was centrifuged at 1, 000 *x g* for 10 mins, supernatant removed and discarded, and pellets resuspended in RLT buffer provided in the kit for extraction of genomic DNA from blood and tissue (Qiagen, 7104, Manchester, UK). The samples were then processed following the manufacturer's instructions.

2.5.2 Isolation of genomic DNA from ear tissue and cervical lymph nodes

Mouse ear and cervical lymph node samples draining the ear inoculation site were processed following Qiagen kit extraction protocol, except for a slight modification when extracting from ear tissue, of doubling the concentration of proteinase K added for overnight digestion to allow complete lysis and removal of any tissue clumps. All other steps were carried out according to the manufacturer's instructions (Qiagen, 7104, Manchester, UK). To collect cervical draining lymph nodes, mice were euthanased post tsetse exposure at the respective time points. Mice were dissected with scissors, and forceps used to harvest the cervical draining lymph node and placed in PBS prior to DNA extraction. While mice ears were collected by euthanasing mice with a schedule 1 procedure and ears removed with a pair of scissors.

2.5.3 RNA Isolation

Ear or cervical lymph node tissues for RNA isolation were removed at the appropriate time points and transferred to sterile DNase/RNase free microcentrifuge tubes containing 500 µl RNAlater (Qiagen, 74104, Manchester, UK). For ear samples, the tissue was fragmented using a sterile scalpel blade prior to placing in the microcentrifuge, to allow RNAlater to more efficiently diffuse into the tissue. Samples were then transferred into M-tubes (Miltenyi, Surrey, UK) containing 600 µl RLT buffer + ß-mercaptoethanol. The tube was then spun on a gentleMACS dissociator (Miltenyi) using a 40s spin. Following the homogenisation of the tissue, subsequent steps were then carried out using the RNeasy mini kit according to the manufacturer's instructions (Qiagen, 74104, Manchester, UK). RNA samples were quantified using a nanodrop and frozen at -80 $^{\circ}$C until needed for use.

2.5.3.1 Measuring concentration of nucleic acids

Nucleic acid (DNA or RNA) concentration was measured photospectrometrically using a NanoDrop 2000 spectrophotometer (ThermoScientific, Paisley, UK).

DNA/RNA samples were quantified using 1.2 µl volume of samples, and elution buffer as blank control.

2.5.3.2 Agarose gel electrophoresis

DNA separations were performed on 1.5-2% agarose gels (Invitrogen), made with 1 x TAE buffer (40mM Tris, 19 mM acetic acid, 1 mM EDTA), and SYBRSafe (Invitrogen). DNA/ RNA samples were electrophoresed in 1 x TAE buffer at 100 V for 1 hr. A 100 bp ladder (NEB, Herts, UK) was used as molecular base pair size marker. DNA samples were then visualised on a GelDoc system (BioRad) using ultraviolet light.

2.5.3.3 Measurement of RNA quality

The quality of RNA extracted from tissue was determined using the Agilent 2100 Bioanalyser (Agilent Technologies, Edinburgh, UK), using approximately 100-200 ng/µl of sample. The RNA concentration was determined and RNA integrity number (RIN) calculated [277]. RIN values of (<5) were considered to be degraded RNA and RIN values >8 were considered to be very good quality RNA suitable for other experimental purposes.

2.5.3.4 Complementary DNA (cDNA) synthesis for Taqman low density arrays

For cDNA synthesis, 1 µg RNA was reverse transcribed using the Precision™ nanoscript reverse transcription kit (Primer design). RNase free water, oligo-dT and random nonamer primers were combined in a master mix to a final volume of 10 µl (Table 1.1).

Table 2-1 CDNA synthesis mix

Nanoscript 10X buffer	2 µl
dNTP mix 10 mM each	1 µl
DTT 100 mM	2 µl

Nanoscript enzyme	1 µl
RNase free water	4 µl

1 µg RNA was made up to a volume of 10 µl with RNase free water, denatured in a hot water bath at 65 °C for 5 mins, and immediately transferred on ice. Ten microlitres master mix was added to the RNA, to make up a total volume of 20 µl. Reverse transcription was carried out using a PCR machine at the following conditions: 25 °C for 5 mins, 55 °C for 20 mins and then 75 °C for 15 mins for heat inactivation.

2.6 Taqman low-density array (TLDA)

Taqman® low-density array microfluidic cards (Applied Biosystems) were designed using two different formats: 32 and 64 genes of interest. The TLDA microfluidic cards with 32 genes were used for the analysing the ear tissue samples and contained probes for chemokines, and inflammatory chemokines. The 64 gene microfluidic card contained murine probes for all murine chemokines with the exclusion of CCL10, CXCL4, CXCL7 and CXCL11. The microfluidic card also contained probes for 9 inflammatory cytokines, 4 pattern recognition receptors, 2 transcription factors and 8 interferon inducible genes. The microfluidic card consisted of 384 wells, which were already customised with the probes and primers for each gene. Two samples were analysed per 32 well card, and four samples per 64 well card respectively. The samples were loaded through the wells present in the microfluidic cards. Each loaded well-contained 100 µl of the reaction mix, prepared in 200 µl volume consisting of 20 µl of RNase free water and cDNA (1 µg total RNA equivalent), and 160 µl of Taqman Universal PCR master mix (Applied Biosystems, Paisley, UK). The Taqman array cards were run on a 7900HT fast real time machine (Applied Biosystems) according to the cycling conditions below:

95 °C 2 mins

95 °C 15 s
65 °C 60 s } 40 cycles

Data was analysed using SDS 2.2 software and RQ manager version 1.2.2 (Applied Biosystems), following the manufacturer's instructions. The relative amount of each target gene was normalised against the chosen endogenous reference gene (18S) in untreated ear or lymph node samples. For lymph node analysis, cervical lymph nodes proximal to the ear skin were collected for processing. Results were reported as fold changes that gives an indication of how much more or less a gene in the experimental group is expressed compared to its expression in the calibrator group or control.

2.7 Parasite quantitation

2.7.1 Polymerase chain reaction (PCR) of tsetse fly bite site tissue

PCR was performed on DNA extracted from tissue following infected tsetse fly bites. Primers were designed that targeted the paraflagellar rod 2 gene, because it is expressed in all the lifecycle stages of *T. b. brucei* [252]. PCR was performed using 100-200 ng template DNA from infected tissue or *T. b. brucei* DNA added to 14.5 µl reddymix PCR master mix with 1.5 mM $MgCl_2$ (Thermoscientific, Paisley, UK), 0.5 µl each of forward and reverse primers (100 mM), and made up with distilled water in a 25 µl reaction volume. The cycling conditions used were an initial 95°C for 15 mins, followed by 45 cycles of 94°C for 15 s, 60°C for 30 s and 72°C for 1 min 30 s, with a final incubation of 72°C for 10 mins. PCR products were routinely stored at -20°C.

2.7.2 PFR2 primers and probe

Gene sequences were downloaded from TriTrypDB Kinetoplastid genomics (www.tritrypDB.org). Primers for qRT-PCR designed using the Applied Biosystems qRT-PCR primer design software and supplied as a kind gift by Dr. Jean Rodgers [252]. PFR2 probe was tagged with FAM and TAMRA at its 5' and 3' ends. Oligonucleotides were then synthesised by Eurofins MWG Operon (www.eurofinsdna.com) as listed in table 2.2. Primers were stored as stock solutions (100 pmol/µl) at -20°C and diluted to a working concentration of 10 pmol/µl when needed.

Table 2-2 Oligonucleotide sequences used for quantification of *T. b. brucei*

Oligonucleotide name	Sequence
PFR2 primers	Forward: AAGTGCTTTCCCATCGCAACT Reverse: GACGCACTAAACCCCTCCAA
PFR2 probe	FAM-CGGTTCGGTGTGTGGCGCC

2.7.3 Preparation of dilutions for standard curve

A plasmid kindly provided by Dr Jean Rodgers was used as standard to estimate the number of copies of PFR2 present in the tissue samples at the different time points quantified [252]. The standard containing 10^7 copies/ 5 µl of the PFR2 gene was serially diluted with sterile DNase/RNase free water to give dilutions ranging from 10^6 to 10^1 copies per 10 µl. All standard dilutions were prepared fresh for each PCR reaction, and used immediately. An example of a standard curve is given in figure 2.4.

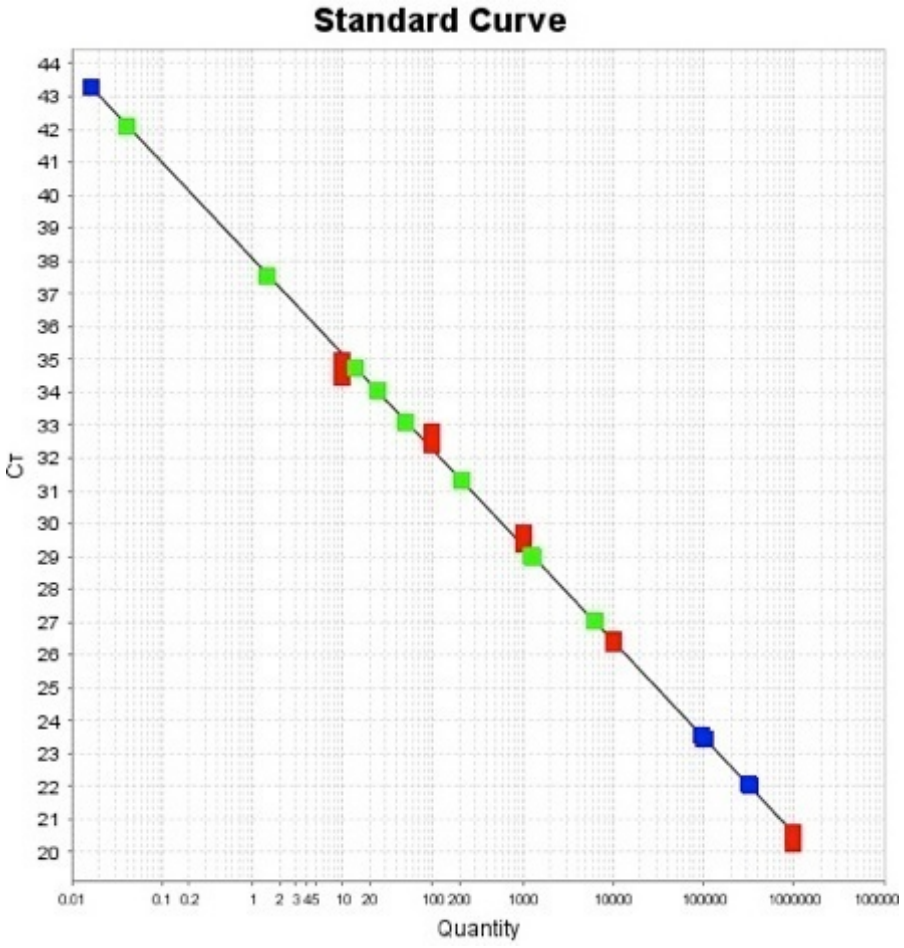

Figure 2-4 Standard curve for quantitation of *T. b. brucei*.
Plasmids were diluted from 10^6 to 10^1 copies and loaded on 384 well PCR wells for analysis on a 7900HT Fast Real-Time machine. Red squares indicate the plasmid dilutions.

2.7.4 Quantitation of parasites in the skin and draining lymph node by QPCR

In order to quantify parasites in the ear skin and cervical draining lymph node (dLN), a taqman semi-quantitative PCR approach was used which was based on designing a taqman probe that relies on the 5'-3' exonuclease activity of Taq polymerase to cleave the PFR2 probe when it binds to its complementary sequence. The QPCR reaction consisted of 12.5 µl Taqman Brilliant II master mix, 0.05 pmol/µl (final concentration) of each primer, 0.1 pmol/µl of the probe (final concentration), 300 ng template DNA, and made up to the final volume of a 25 µl reaction with sterile DNase/RNase fee water. Each sample was analysed in duplicates. The QPCR reaction was performed in an Applied Biosystem, 7900 HT thermocycler. After an initial denaturation step at 95°C for 10 mins, followed

by 95°C for 15 s, 60°C for 1 min for annealing to occur, and finally temperature raised to 72°C for 0.1 s. The reaction consisted of a total of 45 cycles.

2.8 Flow cytometry

2.8.1 Infecting mice ears

Mice to be used for flow cytometry analysis were anesthetized using Hypnorm/Hypnovel injectable anesthesia (10 mL/Kg of a mix of fentanyl/fluanisone/midazolam/H_20 at 1:1:2 by volume) administered intraperitoneally, and placed in a hot box to maintain the body temperature at 37 °C. One infected tsetse fly per universal bottle with a wire gauze underneath to allow probing, was then placed on the ear of the mice for approximately 20 mins or tsetse fly removed once a blood spot was observed on the ear of the mouse (see Figure 2.5 and 2.6).

Figure 2-5 Tsetse probe on mouse ear.
Infected tsetse fly separated into single universal tubes was used to probe on a C57Bl/6 mouse anesthetised with hypnorm/hypnovel. Tsetse fly was exposed to mouse ear for approximately 20 mins in a hot box pre-heated to 37 °C. Following tsetse exposure, mice were recovered in conventional cages and kept till the time point needed.

Figure 2-6 Mouse ear post tsetse exposure.
Once tsetse exposure described in figure 2.5 was over, visible blood spots were observed in the ear of C57Bl/6 mouse as indicated by the black arrow.

2.8.2 Ear tissue preparation

The ear samples for flow cytometry were collected by euthanising the mice by a schedule 1 procedure, and ears removed using scissors (FST, Foster city, USA) at the required time points and immersed in PBS. Ears were then transferred to microcentrifuge tubes (Eppendorf, Stevenage, UK) containing 500 µl, 4 mg/ml collagenase IV (Sigma-Aldrich, Dorset, UK), 2 mg/ml hyaluronidase (Sigma-Aldrich, Dorset, UK)) and DNaseI (Sigma-Aldrich, Dorset, UK) in a 37 °C incubator, 1 hr. The digestion was stopped after an hour by the addition of 1 ml Iscove's modified Dulbecco's medium (Sigma-Aldrich, Dorset, UK) to the samples. Samples were then digested using the program B (2 x 30 s spin) of the MACS dissociator (Miltenyi, Surrey, UK). The tissue suspension was then passed through 40 µm cell strainers (BD, Oxford, UK) and cells were processed for fluorescent activated cell sorting (FACS) antibody staining as described in section 2.8.4.

2.8.3 Flow cytometry analysis of samples

Cell preparation for flow cytometry was performed in 12x75 mm, polystyrene tubes (BD Falcon, Oxford, UK). Cell suspensions were incubated in Fc-receptor blocking agent for 15 mins, at 4 °C cells, resuspended in FACS buffer at 400 *g*, 4 °C for 5 mins, and washed twice. Cells were stained with viability dye e450

(eBioscience, Hatfield, UK), antibodies at 1/100 dilution except for MHCII FITC antibody (see Appendix II for list of antibodies), which was stained using a 1/300 dilution. Cells were then resuspended in 200 µl volume FACS buffer containing 2 mM EDTA. Data were acquired using a MACSQuant flow cytometer (Miltenyi) and analysed using FlowJo software (Tree Star Inc., Oregon, USA).

2.9 Neutrophil depletion in vivo

In order to deplete the neutrophils in mice, 1 mg of anti-Ly6G IA8 clone (BioXcell, West Lebanon, USA) was injected IP into mice 16 hrs before the mice were infected. IgG2a isotype controls (BioXcell, West Lebanon, USA) were injected IP into mice as control in all experiments carried out.

2.10 Imaging the ear using the multiphoton microscope

Multiphoton imaging was performed with a Zeiss LSM7 MP system equipped with both a 10^X/0.3 NA air and 20^X/1.0NA water-immersion objective lens (Zeiss) and a tunable titanium/ sapphire (Ti-S) solid-state 2-photon excitation source (Chameleon Ultra II; Coherent, Santa Clara, USA) from 700 nm to 1050 nm. To extend the wavelength, the output of the Ti-S laser passed through an optical parametric oscillator (OPO, Coherent). When pumped by the Ti-S laser at about 800 nm, outputs up to 1200 nm were obtained. It was also possible to use part of the pump wavelength (800 nm) simultaneously with the OPO output. The intensity of the Ti-S beam bypassing the OPO was regulated by an acousto-optical modulator controlled by an imaging software (Zen 2010, Zeiss). The scan head (Zeiss, LSM7 MP) had a maximum rate of 8 frames per second. The multiphoton had five detectors of non-descanned fluorescence available, three multialkali photodiodes and two GaAsP detectos. All imaging was carried out using the 20^X/1.0NA water-immersion objective lens. Image files were analysed, and videos prepared using Volocity (Perkin-Elmer, Coventry, UK).

2.10.1 Mouse preparation

Mice to be used for imaging were anesthetised using freshly prepared hypnorm/hypnovel, injected IP at 10 µl/g of mice, and were anesthetised for a

maximum of 8 hrs and then euthanased using a schedule 1 procedure. The hair on the mouse ear to be imaged was then removed, by applying a hair removal cream (Nair ®) to the mouse hair for 2 mins, and then excess removed with a wet tissue. The mouse was then placed on a heat mat on a custom built imaging platform (Figure 2.7), and a rectal thermometer inserted to maintain the body temperature of the mouse following anaesthesia, and mice was monitored to ensure body temperature remained at 37 °C. The mouse ear was immobilised on the imaging platform using glue (3M Vetbond) and copious amounts of phosphate buffered saline was added to set the glue (see Figure 2.7 for set up requirements).

Figure 2-7 Setup required for imaging mouse ears.
The figure shows the hair cream, vetbond glue, stage with the rectal thermometer, grease and wet tissue required in setting up the mouse.

2.10.2 Injection of mCherry *T. b. brucei*

Prior to setting the mice under the microscope, mouse ear was exposed to infected tsetses as described in section 2.8.1 or 10 µl microvolumes of blood stream form *T. b. brucei* injected intradermally into the ear skin of anesthetised mice. Mice were anesthetised, ears rolled and adhered on to the bottle top cover of their water bottle, using a double-sided adhesive tape, in order to have a good surface area for precise injections. Intradermal injections were carried out using a 0.3 ml insulin syringe (BD, Oxford, UK) containing 10^6 bloodstream form trypanosomes in 10 µl volume which express mCherry. When infected tsetse was used to inoculate trypanosomes, the tsetse was left on anesthetised mouse ear for approximately 30 mins, with the mouse lying on a heat mat to keep its body warm.

2.10.3 Exogenous fluorescent labels

For imaging trypanosome interactions in C57Bl/6 wild type mice i.e. metacyclic *T. b. brucei* in the ear skin following tsetse bites, or via inoculation of blood stream parasites intradermally into the ear skin, mice were prepared as described in section 2.10.1, post tsetse inoculation/injection of 1 x 10^6 blood stream form parasites in the ear skin (section 2.10.2). Blood plasma was labelled by intravenous injection of dextran 70 kD, 50-70 µl of 100 mg.ml^{-1} conjugated with fluorescein isothiocyanate (Sigma-Aldrich, Dorset, UK), or with quantum dots (QTracker, Invitrogen, Paisley, UK) in 30 µl volume using 0.3 ml insulin syringes (BD, Oxford, UK). Mice were then imaged under the multiphoton microscope within 30 mins post intravenous labelling of blood plasma. Exogenous labelling of blood plasma was not carried out on transgenic mice used in this study.

2.10.4 Placing the mouse under the microscope

Following injection of trypanosomes into the ear of mice, a ring of vacuum grease was made using a syringe around the edge of the ear. The ring was then filled with PBS for imaging under the dipping lens of the multiphoton microscope (Figure 2.8).

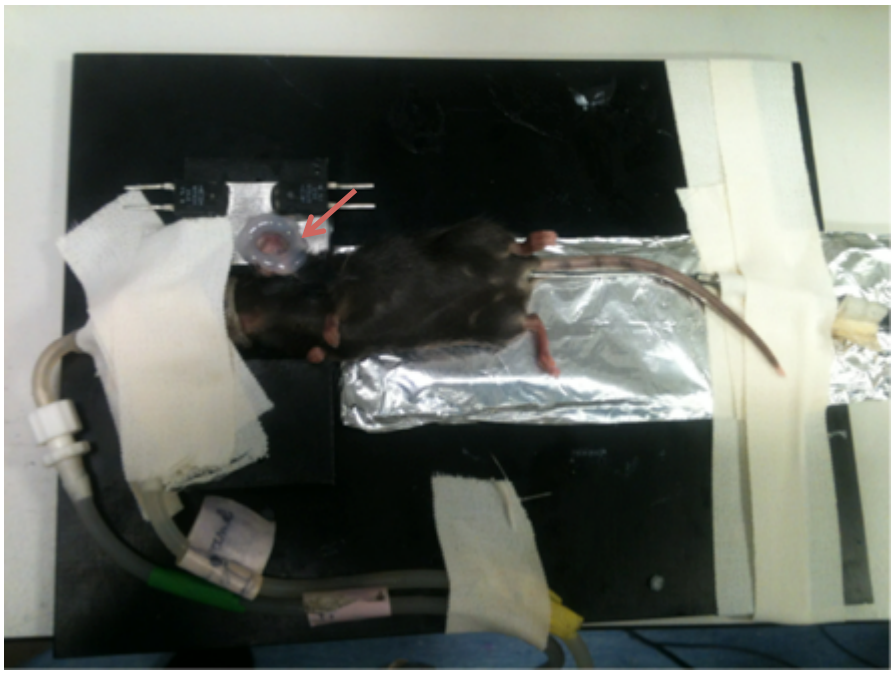

Figure 2-8 A mouse already prepared for imaging.
This is an example of a mouse set up for imaging under the microscope, with a ring of grease made around the ear (red arrow), which served as a well filled with PBS when the dipping lens of the multiphoton laser scanning microscope was used for imaging.

2.11 Hematoxylin and Eosin staining

Whole ears from infected/uninfected mice were removed and fixed in 10% formalin for 24-48 hrs. The samples were then placed into metal moulds and embedded in paraffin wax blocks for sectioning. Tissue sections were cut at 8 µm thick and mounted on Super Frost® Plus slides (VWR, Lutherworth, UK)). Hematoxylin and eosin (H&E) staining was then performed on the slides. Hematoxylin is a dye that forms complexes with metal cations, while eosin is an acidic dye. So when the sections are stained, the there is a reaction between the positively and negatively charged components, resulting in the staining of basophilic cell components such as nucleic acid blue by haematoxylin. While, eosin reacts negatively with the positively charged components acidophilic components of the cell such as the cytoplasm, to give a pink coloration. Prior to H&E staining, sections are deparaffinised and then rehydrated in decreasing ethanol concentrations. The sections were then rinsed in water for 3 min and stained in haematoxylin (Cell Path, Newton, UK) for 5 min. Excess stain was removed under running tap water. Then the slides were immersed in 1% acid alcohol, for few seconds, rinsed in water and placed in Scott's tap water for 30s, followed by another round of rinsing in tap water. Sections were then counter

stained with 1% Eosin Y (Cell Path, Newton, UK) for 2 mins. Excess stain was washed off under running tap water. The stained sections were then dehydrated in a series of increasing ethanol concentrations, and cleared using xylene.

2.12 Transmigration assay

The Bare filter transmigration assay [278] was used to assess the chemotaxis of *T. b. brucei* towards the chemokine CCL21 (R&D, Abingdon, UK)). Transwell transmigration plate (Corning® 3 µm) was pre-incubated for 10 mins, 37 °C with 600 µl CCL 21 (50-500 ng) diluted in chemotaxis buffer (0.5% Bovine serum albumin in Iscove's modified Dulbecco's medium). Following incubation with CCL21, the polycarbonate wells of the transwells were then loaded with 100 µl 1 x 10^5 *T. b. brucei* resuspended in chemotaxis buffer, incubated at 37 °C, 5% CO_2, 7 hrs. After 7 hrs, incubation, cells at the bottom of the well were then counted using a haemocytometer under a light microscope.

3 Development of an experimental tsetse fly infection system

3.1 Introduction

Tsetse flies (male and female) are obligate haematophagous arthropods, and are the only cyclical vector of many trypanosome species in Africa, with both sexes capable of transmitting infection [279]. Sites of maturation of trypanosomes in the tsetse fly vary depending on trypanosome species (Table 3.1). For example, *T. vivax* develops exclusively in the mouthparts, *T. brucei* has its initial establishment in the midgut, matures in the tsetse fly salivary gland, and *T. congolense* also has an initial establishment in the midgut, with further maturation in the mouthparts [280, 281]. Development of trypanosomes within tsetse flies involves a switch from a glycolytic pathway in its mammalian host to a Krebs cycle pathway in the tsetse fly [18, 23, 282]. *T. brucei* when taken up by the tsetse fly are freely motile, and those that survive the immune assault of the tsetse fly, and the new milieu in which they find themselves eventually migrate to the salivary gland. Following migration, the parasites in the salivary gland attach to the microvilli, and multiply as attached epimastigotes. Attachment to the microvilli by the epimastigotes is no longer maintained during differentiation to the mammalian-infective metacyclic trypomastigote, which undergo further metabolic changes and a reacquisition of the metacyclic VSG coat (MVSG) as a pre-adaptation for life in the mammal, before inoculation during a blood feed [18, 20, 283].

Table 3-1 Developmental sites of African trypanosomes in *Glossina spp*.

Species	Trypomastigotes	Epimastigotes	Metacyclics
T. brucei spp.	Midgut	Salivary gland	Salivary glands
T. congolense	Midgut	Proboscis	Proboscis
T. vivax	Proboscis	Proboscis	Proboscis

The duration of trypanosome development in the tsetse fly to achieve mature infections is approximately 27 days in *T. brucei*, 5 days in *T. vivax* and 15 days in *T. congolense* [281]. However, recently it has been shown using fluorescent trypanosomes in a study investigating mating in tsetse flies, that *T. brucei* could appear early in the salivary glands, as early as 13 days post infected feed [284]. Once trypanosomes arrive in the salivary glands, a tsetse fly is capable of

producing hundreds of metacyclic parasites per day and remains infective throughout its life span ~ 3 months [285].

Table 3-2 Factors reported to affect successful trypanosome infection rates in the laboratory using experimentally infected tsetse flies.

Tsetse	Trypanosome
Species/laboratory colony [279]	Species/strain [286]
Fly sex [287-289]	Stage of infection in host [290, 291]
Fly age during first infected feed [292-294]	
Degree of starvation [295]	
Temperature of incubation of pupae [296]	
Temperature of incubation of adult flies [297]	
Host blood for infective feed/maintenance [281, 298, 299]	
Midgut haemolymph lectin activity [286, 300, 301]	
Midgut haemolymph lectin activity [286, 300, 301]	

Natural Infections of tsetse flies with trypanosomes in the field have been investigated. This has been achieved by trapping tsetse flies with nets, dissecting, and examining the gut and mouthparts for parasites. Though this approach is crude and cannot discriminate between trypanosome subspecies e.g. in *T. brucei*, data collected suggests that mature infection in the tsetse salivary gland was generally less than 1% in the field [281, 302]. Various reasons have been attributed for low infection rates of tsetse flies both in the field, and in the laboratory. The factors listed in table 3.2 give a summary of the main challenges encountered in initiating successful experimental trypanosome infections in tsetse flies. These factors influencing transmissibility can collectively be expressed as transmission index (TI) [303, 304]. However, for the purpose of this project, it will be necessary to expand on three key factors that were optimised for successful experimental infections.

The first two are the tsetse fly species, and trypanosome combination. Tsetse fly species and trypanosome combination are important factors that determine the success rate of obtaining mature tsetse fly infections in the laboratory. Taking the tsetse fly species for instance, *G. m. morsitans* has been demonstrated to be susceptible to *T. b. brucei* J10, with 11.3% of flies becoming infected. In contrast, other tsetse fly species, *G. austeni, G. pallidipes* and *G. brevipalpis* were more refractory to infection with the same strain of *T. b. brucei*, with only 1.3% of flies developing mid gut infections [305]. Also, with *T. congolense* stock 1/148, *G. m. morsitans* produced 100% midgut infections, while in *G. p. palpalis*, mature infections where rarely obtained with the same stock [306]. The sex of the tsetse species has also been described to contribute to increase in successful transmission, with male tsetses producing higher infections than females [287-289]. Inherent strain effects also affect maturation in the salivary gland of tsetse flies. For example, there are significant differences in infection between stocks of *T. b. rhodesiense*, which gave much lower infection rates, than *T. b. brucei* in *G. m. morsitans*. Maturation of *T. b. gambiense* is also very rare in any tsetse species, and there could also be great variation between stocks of *T. congolense* in the same tsetse species [286], highlighting that the species of the tsetse fly and the trypanosome strain combination are crucial for successful infections in the laboratory.

Thirdly, the time of feeding the tsetse flies post eclosion with infected blood meal is crucial for obtaining mature infections. This has been described as the teneral phenomenom. Tsetse flies have been demonstrated in various studies to show increased susceptibility to infection when fed within the first 24 hrs post eclosion with an infected blood meal [292, 293, 296, 307, 308], although some workers have argued that this makes little difference to infection rates [295]. The teneral phenomenom has been argued to enhance infections in tsetse flies, because from time points 48 hrs onwards post eclosion age, trypanosome midgut susceptibility decreases due to increasing maturity of the peritrophic matrix, and disappearance of the milk gland protein a constituent of the larval meal remaining in the mid-gut upon eclosion [292].

The ability to achieve experimental infections of tsetse flies in the laboratory is a critical step in enabling investigation of previously uncharted areas in host-trypanosome interactions, using *T. b. brucei* as a model. For the purpose of this project, two strains of *T. b. brucei*, STIB247 and GVR35 [271, 272] were selected because I had access to transgenic parasites for the two strains. Hence, this chapter aims to describe how an experimental tsetse fly infection was set up, used to demonstrate trypanosome kinetics from the skin to the draining lymph node, and establish patency via the ear pinna in mouse models. *G. m. morsitans* were used in combination with tsetse fly transmissible *T. b. brucei* STIB 247 and GVR35 strains.

3.2 Experimental infections of *Glossina* spp.

3.2.1 Tsetse Fly infections

Blood meals for feeds to tsetses were prepared from mice infected with stabilates of *T. b. brucei* STIB247 WT and STIB247 mCherry. At a parasitemia of approximately 1 x 10^8 ml^{-1}, when most (approximately 70%) of the parasites were short stumpy stage as identified by light microscopy, mice were euthanased and blood collected with CBSS/Heparin. The first teneral feed was carried out within 24-48 hrs post eclosion, and repeated twice with an interval of one day between feeds, followed by maintenance on sterile defibrinated horse blood. Following 27 days post exposure, screening was carried out by inducing tsetses to spit on warm glass slides, and examination of extruded saliva by light microscopy for the presence of trypanosomes.

3.2.1.1 *Glossina palpalis* and *G. pallidipes* do not produce mature infections when supplemented with N-acetyl-D-glucosamine

In order to obtain mature infections in the salivary glands of tsetse flies, I attempted to use two different species of tsetse flies combined with a nutritional supplement N-acetyl-D-glucosamine (NAG). NAG is an inhibitor of tsetse midgut lectin, and the decision to add NAG to infected blood was based on previous data indicating tripled infection rates [300, 309]. *G. pallidipes*, and *G. palpalis* were fed with *T. b. brucei* STIB247 WT infected blood meals as

described in section 3.2.1, and modified by addition of sterile 10 mM NAG in order to improve infection rates. Tsetses of each species were given at least two infective feeds through a silicone membrane 24-48 hrs post eclosion [310]. Following infective feeds, tsetse flies were maintained on defibrinated horse blood containing 10 mM NAG, while a batch of 50 flies in a cage for each species of flies were infected without the addition of 10 mM NAG. 200 tsetse flies/species were used for experimental infections with 10 mM NAG.

3.2.1.2 Infection rates and fly survival

After 27 days post infective blood feeds, tsetse flies were separated into single tubes for screening infected flies as described in section 3.2.1. Of the starting batch of tsetses, only 50% of *G. pallidipes* and 55% of *G. palpalis* survived till screening. For control tsetse flies fed with infected blood meals without addition of 10 mM NAG, mortality was at 35-40%. Of all the surviving tsetses, including controls not fed with 10 mM NAG, no positive tsetses with mature salivary gland infections were obtained following saliva screening. These experiments, which included repeated trials by myself and Dr. Marc Ciosi (unpublished), suggested that in our hands *G. pallidipes* and *G. palpalis* were refractory to infection with *T. b. brucei* strain STIB247 so further trials were stopped. This led to the conclusion that independent of NAG or with the addition of NAG I could not achieve mature salivary gland infections using these two species of tsetse flies.

3.2.1.3 Combination of *Glossina* species and strain of *T. b. brucei* are crucial for infection in tsetse flies

Following the unsuccessful attempts at infecting *G. pallidipes* and *G. palpalis,* which I thought would give better infections than *G. m. morsitans,* I switched back to *G. m. morsitans* - a species that has had previous success in the lab with tsetse fly infections, though at very low infection rates. Also, there was the inclusion of two extra strains of *T. b. brucei* (GVR35mCherry and GVR35WT). Blood feeds were prepared in the same manner as previously described, with the exclusion of NAG as a supplement in the infective blood meals. NAG was excluded because of unsuccessful fly infections when the supplement was added, and also previous success we had with *G. m. morsitans* was without the addition of NAG. Tsetse flies were fed within 24-48 hrs post eclosion, and

infected blood meals were repeated twice at one-day intervals, and screened 27 days post feed. Tsetse flies were made to spit on to warm glass slides, and extruded saliva examined under the light microscope (Figure 3.1).

A

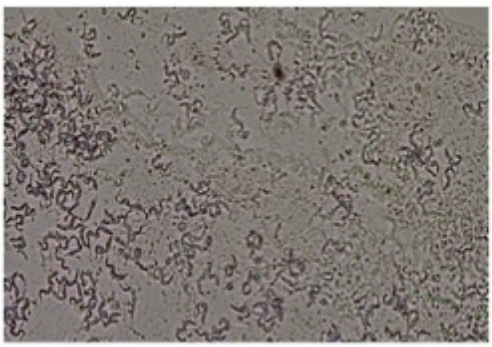

x 40

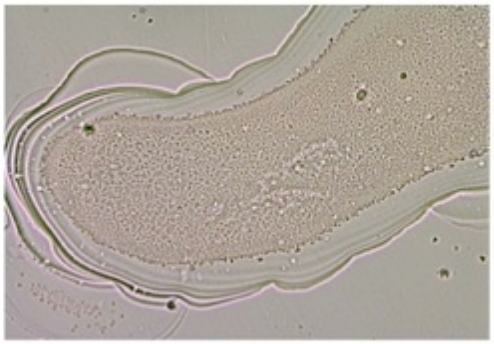

x 40

B

Figure 3-1 Screening for metacyclic trypanosomes.
Tsetse flies fed with infected blood meals, were screened 27 days post feed by probing on warm glass slides for approximately 10 mins on a hot plate pre-heated to 37 °C. Metacyclic trypanosomes can be visualised in (A) positive slide showed *T. b. brucei* in saliva, while (B) showed an example of the saliva of an uninfected tsetse probe lacking trypanosomes.

Of the surviving tsetses, surprisingly a success rate (mature salivary gland infections) of 40% was recorded with *G. m. morsitans* infected with STIB247 WT, 19 and 20% success with STIB247 mCherry and GVR35 mCherry, no success with GVR35 WT (Table 3.3). It is important to mention that in this study, I did not examine the percentage of flies that had mid gut infections of *T. b. brucei*.

Table 3-3 Summary of tsetse fly infections using different strains of *T. b. brucei*

T. b. brucei strain	Number of *G. m. morsitans*	Number of surviving tsetse flies 27 days post infected feed	Percentage of salivary gland infection (%)
247 wild type	200	148	40
247 mCherry	200	145	20
GVR35 mCherry	200	135	19
GVR35 wild type	200	129	0

The mortality rate of *G. m. morsitans* prior to screening for infected tsetse flies was between 25-30%. In subsequent experiments, I obtained similar mortality rates, except when there was a problem during dispatch of the pupae from the

suppliers. Using these approach I achieved mature salivary gland infections of at least 15% consistently during the project. Tsetse fly infections with *T. b. brucei* GVR35 WT was also discontinued.

3.2.1.4 Metacyclic stage *T. b. brucei* express mCherry when passed through tsetse flies

Once tsetses were established to have mature salivary gland infections of *T. b. brucei,* I then examined if the tsetses infected with mCherry expressing parasites maintained fluorescence expression. In order to test retention of fluorescence expression, tsetses were probed on warm slides, and extruded saliva examined by epifluorescence microscopy using a x63 oil immersion objective. I found that all the metacyclics of STIB247 mCherry seen under the bright field objective demonstrated mCherry fluorescence (Figure 3.2). On the other hand, it was observed that approximately 50% of the GVR35mCherry parasites retained fluorescence.

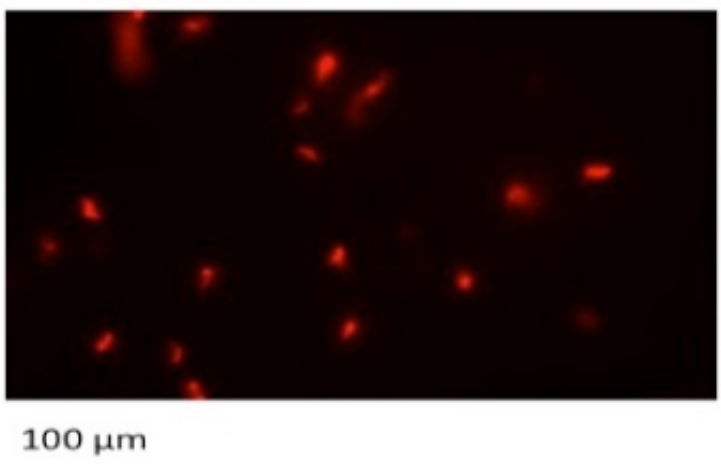

Figure 3-2 mCherry expressing metacyclic *T. b. brucei*.
Infected tsetse flies were made to probe on glass slides, containing 100 µl of warm HMI-9 medium without antibiotics. Immediately tsetses probed, a cover slip was placed on the glass slides and visualised under the microscope within 10-15 mins before the metacyclics die, hence losing mCherry expression. Metacyclic *T. b. brucei* expressing mCherry (STIB247) were visualised in HMI-9 using epi-fluorescence microscopy, excitation/emission at 450nm and 550 nm respectively. Pictures were taken using a x63 oil immersion objective.

In all, the data here demonstrates that *T. b. brucei* STIB247 mCherry passed through tsetses and retained fluorescence expression, and would be suitable for intravital imaging studies. Further trials with GVR35 mCherry were also discontinued, because not all parasites retained fluorescence expression.

3.3 Does infected tsetse bites result in patency via the ear pinna of mice?

In vivo studies in mouse models of African trypanosome infections have been mostly carried out through intraperitoneal and intravenous injections of known numbers of blood stage parasites in order to achieve parasitemia. Hence, it was essential to test the ear pinna if it would be appropriate for establishing patency in mice. For this study, tsetse flies with confirmed *T. b. brucei* 247 wild type infections were used to test if the ear pinna of mice would result in patency in mouse models for subsequent in vivo experiments. Anesthetised mice (C57Bl/6) were placed in a 37 °C incubator and the ventral ear pinna of each mouse was exposed to single tsetse fly probes using diferent tsetse flies per mouse for approximately 20 mins. Following tsetse probe on the ear pinna, confirmed by visible blood spots in the ear, mice were recovered, and blood parasitemia monitored over 25 days by counting using a haemocytometer. It was observed that within 4 days post tsetse exposure, parasites became apparent in the blood (Figure 3.3).

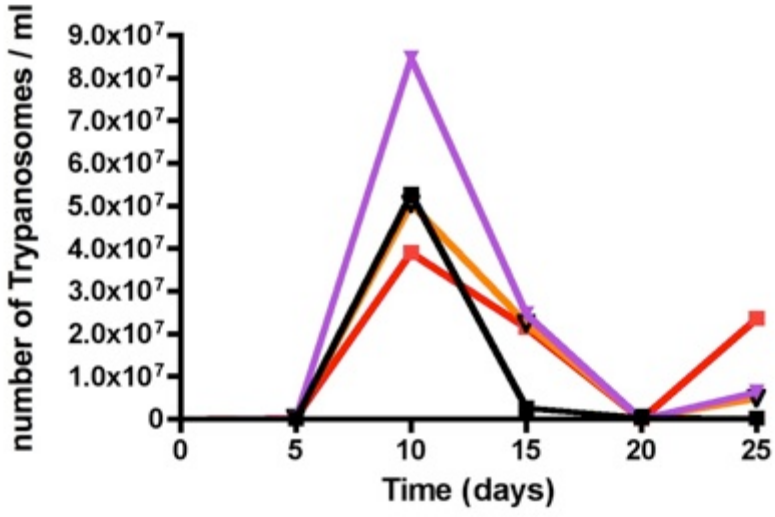

Figure 3-3 Kinetics of parasitemia in C57Bl/6 mice infected with *T. b. brucei* post tsetse exposure to ear pinna of mice.
Five Mice were anesthetised, and ear pinna exposed to infected tsetse probes, that is one tsetse fly per mouse using a separate tsetse fly for each mouse for approximately 20 mins. Following infected tsetse exposure, anesthetised mice were recovered and parasitemia monitored. *T. b. brucei* parasitemia was assessed over 25 days, using the tail prick method to collect 10 µl volume of blood with a Gilson pipette, lysed in equal volume of 0.8% NH_4Cl and parasites counted using a haemocytometer. Lines represent individual mouse, and one mouse was uninfected out of the five

mice post infected tsetse fly exposure. Data shows four infected mice and the kinetics of parasitemia in each mouse.

The data demonstrates that the ear skin is a valid route of infection to analyse early host-parasite interactions following vector-mediated transmission of infection.

3.4 Quantifying *T. b. brucei* in mice

Now that I had established a successful and reproducible model for experimental infection of tsetse flies in the laboratory, I next sought to quantify the number of *T. b. brucei* deposited in the skin and the kinetics of appearance in other tissues. Infected tsetse flies were exposed to the ear pinna of C57Bl/6 mice, ear and lymph node (LN) tissue samples collected at time points 0, 6, 24 and 48 hrs post exposure. Genomic DNA was extracted from tissue and Taqman quantitative PCR (qPCR) was performed on ear and cervical LN samples targeted at PFR2. Ear tissue from tsetse exposed mice for qPCR analysis was standardised by weighing the ears, so approximately 15 mg of ear tissue was used for extraction throughout the studies. For all qPCR analysis, 300 ng of DNA (ear or LN) was used, and copy numbers of PFR2 in total DNA extracted from ear/LN tissue was then computed. Copy numbers of PFR2 were calculated from qPCR values using a standard curve as described in materials and methods (Figure 3.4 & 3.5). Within 0-6 hrs, parasites were already detected in the proximal draining lymph node (dLN) of mice, and the copy numbers of PFR2 in the dLN increased with time peaking at 48 hrs.

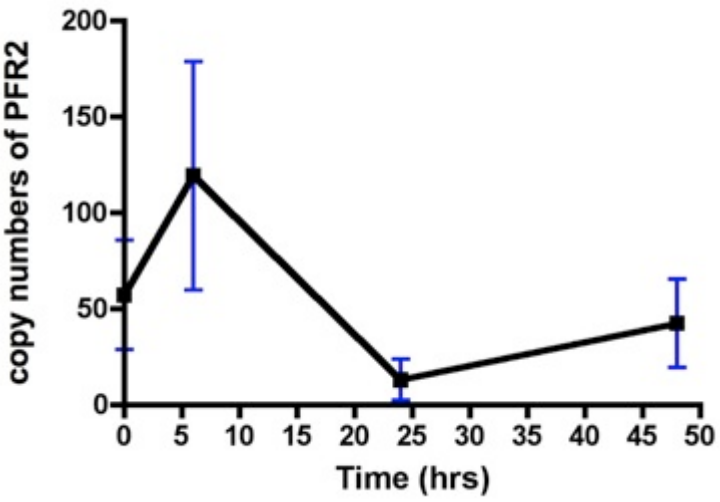

Figure 3-4 *T. b. brucei* kinetics in the ear.
Infected tsetse flies (*T. b. brucei* 247 wild type) in universal bottles with a wire gauze for feeding, were exposed to mice ear pinna (one tsetse fly per mouse) for approximately 20 mins. Mice were euthanased and ears harvested with a scissors. Ear issue was weighed and approximately 15 mg of tissue was used for genomic DNA extraction throughout the studies. QPCR was then performed as described in the materials and methods. A taqman quantitative qPCR approach determined levels of PFR2 gene in tissue and copy number determined against a standard plasmid diluted from 10^6 to 10^1. Data represents 3 mice per group pooled for two independent experiments ± SEM.

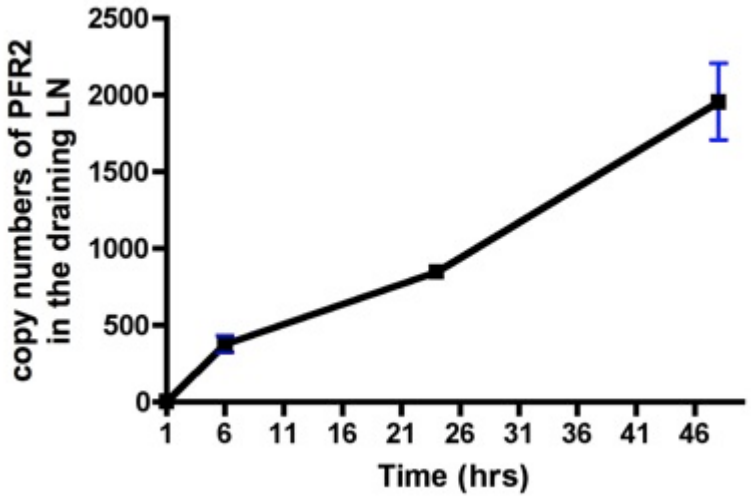

Figure 3-5 *T. b. brucei* kinetics in the draining lymph node.
Infected tsetse flies (*T. b. brucei* 247 wild type) in universal bottles with a wire gauze for feeding, were exposed to mice ear pinna (one tsetse fly per mouse) for approximately 20 mins. Mice were euthanased and cervical LNs draining the inoculation site in the ear were harvested with forceps and placed in PBS prior to genomic DNA extraction. QPCR was then performed as described in the materials and methods. A taqman quantitative qPCR approach determined levels of PFR2 gene in tissue and copy number determined against a standard plasmid diluted from 10^6 to 10^1. Data represents 3 mice per group pooled for one independent experiment ± SEM.

The numbers of *T. b. brucei* parasites detected in the skin within the first 48 hrs was variable across the time points. However 6 hrs post infection, the levels of parasites present in the dLN increased suggesting rapid metastasis of the parasites from the inoculation site. After this period, the level of infection in the dLN continued to increase up to 48 hrs. In all, the data describes the kinetics of egress of parasites from the skin to the dLN.

3.5 General summary

This chapter demonstrated the establishment of a protocol for experimental infections in the tsetse fly, validating the ear pinna of mice as a route of infection, and the use of qPCR to quantify parasites released via exposure of tsetse flies to mice ears. I show that the tsetse fly and trypanosome species, and optimisation of infected blood feeds was crucial for obtaining mature tsetse fly

salivary gland infections. The quantitation of parasites in the skin was a novel attempt describing when parasites appear in the dLN between 0-6 hrs. Also, this study demonstrates that some trypanosomes remain in the skin, and some drained rapidly to the LN. The detection of parasites in the dLN, suggests that the lymphatic vessels were involved in rapid drainage of the parasites from the skin to the blood via the dLN. The mechanisms involved in parasite drainage through the lymphatics, whether it is an active process through its flagella, chemotaxis or through the free flow of the lymph, remain yet unclear. These observations would serve as a good background to investigate the role of the lymphatics in dissemination of African trypanosomes from the skin, which I describe in chapter 5.

3.6 Discussion

3.6.1 Infection rates

Maturation of African trypanosomes from ingestion in a blood meal into infectious stages in the salivary gland of tsetse flies is a tortuous journey for the parasite, both in the field and experimentally in the laboratory. Consequently, a significant outcome of this project was to establish a reliable and reproducible means of infecting tsetse flies experimentally. This experiment was carried out by testing the hypothesis that blocking the trypanocidal effects of the midgut lectins using NAG, could potentially improve the establishment of trypanosomes in the ecto-peritrophic space, and subsequently, maturation in the salivary gland of the tsetse fly [311]. In order to achieve this, I set out to establish infections of tsetse flies using different species (*G. pallidipes, G. m. morsitans* and *G. palpalis*) and the use of a supplement, NAG to enhance infections. The two species of tsetse flies (*G. pallidipes* and *G. palpalis*) previously reported to be permissive to infection [300, 309] were first applied in this study, however successful infections were not achieved.

Previous reports have established that blocking the midgut lectin had resulted in dramatic increases in midgut establishment of *T. brucei* using different tsetse fly and trypanosome combinations [286, 311]. The tsetse species (*G. pallidipes* and *G. palpalis*) that were used, have previously been infected with *T. brucei* in

other studies so were clearly susceptible [312]. The results achieved suggests that in vivo blocking of the midgut lectin using NAG did not result in mature infections in *G. pallidipes* and *G. palpalis*. Another lectin found in the haemolymph when blocked by α-D-melibiose, in addition to inhibiting the midgut lectin by NAG has been demonstrated to enhance maturation rates in male tsetse flies [288]. However, addition of α-D-melibiose and NAG was not considered in this study due to time constraints for optimisation studies. Of note in this study was also the high mortality rate reported here when NAG was added to infected blood feeds. High mortality rates observed were consistent with what has been reported by other workers that have used NAG in optimising experimental infections in tsetse flies. Mortality of tsetses have been reported to begin from the first day post tsetse feed, and was not associated to the sex of the tsetse fly, similar to the observations here [300].

Following the unsuccessful attempts at obtaining mature salivary gland infections using *G. pallidipes* and *G. palpalis* in combination with the addition of NAG to the infected blood meal, I switched to optimising a different tsetse species, *G. m. morsitans* as the host. Infected blood feeds were optimised to contain sufficient numbers of the stumpy stage of the parasite, which is pre-adapted for life in the tsetse midgut and ready for transmission. Differentiation of the slender form parasites to stumpies is an irreversible cell cycle arrest involving morphological and metabolic changes to the life of the parasite [313]. Stumpy form parasites are more tolerant to stresses of the tsetse fly uptake, more sensitive to environmental cues such as *cis*-aconitate [314, 315], and it is thought that they are the only ones capable of differentiation to procyclic forms in the midgut of the tsetse fly [316], although other reports suggests that slender form parasites may be capable of doing same [317]. The tsetse fly strain used for optimisation, *G. m. morsitans* has been reported to have a weak barrier to infection with *T. b. brucei* strain J10 [279], and has previously been used successfully in the lab, albeit with a low rate of mature infection. Optimisation of infected blood feeds involved ensuring that at least 70% of the parasites in the blood were at the stumpy stage, which were identified visually based on their morphology and prepared the infected feed with warm defibrinated horse blood. To my surprise, the first attempt at achieving mature infections using the new strategy described gave over 40% infection success with *T. b. brucei* STIB247

and less mortality was observed compared to *G. pallidipes* or *G. palpalis*. This affirmed previous reports that the tsetse and trypanosome strain combination was essential for mature salivary gland infections. In addition to the tsetse species/trypanosome strain combination used for infection, some workers have used different blood meal sources e.g. goat and pig blood, and reported higher midgut infectivity, compared with tsetse flies fed on other mammalian blood [298, 299]. Although there has been a suggested link between blood source and tsetse infections, only defibrinated horse blood has been used throughout to prepare blood meals in this study. This produced comparable rates of infection in *G. m. morsitans* to those obtained using other blood meal sources for infections [298]. Host blood meal contains species-specific factors that could improve the chances of obtaining mature infections. For example, it has been demonstrated that blood from goats, pigs, and rats enhance infections in most tsetse-trypanosome combinations, whereas, blood from cattle and wild bovidae diminishes infections [299]. Goat blood in particular has been shown to consistently enhance infections better in tsetse flies than blood from other animals, and these results have been repeatable even at lower parasitaemias, and lower incubation temperatures [299].

Another important observation in this study was that not all *T. b. brucei* GVR35 mCherry screened from infected tsetse flies retained expression of mCherry, compared to 100% transmission stability of the mCherry construct when *T. b. brucei* 247 mCherry was passed through tsetse flies. This raised the possibility that it was likely that some form of recombination event was occurring in the tsetse fly. Migration of *T. brucei* from the midgut to the salivary gland is a tortuous process in which the parasite encounters pronounced bottlenecks, which creates the opportunity for genetic exchange between parasites [318]. Mating or genetic exchange between the parasites has been demonstrated to occur in the salivary gland of the tsetse using fluorescent trypanosomes [284]. In *T. brucei* fly transmission, interclonal mating has been identified to occur, which makes it highly likely that the parasite has been genetically altered. Also, intraclonal mating in *T. brucei* and *T. congolense* has also been described to result in recombination events in the parasite [319]. The presence of recombination events in the fly suggests a likely reason why some of the *T. b.*

brucei GVR35mCherry parasites had lost the mCherry construct during development in the tsetse fly.

The data presented here did not attempt to investigate midgut infections, the role of tsetse fly sex in obtaining mature infections, although some studies have suggested there may be a sex bias in infections. These studies generally seem to suggest that male tsetse flies give higher salivary gland infections compared to females, although females survive longer [288, 300]. However, no differences were observed in midgut infections in the tsetse flies when different trypanosomes species (*T. b. brucei*, *T. congolense* and *T. rhodesiense*) were compared in both male and female tsetse flies [288]. These observations supported the view that midgut infection in the tsetse fly is a maternally inherited trait, while salivary gland infections is sex linked trait [320]. Susceptibility of *G. m. morsitans* to infection in this study was variable, and the success reported here for *T. b. brucei* is considerably higher to rates of infection observed in the closely related human pathogenic *T. b. rhodesiense* strains [286].

3.6.2 The ear pinna is a valid route of infection

Following the successful experimental infection of tsetse flies, I next sought to determine if infected tsetse fly feeds on the ear pinna of mice was sufficient to allow the establishment of blood parasitemia. The ear pinna was chosen as the site of inoculation because of its convenience for examining the behaviour of parasites [321-323], host immune cells in the skin [165, 324], and it is a well established technique within our group, that is an amenable site for intravital imaging studies [325]. In addition to its accessibility for intravital imaging studies, this would also serve as an accessible tissue site to investigate cellular recruitment to the skin post tsetse exposure, as already demonstrated in *Leishmania* following sand fly bites [166, 326].

Previous reports on innate and adaptive immune responses during trypanosome infections in mice have been focussed on intravenous or intraperitoneal routes of infection with bloodstream form *T. b. brucei* [132, 327]. However, natural infections occur through the deposition of infective metacyclic stage trypanosomes into the dermis of the skin, after a tsetse fly feed. The feed by a

tsetse fly, injects the parasite along with the saliva. The saliva contains glycosylated proteins, which possess immunomodulatory and enzymatic functions [328-330]. The saliva of the tsetse fly has also been indicated to contribute to the onset of infections in mouse models, suggesting that they contain substances that could contribute to virulence in vivo [330]. These findings are not unique to the tsetse fly, as other vector delivered parasites such as *Leishmania*, have salivary components that modulate transmission dynamics [331, 332]. The outcome of the importance of using the vector for in vivo studies as demonstrated in other parasitic infections such as malaria and cutaneous leishmaniasis necessitated the use of the tsetse fly for this study.

Most studies that have attempted to use tsetse flies for infection have focussed on the flank of mammals for feeds because of the preponderance of blood vessels, and a larger surface area [13, 191, 333, 334]. So the attempt here at using the ear pinna for trypanosome infections was novel, providing a limited surface area, fewer blood vessels, and needed to be tested to determine whether it was sufficient to result in patency in mice. When tsetse flies were exposed to the ear pinna, they were unable to obtain a blood feed as they would on other parts of the mice. Instead, most of the tsetse flies used in this study probed on ear pinna of mice making visible blood spots, or blood pools. The results here demonstrate that probing of the ear pinna post tsetse exposure was sufficient to cause patency, and this confirms previous observations that probing and not necessarily a blood feed was sufficient to establish trypanosome infection in mammals [335]. Mice lacking parasitemia following probes by infected tsetse flies were suspected to occur as a result of unsuccessful tsetse exposures. Both sexes of tsetse flies (male and female) were also established to be capable of transmitting *T. b. brucei*.

The principal conclusion from this part of my study was that tsetse fly probes in the ear pinna of mice, was sufficient to initiate infection despite inability to achieve blood feeds. The findings here was important in order to determine if the ear pinna was a valid route of infection that could be used to characterise immune responses/parasite behaviour by conventional techniques and intravital imaging through the bite of the tsetse fly. The study demonstrates that the ear skin was suitable for establishment and dissemination of parasites into the blood.

3.6.3 *T. b. brucei* kinetics

To my knowledge, the dose of *T. brucei spp.* delivered by tsetse fly vector to the mammalian skin has not been quantified. Interestingly, studies on African trypanosomes have generally focussed on injecting sufficient numbers of parasites to generate patency in their hosts, rather than the physiological relevance of this process. Therefore, in addition to the approximate numbers of trypanosomes used, the use of blood stages rather than transmission stages of parasite, the route of inoculation, as well as the loss of impact of the vector bite makes it difficult to fully appreciate the host/parasite response in infection. In particular, the earliest events that occur within the first few hours of inoculation into the skin by the tsetse fly, and parasite dissemination systemically has yet to be quantified in vivo.

In order to quantify the parasites in vivo, the paraflaggellar rod 2 (PFR2) gene of *T. b. brucei* was an attractive target because it is highly conserved and expressed throughout the life cycle in *T. brucei* and *T. cruzi* [336]. Furthermore, PFR2 has been successfully applied to quantify trypanosomes in mouse models, for example in stage 2 HAT [252], and comparing chemotherapy of *T. b. brucei* GVR35 sensitive and drug resistant strains (Amy Jones, University of Glasgow thesis 2011). Therefore, I optimised a taqman qPCR approach targeting PFR2 using an oligonucleotide probe designed to a section of PFR2 to estimate the copy numbers of parasites following a single tsetse fly probe per mouse over the course of 48 hrs at the bite site and the dLN. At the bite site there was variability within tissues in the copy numbers of parasites recovered back immediately after a tsetse probe. This is likely due to the different probing behaviour of tsetse flies, which would result in injection of different sizes of parasite inoculum. Also, the numbers of metacyclic *T. b. brucei* produced in the salivary glands of tsetse flies varies from one tsetse fly to another. In addition, PCR studies of parasites in the blood at the respective time points was not investigated, so there could be the likelihood of parasites entering the blood stream via routes excluding the LN. Within 0-6 hrs post infected tsetse exposure, parasites were detected in the dLN, and some were still detected at the bite site. The migration of parasites towards the dLN increases over the course of time, with more parasites detected in the dLN by 48 hrs. It was observed that

some of the parasites remained at the bite site and could have differentiated to long slender forms, which are capable of proliferation [14]. Although there is no direct evidence for differentiation of metacyclic *T. b. brucei* in this chapter, *P. berghei* and *P. yoelii* have been demonstrated to differentiate from sporozoites to exoerythrocytic forms in the skin, and may remain in the skin and serve as a secondary reservoir of infective merozoites [183, 184].

Quantification of intracellular parasites such as *Leishmania* and *Plasmodium* has given us an understanding of how the inocula injected into the skin by the their vectors- sand fly and mosquito, contribute to pathogenesis [183, 337]. In *Leishmania* for instance, real time PCR approach has demonstrated that between 10-100,000 parasites could be deposited in the skin following a sand fly probe [257]. The transmission efficiency of sand flies during a probe has been directly linked to the infection levels in the midgut. This simply means that a heavily infected sand fly would deposit large inocula during a feed into the skin of its host [257]. A direct correlation between infection burden in the tsetse fly salivary gland and numbers of metacyclic *T. b. brucei* deposited in the skin has not been established in this study. But it may be appropriate to speculate that variation in numbers of parasites deposited in the dermis through the probe of a tsetse fly could also be linked to the degree of parasitosis in the tsetse salivary gland. The variability in the numbers of parasites transmitted following tsetse fly bites further underscores the need to apply the natural route of infection in understanding the earliest events in pathogenesis.

Here, I have also been able to provide direct evidence that parasites go into the LN via which they may enter into the bloodstream from the skin post tsetse exposure. In *Plasmodium berghei* sporozoites ~30% of the parasites take the lymphatic route and arrive at the first draining LN, where most of the parasites die [183]. In African trypanosomes, most of the parasites that find their way into the LN do not die and have been suggested to replicate in the paracortex of the LN based on intravital imaging studies within our group (unpublished). The detection of trypanosomes very early in the dLN post infected tsetse exposure strongly supports the idea that parasites enter the LN via the lymphatics as shown previously [13, 191]. These findings are fundamental for understanding the earliest events that occur following inoculation of metacyclic *T. b. brucei* in the skin, and might apply to other African trypanosomes.

4 Characterising the skin immune response to the bite of trypanosome infected tsetse fly

4.1 Introduction

Many of the most serious parasitic infectious diseases in the world, ranging from malaria to more neglected tropical parasitic diseases such as filariasis, trypanosomiasis, leishmaniasis, and onchocerciasis, are transmitted by arthropod vector bites during blood feeds [338]. In as much as we know that the transmission of these parasites rely on the vector, most studies investigating the dynamics of parasite transmission and immunity in mammalian hosts have failed to consider the contribution of the vector. Most studies have assumed that parasites transmitted by injection through a syringe adequately reflect vector transmission. However, recent studies have made it very clear that these approaches do not mimic what happens in reality, raising doubts about the applicability of data obtained from such approaches in fully appreciating the host response to infection [165, 339].

Arthropod saliva has been demonstrated to enhance infectivity for several pathogens in their mammalian hosts, for example, sand fly transmission of *Leishmania*, tick transmission of viruses, mosquito transmission of viruses and *Plasmodium* sporozoites [338, 340, 341]. The saliva of arthropod vectors such as mosquito, ticks, tsetse fly and sand fly, has been shown to contain a large number of substances that have pharmacologically important effects on the host, such as anti-haemostatic, vasodilatory, anti-coagulant and anti-inflammatory or immunosuppressive activity [342-351]. Immunologically, the arthropod saliva also has profound consequences on the immune system of its host and on parasite dissemination from the bite site. In *Leishmania spp*, the sand fly vector has been used to demonstrate the early inflammatory processes that occur following inoculation in the ear of mice models. Through sand fly transmission of *Leishmania* it was revealed that the early recruitment of neutrophils to the inoculation site resulted in phagocytosis of parasites, which were still viable, hence transported into macrophages, promoting disease establishment [165, 352]. The saliva of sand flies has also been demonstrated to inhibit T cell activation, macrophage activation, IFN-γ, IL-12, and iNOS production [353-355]. Studies of Chikungunya virus transmission revealed that mosquito bites skewed the host immune response towards a Th2 phenotype through a significant upregulation of IL-4, possibly due to the contribution of

mosquito saliva. In contrast, needle injected Chikungunya virus induced a Th1 immune response as evidenced by the significant upregulation of IFN-γ and IL-2, while Th2 cytokines such as IL-4 and IL-10 did not show significant changes in transcript levels [356]. These findings further emphasised differences in the immune responses elicited between mosquito and needle inoculations. In addition to the contribution of the arthropod saliva to the immune response, mechanical damage from the bite of arthropods or injection via a needle will induce a response from skin-resident immune cells such as Langerhans cells in the epidermis, αß T cells, γδ T cells, mast cells, natural killer cells, macrophages and dendritic cells in the dermis. The mechanical damage in the skin produces endogenous signals that trigger an immune response in order to sterilise and also repair the damaged tissue [357].

In studies carried out using mouse models of trypanosome transmission in the presence or absence of tsetse saliva via needle injections, it was demonstrated that the absence of saliva delayed the progress of parasites into the blood stream and that the saliva biases the host immune response towards a Th2 phenotype, through the production of cytokines IL-4 and IL-5 [330]. What we know about how African trypanosomes interact with its host has been mostly based on intravenous or intraperitoneal injections of bloodstream form parasites into mammals [358-362], which clearly does not represent what happens in nature via the tsetse fly bite. A recent study has used modern analytical tools to analyse the events occurring in mammals in response to African trypanosome infection via the skin, and this was performed using intradermal needle injection of known numbers of bloodstream form parasites. The study demonstrated using B cell deficient mice, that low numbers of *T. b. brucei* and *T. congolense* parasites injected intradermally could be eliminated by the innate immune response [327]. The authors showed that B cell deficient mice exhibited the same degree of resistance when compared to wild type mice injected with the same number of parasites. In contrast, iNOS$^{-/-}$ and wild type mice treated with antibody to TNF-α were more susceptible to infection. This study clearly outlined a role for the innate immune response in controlling low parasite infections. As informative as the study was, it still missed a key part of the parasite's life cycle, which is the metacyclic stage present in the salivary gland

of the tsetse, as well as the contribution of the tsetse fly bite and saliva to the host immune response, and parasite dissemination.

Hence, this study arose out of a need to find answers to some of the questions unanswered regarding the earliest events post tsetse fly bite in the skin of mammals. These questions include, what are the kinetics of earliest events at the bite site following infected and uninfected tsetse fly exposure, does the presence of parasites have an effect on the magnitude of the immune response, what interactions occur between African trypanosomes and immune cells, and what functional role(s) do the cells recruited following inflammation play in pathogenesis. To address these questions, I hypothesised that infections using trypanosome infected tsetse fly would elicit the rapid infiltration of immune cells, and manipulating these immune cells would be important in limiting parasite establishment, and dissemination via the skin into the blood stream. Therefore, this chapter aims to fill in some significant gaps in our knowledge by incorporating the contribution of the tsetse fly in studying the earliest inflammatory processes and how this may relate to parasite dissemination into the bloodstream.

4.2 Kinetics of cellular recruitment in the skin following tsetse fly bite

In order to address the questions mentioned above, a flow cytometry analysis was undertaken of the cells recruited to the skin of *T. b. brucei* infected and uninfected tsetse exposed mice. Prior to characterising the immune cells by flow cytometry, I carried out histological analysis of mice ear samples that had been exposed to tsetse flies to assess whether host cells were recruited to the bite site post infected and uninfected tsetse exposure. For the study in this chapter, all infected tsetses refer to flies infected with *T. b. brucei* 247 wild type.

4.2.1 Cells were recruited to the bite site following tsetse exposure

Infected and uninfected tsetses were exposed to mice ears for 6 hrs, ears were collected and processed as described in materials and methods for Hematoxylin

and Eosin staining (H&E). H&E staining revealed the bite site, and the influx of cells post tsetse exposure. Cells were shown to infiltrate the lesion post-bite in both infected and uninfected ear samples, and appeared to congregate towards the dermal papillary lesion (Figure 4.1).

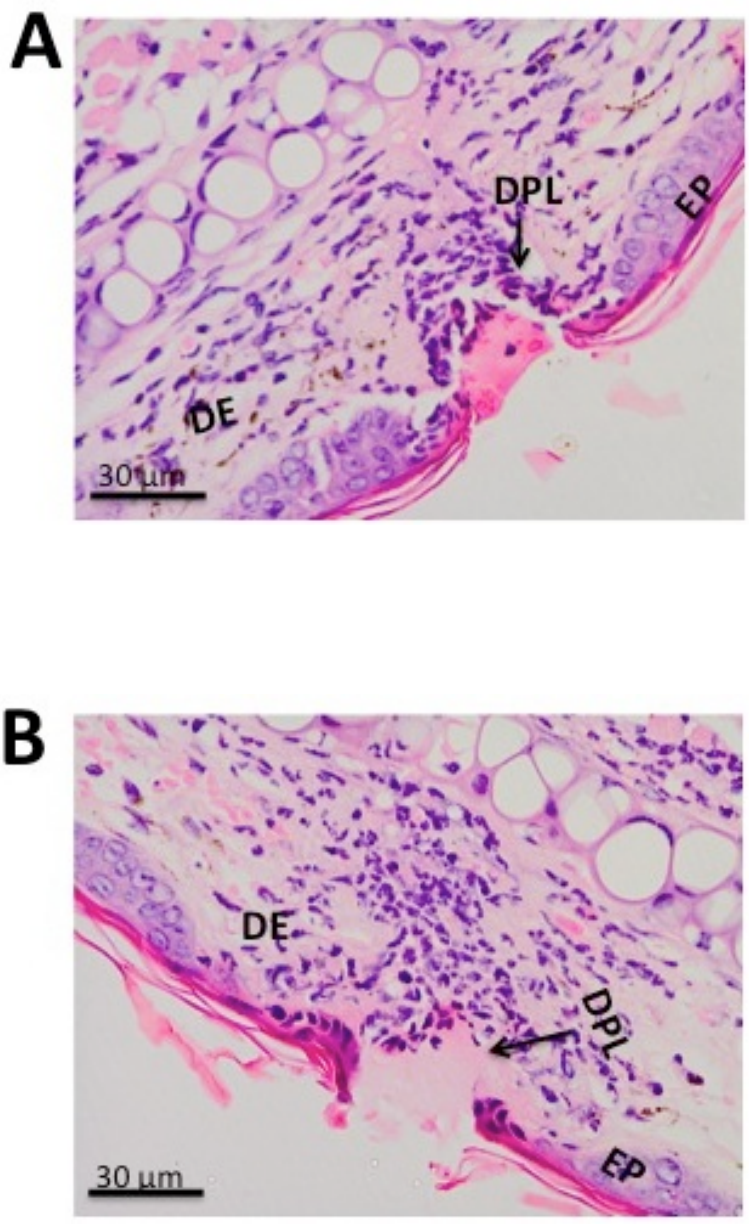

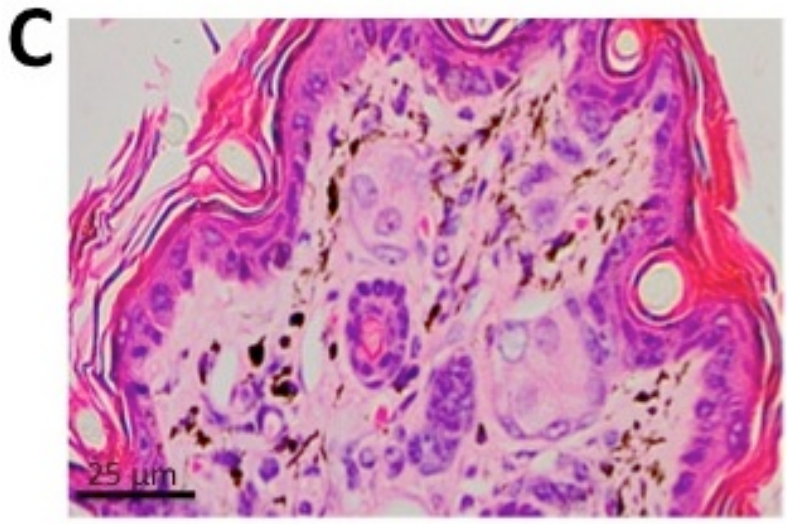

Figure 4-1 Infected and uninfected tsetse exposure caused recruitment of cells
Mice were anesthetised, ears were exposed to feeding by infected and uninfected tsetses, ears harvested 6 hrs post tsetse exposure and stained with hematoxylin and eosin for morphological examination, as described in materials and methods. (A) Post exposure to infected tsetse, (B) post exposure to uninfected tsetse, (C) untreated ear control. Images were acquired using x40 magnification on a Zeiss Axiostar Plus microscope fitted with AxioVision software; arrow points to the dermal papillary lesion (DPL) in response to tsetse fly bites, DE = dermis, EP = epidermis.

4.2.2 Flow cytometry for identification of recruited leukocytes

Once it was established by H&E that cells were indeed recruited to the tsetse bite site, I next sought to characterise the phenotype of cells that were recruited. In order to characterise the cells recruited, a flow cytometry approach was applied. This was carried out by processing tissues to isolate single-cell suspensions, by digestion of ear tissue, and staining with fluorescent antibodies. Once the process of isolation of cells from tissues was optimised for concentration of enzymes (Hyaluronidase and collagenase IV) with minimal damage to isolated cells, a gating strategy for identification of leukocytes was set up. The approach used here first involved drawing a gate on all cells using the forward scatter and side scatter plot, followed by the use of a live dead stain for exclusion of dead cells. For standardisation of total cell numbers in tissue samples, isolated cell suspensions were resuspended in 200 µl FACS buffer, and 100 µl volume taken up and analysed by the Miltenyi seven colour flow cytometry machine (MACSQuant analyzer) with automatic calibration features. The MACSQuant has an automated cell counter software, so by drawing a gate on viable cells as described below (Figure 4.2), the absolute number of cells was automatically calculated by the flow cytometry software. The number of cells

counted in 100 µl volume by the MACSQuant was then multiplied by two to get the total number of viable cells per ear tissue. For analysis of cell numbers in the refined populations of cells analysed, the same approach was applied by drawing a gate on the subset of cells I was interested in using the MACSQuant analyser. Leukocytes were gated by use of the CD45 marker. The $CD45^{+}$ cell population was subsequently refined into leukocytes such as neutrophils, macrophages and monocytes using the appropriate lineage markers as described in Figure 4.2. Figure 4.2 shows that after tsetse exposure to a single mouse, approximately 3.73% of the viable cells expressed the CD45 marker. Further refinement of the $CD45^{+}$ viable cells revealed that neutrophils constituted 27.4% of the cell type present in the skin post tsetse exposure. The gating strategy described in figure 4.2 was then applied throughout this study for characterisation of leukocytes post tsetse exposure in all cases. The percentage of $CD45^{hi}$ cells observed here was lower than what I expected following tsetse exposure. I anticipated a much more significant recruitment of cells to the bite site, this observation suggested that the tsetse bites did not induce excessive inflammation to the inoculation site.

For this analysis and others, it should be noted that untreated controls refer to ear or lymph node samples not exposed to tsetses (naïve controls), while infected tsetse samples refers to mice tissues exposed to tsetses carrying *T. b. brucei* 247 wild type strain infections, and uninfected tsetse samples refers to mice tissue exposed to tsetses not infected with *T. b. brucei* 247.

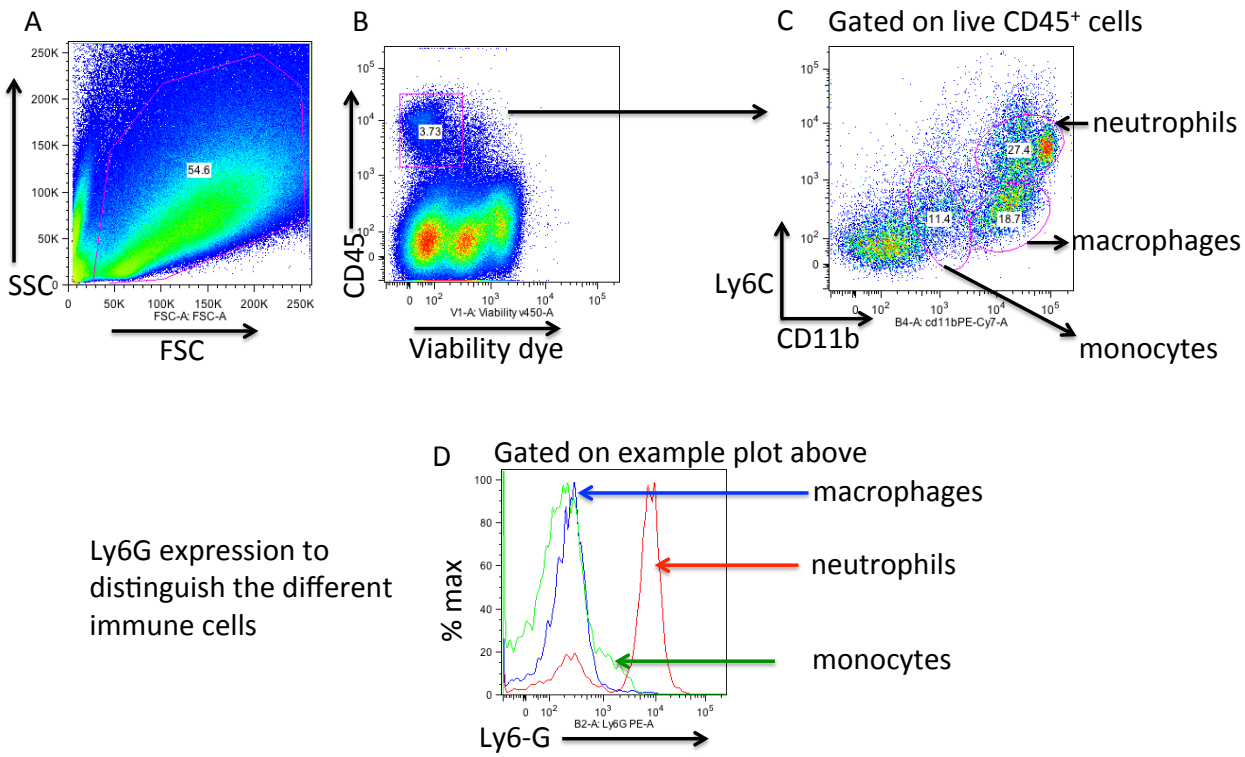

Figure 4-2 Example plots of the flow cytometry-gating strategy for identification of leukocytes in the ear skin.
Following tsetse exposure to mice ears, ears were harvested and samples were processed for isolation of single-cells and then stained with appropriate antibodies as described in the materials and methods. (A) Intact cells were identified based on size and granularity, (B) followed by selecting viable cells with a viability dye, and then identification of leukocytes based on $CD45^{hi}$ expression. (C) Identification of the different leukocyte populations was performed using $CD11b^{+}$ and $Ly6C^{+}$ expression to distinguish the three populations: neutrophils ($CD11b^{+}Ly6C^{hi}$), macrophages ($CD11b^{+}Ly6C^{int}$) and monocytes ($CD11b^{+}Ly6C^{lo}$). (D) The expression levels of different populations could also be distinguished using a histogram to show Ly6G purity levels. Data is representative of 3 mice exposed to tsetse bites.

4.2.3 $CD45^{+}$ cells were identified post tsetse exposure by flow cytometry

Inflammation is a fundamental process in mammals for removal of substances that are foreign or injurious to its host. A key event in the inflammatory response is the localised recruitment of leukocyte subsets. CD45 is a pan-leukocyte marker expressed by all bone marrow derived cells except erythrocytes and platelets [363]. Hence, to allow for identification and quantification of leukocytes by flow cytometry, CD45 expression was used for phenotypic analysis. There was recruitment of cells to the inoculation site post tsetse exposure (Figure 4.3). However, no significant differences in $CD45^{+}$ cells

recruited between infected and uninfected tsetse exposed samples (P>0.05; One way ANOVA with Tukey's test). Tsetse exposed samples showed that there was recruitment of cells to the bite site.

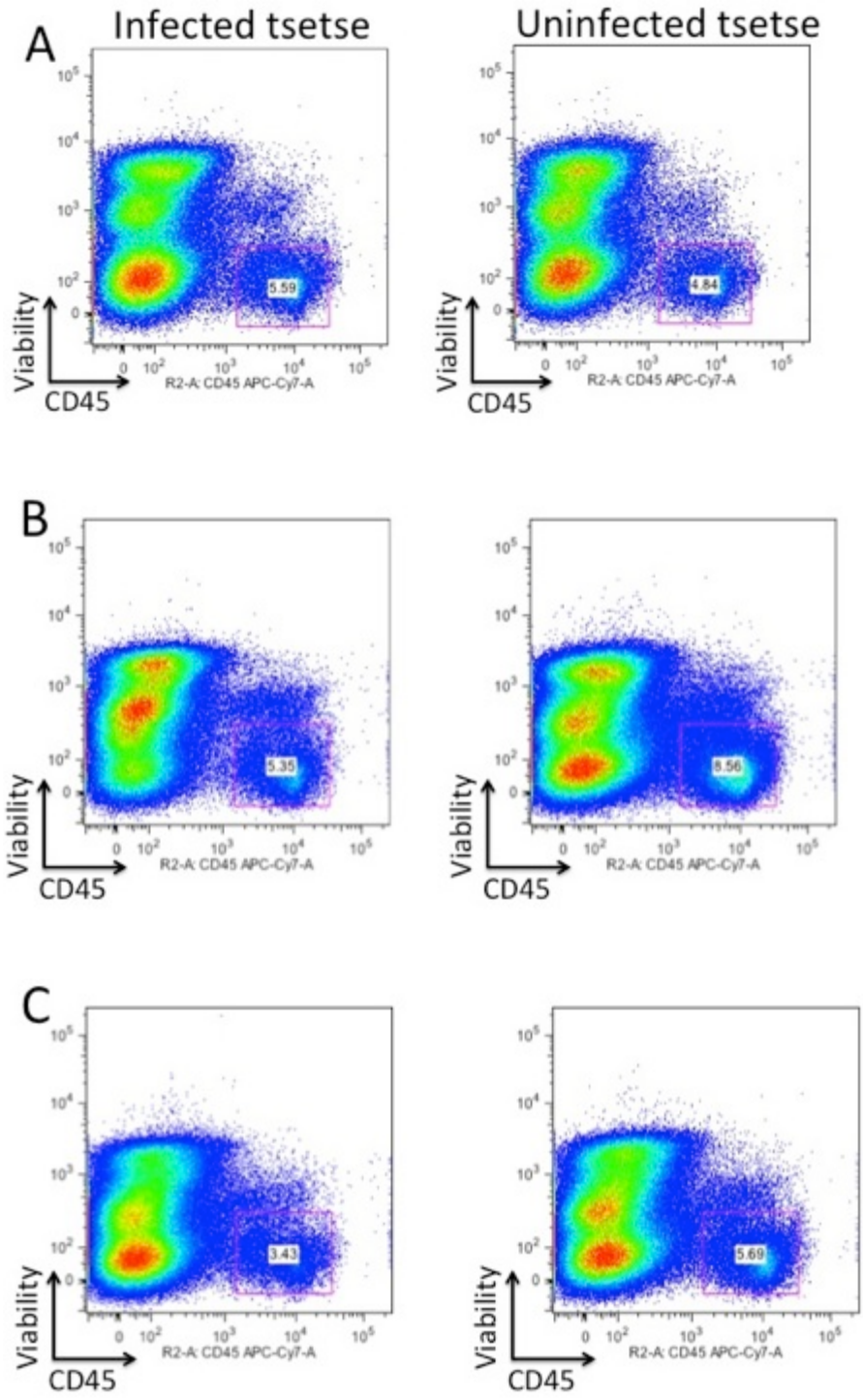

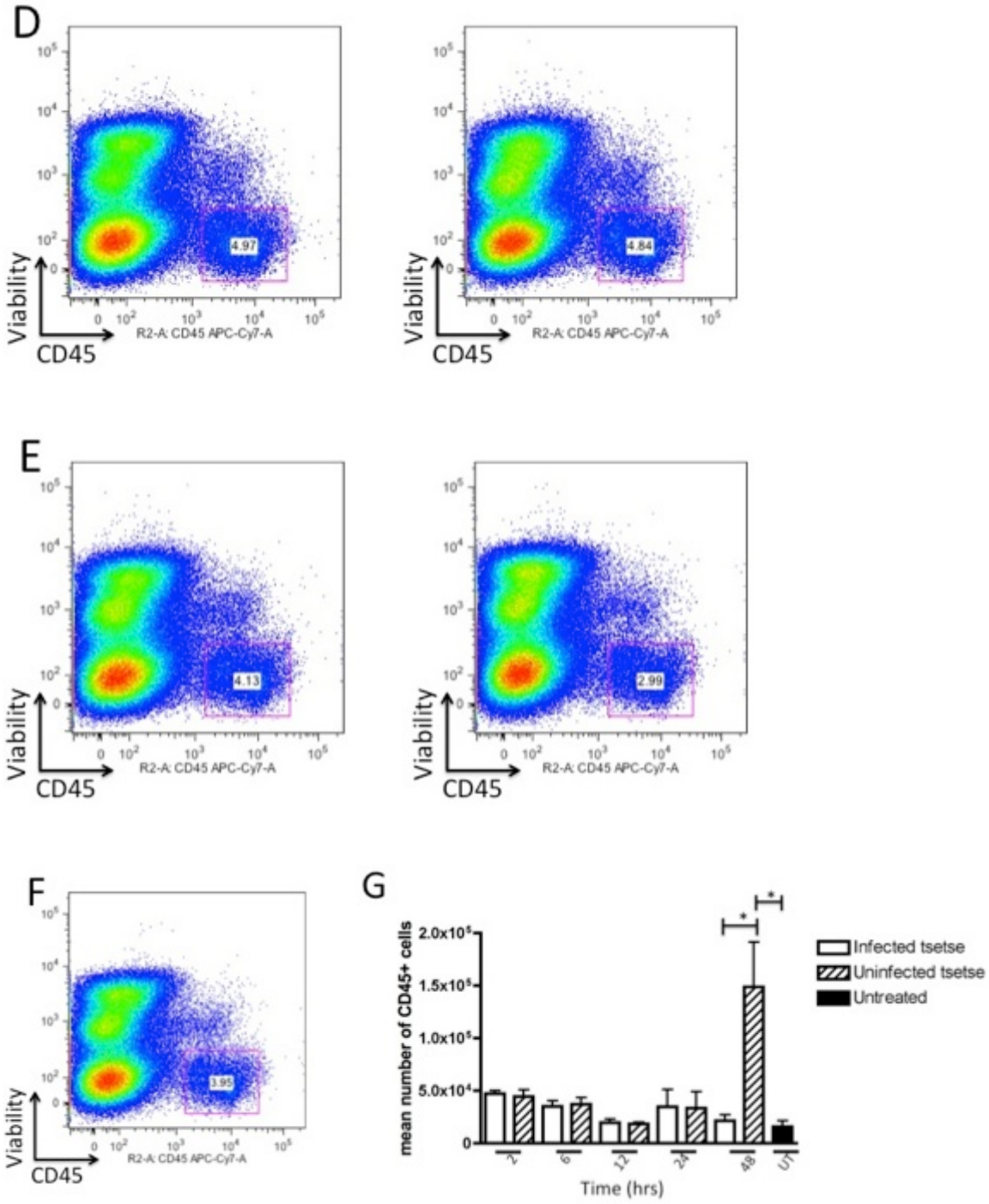

Figure 4-3 Total leukocyte populations in the ear skin post tsetse exposure.
Mice were anesthetised and ears exposed to infected/uninfected tsetse bites, and ears harvested at the respective time points. Following ear sample processing to isolate single-cell suspensions post tsetse exposure, processed samples were resuspended in 200 µl volumes FACS buffer. For flow cytometry analysis, 100 µl of cell suspension was analysed on the MACSQuant analyser, and the total number of cells present in the sample tube was estimated by Miltenyi software, and number obtained multiplied by two to calculate the total number of cells in the ear tissue. Total absolute numbers of $CD45^+$ cells present over 48 hrs were quantified and plotted. Example plots at the time points analysed for infected and uninfected tsetse samples are presented: infected and uninfected tsetse ears at 2 hrs (A), 6 hrs (B), 12 hrs (C), 24 hrs (D), 48 hrs (E), and untreated naïve ear control (F), respectively. (G) Line graph depicts the absolute numbers of $CD45^+$ cells in the skin post tsetse exposure, ± SEM. Data represents pooled data from 3 mice per group from 3 independent experiments. No difference was observed between uninfected and infected tsetse samples ($P>0.05$; not significant, ns) carried out using a One-way ANOVA with Tukey's post test.

Leukocyte subtypes accumulating post tsetse exposure were further refined based on expression of neutrophil, macrophage, and monocyte markers in the subsequent sections.

4.2.4 Neutrophils were recruited within the first 24 hrs post tsetse exposure

Neutrophils are rapidly recruited through blood vessels to sites of inflammation or sterile injury, through a series of steps tightly regulated by integrins [364]. They are usually the first immune cells that extravasate from the blood to tissue sites in inflammation. Hence, the kinetics of neutrophil influx post infected and uninfected tsetse exposure to mice ears was characterised. Following the identification of $CD45^+$ cells in the skin, neutrophils were analysed through their combined expression of $CD11b^+$ and $Ly6G^{hi}$. Consistent with their role as early responders at sites of tissue damage, neutrophils were detected in the ear pinna within the first 2 hrs in both infected and uninfected tsetse samples. Neutrophil recruitment at the time points analysed (2, 6, 12 and 24 hrs) was compared between infected and uninfected tsetse samples, and was found to be statistically insignificant ($P>0.05$; One way ANOVA with Tukey's post test). However, comparison of either infected or uninfected tsetse exposed samples with untreated controls gave statistically significant results ($P<0.05$; One way ANOVA with Tukey's post test) for the time points analysed in all samples, except for uninfected tsetse sample at 24 hrs, which showed no difference (Figure 4.4).

Overall the data suggests that there was transient recruitment of neutrophils, with peak influx into the bite site occurring within the first 2 hrs, and there was no significant difference between infected and uninfected tsetse samples

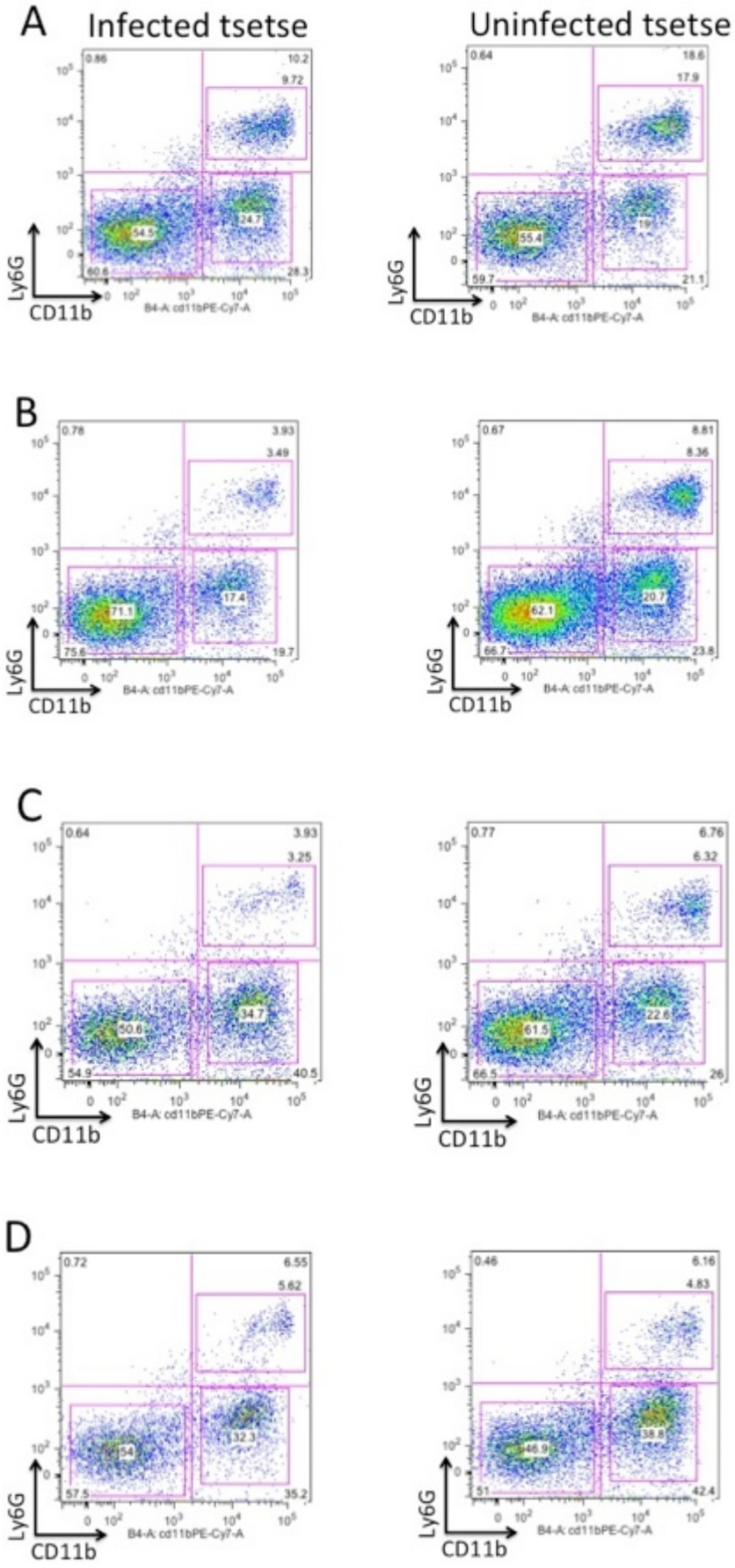
A
Infected tsetse
Uninfected tsetse
B
C
D
Ly6G
CD11b
B4-A: cd11bPE-Cy7-A

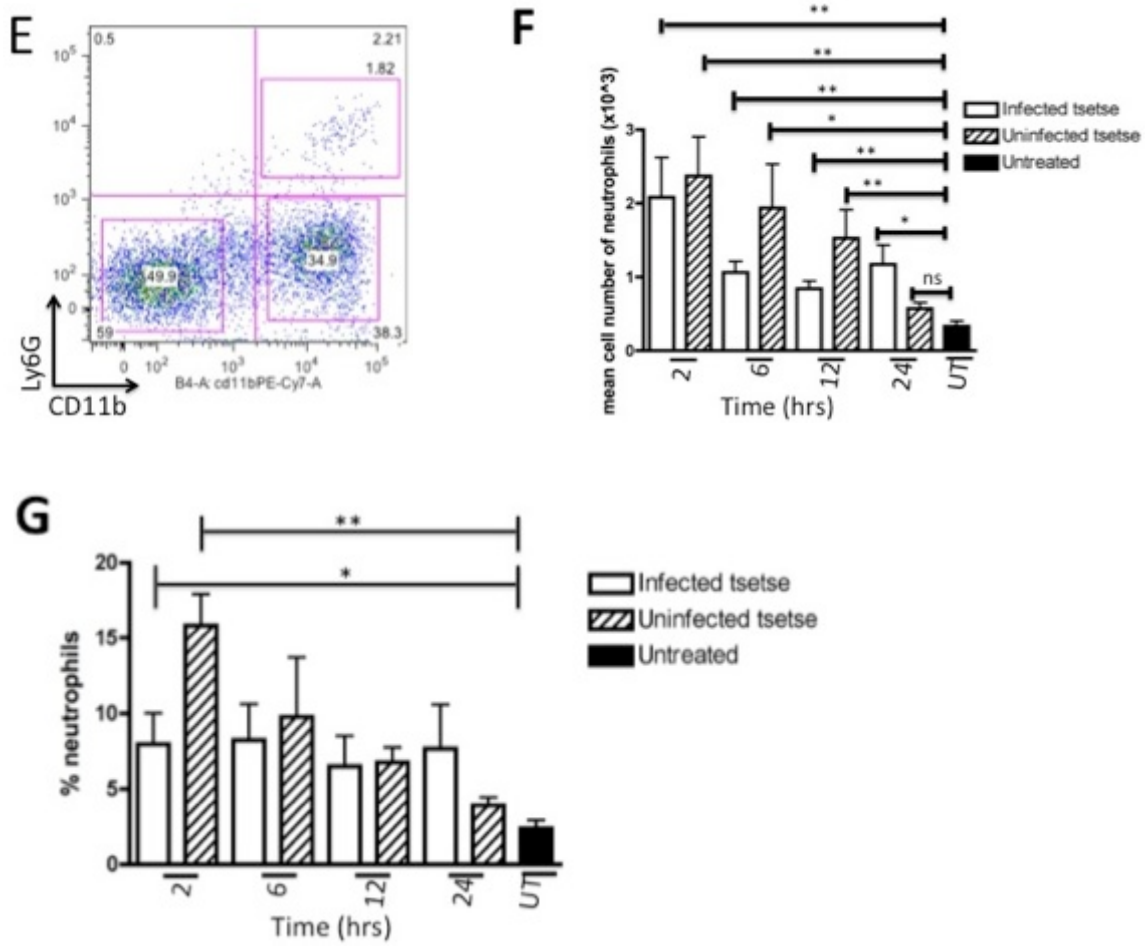

Figure 4-4 Estimation of the kinetics of neutrophil recruitment in the ear post tsetse exposure

Mice were anesthetised and ears exposed to infected/uninfected tsetse bites, and ears harvested at the respective time points. Following ear sample processing to isolate single-cell suspensions post tsetse exposure, processed samples were resuspended in 200 µl volumes FACS buffer. For standardisation of absolute cell numbers, 100 µl of cell suspension was analysed on the flow cytometry machine, and the total number of cells present in the sample tube was estimated by Miltenyi software, and number obtained multiplied by two to calculate the total number of cells in the ear tissue. Neutrophils were gated as described in Figure 4.2. Neutrophils ($CD11b^+Ly6G^+$) are present in the top right hand quadrant of the live $CD45^+$ cells gate. Representative dot plots of an infected and uninfected tsetse sample at 2 hrs (A), 6 hrs (B), 12 hrs (C) 24 hrs (D), and (E) untreated ear controls from naïve mice. (F) Bar graph summarised the mean neutrophil numbers, and (G) the proportion of neutrophils in infected, uninfected tsetse and untreated ears. Statistical test was estimated by comparing either infected or uninfected samples with untreated (UT) ear controls (*P<0.05, **P<0.01), and between infected and uninfected tsetse samples (P>0.05; not significant, ns) using One way ANOVA with Tukey's post test. Data represents the mean ± SEM, pooled together from 3 mice per group for three independent experiments.

4.2.5 Macrophage numbers in the ear skin do not change following tsetse exposure

Macrophages belong to the professional phagocyte pool comprising monocytes, DCs, mast cells and neutrophils, due to their efficiency at phagocytosis. They are described as professional phagocytes due to the expression of receptors such as scavenger receptors or TLRs that can detect signals not normally found in

healthy tissues, non-self or damage responses [365]. During tissue injury, macrophages develop a pro-inflammatory phenotype and secrete inflammatory mediators such as TNF-α, NO and IL-1, which participate in the activation of antimicrobial mechanisms that contribute to the killing of microorganisms in vivo [366]. The significance of macrophages during inflammation led to the analysis of macrophages in ear skin post tsetse exposure, to ask if there were changes in numbers during inflammation in tsetse exposed samples. Macrophages were gated on live $CD45^{+}$ $CD11b^{int}$, and examined for the combined expression of $F4/80^{+}$ and $CD11b^{+}$ (Figure 4.5). Comparison of macrophage numbers in the skin of infected and uninfected tsetse exposed samples clearly shows that there was no statistically significant difference ($P>0.05$; One way ANOVA with Tukey's post test). Further comparison of tsetse exposed samples with untreated controls also revealed no statistically significant changes in macrophage numbers ($P>0.05$; One way ANOVA with Tukey's posttest). Overall, the data suggests no differences in macrophage numbers in the skin post tsetse bites at the time points analysed.

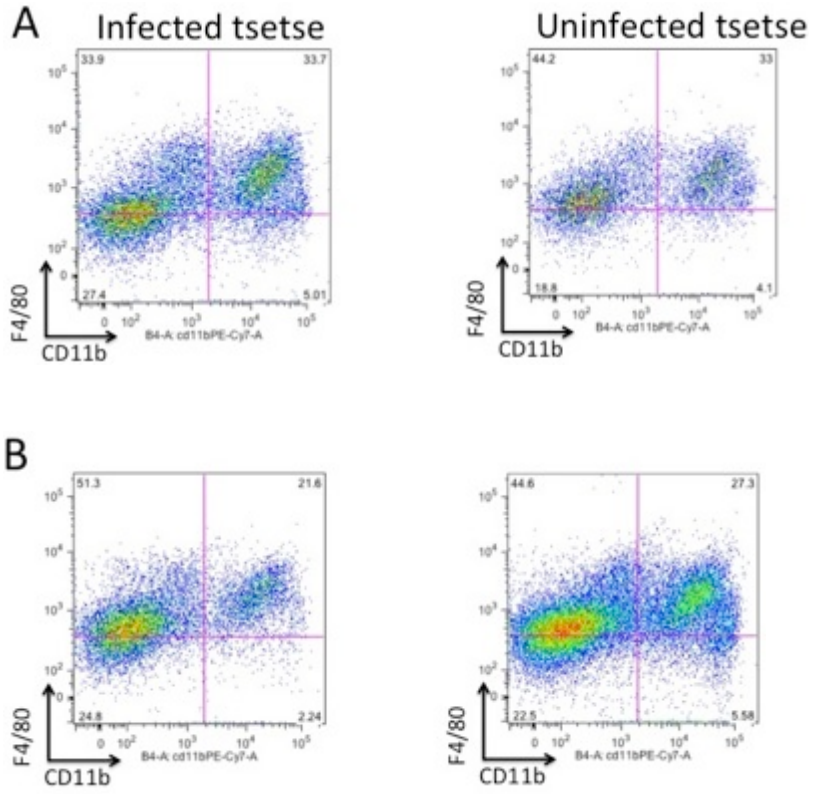

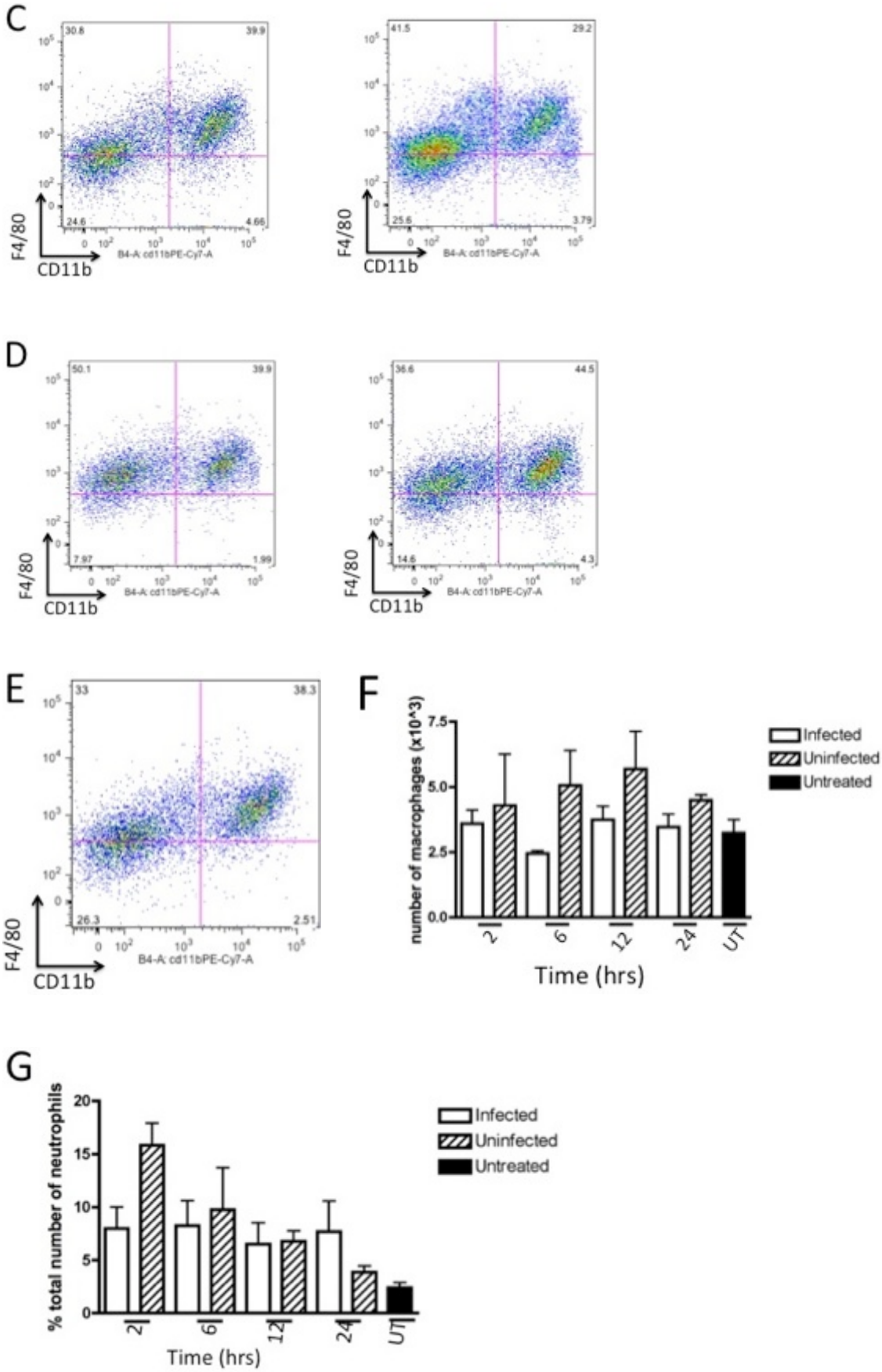

Figure 4-5 Kinetics of macrophage numbers following tsetse exposure.
Following ear sample processing to isolate single-cell suspensions, processed samples were resuspended in 200 µl volumes FACS buffer. For flow cytometry analysis, 100 µl of cell suspension was analysed on the MACSQuant analyser, and the total number of cells present in the sample

tube was estimated by Miltenyi software by drawing gates on cells phenotyped to be macrophages. Identification of macrophages was carried out on live CD45^{+} cells that were double positives for CD11b and F4/80. Example dot plots for macrophages at the time points in infected and uninfected tsetse samples at 2 hrs (A), 6 hrs (B), 12 hrs (C) and 24 hrs (D), respectively. (E) Example plot of macrophages in untreated ear skin of naïve mice. (F) Bar graph represents mean macrophage numbers ± SEM, and (G) the proportion of macrophages in tissue. Statistical analyses were carried out by comparing either infected or uninfected samples to untreated controls, also between infected and uninfected tsetse samples (P>0.05; not significant, ns), using One way ANOVA with Tukey's post test. Data represents the mean ± SEM, pooled together from 3 mice per group for three independent experiments.

4.2.6 Inflammatory monocytes do not appear within 24 hrs post tsetse exposure.

At sites of inflammation, inflammatory monocytes may be recruited from the blood, characterised by the expression of CD11b^{+} and Ly6C^{hi} cells. Recruitment of inflammatory monocytes to the skin following tsetse exposure was therefore examined, and it was demonstrated that inflammatory monocytes were not recruited in the first 24 hrs post tsetse exposure (Figure 4.6). Rather, monocytes resident in the skin characterised by the expression of CD11b^{+}, Ly6C^{lo}, and Ly6G^{-} were identified. Statistical comparisons of infected and uninfected tsetse exposed samples at each time point, suggests no significant difference (P>0.05; One way ANOVA with Tukey's post test), and there was also no difference when infected and uninfected tsetse exposed samples were compared to untreated controls.

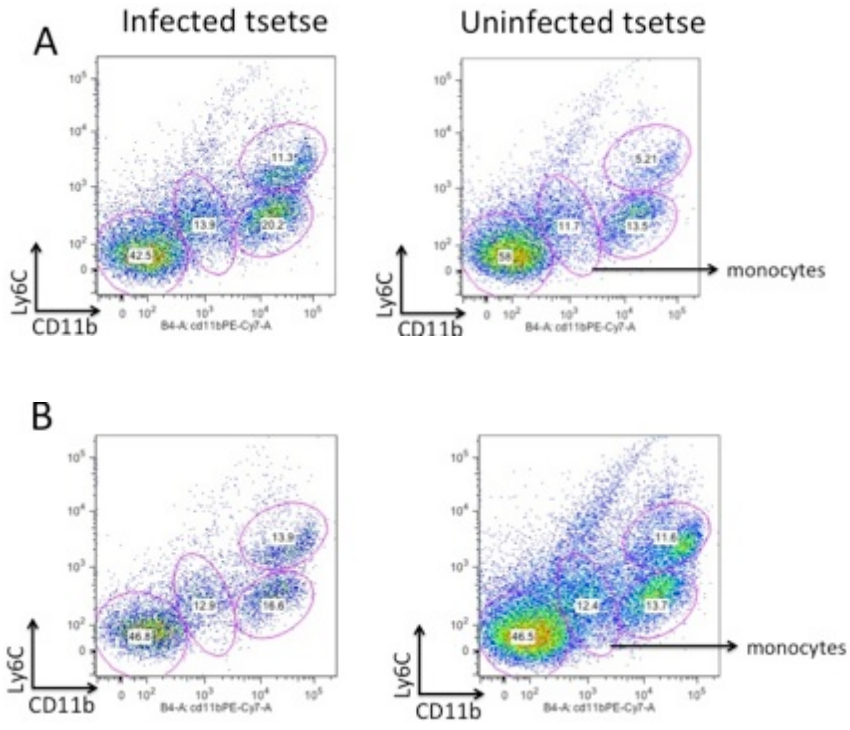

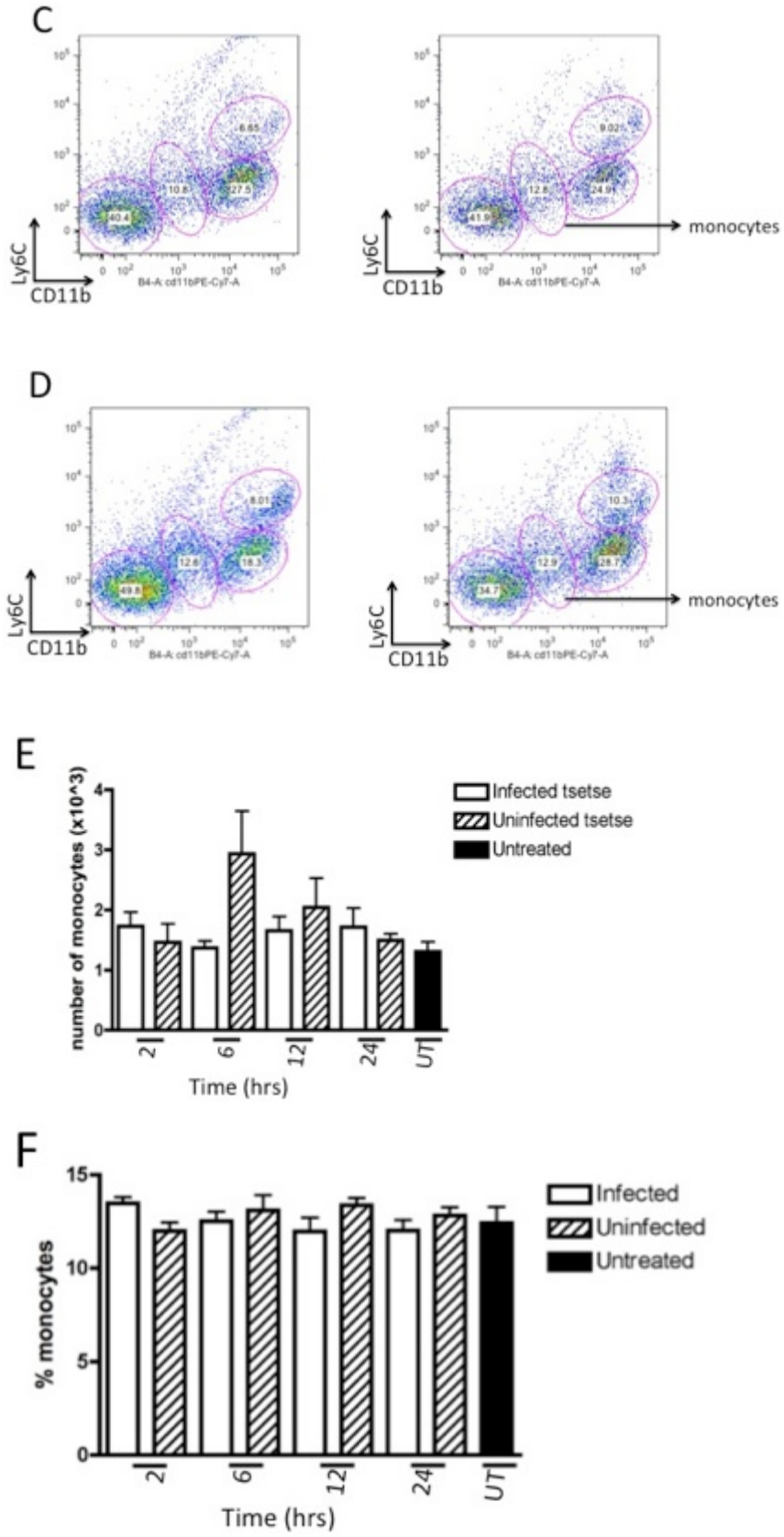

Figure 4-6 Kinetics of resident monocytes in the skin post tsetse bites.
Following ear sample processing to isolate single-cell suspensions, processed samples were resuspended in 200 µl volumes FACS buffer. For flow cytometry analysis, 100 µl of cell suspension was analysed on the MACSQuant analyser, and the total number of monocytes present in the sample tube was estimated by Miltenyi software, by drawing gates on monocytes and number of cells counted multiplied by two. Identification of monocytes was carried out on live $CD45^{+}$ cells that were double positives for $CD11b^{+}$ and $Ly6C^{lo}$. Example dot plots for monocytes at the time points in

infected/uninfected tsetse samples at 2 hrs (A), 6 hrs (B), 12 hrs (C) and 24 hrs (D), respectively. (E) Absolute cell counts were carried out and mean cell numbers depicted, and (F) the proportion of monocytes in tissue, were summarised in the bar graph. Statistical analyses was carried out by comparing infected/uninfected samples to untreated controls (UT), and between infected and uninfected tsetse samples. No statistically significant (ns) result was obtained using One way ANOVA with Tukey's post test. Data represents the mean ± SEM, pooled together from 3 mice per group for three independent experiments.

Together, the monocyte data here suggests that only skin resident monocytes were still present in the skin very early post tsetse exposure to mice ears.

4.2.7 Activation of macrophages in the skin post tsetse exposure

In African trypanosome infections, a type I cytokine environment typically predominates which fuels the generation of classically activated macrophages [131, 367-371]. Classically activated macrophages are developed in response to IFN-γ and exposure to microbes or microbial products such as LPS [372]. Classically activated macrophages secrete nitric oxide as well as costimulatory molecules such as CD86, upregulate MHCII, possess an enhanced antigen presenting capability and intracellular pathogen destruction [373]. MHCII is expressed on antigen presenting cells (APCs) such as macrophages and helps APCs in presenting antigens on their surface to cognate cells following processing in the lysosomal compartment of the cell [374]. Since the markers I used in phenotypic characterisation of macrophages post tsetse exposure consisted of anti-MHCII antibody, I measured the upregulation of MHCII on macrophages following tsetse exposure to determine its activation status. The data here was analysed using the mean fluorescent intensity (MFI) numbers to plot the expression levels of MHCII on macrophages in infected, uninfected tsetse samples, and untreated controls (Figure 4.7). At 2, 6, and 12 hrs MHCII MFI values on macrophages was significantly different compared to untreated controls ($P<0.05$; One way ANOVA with Tukey's post test) in infected and uninfected tsetse samples with the exception of infected tsetse samples at 2 and 12 hrs ($P>0.05$; One way ANOVA with Tukey's post test). At 24 hrs infected and uninfected tsetse samples, were not significantly different from untreated controls ($P>0.05$; One way ANOVA with Tukey's post test).

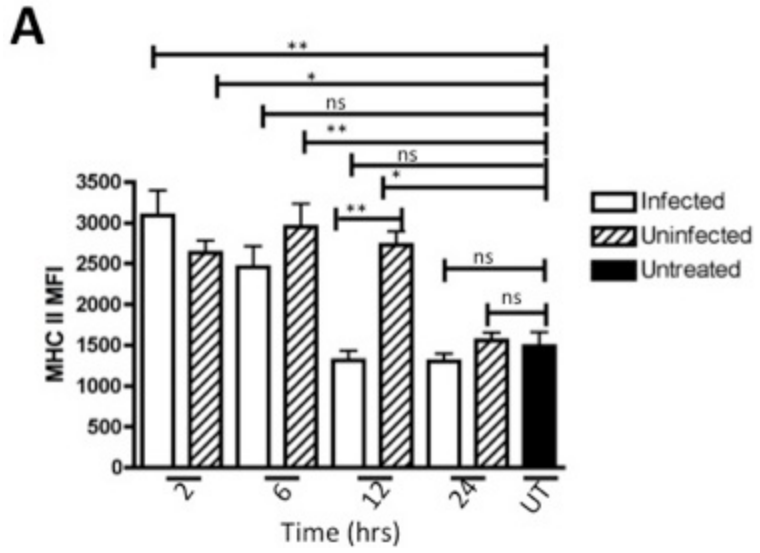
A
**
*
ns
**
ns
*
ns
ns
MHC II MFI
3500
3000
2500
2000
1500
1000
500
0
Infected
Uninfected
Untreated
2
6
12
24
UT
Time (hrs)

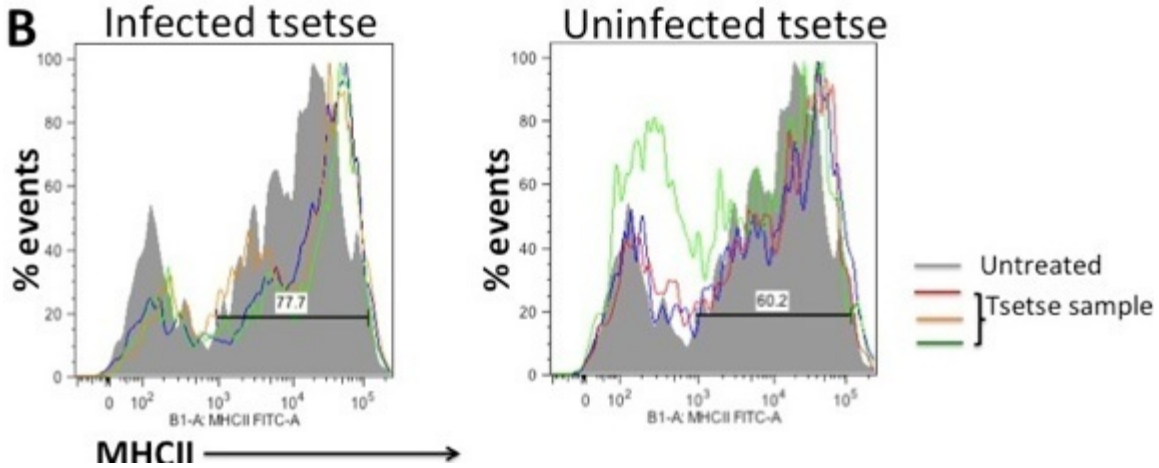
B
Infected tsetse
Uninfected tsetse
% events
77.7
60.2
B1-A: MHCII FITC-A
MHCII
Untreated
Tsetse sample

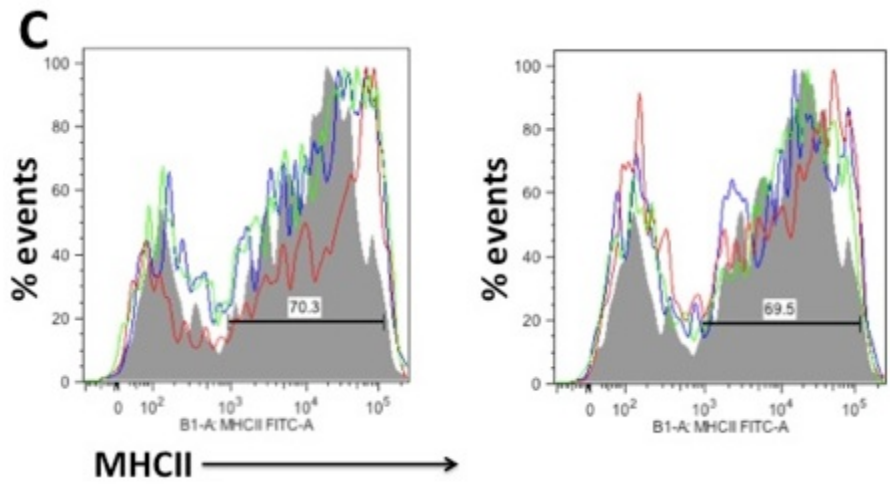
C
% events
70.3
69.5
B1-A: MHCII FITC-A
MHCII

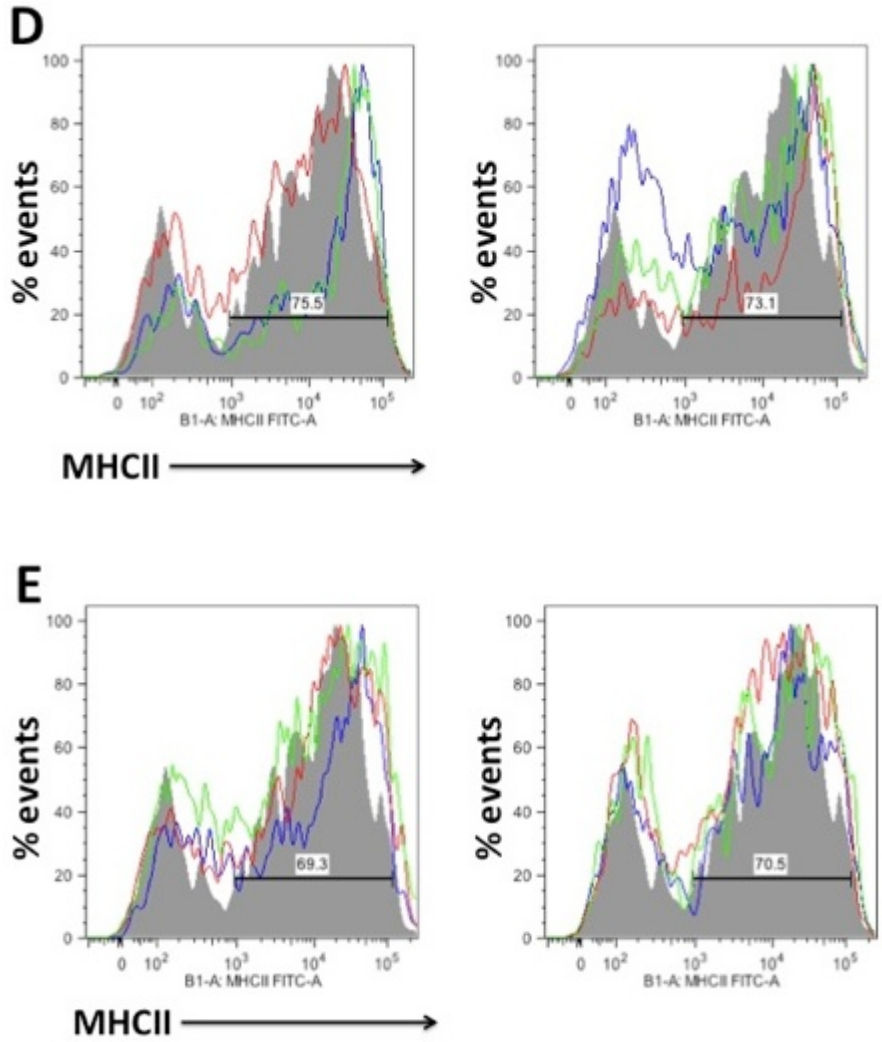

Figure 4-7 Upregulation of MHCII on macrophages in the ear skin post tsetse exposure. Following the processing of tissue and identification of macrophages (gated as described in Figure 4.2), expression levels of MHCII was investigated. (A) Bar graph depicting MFI values of MHCII expression on macrophages. Histogram plots for macrophage expression of MHCII at the time points in infected and uninfected tsetse exposed samples at 2 hrs (B), 6 hrs (C), 12 hrs (D) and 24 hrs (E), respectively. Statistical analysis was carried out using One-way ANOVA with Tukey's post test (*P<0.05, **P<0.01). No significant (ns) difference was observed between infected and uninfected tsetse samples. Data represents the mean ± SEM, pooled together from 3 mice per group for three independent experiments. Green, yellow, red and grey lines represent a single mouse.

4.2.8 Characterisation of the inflammatory profile in the ear

4.2.8.1 Assessment of RNA quality from ear and draining lymph node of mice exposed to tsetse

Following the identification and characterisation of the kinetics of cells recruited post tsetse exposure to ear samples, I next sought to characterise the expression profile of inflammation-associated genes in the skin and draining lymph node of C57Bl/6 mice. Two and twelve hours were identified as

appropriate time points based on the kinetics of neutrophil recruitment to the skin post tsetse exposure. Characterisation of inflammation associated genes was carried out by exposing infected and uninfected tsetses to mice ears, sampling tissues at 2 and 12 hours post exposure, extracting total RNA, and analysing the RNA obtained on a custom Taqman Low-Density Array (TLDA) microfluidic card. Prior to the TLDA analysis, the quality of RNA obtained from tissues was analysed using the Agilent 2100 Bioanalyser platform. The Agilent 2100 Bioanalyser provides the RNA integrity number (RIN), a ratio of 28S/18S, as well as an electrophoregram that gives information on the degree of noise and low molecular weight contamination [277], as shown in Figure 4.8. The electrophoregram also showed distinct and clear 18S and 28S bands, which was also an indicator of RNA quality. Only samples with RIN > 8.0 were used for downstream TLDA analysis. After confirmation of the quality of RNA to be used for analysis in the TLDA assay, approximately 1500 ng of total RNA was used for complementary DNA (cDNA) synthesis and downstream TLDA analysis.

TLDA is a customised 384-well microfluidic card (Applied Biosystems) containing primers and probes for pre-selected chemokines and inflammatory cytokines. In all, the format selected was able to allow profiling for 32 genes for total RNA from skin, and 64 genes for total RNA from lymph node implicated in inflammatory responses. All gene expression levels were firstly normalised to 18S, and then calibrated to untreated controls to obtain fold changes ($\Delta\Delta C_T$, where C_T is the threshold cycle). Therefore for these studies, a fold change of ≥1 or ≤1, meant that exposure to tsetse (infected and uninfected) induced upregulation or downregulation in that gene's expression compared to untreated controls respectively. To allow a direct comparison of the modulation of gene expression in response to infected and uninfected tsetse exposure, fold changes were plotted on a logarithmic scale. Statistical significance for differences in fold change in expression of each gene was calculated using a 2-tailed Mann Whitney U test.

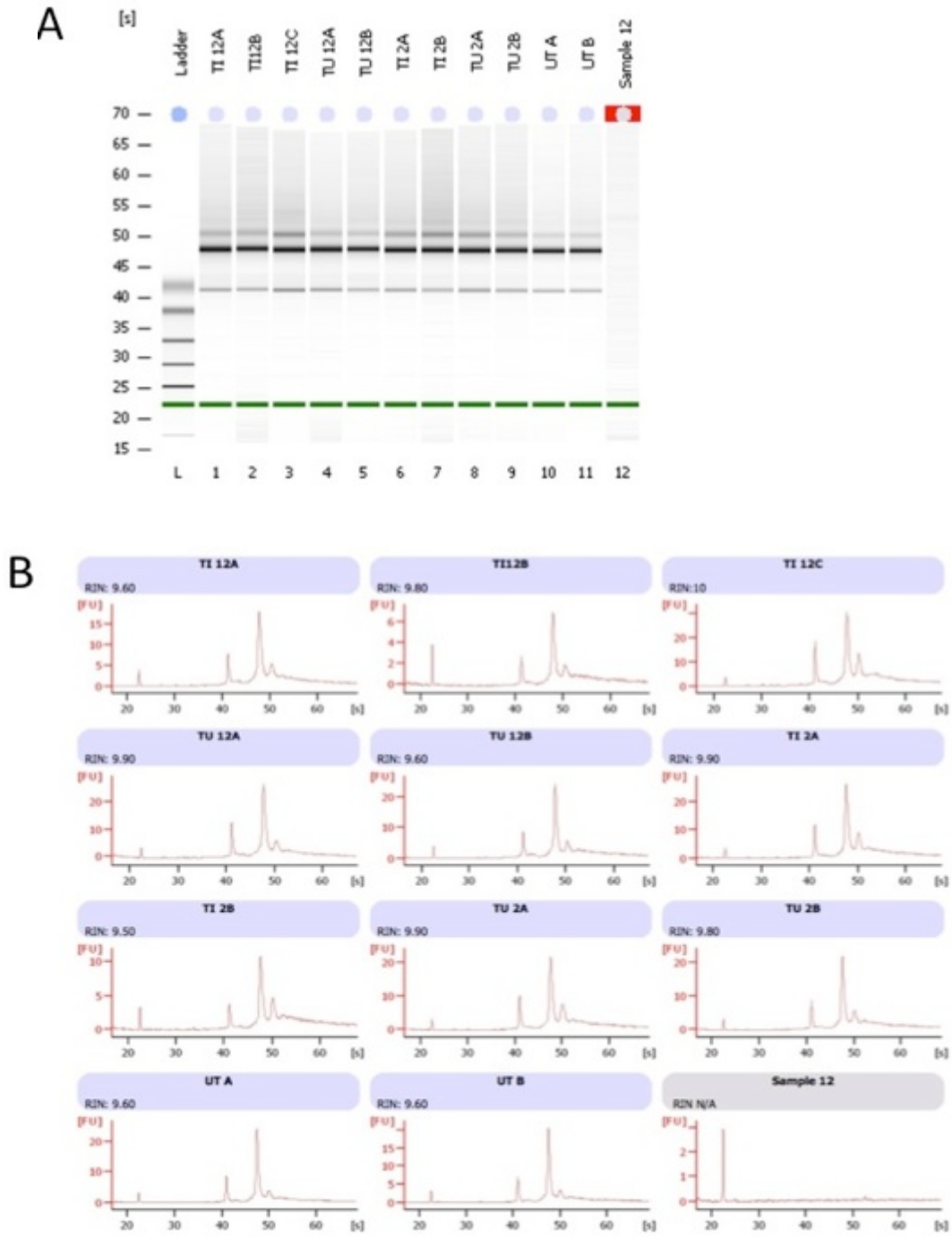

Figure 4-8 Assessment of RNA quality isolated from mouse ear skin and draining lymph node tissues isolated post tsetse exposure.
Total RNA was isolated from mouse ears, and draining lymph nodes (dLN) exposed to tsetses or untreated control tissues as described in materials and methods. RNA quality was assessed using the Agilent 2100 Bioanalyser. (A) Representative gel image of total RNA isolated from ears of infected tsetse exposed ear samples (lanes 1-3, 6-7), uninfected tsetse exposed ears (lanes 4-5, 8-9) isolated 12 hrs post probes, untreated controls (UT) (lanes 10-11), lane 12 is the internal control for the assay, Lane L: size marker (nucleotides, nt). (B) Electrophoregrams for each sample in the gel (A) is shown. The x-axis represents amplicons size (nt), while the y-axis represents the fluorescence units (FU). The electrophoregrams shows two peaks, 18S and 28S.

4.2.8.2 Inflammatory profile in the ear at 2 and 12 hrs post tsetse exposure

To better understand the mechanisms guiding leukocyte recruitment to the skin post tsetse exposure, an assessment of inflammation-associated genes in the skin was carried out by TLDA. The TLDA microfluidic card consisted of 32 genes, and the genes analysed were cytokines: TNF-α, IL-6, IL-10, IL-13, CD45, GM-CSF, CC chemokines: CCL2, 3, 4, 6, 7, 19, 27, CXC chemokines: CXCL1, 2, 3, 5, 10, 11, 12, 13, CC receptors: CCR2, 3, 4, 5, 7, 10, CXC receptors: CXCR2, 4, 5 and Fractalkine receptor, comprising wells preloaded with reagents for qPCR to detect the cDNA, therefore expression level of an array of 32 genes. Samples were analysed as described in section 4.2.8.1.

4.2.8.3 CC chemokine upregulation in mice ears at 2 and 12 hrs post tsetse exposure

The CC chemokines that were upregulated at 2 hrs were CCL2, CCL4 and CCL7 (Figure 4.9A). For CCL2 gene expression in the skin following tsetse exposure, there was a <10-fold increase in infected and uninfected tsetse samples. For CCL4, there was a 10-fold change in gene expression in both infected and uninfected tsetse samples. Lastly, at 2 hrs CCL7 gave a fold change in expression of <10 in both infected and uninfected tsetse samples. In all, the CC chemokines upregulated at 2 hrs were not statistically different between infected and uninfected tsetse exposed samples ($P>0.05$; 2-tailed Mann Whitney U test).

Next, I investigated infected and uninfected tsetse samples post exposure at 12 hrs. CCL2, CCL5 and CCL7 were the three CC chemokines upregulated (Figure 4.9B). At 12 hrs, CCL2 and CCL7 gave fold change in gene expression ≥1≤10 in both infected and uninfected tsetse samples, while CCL5 fold change in gene expression was only observed in uninfected tsetse samples (Figure 4.9B). Fold changes in gene expression of CCL2, CCL5 and CCL7 post tsetse exposure were not significant ($P>0.05$; 2-tailed Mann Whitney U test).

In summary, the presence or absence of *T. b. brucei* in the tsetse fly made no significant impact on inflammatory CC chemokines upregulation.

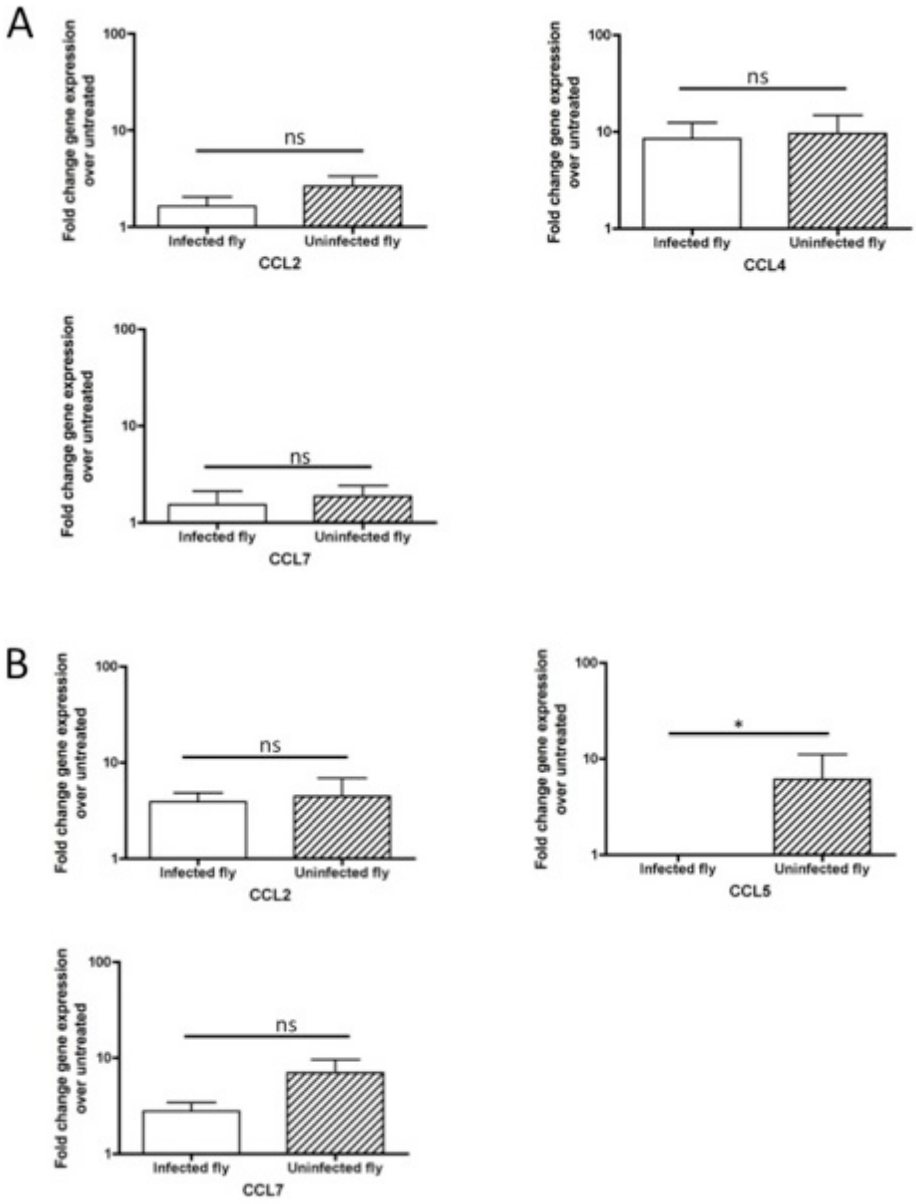

Figure 4-9 CC-chemokine expression did not differ at 2 and 12 hrs in infected and uninfected samples post tsetse exposure to the ear skin.
Infected and Uninfected tsetses were exposed to ears of C57Bl/6 mice, and ears collected at 2 and 12 hrs for total RNA isolation. 1500 ng of total RNA was used for cDNA synthesis diluted 1:5 and then used for chemokine gene analysis using Taqman Low Density Analysis. Gene expression was normalised with the housekeeping gene 18S, then RQ (relative quantification) values were set to 1 using an untreated ear control to calibrate samples and work out gene expression levels to obtain fold changes ($\Delta\Delta C_T$). RQ values in the plots were depicted as fold changes. Each sample was tested in triplicate and data represents the mean ± SEM. (A) Bar graph show CC genes that gave fold changes ≥ 1 at 2 hrs were CCL2, CCL4, and CCL7. (B) CCL2, CCL5, and CCL7 gave fold changes ≥ 1 at 12 hrs. Statistical analysis to compare fold changes in gene expression induced following tsetse exposure was carried out using 2-tailed Mann-Whitney U test. No significant (ns) differences ($P>0.05$) were observed between infected and uninfected tsetse samples with the exception of CCL5 at 12 hrs (*$P<0.05$). Data depicts fold changes of pooled values from 3 mice per group.

4.2.8.4 CXC chemokine upregulation in mice ears at 2 and 12 hrs post tsetse exposure

The CXC chemokine signatures followed a similar differential regulation pattern to the CC chemokines. At 2 & 12 hrs, CXCL1 and CXCL2 were the CXC chemokines that were upregulated post tsetse exposure. At 2 hrs, CXCL1 in uninfected tsetse exposed samples gave fold change values >10 fold in both infected and uninfected tsetse samples with no statistically significant difference ($P>0.05$; 2-tailed Mann Whitney U test) between infected and uninfected tsetse samples. At 12 hrs post tsetse exposure, CXCL1 expression was at base line level (similar to untreated controls i.e. gave a value of 1) in infected and uninfected tsetse exposed samples.

For CXCL2 expression in infected tsetse samples at both time points (2 and 12 hrs), fold changes were at base line level. While uninfected tsetse gave fold change values of ~1.5 and 6.5 respectively at 2 and 12 hrs (Figure 4.10).

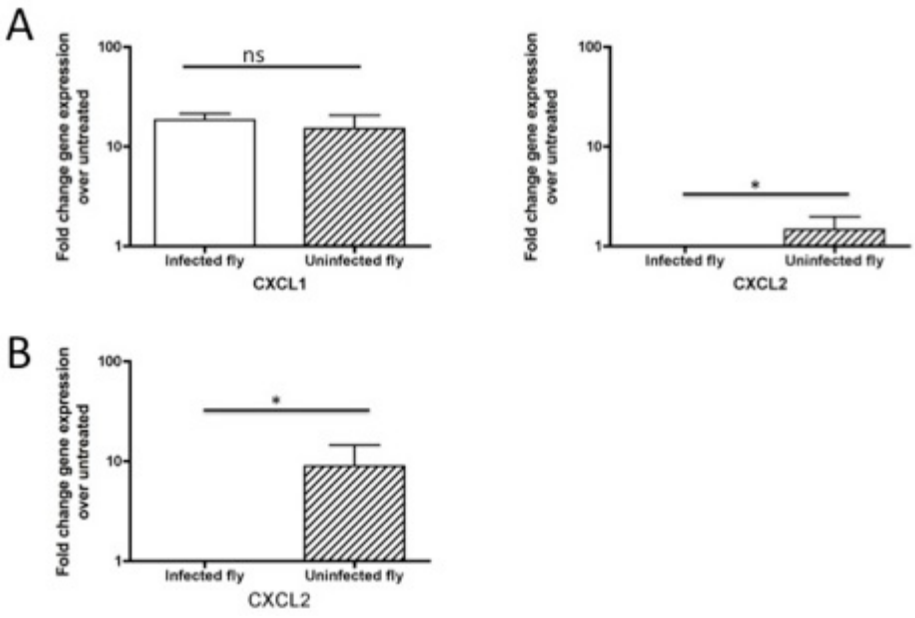

Figure 4-10 CXC-chemokine expression did not differ at 2 and 12 hrs in infected and uninfected samples post tsetse exposure to the ear skin.
Infected and Uninfected tsetses were exposed to ears of C57Bl/6 mice, and ears collected at 2 and 12 hrs for total RNA isolation. 1500 ng of total RNA was used for cDNA synthesis diluted 1:5 and then used for chemokine gene analysis using Taqman Low Density Analysis. Gene expression was normalised with the housekeeping gene 18S, then RQ (relative quantification) values were set to 1 using an untreated ear control to calibrate samples and work out gene expression levels to obtain fold changes ($\Delta\Delta C_T$). RQ values in the plots were depicted as fold changes. Each sample was tested in triplicate and data represents the mean ± SEM. (A) Bar graph show fold changes ~12 at 2 hrs for both CXCL1 and CXCL2. (B) At 12 hrs, CXCL2 expression was detected only in uninfected tsetse samples with fold change of ~6.5. Statistical analysis to compare fold change in gene

expression induced following tsetse exposure was carried out using 2-tailed Mann-Whitney U test. No significant (ns) differences were observed between infected and uninfected tsetse samples (P>0.05) with the exception of CXCL2 (*P<0.05) in both infected samples at 2 and 12 hrs. Data depicts fold changes of pooled values from 3 mice per group.

4.2.8.5 CX_3CL1 expression in mice ears at 12 hrs post tsetse exposure

CX_3CL1 a potent chemoattractant of T cells and monocytes was investigated at 2 and 12 hrs. At 2 hrs, in infected and uninfected tsetse exposed samples, CX_3CL1 was expressed at levels similar to naïve controls, while at 12 hrs fold changes were ~ 1.5 in both infected and uninfected tsetse samples (Figure 4.11). Hence at 12 hrs, CX_3CL1 expression was not significantly different between infected and uninfected tsetse samples (P>0.05; 2-tailed, Mann Whitney U test).

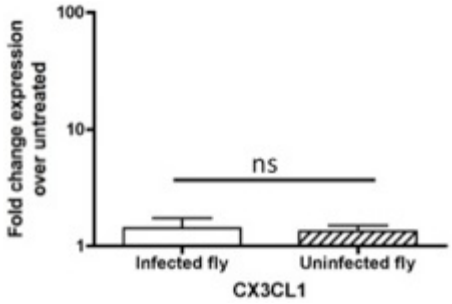

Figure 4-11 CX_3CL1 expression in the ear skin at 12 hrs post tsetse exposure.
Infected and Uninfected tsetses were exposed to ears of C57Bl/6 mice, and ears collected at 12 hrs for total RNA isolation. 1500 ng of total RNA was used for cDNA synthesis diluted 1:5 and then used for chemokine and cytokine gene analysis using Taqman Low Density Analysis. Gene expression was normalised with the housekeeping gene 18S, then RQ (relative quantification) values were set to 1 using an untreated ear control to calibrate samples and work out gene expression levels to obtain fold changes ($\Delta\Delta C_T$). RQ values in the plots were depicted as fold changes. Each sample was tested in triplicate and data represents the mean ± SEM. Bar graph shows CX_3CL1 gene expression, fold changes ~ 1.5 at 12 hrs in both infected and uninfected samples. No significant (ns) difference (P>0.05) was observed between infected and uninfected tsetse samples, 2-tailed Mann-Whitney U test. Data depicts fold changes of pooled values from 3 mice per group.

4.2.8.6 Inflammatory cytokine expression post tsetse exposure at 2 and 12 hrs

The cytokine genes upregulated at 2 hrs in response to infected and uninfected tsetse exposure were IL-1ß, macrophage colony stimulating factor (M-CSF) and IL-6 (Figure 4.12A). IL-1ß gave fold change expression of <10 fold in both tsetse exposed samples, while IL-6 gave ~100 fold increase in infected and uninfected tsetse samples. M-CSF fold change values of <10 was also observed in infected

and uninfected tsetse exposed samples at 2 hrs, with no statistically significant difference in cytokine fold changes between infected and uninfected tsetse exposed samples at 2 hrs (P>0.05; 2-tailed, Mann Whitney U test).

At 12 hrs only IL-1ß was upregulated (Figure 4.12B), following infected and uninfected tsetse exposure. IL-1ß gave fold changes ~8 and 12 fold in infected and uninfected tsetse samples respectively. No statistically significant difference was observed when both tsetse-exposed groups were compared (P>0.05; 2-tailed, Mann Whitney U test). Unexpectedly, I observed a 30-fold change in the anti-inflammatory cytokine IL-10 in infected tsetse sample at 2 hrs, which was completely undetected in uninfected tsetse samples. Further analysis to investigate the upregulation of IL-10 at 12 hrs, or absolute quantification by qPCR did not detect its expression.

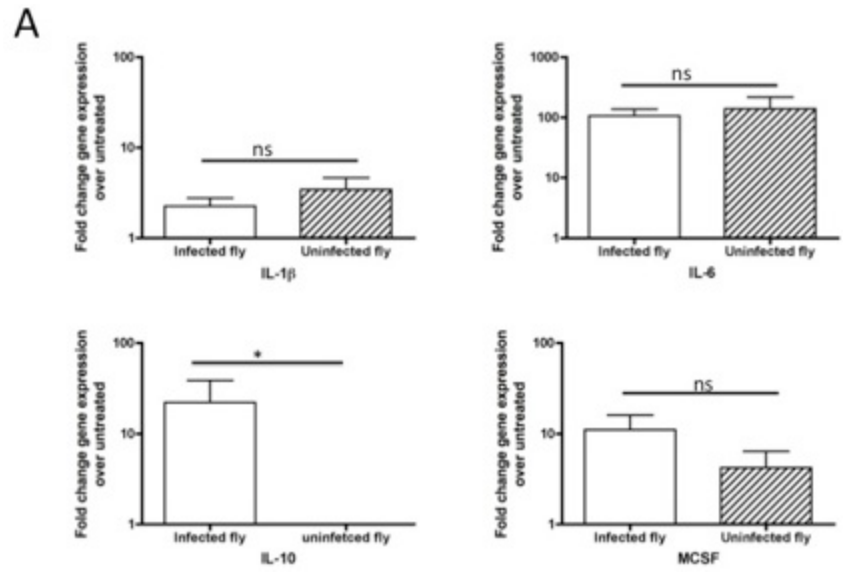

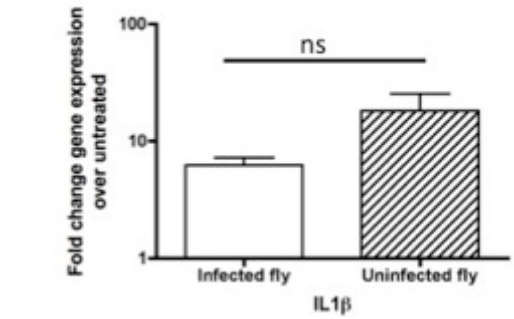

Figure 4-12 Inflammatory cytokine expression at 2 and 12 hrs in the ear skin post tsetse exposure.
Infected and Uninfected tsetses were exposed to ears of C57Bl/6 mice, and ears collected at 2 and 12 hrs for total RNA isolation. 1500 ng of total RNA was used for cDNA synthesis diluted 1:5 and then used for chemokine and cytokine gene analysis using Taqman Low Density Analysis. Gene expression was normalised with the housekeeping gene 18S, then RQ (relative quantification) values were set to 1 using an untreated ear control to calibrate samples and work out gene expression levels to obtain fold changes ($\Delta\Delta C_T$). RQ values in the plots were depicted as fold changes. Each sample was tested in triplicate and data represents the mean ± SEM. (A) Bar graph showing IL-1β, IL-6, IL-10 and M-CSF fold changes at 2 hrs. (B) At 12 hrs, bar graph shows IL-1β fold change. No significant (ns) difference was observed using 2-tailed Mann-Whitney U test, $P>0.05$, with the exception of IL-10 ($^*P<0.05$). Data depicts fold changes of pooled values from 3 mice per group.

A summary of the results of all the genes analysed is given in Table 4.1 below.

Table 4-1. Summary of the results of bar graphs presented for genes analysed at 2 and 12 hrs.

Genes analysed at 2 and 12 hrs	Infected tsetse Upregulated/downregulated (+/-)	Uninfected tsetse Upregulated/downregulated (+/-)
CCL2	+	+
CCL4	+	+
CCL5	-	+
CCL7	+	+
CXCL1	+	+
CXCL2	-	+
CXC3CL1	+	+
IL-1β	+	+
IL-6	+	+

IL-10	+	-
MCSF	+	+

+ = upregulated, - = downregulated

4.2.9 Summary of gene upregulation in the skin post tsetse exposure

The aim of this section was to characterise the inflammatory profile in the skin following *T. b. brucei* infected and uninfected tsetse exposure, and also investigate whether there were differences between infected and uninfected tsetse samples. There were no statistically significant differences in inflammatory chemokine and cytokine genes upregulated between infected and uninfected tsetse exposed samples at the time points analysed.

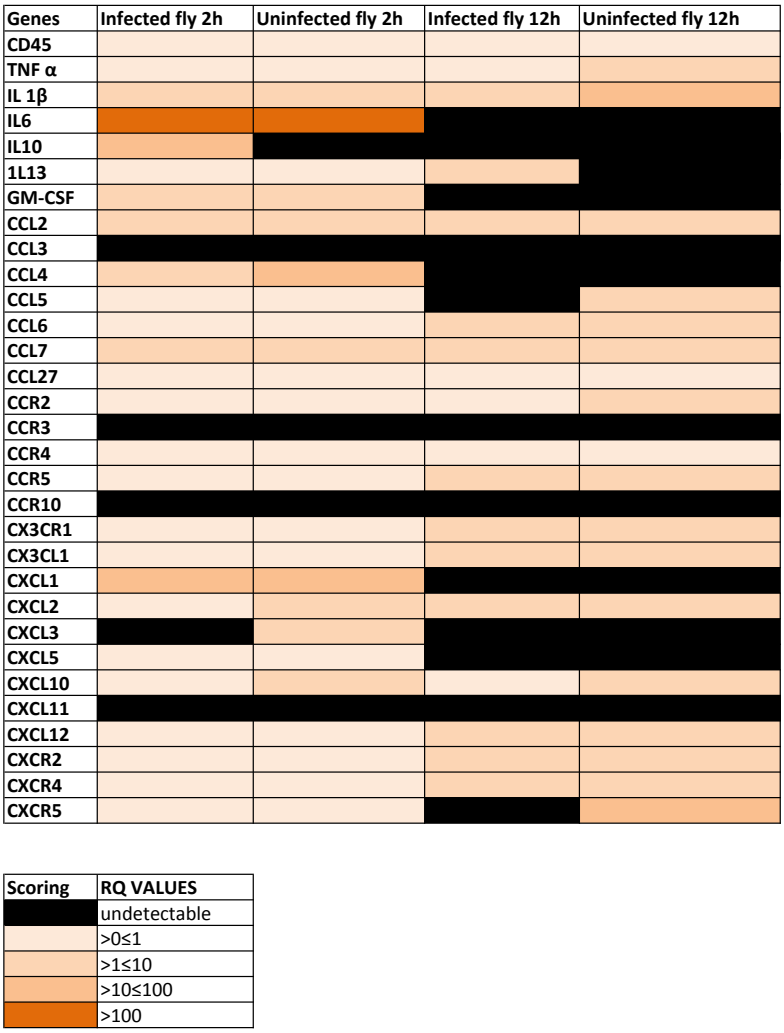

Scoring	RQ VALUES
	undetectable
	>0≤1
	>1≤10
	>10≤100
	>100

Figure 4-13 Summary of total genes analysed by Taqman Low Density Arrays at 2 and 12 hrs in the ear skin post tsetse exposure.
Infected and Uninfected tsetses were exposed to ears of C57Bl/6 mice, and ears collected at 2 and 12 hrs for total RNA isolation. 1.5 µg of total RNA was used for cDNA synthesis diluted 1:5 and then used for chemokine and cytokine gene analysis using Taqman Low Density Analysis. Gene expression was normalised with the housekeeping gene 18S, then RQ (relative quantification) values were set to 1 using an untreated ear control to normalise samples and work out gene expression levels to obtain fold changes ($\Delta\Delta C_T$). Fold change values were computed as an increment over untreated controls. The expression data obtained from all the genes analysed at 2

and 12 hrs post tsetse bites are summarised above. The scoring system for classifying the colours is also indicated above. Genes that were undetectable on the TLDA microfluidic card are coloured black.

Chemokines are important for leukocyte trafficking to sites of inflammation, and perform immunosurveillance roles in the skin. In this study, it has been shown that the CXC chemokines CXCL1, CXCL2, and CXCL5 were in the skin post tsetse bites. The pro-inflammatory chemokines CXCL1, CXCL2, and CXCL5 are associated with neutrophil extravasation from blood and bind the receptor CXCR1/CXCR2 during infection. CXCL1 and CXCL2 together with other proinflammatory CC chemokines upregulated in this study, such as CCL2, CCL4, CCL5 and CCL7 are important for neutrophil, macrophage and monocyte recruitment during inflammation. The presence of neutrophils in my model post tsetse exposure as confirmed by flow cytometry lends credence to the role of these pro-inflammatory chemokines in neutrophil extravasation [375]. Also, the fractalkine receptor CX_3CL1 was upregulated at 12 hrs, and has been indicated to induce the accumulation of mature mast cells in the skin during inflammation.

In the course of the transcript analysis from the skin post tsetse bites, I also identified the upregulation of pro-inflammatory cytokines IL-6 and IL-1ß. IL-1ß which can be produced by activated cells such as monocytes and macrophages, or non-immune cells such as fibroblasts and endothelial cells during injury, infection or inflammation, was consistently secreted at the two time points (2 and 12 hrs) used for TLDA studies. The production of IL-1ß, which was present in both infected and uninfected tsetse samples, may be likely due to the damage from the tsetse proboscis to the skin. IL-6 a pleiotropic cytokine was upregulated, albeit only at 2 hrs. The role of IL-6 has described to be essential in the differentiation of Th_{17} cells and it is involved in a wide range of biological activities such as immune regulation, hematopoiesis, inflammation and oncogenesis. Interestingly, there was also the upregulation of an anti-inflammatory cytokine IL-10 in the infected tsetse sample at 2 hrs, which was significant when compared with the uninfected tsetse sample, which showed no upregulation. Anti-inflammatory cytokines dampen the expression of pro-inflammatory cytokines. In the context of this infection model, IL-10 may dampen the production of pro-inflammatory cytokines in order to allow for parasite establishment in the skin, prior to dissemination into the blood stream [122]. Other chemokines such as CCL5 and CXCL2 were also downregulated in

the infected tsetse samples only. This might suggest that the presence of parasites in the tsetse was contributing to some form of anti-inflammatory role following tsetse bites. The upregulation of an anti-inflammatory cytokine IL-10 and the downregulation of monocyte/neutrophil chemokines CCL5 and CXCL2 in infected tsetse samples, suggests that *T. b. brucei* may possess an anti-inflammatory role.

Taken together, the gene expression data here agrees with the flow cytometry data that there were no significant differences between infected and uninfected samples post tsetse exposure. The data here aso suggests a significant downregulation of chemokines involved in leukocyte chemotaxis (CCL5 and CXCL2) and a significant upregulation of an anti-inflammatory cytokine (IL-10) in infected tsetse samples. This suggests that inflammation events very early in the skin may be triggered by the tsetse damage and the presence of parasites in the skin might contribute to an anti-inflammatory role in vivo.

4.2.10 Inflammatory profile of the lymph node post tsetse exposure

Following the analysis of the inflammatory genes triggered post tsetse exposure to mice ears, the inflammatory profile of the draining lymph node (LN) of mice was also analysed using TLDA. This was carried out using a customised TLDA microfluidic card that consisted of 64 customised genes, and was kindly supplied as a gift by Dr. Clive McKimme. The TLDA microfluidic card contained CC ligands (CCL) 1-28, CXC ligands (CXCL) 1-17, CX_3CL1, XCL1, innate immunity genes TNF-α, IL-6, IL-1α, IFN-α, IFN-β, IL-1β, adaptive immune genes and pathogen recognition receptors, comprising wells preloaded with reagents for qPCR to detect the cDNA, therefore expression level of an array of 64 genes. The housekeeping gene, 18S that was constitutively expressed in the LN was used to normalise gene expression levels prior to determining fold expression changes by calibrating with untreated control samples. Analysis was carried out in a similar manner to TLDA analysis of skin data as described in section 4.2.8.1.

4.2.10.1 Expression of chemokines in the draining lymph node at 2 and 12 hrs post tsetse exposure

At 2 hrs, the chemokines and cytokines analysed suggested that there were no fold changes in gene expression above base line levels (i.e. untreated controls) in the lymph node.

At 12 hrs, only 7 of the 64 genes analysed on the TLDA microfluidic cards were upregulated following exposure to infected and uninfected tsetses. Those genes upregulated were CC ligands; CCL7, CCL20, CCL28, and CXC ligands; CXCL2, CXCL5, CXCL10, and CXCL17. For CCL7 and CCL20, fold changes of <10 were observed in infected and uninfected tsetse exposed samples (Figure 4.14A). For CCL28, infected and uninfected tsetse exposed samples gave fold change values >500 at 12 hrs. No statistically significant difference between infected and uninfected tsetse samples was observed in the CC chemokines that were upregulated ($P>0.05$; 2-tailed, Mann Whitney U test).

The CXC chemokines that were upregulated following infected and uninfected tsetse exposure at 12 hrs were CXCL2, CXCL5, CXCL10, and CXCL13 (Figure 4.14B). CXCL2, CXCL5 and CXCL10 gave fold changes ≥10<100 in infected and uninfected tsetse samples. CXCL17 gave fold change values of >10<100 in infected and uninfected tsetse samples. No statistically significant difference ($P>0.05$; 2-tailed, Mann Whitney U test) was observed for CXC chemokine fold change gene expression between infected and uninfected tsetse samples in the draining LN at 12 hrs.

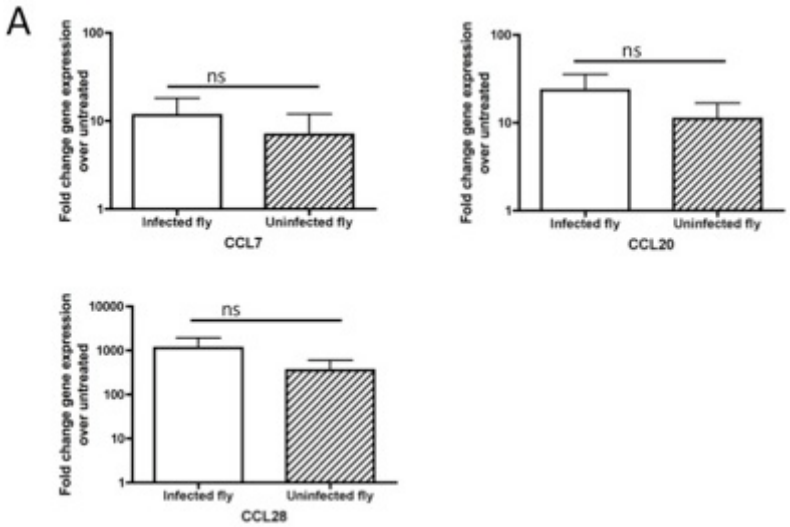

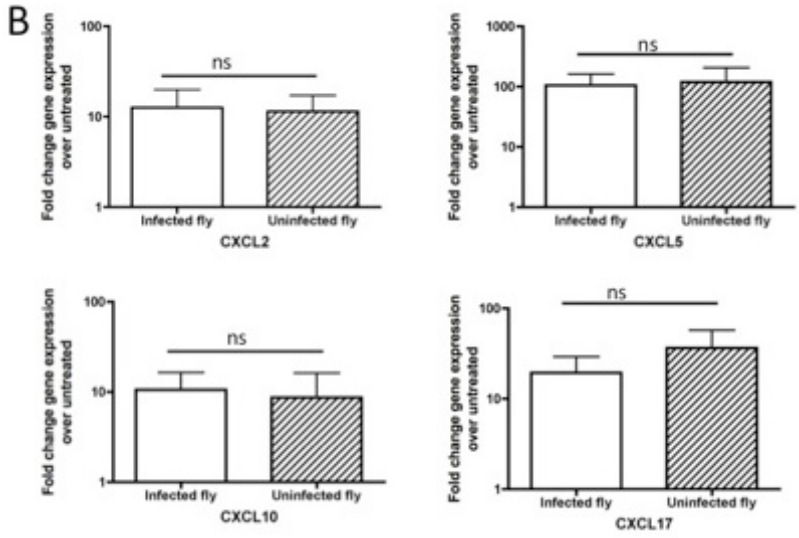

Figure 4-14 CC and CXC-chemokine upregulation at 12 hrs in the draining lymph node post tsetse exposure
Infected and Uninfected tsetses were exposed to ears of C57Bl/6 mice, and ears collected at 12 hrs for total RNA isolation. 1500 ng of total RNA was used for cDNA synthesis diluted 1:5 and then used for chemokine and cytokine gene analysis using Taqman Low Density Analysis. Gene expression was normalised with the housekeeping gene 18S, then RQ (relative quantification) values were set to 1 using an untreated lymph node control to calibrate samples and work out gene expression levels to obtain fold changes ($\Delta\Delta C_T$). RQ values in the plots were depicted as fold changes. Each sample was tested in triplicate and data represents the mean ± SEM. (A) Bar graphs show CCL7, CCL20 and CCL28 fold changes, (B) CXCL2, CXCL5, CXCL10 and CXCL17. No significant (ns) difference ($P>0.05$) was observed between infected and uninfected tsetse samples using 2-tailed Mann-Whitney U test. Data depicts fold changes of pooled values from 3 mice per group.
.

In summary, the chemokine genes that were upregulated in the draining LN at 12 hrs post tsetse exposure were not significantly different between infected and uninfected tsetse samples.

4.2.11 Summary of gene upregulation in the draining LN post tsetse exposure

At 12 hrs, it was demonstrated that only inflammatory CC chemokines CCL7, CCL20 and CCL28 were upregulated, while CXC chemokines, CXCL2, CXCL5, CXCL10 and CXCL17 were upregulated in both infected and uninfected tsetse exposed samples.

CXCL10, which was upregulated in the LN at 12 hrs, is an agonist for CXCR3, which is expressed on Th1 cells, and also antagonizes CCR3 expressed on Th2 cells. This suggests that the upregulation of CXCL10 in the lymph node post tsetse exposure could contribute to the polarisation of the immune response to a

Th1 type [376]. CXCL5 an LPS-induced CXC chemokine could have been upregulated in the lymph node as a result of the bacteria released from the saliva components of the tsetse fly. CXCL5, similar to CXCL2 binds CXCR2 a neutrophil receptor, and has a role in neutrophil recruitment, as it has been described to be involved in neutrophil recruitment in lungs of mice infected with *M. tuberculosis* [377].

In all, temporal upregulation of inflammation-associated genes in the draining LN was < 100 fold in almost all the genes analysed, and there was no difference between infected and uninfected tsetse exposed LN samples, similar to the findings reported in tsetse exposed mice ears.

4.2.12 Depletion of neutrophils

4.2.12.1 Establishing the protocol for neutrophil depletion

From section 4.2.4, it was established that neutrophils were the first cells that were recruited very early to the bite site, either in infected or uninfected tsetse exposed samples. The aim of this section was to investigate the depletion of neutrophils and the functional consequence of depletion in parasite dissemination from the bite site to the blood stream. In order to deplete neutrophils from C57Bl/6 mice, a well-established model for neutrophil depletion was applied [378, 379]. Following administration of anti-Ly6G or isotype control antibodies, mice were kept for 16 hrs prior to infections. The first experiment was to test that depletion of neutrophils using anti-Ly6G was successful. Sixteen hours post administration of anti-Ly6G and setting up the appropriate controls, mice were treated with 10 µg/ml LPS to observe the recruitment of neutrophils for 6 hrs, when neutrophils were previously reported to be observed in the skin in our lab. LPS was used as a model to test the success of neutrophil depletions in mice, because it is a well-established model of inflammation in tissues [380-382]. As shown in Figure 4.15 neutrophils were successfully depleted in anti-Ly6G treated mice post LPS treatment.

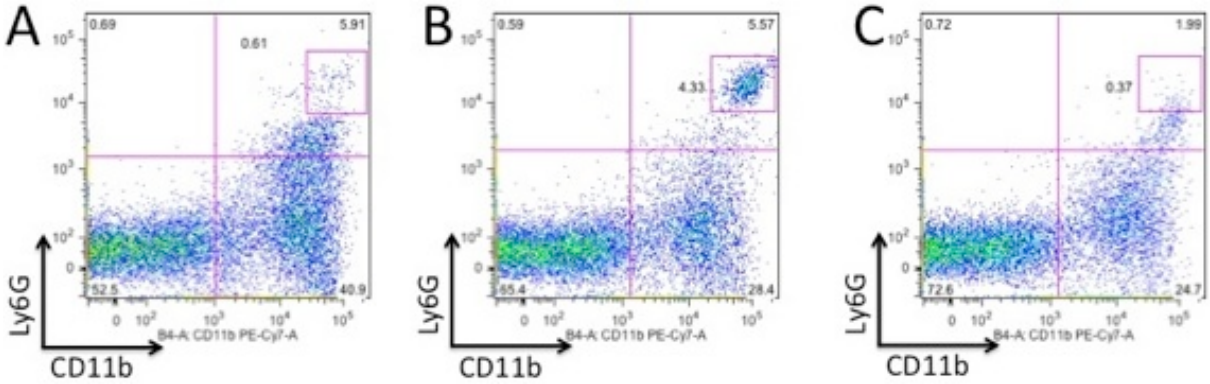

Figure 4-15 Setting up the neutrophil depletion study.
C57Bl/6 mice were injected intraperitoneally with 1 mg anti-Ly6G or isotype control antibodies and left for 16 hrs. Sixteen hours post injection of mice with antibodies, ear pinna of anti-Ly6G (1A8) and isotype treated mice were injected subcutaneously with 10 µg/ml of LPS. Six hours later, ear skin was collected and digested using hyaluronidase and collagenase type IV, and ground in a tissue-lysing machine. Cell suspension was spun down and passed through a 40- µm cell strainer to collect cells. Cells were then prepared for leukocyte staining as described in the materials and methods. The gating strategy described in figure 4.2 was applied, and neutrophils identified by the markers CD11b and Ly6G. Representative plots of neutrophils in the top right hand quadrant in (A) naïve control, (B) isotype control, and (C) anti-Ly6G treated mice. Data representative of 3 mice per group.

4.2.12.2 Impact of Neutrophil depletion on African trypanosome infection via tsetse transmission

Once it was established that depletion of neutrophils was successful, it was then applied to *T. b. brucei* infection model. One mg anti-ly6G or isotype antibody was administered 16 hrs prior to *T. b. brucei* infected tsetse exposure to mice ear skin. Parasitemia was observed on a daily basis for the first 9 days. Mice treated with anti-ly6G showed parasitemia, as early as 2 days post infected tsetse exposure compared with isotype control antibody treated and naive controls. Isotype and untreated controls gave parasitemia from 3 and 4 days post infection in C57Bl/6 mice. Statistical analyses to compare the parasitemia in mice from the three groups revealed no statistically significant difference across the time points analysed ($P>0.05$; One way ANOVA with Bonferroni multiple test). Together, the data suggests that neutrophil depletion resulted in a minor increase in the appearance of parasites with no further impact on parasite dissemination.

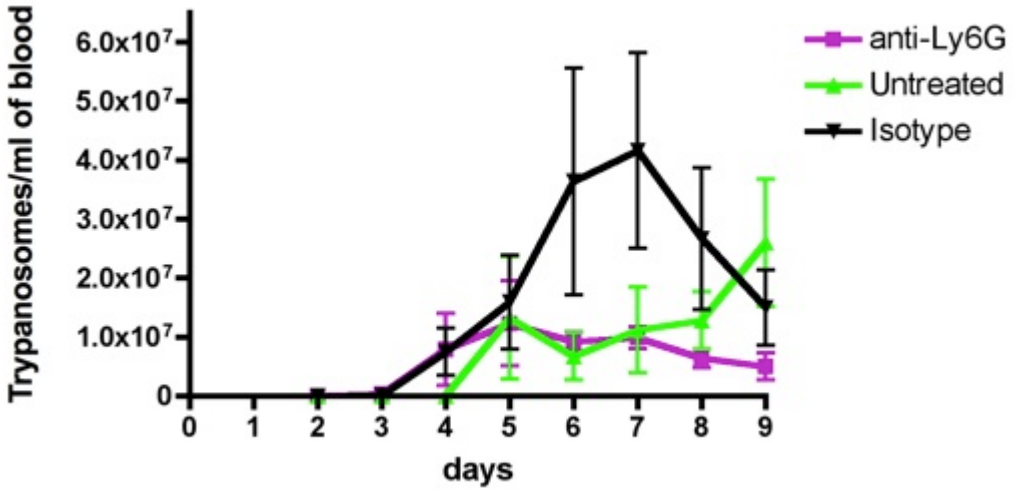

Figure 4-16 Depletion of neutrophils causes an early appearance of parasitemia.
Mice were administered anti-Ly6G or isotype control 2A3 antibodies for 16 hrs prior to infection via tsetse flies. Untreated control mice were also included in the infections. Parasitemia was monitored over 9 days with neutrophil depleted mice producing an earlier appearance of parasites from day 2 compared with isotype controls and untreated mice. Statistical analyses to compare differences in parasitemia between the three groups were carried out using one-way ANOVA (Bonferroni multiple test) [(Data pooled from 4 mice per group for 2 independent experiments)]. No significant differences were observed ($P>0.05$).

4.3 General summary

At the start of this study, it was hypothesised that tsetse exposure to the skin would cause a rapid influx of inflammatory cells to the bite site, which would differ significantly between infected and uninfected tsetse exposed samples. To test the hypothesis, I set out to carry out flow cytometry to characterise the kinetics, and identity of cells that were recruited to the bite site, followed by a transcript analysis to identify inflammatory mediators. The findings here suggest that the presence or absence of infection in the tsetse did not impact on the recruitment of cells to the bite site when infected and uninfected tsetse exposed samples were compared statistically. However, in both groups (infected and uninfected tsetse exposed), there were statistically significant differences in cellular recruitment compared to untreated controls. This suggested that mechanical trauma from probing, and the saliva of the tsetse fly may be responsible for the influx of neutrophils into tissue. Transcript analysis of inflammatory mediators revealed the fold changes of chemokines and cytokines during tsetse induced inflammation. Overall, the TLDA data here followed a similar pattern with the flow cytometry data indicating no significant difference

between infected and uninfected tsetse exposed samples in most of the chemokines and cytokines analysed. However, I observed the downregulation of leukocyte attracting chemokines such as CCL5 and CXCL2, and an upregulation of IL-10 in infected tsetse samples. CXCL1/CXCL2, chemokines associated with neutrophil extravasation were also upregulated. The transcript data agree with the findings from my flow cytometry data that it was the impact of the vector, and not the parasites that mediated inflammation in the skin. A summary of the earliest events in the skin and draining lymph node post tsetse exposure is described in figure 4.17.

The identification of neutrophils as the main immune cell type recruited within the first 24 hrs, led to further investigation of its role in pathogenesis. Hence the need to ask how mechanical trauma caused by tsetse probing would have an impact on parasite dissemination from the skin into the blood via the lymphatics. To address this, infections were carried out via the tsetse fly in neutrophil depleted mice. Depleting neutrophils from mice prior to infection gave similar parasitemia in neutrophil replete and deficient mice. A general discussion of the key findings of the results section and how it relates to pathogenesis are discussed below.

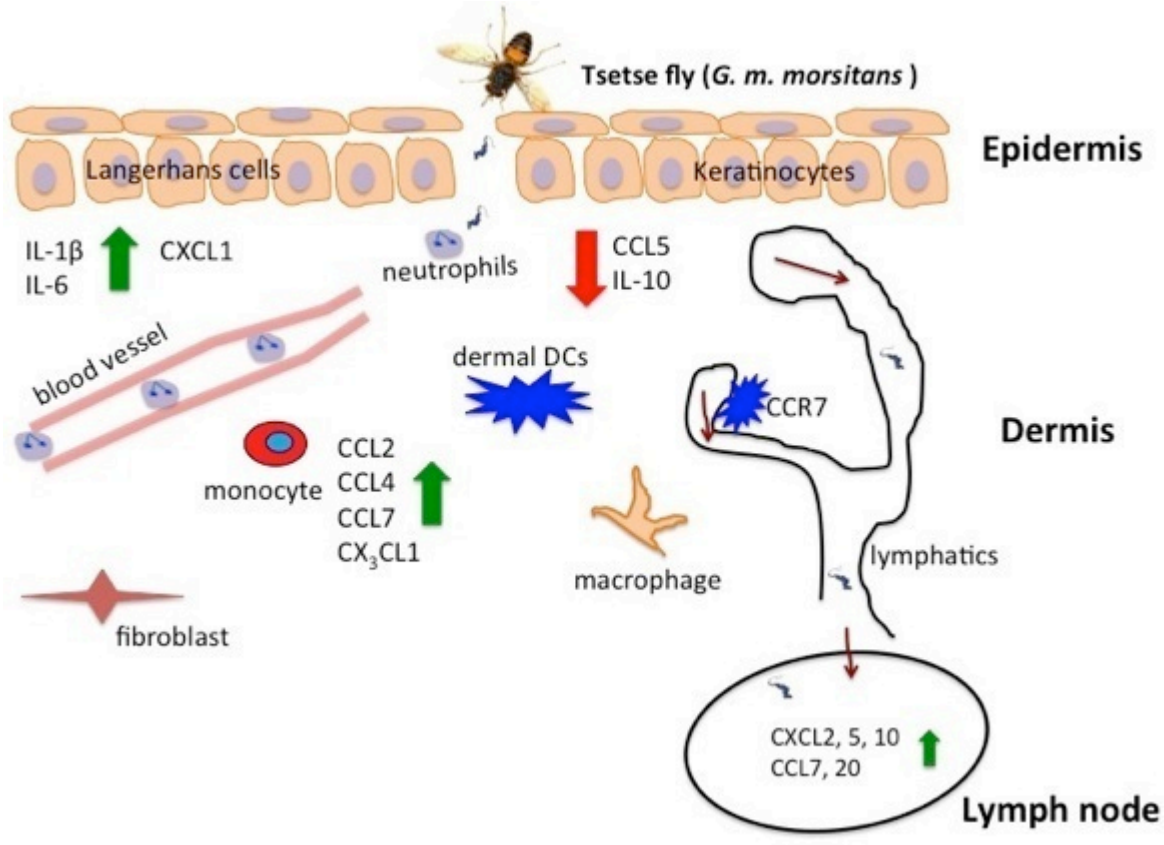

Figure 4-17 Summary of the earliest events in the skin and draining lymph node at the molecular and cellular level post tsetse exposure.
Disruption of mice skin barrier by infected or uninfected tsetse exposure triggers a coordinated immune response to maintain skin homeostasis. Keratinocytes, which are normally present in the epidermis, can respond through production of pro-inflammatory cytokines such as IL-1β, and IL-6, that were upregulated within the first 12 hrs as shown by TLDA. Langerhans cells (not characterised by flow cytometry) present in the epidermis also act as key immunological sentinels. Macrophages and monocytes in the skin were activated and released pro-inflammatory chemokines such as CCL2, CCL4, CCL5, CCL7 and the fractalkine receptor (CX_3CL1), which are involved in the recruitment of cells to sites of inflammation or infection post tsetse exposure. Dermal DCs which express CCR7 and have migratory capabilities can are also present in the skin (not characterised by flow cytometry). Neutrophils were recruited from the blood within the first 2 hrs post tsetse exposure (as shown by flow cytometry) through the blood vessels to the site of tissue damage- most likely in a CXCL1/CXCL2 dependent manner based on the upregulation of these chemokines by TLDA. Metacyclic *T. b. brucei* injected into the dermis can also navigate through the anatomy and migrate into the lymphatics (see chapter 5 for further details) and access the draining LN within the first 6 hrs. In the LN, the molecular events within the first 12 hrs involved upregulation of pro-inflammatory chemokines such as CXCL2, CXCL5, CXCL10, CCL7, CCL20 and CCL28. The chemokines upregulated in the draining lymph node can promote recruitment of neutrophils and monocytes. Green arrow= upregulated, red arrow= downregulated chemokines/ cytokines in the skin/LN.

4.4 Discussion of the molecular and cellular events in the skin post tsetse bites

To my knowledge, no study has been carried out to investigate the very earliest events (within 24 hrs) at the inoculation site using the tsetse, and characterisation of the kinetics of these events. Most studies on the immune response in African trypanosomes have been based on intravenous or intraperitoneal routes of infection, which investigated the downstream immune events [359, 361, 362, 383, 384]. Other studies have focussed on events in the stage 2 of the disease in mouse models, especially invasion of the central nervous system [237, 385-387]. As important as these studies are, most have neglected the skin stage of disease, which is the first step in parasite entry into mammals, where parasites encounter cells and interact with host anatomy prior to dissemination into the blood.

This study identified the leukocytes recruited to the skin, and the kinetics of recruitment within the first 24 hrs in response to tsetse exposure. Temporal analysis of the events in the skin revealed that neutrophils were the predominant responders post tsetse exposure. As early as 2 hrs following tsetse exposure, neutrophils rapidly influxed the bite site, with maximum neutrophil numbers at that time point. Neutrophil recruitment appeared to be initiated by

damage caused by the tsetse fly probe rather than parasite entry into the skin, as demonstrated by lack of any statistically significant difference between infected and uninfected tsetse exposed samples. The early influx of neutrophils at the bite site is in agreement with the role of neutrophils as the first responders during wound healing, and clearance of pathogenic substances from tissues [388]. Neutrophils as key players of innate immunity carry out their primary function, which is to protect against bacteria or parasitic infections through their ability to recognize, phagocytose, and destroy pathogenic organisms via the release of proteases and reactive oxygen species [389-392]. Neutrophils also regulate the immune response through the release of IL-1, IL-3, IL-6, IL-12 and TNF-α, as well as chemokines such as CCL2, CCL3, CCL19 and CCL20. Neutrophil recruitment to sites of inflammation could be in response to endogenous factors released from the site of tissue damage, as demonstrated in the influx of neutrophils to laser induced brain injury [393]. This suggests that the initial influx of neutrophils to the bite site may be in response to endogenous factors released following mechanical trauma to the skin by the tsetse fly, the presence of tsetse derived factors in the saliva which could mimic a tissue damage signal, or possibly activate chemokine/chemokine receptor pathway to cause neutrophil recruitment [394].

In cutaneous leishmaniasis delivered by the bite of the sand fly vector, neutrophils recruited to the site of tissue damage have been implicated in two roles in vivo- in protecting the host during infection, and also promoting disease following transmission of parasites [395-400]. The use of sand fly in initiating *Leishmania* spp. infection also demonstrated the persistence of neutrophils at the inoculation site when infected and uninfected sand flies were used for pathogen delivery [165, 339]. In this study however, using infected and uninfected tsetse flies, I do not observe a persistence of neutrophils following tsetse exposure, as observed in cutaneous leishmaniasis. However, the findings here were consistent with the *Leishmania* model, where the vector bite was sufficient to drive in a rapid and robust neutrophil influx irrespective of the infection status of the vector [166].

The saliva of the tsetse fly is made up of a number of substances capable of initiating cellular recruitment, aiding tsetse fly feed, and parasite establishment in the skin of mammals. The tsetse fly saliva constituents include tsetse

thrombin initiator which facilitates blood feeding [401], putative endonucleases such as tsetse salivary gland proteins 1 and 2 [402], and an antigen5 related allergen [403]. The tsetse fly saliva also contains a number of proteins with unknown functions which are essential for the haematophagous behaviour of the tsetse fly by antagonising mammalian host responses such as vasoconstriction, platelet aggregation and coagulation reactions [329, 401, 404]. In the tsetse fly, an anti inflammatory role for the saliva has been described where it biases the host immune response towards a Th2 associated cytokine response, and also enhanced an early onset of infection in mouse models, when blood stage *T. b. brucei* were coinjected with tsetse saliva, compared to wild-type control mice infected without tsetse saliva [186, 188]. The occurrence of a Th2 associated cytokine response due to the saliva components of the vector has also been described in ticks [405, 406]. Similar observations of host immune modulation have been made with the saliva of sand flies in promoting parasite establishment. For example, salivary gland homogenates of *Lutzomyia longipalpis* induced the expression of CCL2, which led to the recruitment of macrophages, while saliva from *Phlebotomus papatasi* also attracted macrophages with increased parasite loads in order to aid parasite dissemination [394, 407]. In general, the saliva of vectors seems to produce an anti-inflammatory response, inhibiting pro-inflammatory responses that help to promote parasite establishment.

T. b. brucei being extracellular parasites, which release a number of proteases, and with rapid motility in vivo was hypothesised to trigger the innate immune response generated by the host post tsetse exposure. To my surprise this was not the case, it appeared that the presence of these extracellular free-living parasites in the skin, which are highly motile did not influence the outcome of the innate immune response within the time points analysed. The findings here are similar to observations in cutaneous leishmaniasis studies using the sand fly, suggesting there is no significant impact of *T. b. brucei* parasites in modulating the early inflammatory response [388, 408]. Although I report in this part of my study that there was no significant difference between infected and uninfected tsetse samples, there is the likelihood that the sample sizes used in this study was not sufficient enough to produce statistically significant difference between

the two groups. Hence, it is important to note this limitation in sample size when considering the findings in this part of the study.

The functional role of neutrophils in pathogenesis, has been described in *Leishmania spp.* infections, where the use of neutrophil replete and deficient mice have been used to describe the Trojan horse hypothesis for *Leishmania* pathogenesis [166, 395]. Depleting neutrophils in our model suggests that the absence of neutrophils at the bite site was not sufficient to impair parasite dissemination or promote host resistance contrary to reports in *Leishmania major* sand fly transmitted infections [166]. *T. b. brucei* parasites did not demonstrate any difference in neutrophil deficient mice compared to neutrophil replete mice, with parasitemia in both groups adopting a similar pattern later on in infection. Neutrophil depletion in cutaneous leishmaniasis promotes host resistance to infection, hence restricting pathogenesis [166]. However, dissemination of *T. b. brucei* from the skin post tsetse exposure appears to be independent of the presence or absence of neutrophils. However, this neutrophil response when present in mice appears to be ineffective in limiting pathogenesis or could potentially suggest that *T. b. brucei* have efficient mechanisms of evading the early neutrophil response [409, 410]. Neutrophils despite possessing a potent arsenal against pathogens, quite a few pathogens have evolved mechanisms to avoid direct killing. These pathogens include *Helicobacter pylori*, *Francisella tularensis*, and *Anaplasma phagocytophilum* [411, 412]. The possibility of such mechanisms in *T. b. brucei* is yet to be investigated.

African trypanosomes being parasites with a digenetic lifecycle, have adapted to surviving in harsh environmental conditions of its hosts i.e. in both the tsetse fly and mammals. A well-defined mechanism for evading the host immune response is the expression of VSGs [9, 15, 16, 205], however, this is only one of several mechanisms employed by African trypanosomes in evading the host immune system. In addition to the switching of the VSG coat, bloodstream form trypanosomes are known to evade host complement activity through the expression of a protein GP63 on its surface, and its rapid motility through its flagellum [220, 233, 237, 240, 413]. The rapid motility of *T. b. brucei* characteristic of the metacyclic and bloodstream stages, which is crucial for infection in the tsetse fly [230], and possibly pathogenesis in mammals, has been described as an immune evasion strategy employed by the parasite to wade off

immune cells [414]. *T. b. brucei* being an extracellular parasite is in constant contact with host tissues, and moves in an ordered sequence in the tsetse fly-travelling from the midgut to the salivary gland, and in mammals travelling from the skin to the bloodstream via the lymphatics [13, 191, 334]. This motility process is an active one, and motility mutants were unable to proceed beyond the midgut of the tsetse fly [230]. In the context of this work, rapid motility by *T. brucei* has been hypothesised to thwart phagocytic processes, in a manner similar to what happens in the bloodstream, where the flagellum removes host immunoglobulin bound to surface VSGs through hydrodynamic forces generated by its rapid movement [240]. Furthermore, in blood stream form *T. b. brucei* there is high-level expression of GP63. GP63 has been identified and extensively studied in *Leishmania* [415, 416] and *Crithidia* [417], prior to the identification of a homologue in *T. b. brucei* [418]. In *Leishmania spp.*, GP63 has been described to play a role in the interaction between infective promastigotes and macrophages. GP63 contributes to the entry and survival of *Leishmania* promastigotes in macrophages [413]. This suggests that metacyclic *T. b. brucei,* like blood stages may also have high expression levels of GP63. Hence, GP63 may likely have a potential role in parasite evasion of host neutrophil response in the mammalian skin, in order for metacyclic *T. b. brucei* to establish itself.

Other recruited cells such as inflammatory monocytes and DCs, which have been observed very early in other parasitic infections such as *Leishmania* [166] and *Plasmodium spp.*, [379] following vector bites were absent in this model at the time points analysed. Intradermal injection of *Plasmodium* sporozoites into the skin, describes a two wave inflammatory response, characterised first by the appearance of neutrophils, followed by the onset of Ly6C^{hi} cells (inflammatory monocytes) from 24 hrs [379, 419]. Inflammatory monocytes were not detected in this study within the first 24 hrs, but might likely appear at latter time points.

In order to understand the inflammatory events occurring at the molecular level, this study identified two chemokine ligands, CXCL1 and CXCL2 that were differentially upregulated in the skin following transcript analysis, and act selectively on neutrophil recruitment [420, 421]. CXCL1 and CXCL2 bind the CXCR2 receptor, which is abundantly expressed on natural killer cells and granulocytes [422, 423]. CXCL1 and CXCL2 are both constitutively expressed in the epithelia and on endothelial cells [424, 425]. The transcript analysis in this

study demonstrated the upregulation of CXCL1 and CXCL2 in the skin post tsetse exposure, suggesting they have a role in neutrophil recruitment, although CXCL2 was downregulated in infected tsetse samples. Pro-inflammatory cytokines such as IL-1 and TNF-α were also upregulated, and have been demonstrated in vitro to induce CXCL2 expression in murine endothelial cells [426]. IL-1 has also been demonstrated in vivo to be an important inducer of CXCL2 expression and subsequently hepatic neutrophil recruitment [427]. CXCL1 and CXCL2 can also act locally to mobilize neutrophils from the bone marrow. This has been demonstrated in a study where CXCL2 was injected into the blood, and resulted in a response that was similar to acute peritonitis when the peripheral neutrophil blood count was analysed [428]. So in the model described in this study, it is most likely that there could be a release of CXCL1 and CXCL2 in the skin through activation of the endothelia, which drives in neutrophils post tsetse exposure to the bite site. It would be interesting to investigate if the absolute copy numbers of the transcripts upregulated in tissues samples, and protein expression levels in tissues would be different between infected and uninfected tsetse samples. This would further define the molecular events occurring in the skin post tsetse bites. It is also important to note that a major limitation of using mouse models is the absent of the chancre at the bite site post inoculation by tsetse flies. However, how the absence of the chancre would impact on the outcome of immune responses when compared to that of cattle/humans is yet unclear.

Taken together, the data here suggests there is no difference in the very earliest immune events in the skin between infected and uninfected tsetse exposed samples. This led me to propose that the very earliest immune events in the skin are driven by mechanical damage caused by the tsetse fly rather than the presence of metacyclic *T. b. brucei*. The findings here using flow cytometry, and transcript analysis of inflammatory mediators support this view. The data here also suggests that neutrophil depletion does not have a significant impact on pathogenesis in mice models. Further studies to identify the components of the tsetse saliva involved in neutrophil recruitment would shed more light on the temporal events occurring in the skin, and how this could be manipulated to further understand the earliest events in African trypanosome pathogenesis in vivo.

5 Imaging African trypanosomes and host interactions

5.1 Introduction

In order to investigate the dynamics of what happens in vivo in the skin during the infection process, it is necessary to have transgenic parasites, and genetically modified mice, which can be used for visualisation of the events [266, 429-432]. The first demonstration of the applicability of imaging infection dynamics in mouse models was in the malaria parasite [322, 433-435]. Using fluorescent sporozoites injected by infected mosquitoes into the skin of anesthetised mice and imaged using a wide field fluorescent microscope, the authors were able to follow the fate of injected sporozoites in vivo [434]. Further studies have also shown the egress of the sporozoites from the skin into blood vessels or the LN via the lymphatics where sporozoites were degraded [183]. In vivo imaging approaches have also helped in understanding the motility behaviour of sporozoites, and how sporozoites invade the liver through Kupffer cells [322, 337, 436]. These observations have provided new insights about our understanding of the infection process in the malaria parasite.

In *Leishmania spp.*, a sand fly delivered pathogen that is the cause of cutaneous and visceral leishmaniasis, which has been studied in detail to provide insights into the events in the skin, direct entry of *Leishmania* into macrophages was thought to occur following deposition by the sand fly [437]. However, through intravital imaging, it has been revealed that neutrophils were recruited to the skin in both infected/uninfected sand fly bites. The neutrophils that were recruited to the skin were found to be infected by *Leishmania*, and these parasites remained viable [165]. Intravital imaging studies revealed that when *Leishmania* infected neutrophils were taken up by macrophages, they could potentially serve as a means of dissemination [165].

In addition to understanding the events that occur in relation to parasite dissemination, intravital imaging has also revealed how the hosts' innate and adaptive immunity is activated. The draining of pathogens from the bite site to the LN has been suggested to initiate an innate immune response, analogous to that seen in non-lymphoid tissues in the LN following the arrival of lymph borne parasites [438]. In *Toxoplasma gondii* infection, neutrophils recruited form dynamic swarms around the foci of infection in the subcapsular sinus of the LN.

This was then followed by the appearance of larger number of neutrophils later, which also formed swarms, suggesting a chemoattractant effect was in operation [152]. Intravital imaging has also helped assess how antigen specific T cells interact with APCs [439-441]. $CD4^+$ T cell effector responses have been visualised in the skin of *L. major* infected animals, which defined two physiologic modes of antigen recognition by activated $CD4^+$ T cells. In the first instance, there was a stable interaction in which T cells were completely arrested, and secondly, the interactions were dynamic during which T cells maintained a scanning behaviour [439]. The study also highlighted the limitations in $CD4^+$ T cell responses to *L. major*, by demonstrating that antigen specific T cell responses in the skin was highly variable, suggesting lack of T cell accessibility in some areas [439]. Together, these studies have demonstrated through intravital imaging important immunological information that would otherwise have been near impossible using conventional techniques.

The life cycle of African trypanosomes begins with an infected tsetse fly injecting metacyclic trypanosomes into the skin. African trypanosomes have been described to be established in the skin, egress from the skin to the lymphatics, and into the blood [189, 191, 442]. *T. b. brucei* were observed to appear in the lymph in goats that were cannulated within 24-48 hrs prior to detection of blood parasites, and prior to the onset of the chancre [191]. A similar observation has also been made in *T. vivax*, suggesting that the lymph is the principal route of dissemination [334]. The damage or wounding to the skin by the tsetse fly also generates the first wave of immune cells that infiltrate the bite site, similar to observations in sterile inflammation and in the sand fly [165, 357, 443].

The Multiphoton Laser Scanning Microscope (MPLSM) can been applied to provide further optical resolution of parasites, and also complement information about the precise location, behaviour, and interactions that occur within host tissues [444, 445]. MPLSM also provides deep tissue imaging, superior spatiotemporal resolution [446], and has been used to reveal that *T. b. brucei* GVR35 invade the meninges as early as day 5 post infection [252].

As already mentioned *T. b. brucei* enter the lymphatics from the skin following tsetse fly bite, but the exact mechanisms of entry and possibility of tropism for lymphatics have not been investigated to date. The detection of parasites in the LN before appearance in the blood by qPCR in chapter 3, and also the detection of *T. b. brucei* in the lymph prior to blood through the cannulation of goats [191], led us to hypothesise that African trypanosomes may exhibit tropism for lymphatics. Here, I used MPLSM to visualise the motility of mCherry tagged *T. b. brucei* in the skin, trafficking of neutrophils to the bite site in response to tsetse fly bites, and egress of *T. b. brucei* from the skin to the lymphatic vessels. All image files were then analysed and movies prepared using Volocity. This was possible through the use of the tsetse fly infection model set up in chapter 3, C57Bl/6 mice, transgenic mice (Prox-1 mOrange and LysM-GFP) and reporter dyes.

5.2 Metacyclic stage *T. b. brucei* can be visualised in the skin

In order to visualise metacyclic stage *T. b. brucei* in the skin of C57Bl/6 mice following successful infection of tsetse flies, anesthetised mice ears were probed using one infected tsetse fly per mouse ear. Mice were placed on a heat mat to keep the body temperature warm, or the microscope stage was pre-heated to 37 °C and used as the base for tsetse fly probes. Tsetse flies were allowed to probe on mice ears until a blood spot/obvious puncture in the skin was visible – for approximately 30 mins. Mice were then prepared and imaged as described in materials and methods.

Once the infected tsetse flies had probed mouse ears, mice were placed under the MPLSM for imaging. *T. b. brucei* were found to be injected into the extracellular matrix, and metacyclic *T. b. brucei* detected using the dermal puncture in the skin as a landmark. Metacyclic *T. b. brucei* were readily found near areas in the skin were the tsetse fly probe was carried out and was visualised approximately 30 mins post tsetse bite. Approximately 5-10 metacyclic *T. b. brucei* were visualised at the bite site, and parasites were spread over the different areas of the skin were tsetse fly probes had taken place. Metacyclic *T. b. brucei* were located in the dermis of the skin and

exhibited vigorous cell motility (Figure 5.1A). *T. b. brucei* motility might be driven by the flagella from the tip to the base, and the cells moved for extended periods in one direction, tumbled or occasional spinning as previously described [447].

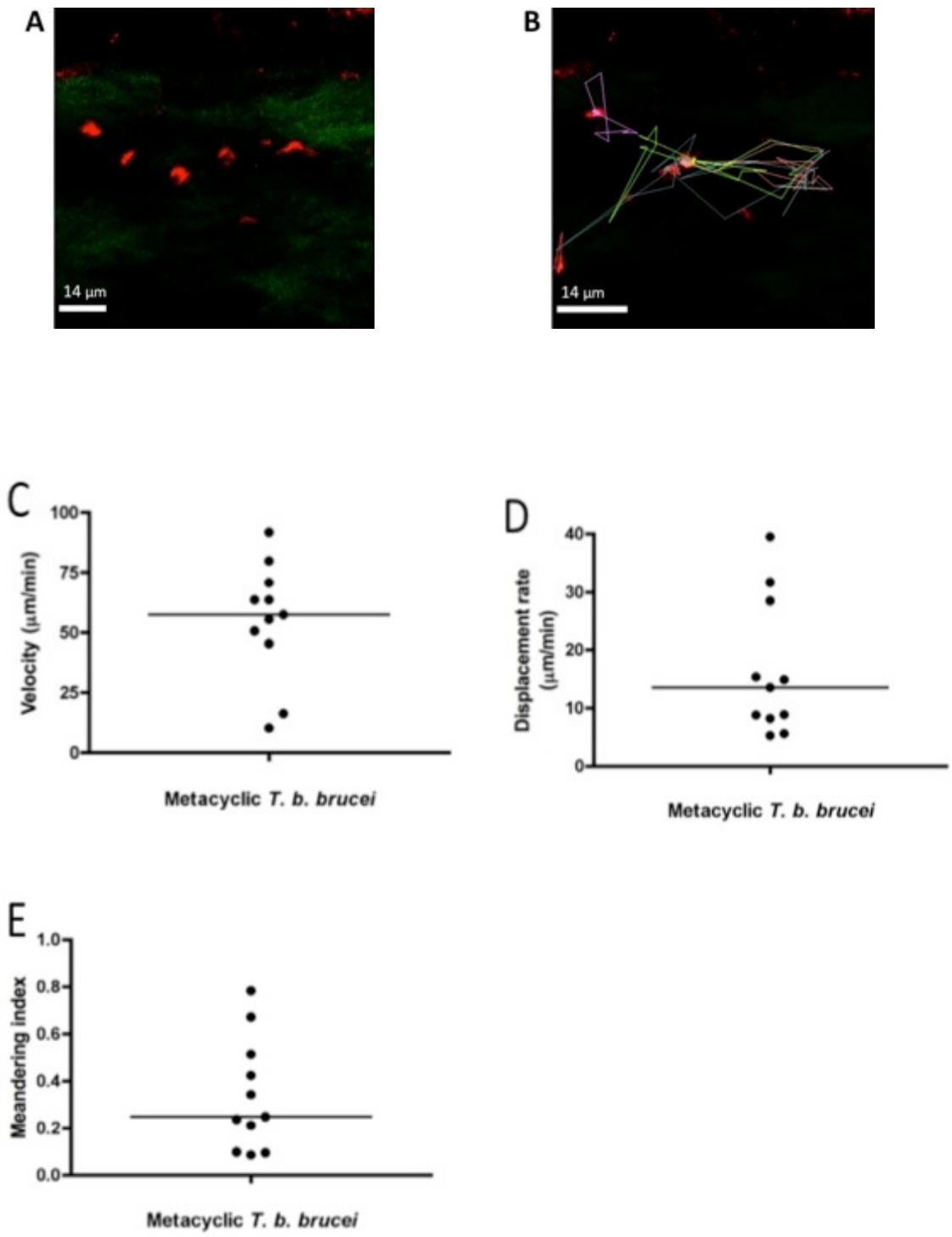

Figure 5-1 Visualising metacyclic *T. b. brucei* in the skin
Following infected tsetse fly bites in the ear pinna of anesthetised C57Bl/6 mice, mouse ear was prepared for imaging immediately after tsetse fly probe. *T. b. brucei* were imaged in the skin within 30 mins post tsetse fly bite. Image acquisition under the MPLSM was carried out for ≥ 20 mins. Laser generation of the second harmonic signal shows collagen as green. (A) Representative

image of metacyclic *T. b. brucei*, (B) volocity software was used to track metacyclic *T. b. brucei* to allow calculation of, (C) velocity, (D) displacement rate, and (E) meandering index. Values represent data showing the median as indicated using the horizontal bar. Data represents tracks pooled from 2 independent animals, scale bar denotes 14 μm. No significant differences were observed between the two independent animals (P>0.05; 2 tailed Mann Whitney U test).

In vitro experiments on blood stream form African trypanosomes have reported high swimming velocities of 20 μm/s, and that trypanosomes are capable of highly directional cell motility [447]. The tracking of *T. b. brucei* in the skin (Figure 5.1B) enabled the calculation of motility parameters related to metacyclic *T. b. brucei* in the skin, such as the meandering index, displacement and velocity using Volocity software (Improvision). Motility of *T. b. brucei* in the skin gave median velocity of 57.42 μm/min (Figure 5.1C), and median displacement rate (shortest distance between two positions at two time points) of 13.56 μ/min (Figure 5.1D). The meandering index (the total displacement/path length of a cell track) allowed for a more detailed analysis of the straightness of *T. b. brucei* with a value of 1 representing a completely linear track. As shown in Figure 5.1E, metacyclic *T. b. brucei* had a median meandering index of 0.25.

Entry of malaria sporozoites into blood vessels following *Anopheles* mosquito injection into the dermis in *P. yoelii* and *P. berghei* has been reported [321]. Given the previous data indicating that trypanosomes migrate via lymphatics, I speculated that I would not be able to detect *T. b. brucei* entering skin blood vessels following tsetse fly bite. To test this, blood vessels of C57Bl/6 mice were labelled intravenously (i.v.) using a vascular tracer dye, by injection of 70 Kda dextran conjugated with fluorescein isothiocyanate (FITC). I report here that metacyclic *T. b. brucei* imaged were highly motile, and no parasites were detected inside blood vessels (Figure 5.2A).

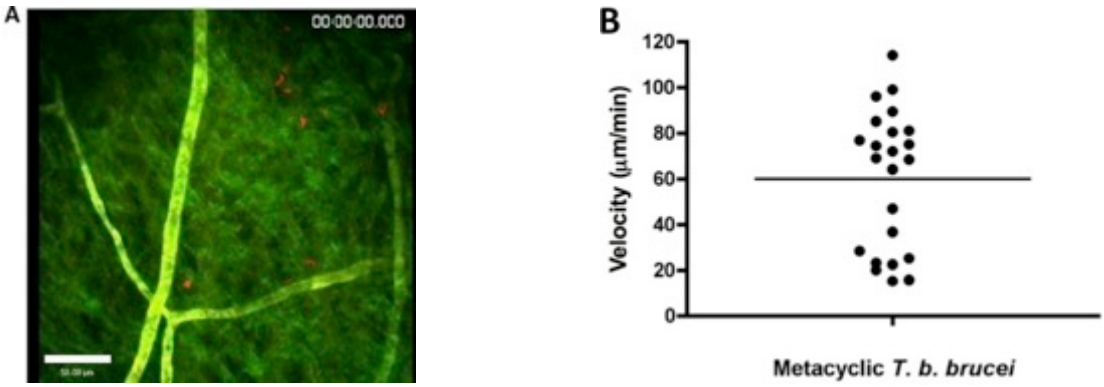

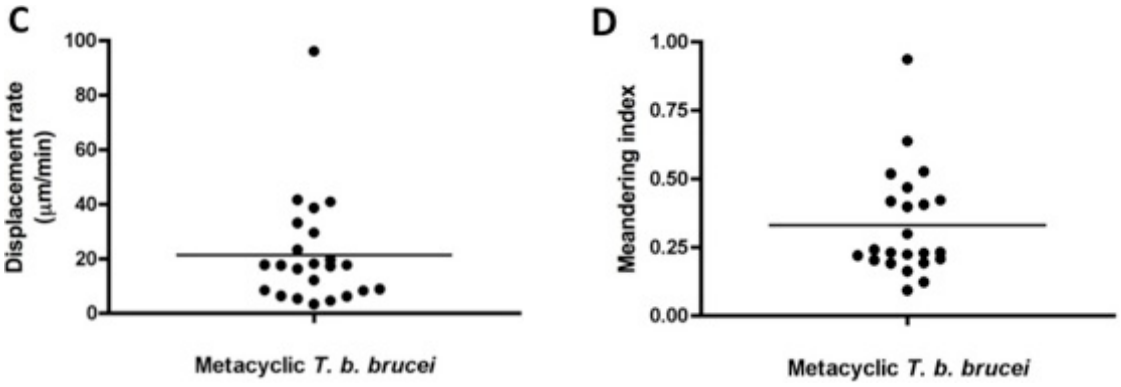

Figure 5-2 Metacyclic *T. b. brucei* parasites do not enter skin blood vessels
Following infected tsetse fly bites in the ear pinna of anesthetised C57Bl/6 mice, mouse ear was prepared for imaging immediately after tsetse fly probe. C57Bl/6 mice were injected i.v. with FITC dextran to label blood vessels. Blood vessels (green) and laser induced second harmonic signal appears green for collagen. *T. b. brucei* were imaged in the skin within 30 mins of tsetse fly bite. Image acquisition under the MPLSM microscope was carried out for ≥ 20 mins. (A) Metacyclic *T. b. brucei* in the skin with labelled blood vessels, (B) velocity, (C) displacement rate, and (D) meandering index. Horizontal bar shows the mean. Data represents tracks pooled from 2 independent animals, scale bar denotes 50 μm.

From the movies acquired, blood flow was still apparent indicating that the mouse was alive. Also in the movies of the mice acquired, I could visualised cells moving through the blood vessls potentially leukocytes. Metacyclic *T. b. brucei* had mean velocity of 59.46 ± 30.41 μm/min (Figure 5.2B), and displacement rate of 21.33 ± 20.08 μm/min (Figure 5.2C) respectively. Meandering index of metacyclic *T. b. brucei* was 0.33 ± 0.19 (Figure 5.2D).

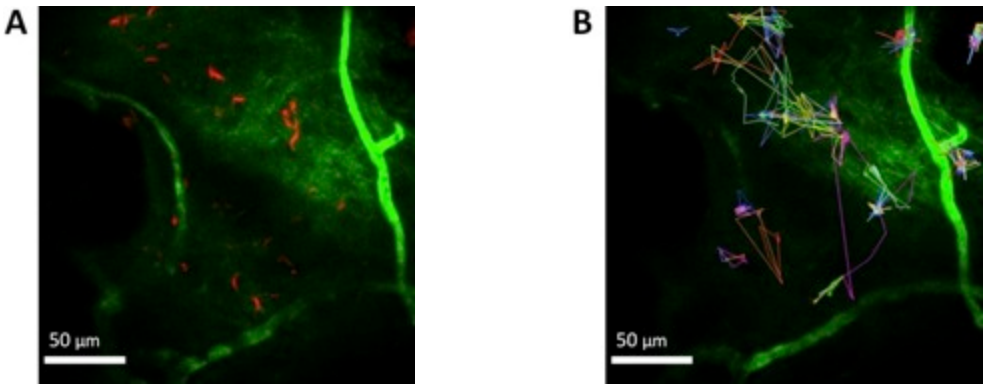

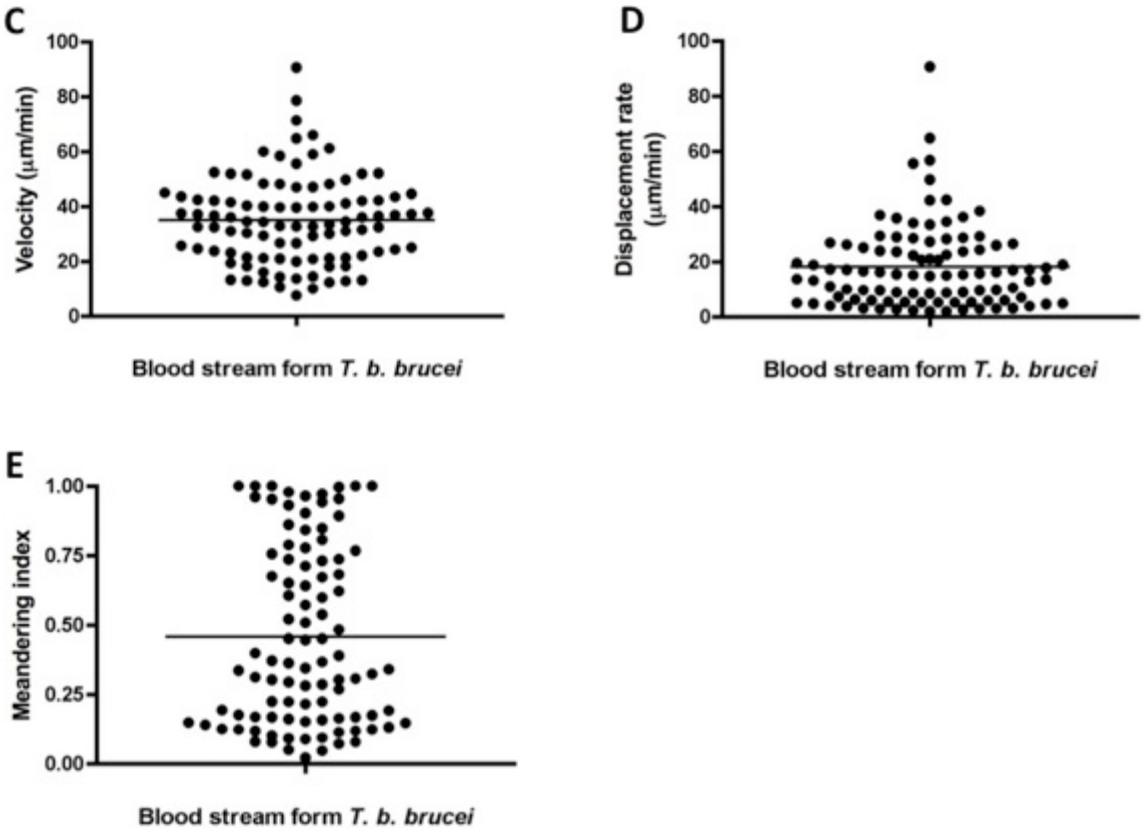

Figure 5-3 Bloodstream form *T. b. brucei* parasites do not enter skin blood vessels
Following injection of bloodstream form *T. b. brucei* intradermally into the ear pinna of anesthetised C57Bl/6 mice, mouse ear was prepared for imaging. C57Bl/6 mice were injected i.v. with FITC dextran to label blood vessels. Blood vessels (green) and laser induced second harmonic signal appears green for collagen. *T. b. brucei* were imaged in the skin within 10 mins of intradermal injection. Image acquisition under the MPLSM microscope was carried out for ≥ 30 mins. (A) *T. b. brucei* in the skin with labelled blood vessels, (B) tracked *T. b. brucei* to allow for calculation of, (C) velocity, (D) displacement rate, and (E) meandering index. Horizontal bar shows the mean. Data represents tracks pooled from 2 independent animals, scale bar denotes 50 μm.

As a control in this study, I also injected 1 x 10^6 blood stream form parasites into the skin, and no blood stage *T. b. brucei* were detected in blood vessels in the skin (Figure 5.3A). Blood stream form *T. b. brucei* had a mean velocity and mean displacement rate of 34.94 ± 16.04 (Figure 5.3C) and 18.19 ± 15.32 μm/min (Figure 5.3D), respectively, and mean meandering index of 0.46 ± 0.32 (Figure 5.3E). Mean velocity of metacyclic *T. b. brucei* was significantly different from blood stream form *T. b. brucei* (Figure 5.4A; $P<0.0001$), while the displacement rate and meandering index were not significantly different (Figure 5.4B & 5.4C).

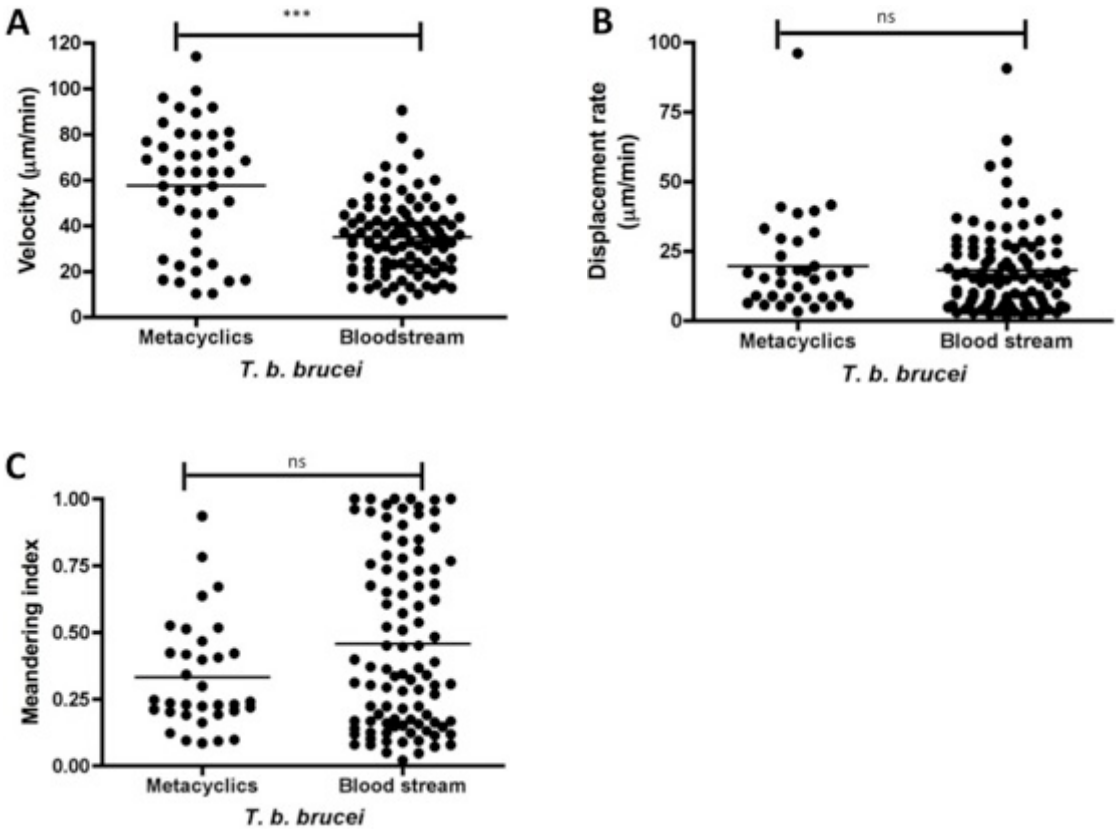

Figure 5-4 Metacyclic *T. b. brucei* migrate faster than blood stream forms.
Statistical analysis was carried out on velocity, displacement rate and meandering index of Metacyclic and blood stream form *T. b. brucei* injected into mice ears. (A) velocity (***p<0.0001), (B) displacement rate (not significant) & (C) meandering index (not significant). Data were pooled from 3 independent animals, and a 2 tailed unpaired t-test used for statistical analysis.

These results suggested that rapid motility might be a crucial step for metacyclic *T. b. brucei* dissemination from the skin. Furthermore, the absence of *T. b. brucei* metacyclics or bloodstream forms in skin blood vessels suggested that lack of penetration of blood vessels might not be dependent on the life cycle stage of *T. b. brucei* injected into the skin, and that *T. b. brucei* may not disseminate via skin blood vessels, consistent with previous studies. A few parasites were also observed in the dermis near hair follicles (data not shown), which are immune privileged sites.

It is also important to mention that metacyclic *T. b. brucei* could still be visualised in the skin for at least 2 hrs post tsetse transmission. In summary, *T. b. brucei* was not detected in the blood vessels of C57Bl/6 mice when both metacyclic and blood stream stages were injected via the tsetse fly and needle. *T. b. brucei* exhibited tumbling motion with significantly higher velocity in metacyclic *T. b. brucei* than blood stream stages in the skin. MPLSM imaging was

carried out using 800 nm and 1200 nm excitation wavelengths for imaging parasites and blood vessels in vivo.

5.3 Neutrophils can be imaged in the skin following infected tsetse fly bites and do not form dynamic clusters

In chapters 3 & 4, it was established that *T. b. brucei* remained in the skin and neutrophils were recruited to the bite site following tsetse fly probe in the skin. My findings were in agreement with previous work that skin wounding was sufficient to cause recruitment of phagocytes to site of injury [448]. It was also shown that there were no significant differences in neutrophil absolute numbers between ears exposed to infected and uninfected tsetse flies. Through intravital imaging, the previous section has also established that indeed, *T. b. brucei* were present in the skin and could differentiate into long slender forms in the skin based on preliminary experiments carried out in the lab. So I sought to ask if I could visualise the trafficking of neutrophils to the bite site, investigate the behaviour of neutrophils, and possibly image the interactions between *T. b. brucei* and neutrophils using LysM-GFP reporter mice. Although I had previously established that neutrophil recruitment was independent of the presence of trypanosomes, I carried out further investigations with neutrophils to examine if there was formation of NETs, which is found in other intracellular parasites and bacteria infections.

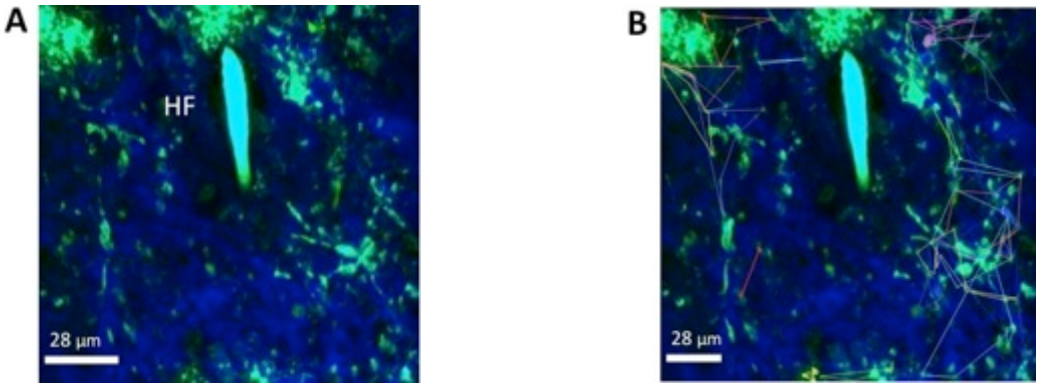

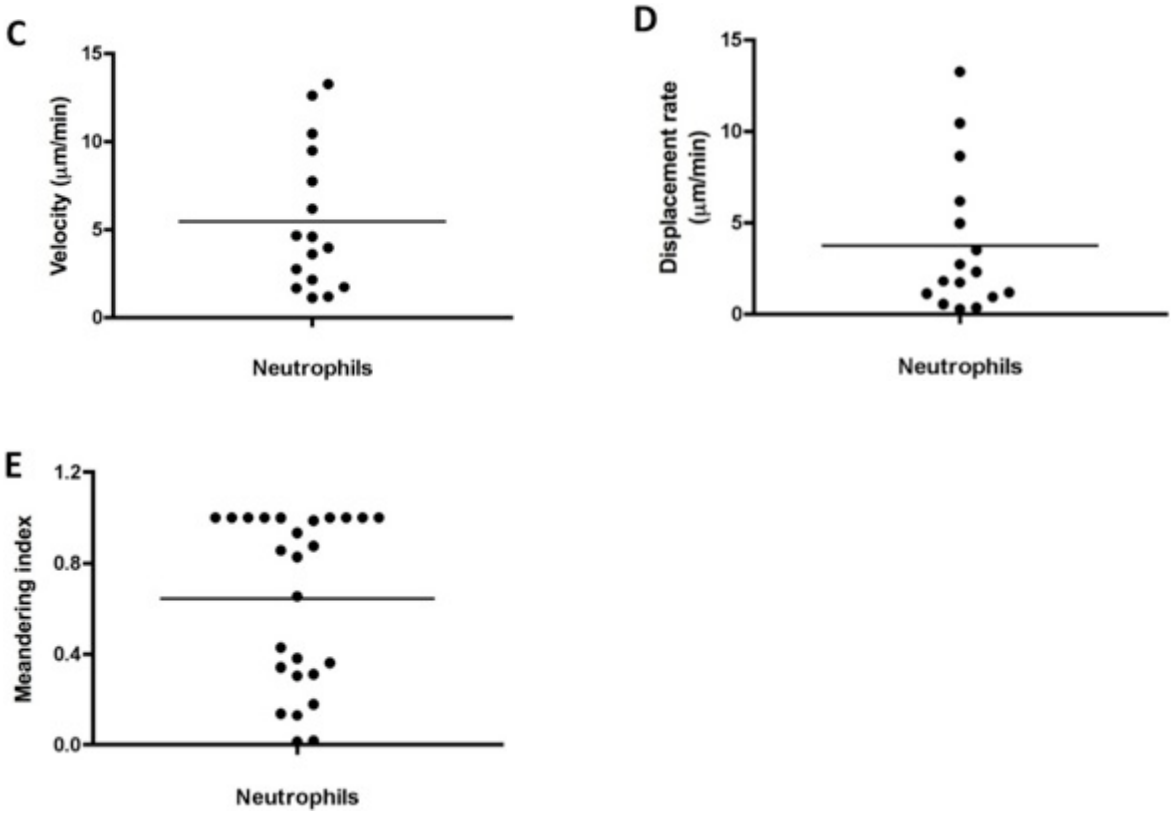

Figure 5-5 Neutrophils do not swarm following inoculation of metacyclic *T. b. brucei*. Following infected tsetse fly bites in the ear pinna of anesthetised LysM-GFP reporter mouse, mouse ear was prepared for imaging 3 hrs post tsetse fly probe. Laser generation of second harmonic signals was used to visualise collagen (blue). Neutrophils were imaged for ≥ 20 mins. (A) Neutrophils migration to the bite site, hair follicle (HF), (B) neutrophil tracks to allow calculation of, (C) velocity, (D) displacement rate, and (E) meandering index. Data represents tracks from 2 independent animals, horizontal bar shows the mean. Scale bar denotes 28 μm.

LysM-GFP mouse expressed a green fluorescent protein under the control of the lysozyme M (LysM) promoter [267]. LysM is expressed specifically by macrophages and neutrophils [449], and the LysM-GFP mouse is well established in investigating neutrophil recruitment. In this mouse, endogenous neutrophils are brightly labelled, while macrophages and monocytes are labelled to a lesser extent [267, 450]. LysM-Gfp mice has been used in investigating leukocyte trafficking in pulmonary inflammation, where the neutrophils recruited formed dynamic clusters [451], in intracellular infections such as *Toxoplasma gondii*, where the parasites invade neutrophils recruited to the small intestine and use as a potential mechanism for spreading infection [452], and also in *Leishmania* infections for investigating the behaviour of neutrophils following sand fly bites [326].

Within 3 hrs of tsetse fly probe to the ear, neutrophils were rapidly recruited to the site of tissue damage, visualised and movies acquired. As shown in Figure

5.5A, there was migration of neutrophils in a directed manner, with a mean velocity of 5.45 ± 4.08 μm/min (Figure 5.5C) and displacement rate of 3.75 ± 3.90 μm/min (Figure 5.5D). Migrating cells exhibited very little deviation from their path, indicated by the meandering index as a measure of directionality: 0.64 ± 0.38 (Figure 5.5E), and recruited cells remained around the site of injury. In other models of inflammation, neutrophil swarms have been reported [431]. I observed that there was no formation of neutrophil swarms at the site of tissue injury. I was however unable to visualise *T. b. brucei* and neutrophils together simultaneously, due to spectral overlap. However, neutrophils were detected in the same plane as *T. b. brucei*.

In summary, these results reveal a notable behaviour of neutrophils in African trypanosome infections, which is absence of neutrophil swarms and rapid recruitment of neutrophils to the site of tsetse fly probe.

5.4 African trypanosomes migrate towards lymphatic vessels

To date no study has demonstrated whether *T. b. brucei* have preference for lymphatics in mammalian hosts. From my data in chapter 3 where *T. b. brucei* were detected in the LN within 6 hrs, I postulated that African trypanosomes might have tropism for lymphatic vessels. To test this hypothesis, I began by injecting lymphatic vessel endothelial hyaluronan receptor-1 (Lyve-1) antibodies to label lymphatics. This was unsuccessful, and I subsequently switched to the use of Prox-1 mOrange mice to investigate interactions of *T. b. brucei* with lymphatic vessels.

5.4.1.1 Imaging lymphatic vessels using Prox-1 mOrange

Following the unsuccessful application of lyve-1 antibody in imaging lymphatic vessels and fluorescent trypanosomes, a transgenic reporter mouse, Prox-1 mOrange was then used. These transgenic mice have a lymphatic endothelial cell specific *Prox1* promoter-driven fluorescent reporter, and *Prox1* is faithfully expressed on lymphatic endothelial cells [268, 269]. In Prox-1 knockout mice, lymphatics do not develop, whereas blood vessels appear normal [453]. The use

of transgenic constructs under *Prox1* transcripional control has been used in studies of dendritic cell migration, lymphatic vessel morphology during the early phases of cutaneous inflammation and in lymphangiogenesis [454]. In this study, the first set of experiments performed was to visualise lymphatic vessels under the MPLSM prior to infection studies.

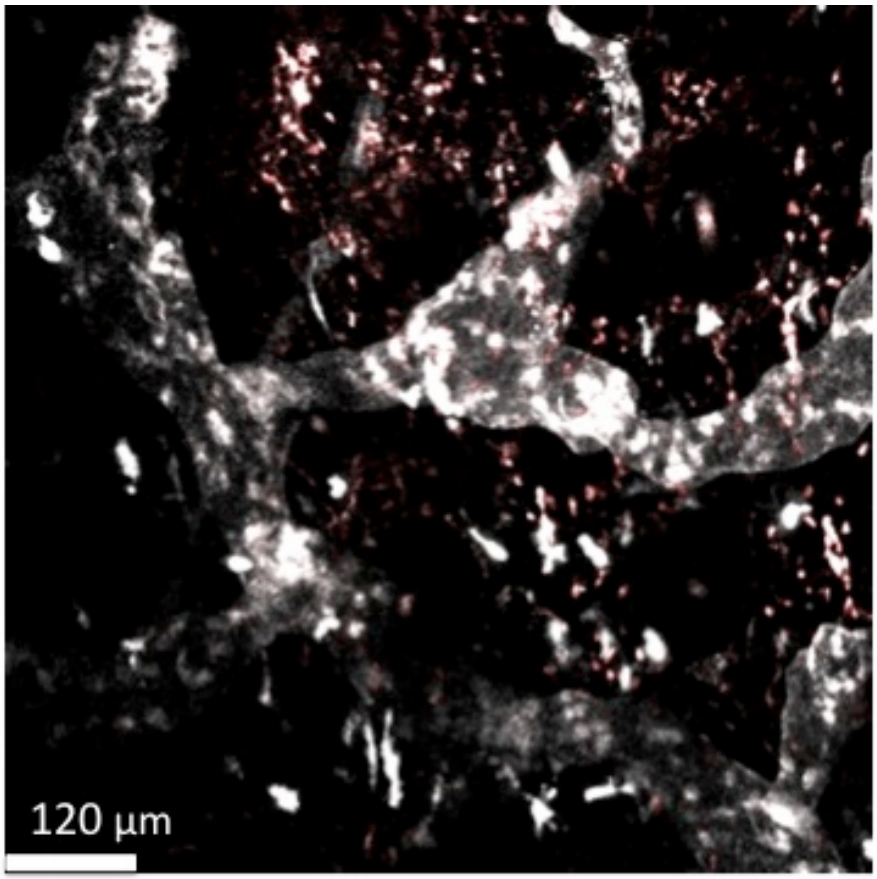

Figure 5-6 Visualising lymphatic vessels in Prox-1 mOrange mice.
Prox-1 mOrange mice was anesthetised and prepared for ear imaging as previously described in the materials and methods. Lymphatics in the ear of Prox-1 mOrange mice were imaged at 800nm and 1200 nm excitation wavelengths. The distinctive oak leaf patterning of lymphatic endothelial cells in the lymphatic vessels was detected shown in white, lymphatic vessels reveal blind endings and lymphatic vessels in the skin have irregular sizes compared to blood vessels (e.g. Figure 5.2A), Scale bar: 120 µm. Representative image of several images collected.

Lymphatic vessels were visualised in the ear skin of Prox-1 mOrange mouse. Lymphatic vessels appeared wider and more irregular shaped than blood vessels (Figure 5.2A), and formed a network of vessels (Figure 5.6). Lymphatic vessels displayed lack of uniformity in size compared to blood vessels, and possessed blind endings.

In summary the ear skin of Prox-1 mOrange mouse has irregular anastomoses of lymphatic vessels with blind endings in the dermis of the skin, and were wider than blood vessels.

5.4.1.2 *T. b. brucei* penetrate skin lymphatic vessels

In the previous section, it was established that Prox-1 mOrange mice lymphatic vessels were sufficiently bright for MPLSM imaging and the settings optimised.

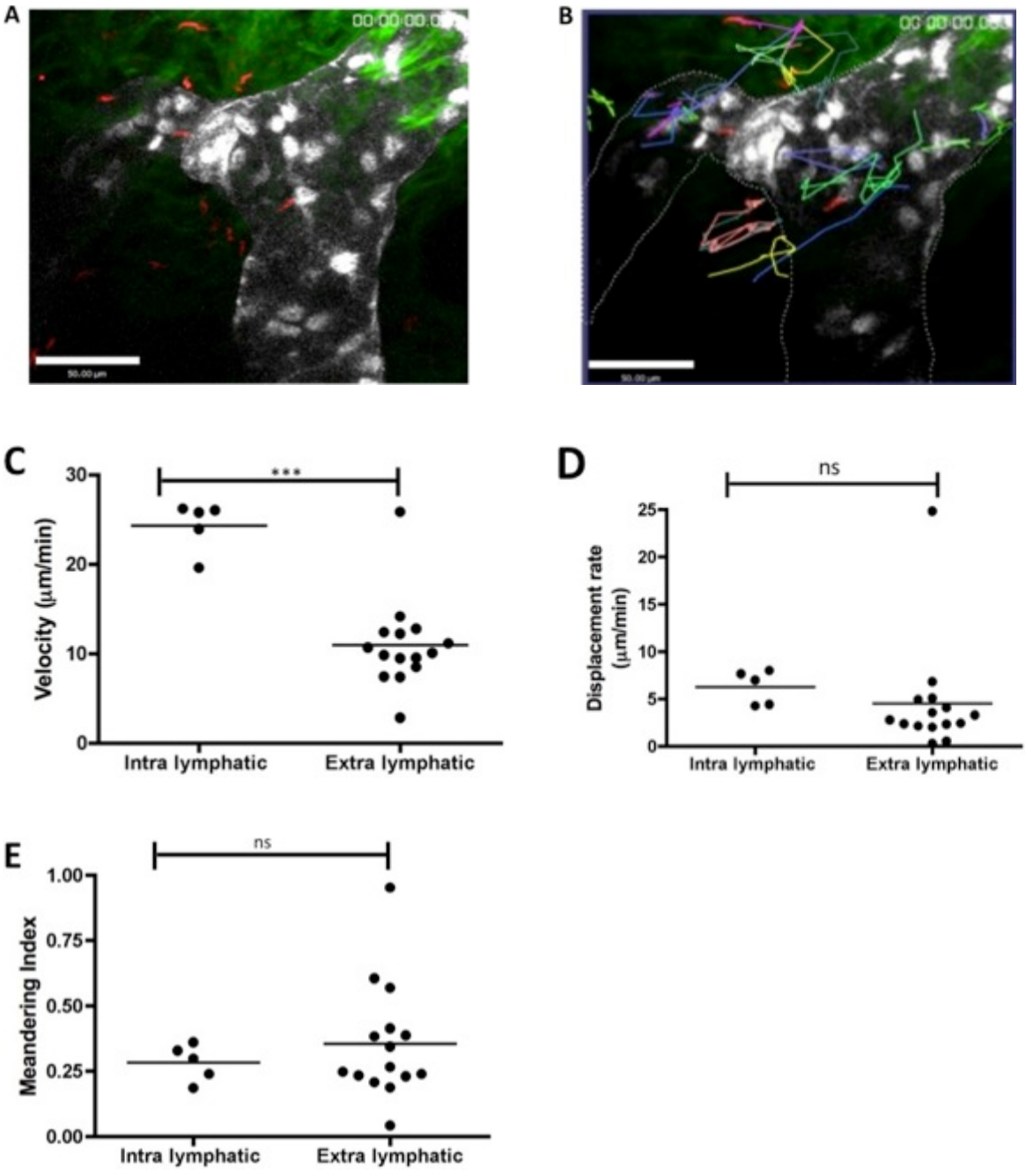

Figure 5-7 *T. b. brucei* migrates into lymphatic vessels.
$1x10^6$ bloodstream *T. b. brucei* were injected intradermally into the ear pinna of mice and imaged after 1 hr. Mouse ear was prepared for imaging as described in the materials and methods.

Collagen was visualised using second harmonic signal from the laser, indicated as green (A) Intra and Extra lymphatic *T. b. brucei* (B) dotted lines indicate the outline of the lymphatics, tracked to calculate (C) velocity, (D) displacement rate, and (E) meandering index for intra/extra lymphatic *T. b. brucei* respectively. Data presented in the plots show mean as indicated with the horizontal bar, [(***P<0.0001; not significantly different (ns), statistical analysis was calculated using 2-tailed, unpaired t-test)].

The next approach was to ask if I could image the lymphatic vessels and mCherry *T. b. brucei* simultaneously, and possibly visualise trypanosomes entering lymphatics. To answer this question, Prox1-mOrange mice were intradermally injected with 1 x 10^6 blood stream form *T. b. brucei* in the ear pinna. Following injection, mice were left for approximately 1 hr, before MPLSM imaging. Once the mice ears were prepared and imaged, I observed that most of the parasites injected into the skin remained extra lymphatic, residing in the extracellular matrix of the skin. However, to my surprise, I observed that a few parasites were intra lymphatic, and all parasites imaged were in the same plane with the lymphatic vessels.

Hence, through intravital imaging and single cell tracking it was revealed that *T. b. brucei* parasites were both intra and extra lymphatic, and were highly motile in the lymphatic vessels (Figure 5.7A&B). It was surprising to detect intra lymphatic *T. b. brucei,* because previous imaging experiments carried out using infected tsetse flies and intradermal injection of blood stream form *T. b. brucei* had not shown the presence of parasites in the lymphatics. *T. b. brucei* were tracked (Figure 5.7B), and the following motility parameters computed: velocity, displacement rate and meandering indices. Following extrapolation of the parameters, and relating each parameter to parasites individually tracked, I found that *T. b. brucei* within the lymphatics had a significant increase in velocity than those that were extra lymphatic (24.25 ± 1.3 and 11.01 ± 1.32 μm/min; P<0.001, Figure 5.7C). The mean displacement rate (6.29 ± 0.81 and 4.51 ±1.52 μm/min; Figure 5.7D), and mean meandering index (0.28 ± 0.03 and 0.35 ± 0.06; Figure 5.7E) for both intra and extra lymphatic *T. b. brucei* were not significantly different.

The detection of *T. b. brucei* in the lymphatics in this study is novel, and demonstrated that there may be a tropism for lymphatics by *T. b. brucei* due to the movement of some of the parasites towards the lymphatic vessels. Hence,

these observations led to further investigate whether the entry into lymphatics was chemokine mediated, specifically CCL21.

5.4.1.3 *T. b. brucei* do not migrate towards CCL21 in vitro

Following the detection of intra lymphatic *T. b. brucei* within 2 hrs of intradermal ear injections, I then attempted to decipher how these trypanosomes gain access to lymphatic vessels. To address this question, I investigated the role of a chemokine, CCL21, in chemotaxis of *T. b. brucei* towards lymphatic vessels. CCL21 is a chemokine involved in lymphocyte recruitment and is highly expressed on high endothelial venules (HEVs) and lymphatics [455, 456]. CCL21 was chosen as the chemokine to be tested because of the role it plays in lymphocyte recruitment to LNs via HEVs, and in DC transmigration through lymphatic vessels. This was tested in vitro using a transmigration assay (see materials and methods) that was set up to include different concentrations of recombinant CCL21, and 1 x 10^5 *T. b. brucei* added to the wells to assess chemotaxis.

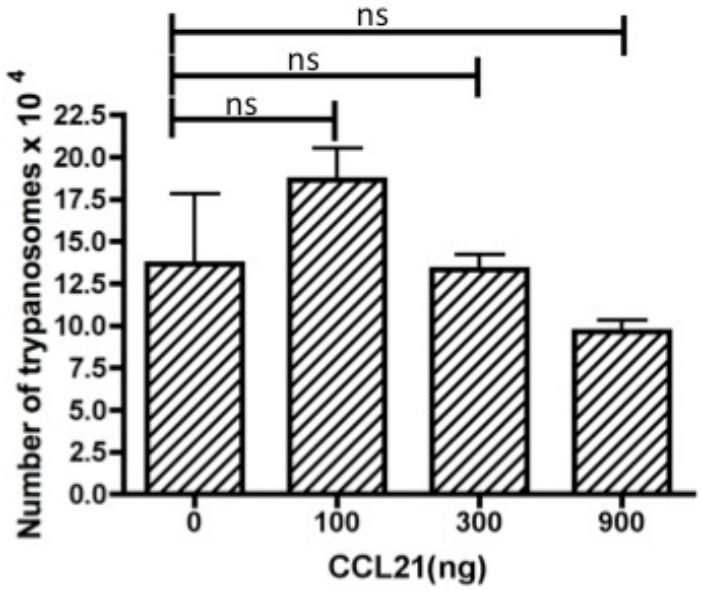

Figure 5-8 There is no chemotaxis of *T. b. brucei* towards CCL21.
Chemokine concentrations of 0, 100, 300 and 900 ng of CCL21 were added to media, and incubated with the transmembrane for 10 mins at 37 °C, 5% CO_2 for equilibration to occur. 10^5 *T. b. brucei* was added to the different chemokine concentration gradients and incubated for 7 hrs. Using a haemocytometer to count parasites, 10 µl of media containing transmigrated parasites was added and counted under a compound microscope. There were no statistically significant (ns) differences when compared to untreated controls (0 ng), statistical analyses was carried out using 2-tailed unpaired t test. Data presented in the bar graphs were mean ± SEM, n=3, for 3 independent experiments.

Following incubation for 7 hrs, the data suggests no statistically significant difference between *T. b. brucei* that were incubated in at the different CCL21 concentrations (Figure 5.8). Seven hours incubation was chosen because at later time points, *T. b. brucei* began to die and exhibit reduced motility, while at earlier time points only few parasites had migrated across the membrane. In the absence of CCL21, *T. b. brucei* were still able to migrate across the membrane at a similar rate compared to when 300 ng CCL21 was added.

Together, the data suggests that there is no chemotaxis of *T. b. brucei* towards CCL21.

5.5 General summary

In this chapter I started by stating that I had shown in chapter 3 that *T. b. brucei* was detected in the LN from 6 hrs, and in chapter 4, neutrophils trafficked to the bite site following tsetse fly bites (infected and uninfected). Here, I have gone a step further to visualise interactions of *T. b. brucei* and its host spatiotemporally using the MPLSM. Firstly, metacyclic *T. b. brucei* were visualised for the first time directly in the extracellular matrix of the skin after tsetse fly probes, and these parasites were very motile (significantly more so than bloodstream forms). I also demonstrated that *T. b. brucei* were not detected in blood vessels in the skin immediately after a tsetse fly probe or intradermal needle injection of blood stream stage *T. b. brucei*. In addition, it was shown using LysM-GFP reporter mice that the recruitment of neutrophils to the bite site was rapid and did not result in the formation of swarms.

Lastly, using the Prox-1 mOrange mice, it was demonstrated that *T. b. brucei* that were intra lymphatic behaved differently from those that were extra lymphatic, and also present data suggesting CCL21 is not involved. The data here may also suggest the possibility of tropism for lymphatic vessels by *T. b. brucei,* when injected into the skin. Altogether, in this chapter I present novel data specifically shedding light on *T. b. brucei* dissemination from the skin to lymphatic vessels in Prox-1 reporter mice through intravital imaging studies. The key findings of this chapter are discussed below.

5.6 Discussion

To evaluate interactions that occur between *T. b. brucei* and its host following tsetse fly bites, I used the 247 strain of *T. b. brucei* that was pleomorphic and had been successfully used to infect tsetse flies in chapter 3. This strain was also used in characterising the nature of the early immune events in the skin, which identified neutrophils as the main cells recruited. Once infected tsetse flies had probed into the skin, metacyclic *T. b. brucei* were imaged under the MPLSM. *T. b. brucei* metacyclics were actively motile and navigated rapidly through the skin. Motility in African trypanosomes has been a subject of interest, as parasite movement in specific host tissues are key events in pathogenesis, immune evasion and disease transmission. Motility in African trypanosomes is driven by a single flagella that runs across the cell, laterally connected to the cell body [220], and is important for the establishment of infection in the tsetse fly and possibly in mammalian hosts.

In the blood stream, rapid motility of *T. b. brucei* helps to evade antibody clearance. Antibodies that bind the VSGs expressed on *T. b. brucei* were sorted from the surface to the flagellar pocket where they are internalized and endocytosed [240]. The hydrodynamic forces required for sorting antibodies from the surface of trypanosomes are produced by forward motility of *T. b. brucei*. This was described through RNAi mediated transcript depletion of genes to inactivate trypanosome endocytosis (by targeting clathrin) [457], cell directionality (by targeting flagellum adhesion glycoprotein, *fla1*) [458], or plasma membrane recycling (by targeting actin) [230]. Of significance was that the removal of *fla1* resulted in a loss of antibody-VSG complex sorting to the posterior, consequently blocking the first step of antibody clearance [240]. Hence besides antigenic variation as the well known mechanism applied by trypanosomes to evade immune responses [9], directional cell motility and plasma membrane recycling functions cooperate in removing host antibodies [240]. The findings established that physical flow forces generated by the beat of the flagella while swimming were essential not only for motility but also survival in the blood stream of mammals. This further suggested that high cellular motility might be essential for parasite survival [219, 223, 224].

In the tsetse fly, motility is important for infection of the salivary glands to occur. *T. b. brucei* forward motility is essential for migration in the tsetse fly [230]. Inducible RNAi silencing of the dynein intermediate chain (DNAI1) of the flagella axoneme led to a loss of trypanosomes ability for propulsive wave and forward motility [217]. Motility impaired trypomastigote parasites were unable to complete the first crucial step in infection, which was migrating from the foregut to the midgut, although they could still proliferate, albeit at half the normal duplication rates [230]. This observation of the importance of motility in the tsetse fly has led to investigations of the potential impact of motility mutants in pathogenesis in mammals [232]. In order for African trypanosomes to migrate from the skin into the lymphatics and then the draining LN, motility is most likely essential. My data suggests that metacyclic *T. b. brucei* have a significantly higher velocity than bloodstream form *T. b. brucei*, which may serve an advantage in establishing and migrating rapidly to the skin lymphatics.

In addition, intra lymphatic *T. b. brucei* showed a significant increase in velocity, compared to extra lymphatic *T. b. brucei,* which is a key step in systemic dissemination [191, 334]. However, it was also observed that the mean velocity of blood stage parasites in the extravascular matrix of Prox-1 mOrange was slightly more than those on C57Bl/6 mice. This difference though not significant, could be due to the differences associated with the use of transgenic mice in this study, or possibly suggests the need for more replicates to further verify my findings. Data here shows that *T. b. brucei* may need to navigate quickly through the skin in order to survive the immune assault of the host, thrive in its new environment, and disseminate into the blood, via the lymphatics. In stage 2 of HAT, penetration of the vascular endothelium or the CNS by blood stream form *T. b. brucei* requires actively motile parasites [252]. In a study to decipher the role of motility mutants in vivo with blood stream form *T. brucei* 427 (monomorphic parasites), it was shown that *T. b. brucei* propulsive motility was dispensable for blood stream form infections [232]. The authors concluded that motility made no difference in their model through intraperitoneal injections. However their study has some drawbacks, which include; the use of an acute infection *T. b. brucei* model, so migration of *T. b. brucei* into the brain could not be monitored. Secondly, the route of infection was intraperitoneal, hence neglecting the skin stage as well as lacking the

appropriate parasite life cycle stages (i.e. metayclics), resulting in a model that does not accurately mimic establishment of infection and parasite dissemination [191]. So in the context of my work, I would argue that motility mutants of *T. b. brucei* transmitted through the tsetse fly into the skin might be unable to establish parasitemia in mammalian hosts. Motility mutants of metacyclic *T. b. brucei* may become trapped in the skin, allowing the immune system to clear the infection.

The data in this study also did not detect *T. b. brucei* in blood vessels following tsetse fly. This is in contrast to what has been seen in *Plasmodium spp* sporozoites injected by the mosquito bites. Sporozoites were shown to rapidly migrate into both blood and lymphatic vessels [183, 434]. Most of the sporozoites released by the mosquito enter into the dermis of the skin and glide into blood vessels, while the few that migrate into lymphatics, remain in the LN where they were killed [183]. The lymphatic route of sporozoite dissemination for malaria parasites appeared to be a dead end. In contrast, in this study, I report the presence of *T. b. brucei* into only the lymphatics; *T. b. brucei* were not detected in blood vessels (either metacyclic or blood stream forms of *T. b. brucei*), despite repeated trials using both tsetse fly inoculation and needle injection of blood stream form *T. b. brucei*. The absence of *T. b. brucei* in blood vessels post tsetse fly bite reflects the importance of the intravital imaging tools in understanding *T. b. brucei* pathogenesis in vivo. It also agrees with previous reports that the lymphatics is a route of dissemination of parasites [191, 334].

In mammals, apart from laboratory rodents that have been used for experimental *T. brucei* infection studies via the tsetse fly, there is the development of a chancre (skin lesion) in the skin within 4-5 days [333]. In the chancre, *T. b. brucei* were observed to proliferate, and neutrophils detected at day 11-post infection [13, 191, 333, 459]. Although there was no chancre observed in our mouse model, which might suggest a difference in immune response in humans or cattle. This difference is a limitation of the study in using mice models for analysing the earliest interactions in the skin. *T. b. brucei* also remain in the skin as detected by MPLSM imaging for at least 24 hrs post tsetse fly bites and qPCR data in chapter 3, suggesting that the skin may be a ‘reservoir’ for *T. b. brucei*. In *Plasmodium spp.*, sporozoites have been shown to remain and differentiate into merozoites in the skin, and serve as a potential

source of parasitemia in relapsing infections [337]. Though there is no direct evidence to prove a similar phenomenom happens in *T. b. brucei*, this possibility can't be ruled out. Here, I observed that some *T. b. brucei* remain in the skin and differentiate into blood stages within 20 hrs post infected tsetse fly bites, though the fate of these parasites in the skin is yet unclear.

Next, I investigated the recruitment of neutrophils to the bite site following tsetse fly bites, since they were already identified as the first cells recruited to the tsetse fly bite site. Neutrophil recruitment from the blood to infectious sites or in response to tissue damage is a key feature of the early innate immune response [460, 461]. Further investigation on neutrophil recruitment was to determine if the presence of neutrophils at the bite site resulted in NET formation, which is used in killing parasites or bacteria in vivo. In my model, the recruitment of neutrophils to the bite site did not result in swarm formation as observed in inflamed, infected or sterilely wounded tissues [326, 408, 450, 451, 462-469]. In a model to demonstrate the formation of neutrophil swarms in extravascular spaces, and the molecular events guiding swarm formation, it was reported that neutrophil cell death initiated dramatic neutrophil swarm formation. Leukotriene B4 (LTB4) was shown to play a key role as a unique intercellular communication signal between neutrophils, allowing a rapid integrin-independent neutrophil recruitment through the tissue [470]. This suggests that the absence of neutrophil swarms in my model could possibly be due to the absence of LTB4 needed at sites of cell death in order to mediate neutrophil swarm formation [470]. Parasite infections such as *T. gondii* and *L. major* have been described to form dynamic neutrophil clusters in the LN and skin respectively [408, 471]. The absence of neutrophil swarms was a novel observation of the behaviour of recruited neutrophils during *T. b. brucei* infection in the skin. The recruitment of neutrophils to the bite site was rapid, and directed towards the site of injury, suggesting chemotactic factors such as CXCL1/CXCL2 were at play. In a model of liver injury, neutrophil migration was found to depend on an intravascular CXCL2 gradient for migration to sites of tissue necrosis [472]. The role of neutrophils in carrying out its phagocytic functions have been described in bacterial and parasitic infections, where antigens are transported through lymphatic vessels to the draining lymph node [473]. From the intravital data on neutrophils described here, this suggests that

at sites of *T. b. brucei* deposition/tsetse fly probe, neutrophils rapidly migrated from the blood to phagocytose parasites.

The lymphatic vessels are responsible for draining excess fluid, soluble proteins, migratory DCs and antigens through lymphatic vessels into the LN. The draining function of lymphatic vessels is important for maintaining tissue homeostasis, and in inflammatory conditions there is increased fluid and cellular activity [194, 195, 474]. Dissemination of *T. b. brucei* through the lymphatics has been described for over three decades [191, 333], but the likely mechanisms involved have yet to be described. Based on the observation of intra lymphatic *T. b. brucei*, and extra lymphatic parasites migrating towards the lymphatic vessel, it led me to propose that the mechanism of entry of *T. b. brucei* into lymphatic vessels may be similar to leukocyte transmigration into lymphatics, in particular DC entry into lymphatics. Transmigration of leukocytes through endothelial cell junctions occurs in a tightly regulated manner, requiring integrins such as PECAM, CD99 and other proteins [430, 475-477]. This process involves sequential interactions between adhesion molecules on the leukocytes and the endothelial cell, and during acute inflammation there is an increase in vascular permeability to fluid, without an alteration to the barrier functions which prevents the exit of solutes [475].

Dendritic cells (DCs), described as professional APCs, unlike other leukocytes do not require an integrin mediated cell-cell and cell-matrix interactions to enter the lymphatics in mouse dermis [478]. DCs enter lymphatics through expression of chemokine receptor CCR7, while CCR7 non-expressors DCs are unable to migrate into the lymphatics [193, 479]. CCR7 is upregulated on migratory DCs and acts as a gatekeeper during their mobilization [480, 481]. CCR7 deficient DCs can crawl as fast as CCR7 sufficient DCs, but do not enter the lymphatics, and fail to gain access to LNs [203]. CCR7 recognizes the ligands CCL19 and CCL21, which together coordinate the trafficking of DCs and T cells to, and within secondary lymphoid organs under steady and inflammatory conditions [479]. CCL21 is a chemokine associated with lymphocyte ingress into LNs, and DCs have been described to migrate directionally along CCL21 gradients [482, 483]. Two types of CCL21 are expressed (CCL21-ser and CCL21-Leu). CCL21-Leu is expressed on lymphatic endothelial cells and CCL21-Ser on fibroblastic reticular cells [484]. DCs gain access into lymphatics through perforations or

button like junctions that are present in the initial lymphatics. These button-like junctions are equipped with flap valves to allow entry but prevent exit of solutes and small particles [204]. Hence, to access the lymphatics, DCs seek out areas with sparse basement membrane on initial lymphatics, where they are able to squeeze in, at or near blind-ended tips of initial lymphatics [204], and localize in the subcapsular sinus of the LN [485-487].

From my observation of intra lymphatic *T. b. brucei*, some of the extra lymphatic *T. b. brucei* were observed to migrate towards lymphatic vessels in a CCL21 independent manner as shown from the transwell assay. Hence, *T. b. brucei* may interact with lymphatic vessels through its rapid motility, seeking out perforations through which they may gain entry. The architecture of the lymphatics being a one-way drainage system may also favour the entry of *T. b. brucei*. DCs also interact with the endothelium using their lamellipodia, and are guided by lymph flow and other cues, which lead them to the LN [203]. *T. b. brucei* appear to behave similarly, traversing at significantly higher velocities compared to extra lymphatic parasites in a random manner, probably due to the weak current of the lymph flow and rapid flagella motility. Cells migrate in the direction of lymph possibly due to chemotactic cues produced by the lymphatics or endothelial cells [488]. In the intracellular parasite *T. cruzi,* a closely related parasite to *T. b. brucei,* it has been described to bind CCL2. Injection of CCL2 into the air pouch of infected mice increased *T. cruzi* migration to different tissues and leukocyte recruitment in a concentration dependent manner [489]. The run and tumble behaviour of *T. b. brucei* in vivo which is characteristic of bacterial chemotaxis [490, 491], also raises the intriguing possibility of *T. b. brucei* migrating in a chemotactic manner both in the lymphatics and the skin.

Although the data presented here is novel with respect to the observation of parasites in the extravascular matrix, intralymphatic parasites and neutrophil migration to the bite site post infected tsetse exposure. The experiments described in this study have some drawbacks. Firstly is the suggestion that I was unable to detect parasites in blood vessels using tsetse flies (metacyclics) and needle injections of blood stream form parasites. Inability to detect parasites in the blood vessels could possibly be due to direct injection of parasites into the blood vessels or rapid transit of the parasites into the blood stream of the mouse from the skin, hence making it undetectable. Although the injection of parasites

directly into blood vessels is atypical of dipteran vectors, hence it is highly unlikely this was the case. Secondly, the observation of intralymphatic parasites was carried out using blood stream form parasites without sufficient replicates. Parasites in the Prox1 mOrange mice also had higher velocities compared to their counterparts imaged in wild type mice. This suggests that the phenotype of the mouse used could be attributed to the difference in velocities, and the need to carry out more replicates to properly draw conclusions regarding the migration of parasites towards lymphatic vessels and also account for the difference in velocities. Furthermore, there is the need to carry out these studies using infected tsetse flies (i.e. with metacyclics injected into the skin), to decipher whether the results obtained with blood stream injections would be similar or different. The use of infected tsetses for inoculation during lymphatic imaging would however pose considerable challenges with imaging due to the low numbers of parasites injected with the strain used in this study. I was also unable to compare the behaviour of neutrophils in uninfected tsetse and infected tsetse exposed mice. This would also be necessary to account for the contribution of the parasite to neutrophil behaviour in vivo. It would be interesting to find out whether uninfected tsetse exposed mice would form neutrophil swarms which was absent in infected tsetse exposed mice. Hence further studies taking note of these limitations, need to be carried out, and also taking into account that these observations have been made in mice, which might be different in humans/cattle. So interpretations of data from mice models have to been done with caution when drawing conclusions on trypanosome host interactions occurring in the skin post tsetse exposure. The limitations outlined here, however does not diminish the novelty of the data presented in this chapter.

Overall, my findings in this study outline the events observed following the injection of *T. b. brucei* into the dermis of the skin via the tsetse fly bite, and the host cellular recruitment that follows. Metacyclic *T. b. brucei* were highly motile in the skin, migrating rapidly in the dermis of the skin, and blood stream forms rapidly migrating towards lymphatics. Intravital imaging also revealed that the damage to the skin by the tsetse fly caused the recruitment of neutrophils, which do not form swarms and maintain directionality towards the site of injury.

A thorough understanding of the molecular mechanisms guiding this process would deepen our understanding of the pathogenesis of African trypanosomes in mammals.

6 General Discussion

6.1 Introduction

For arthropod delivered parasites, the skin represents the first contact the vector and parasites have with the mammalian host. This serves an opportunity for the parasite to establish itself, and also for the host to mount an innate immune response to clear or control infection [492]. In African trypanosomes, transmitted by the bite of the tsetse fly, the skin is needed for the parasites to establish and disseminate to other organs of the mammal [18, 23]. The skin also serves as a physical barrier to prevent the entry of parasites, and it is also host to a plethora of immune cells [82, 93]. The bite of the tsetse fly is capable of eliciting an immune response as observed in other arthropod delivered parasites such as *Leishmania* spp [166]. During infection, the first line of cellular defence is the recruitment of neutrophils within minutes, which is followed later by monocytes, which can differentiate into macrophages and DCs, and are recruited by chemotaxis through local production of CCL2, CCL3, CCL4 and CCL5 [488]. Once the parasites are established, next is dissemination from the bite site, which for some intracellular parasites such as *Leishmania* involves capture and dissemination by neutrophils [165, 166].

In African trypanosomes infected cattle, cannulation of the flank of these animals indicates the presence of trypanosomes in the lymph prior to blood detection. This suggests that parasites may use the lymphatics as a principal route of dissemination [13, 191]. In mammals, leukocytes transmigration into lymphatics has been described extensively, especially that of DCs [430, 475]. Migratory DCs express CCR7, which recognize the ligands CCL19 and CCL21 that participate in trafficking DCs into the lymphatics along CCL21 gradients [193, 479, 486]. This suggests that DC entry into lymphatics involves cells following a chemotactic gradient. In African trypanosomes, it has yet to be established whether chemokines, active parasite motility or events similar to leukocyte transmigration are involved in parasite ingress into lymphatics. Dissecting the events in the skin would help shape our understanding of parasite dissemination and interactions that may occur within host tissues. This present study has described some of those very early events in the host occurring in the skin post tsetse fly bites, at the molecular and cellular level, using conventional techniques and intravital imaging studies.

6.2 Tsetse fly infections and *T. b. brucei* egress from the skin to the lymph node

In this study, I successfully established a method for experimental infections of mice via trypanosome infected tsetse flies in the laboratory. This was important in order to carry out studies in vivo that mimic the natural route of infection in the field through injection of the right dose and life cycle stage (metacyclics) of parasites via the tsetse fly. My method of infecting tsetse flies by optimising the blood meal, trypanosome and tsetse strain combination (*T. b. brucei* 247 and *G. m. morsitans*) was consistent with previous reports that optimising these parameters could enhance successful salivary gland infections in tsetse flies [298, 493]. This approach gave a consistently high level of mature infections in tsetse flies. Following tsetse infections, mice ear pinna was then exposed to infected tsetse flies, which demonstrated the successful establishment of *T. b. brucei* in mice. There was detection of parasitemia, and this validated that the route of infection (ear pinna) was appropriate for further in vivo studies.

I also report here the establishment/proliferation of parasites in mouse skin by qPCR, which is consistent with what has been observed in goats [11, 13, 191, 192]. Also, the presence of parasites in the LN suggested that the lymphatics were used to transit into the blood stream. The presence of parasites in the skin for up to 48 hrs suggests the importance of the skin stage in pathogenesis, and points to other critical roles it may play in infection yet to be identified. The lymphatics drain antigens and excess fluid from the skin and maintain normal tissue homeostasis. In relation to this study, this suggests lymphatics are important in trafficking *T. b. brucei* as observed for immune cells e.g. dendritic cells from tissues to the LN. Other vector-transmitted parasites such as *Plasmodium* sporozoites have also been demonstrated to transit to the LN through the lymphatics, although the LN is a dead end for these parasites [184]. In African trypanosomes following infections initiated by the bite of infected tsetse flies on the flanks of cattle, parasites multiply at the bite site, followed by the onset of a localised skin reaction (chancre). Lymph collected from the nodes of these mammals via the efferent lymphatics were shown to contain parasites, preceding the appearance of parasites in the blood, suggesting that

the LN also serves for proliferation of trypanosomes and a passage route for dissemination into the blood [11, 494].

In all, the data presented shows that African trypanosomes migrates towards the lymphatics, and enters the lymphatics during infection as previously described [191], but further studies are needed to prove there is tropism for lymphatics.

6.3 Identification of the molecular and cellular events in the skin post tsetse fly bites

The very early events following the bite of infected/uninfected tsetse flies remained an area that was uncharted prior to this study. African trypanosomes inject metacyclic stage parasites into the skin, and as previously discussed, the damage to the skin itself from the probe caused the recruitment of cells to the bite site. The first cells identified to enter the skin from the blood post tsetse bite were neutrophils, which were $CD11b^+$ and $Ly6G^+$. The presence of neutrophils in the skin post tsetse fly bite was consistent with the recruitment of neutrophils in other arthropod transmission models such as *Phlebotomous duboscqi* [326, 396]. However, the presence of neutrophils was not different in infected or uninfected tsetse fly bites, suggesting that the break in the skin caused by the probe was responsible for the early influx of cells.

Neutrophils are recruited to sites of inflammation or sterile injury to either clear invaders or participate in the tissue repair process in the skin [462, 495]. Neutrophils can become primed by chemokines and cytokines such as TNF-α, IL-8, and become mobilized to sites of infection, releasing proteases and reactive oxygen species for clearing pathogens [496]. Neutrophil derived proteases could also be responsible for proteolytic activation of IL-1ß and IL-6, and both cytokines were upregulated in the skin post tsetse fly exposure. Membrane-associated proteinase 3 could cleave IL-1ß, while neutrophil elastase could play a role in degradation of soluble IL-6 [497]. At sites of infection, neutrophils could also release cytokines, chemokines and anti-microbial peptides in order to carry out its phagocytic function [498]. The recruitment of neutrophils to the bite site during infection results in immunity against the invading pathogens, through phagocytosis [152].

TLDA analysis in the skin also revealed the upregulation of two chemokines associated with neutrophil recruitment, CXCL1 and CXCL2, which bind the chemokine receptors CXCR1/2 that are involved in neutrophil extravasation from the blood [499]. The saliva of *Anopheles stephensi* contains a 200 Kda neutrophil chemotactic factor, which serves as a chemoattractant for neutrophils [500]. The saliva of the tsetse fly is highly heterogeneous, with several proteins with hypothetical functions. These saliva components could contain substances that modulate the innate immune response, which is characteristic of the saliva of vectors [501, 502]. The tsetse fly saliva has been suggested to modulate the T helper response in African trypanosome infections towards a Th2 phenotype, when injected with or without trypanosomes intraperitoneally [186]. Furthermore, neutrophils have been effective in clearing *Trypanosoma congolense* in the chancre formed after a tsetse fly bite, confirming their phagocytic role in *Trypanosoma* infections [13]. The presence of neutrophils in the chancre at day 11-post infection suggests they are beneficial to the host during infection [503]. In contrast to the protective roles of neutrophils in infection, neutrophils have been demonstrated through depletion studies to facilitate the onset of parasitemia in *Leishmania major* [339]. Given the contrasting activity of neutrophils it was important to establish their role in tsetse mediated trypanosome infection. Using antibody mediated neutrophil depletion, there was no difference observed in parasitemia.

Overall, the data here seems to suggest that the very earliest immune events post tsetse fly bite resulted in the influx of neutrophils to the skin, which may play a protective role in clearing parasites. However, sufficient parasites were able to evade neutrophil killing and successfully establish parasitemia. This study also shows that it is the impact of the vector probe and its saliva that drives and sustains the migration of neutrophils from the blood to the skin, rather than the presence of trypanosomes.

6.4 Proposed mechanism for *T. b. brucei* dissemination through the lymphatics

The life cycle of African trypanosomes in mammals begins in the skin where parasites are deposited, gain access into the blood via the lymphatics, and continue through parasite uptake from the skin during a tsetse fly feed. At each stage of *T. b. brucei* infection, the parasites possess unique features for adapting to its new environment [18, 23]. The first stage during the tsetse bite is the release of metacyclic *T. b. brucei*, which then differentiate into long slender forms present in the blood stream, which then differentiate into short stumpy stages that are taken up in the skin during tsetse fly feeds. The very early events in parasite dissemination from the skin have yet to be investigated. This led me to investigate intravitally the spatiotemporal events in the skin stage of the lifecycle of *T. b. brucei* in mammals.

Metacyclic *T. b. brucei* injected into the skin via tsetse bites were actively motile with a higher velocity than bloodstream forms, and moved randomly in the skin. Metacyclic parasites were not detected in blood vessels. I also observed the presence of *T. b. brucei* in the ear skin lymphatic vessels using Prox-1 mOrange, lymphatic vessel reporter mice. Intralymphatic parasites were clearly motile and moved rapidly within the lymphatic vessel. During leukocyte trafficking, DCs enter the lymphatics through the initial lymphatic vessels present in the dermis, through the interaction of the chemokine receptor CCR7 with the ligand CCL21 expressed on lymphatic vessels [482, 504]. However, CCR7 deficient DCs have been found to still gain access into the T cell area of the LN though in lower numbers, possibly through other chemokine receptors CXCR4 [505] or CCR8 [506] which partially overlap with CCR7 signalling. CCR7 and CCL21 have not been identified to be involved in migration towards lymphatics for *T. b. brucei*, but the use of host chemokine receptors by the parasite can't be ruled out, and needs to be investigated further.

Parasite derived chemokine homologues have also been described which could induce cell migration. For example parasite macrophage migratory inhibitory factor has been isolated from nematodes [507, 508], and protozoa [509, 510]. Also, *Strongyloides stercoralis* can interact with chemokine receptors to induce

eosinophil migration [511]. Through these homologues, parasites have evolved mechanisms to prolong survival and dissemination in their hosts. This suggests it is likely that *T. b. brucei* secrete molecules that could bind host factors in order to gain access to the lymphatics.

I also observed *T. b. brucei* parasites migrating towards the lymphatic vessels in the skin, suggesting they might penetrate by seeking out perforations in the lymphatics. DCs actively crawl along the endothelium and their migration in the initial lymphatics was not due to lymph flow current alone [203]. My findings seem to mimic that, with parasites actively migrating in lymphatic vessels and not appearing to be pushed along by the weak lymph current. Here, I also report that the crawling movement along the endothelium reported for DCs is absent in our *T. b. brucei* model [203]. The study presented in this thesis is the very first intravital observation of the migrationof *T. b. brucei* towards lymphatic vessels and observation of intralymphatic parasites.

I propose that African trypanosomes may gain access into the lymphatics using a mechanism similar to DCs, by seeking areas on the lymphatics with perforations. Once in the initial lymphatics, through a combination of active motility by their flagella and by sensing direction of lymph flow they migrate towards larger collecting vessels where they may now be sufficiently pushed by the shear force of the lymph [512, 513].

6.5 Conclusions

The aim of this thesis was to characterise the very early immune events in the skin post tsetse fly bites with infected/uninfected tsetse flies, and also visualise the events that occur in the skin using *T. b. brucei* as a model for African trypanosomes. The study presented here draws the following conclusions:

1. The recruitment of cells to the bite skin post tsetse bite is independent of the presence or absence of parasites. The damage caused by the tsetse fly drives the influx of host cells, which were predominantly neutrophils.

2. *T. b. brucei* are detected in the LN prior to blood dissemination, and infection of tsetse flies is best achieved through optimisation of the infected blood feed, trypanosome strain and tsetse fly combinations.
3. Metacyclic *T. b. brucei* are actively motile in the skin
4. *T. b. brucei* migrates towards lymphatic vessels and gain entry.

Overall the data presented in this thesis demonstrates that chemokines drive neutrophil influx to the skin, specifically CXCL1 and CXCL2. Also, neutrophil behaviour in the skin in African trypanosome infections was unique in that neutrophil swarms were absent during intravital imaging studies. *T. b. brucei* were also detected, and could possibly gain access to the initial lymphatics through gaps in the basement membrane where they could squeeze in. The data presented here also excludes the possibility of CCL21 contributing to *T. b. brucei* ingress into lymphatic vessels.

6.6 Future work

In the light of the findings from this thesis as outlined above, it would be interesting to carry out the following studies to provide more insights into the very early events in African trypanosome infections. Firstly, the characterisation of the factor(s) present in the tsetse fly salivary gland that could potentially drive neutrophil influx to the bite site - this would shed more light on the neutrophil influx data I have presented in chapter 4 of my thesis. Secondly, it would also be interesting to dissect the molecular mechanisms underlying the entry of African trypanosomes into the lymphatics, first through in vitro chemotaxis assays using a broad range of chemokines, and followed by the use of mice deficient in skin lymphatics in order to define the impact this would have on pathogenesis.

In summary, these studies together with the data from my thesis would undoubtedly provide further insights into African trypanosome dissemination through the skin, hence uncovering the ‘black box’ of the very earliest events in the skin.

Appendices

I General solutions

Complete medium: 500 mL IMDM [Iscove's Modified Dulbecco's Medium, (Invitrogen, Paisley, UK)] containing 4%v/v foetal calf serum (FCS), penicillin (100 units/mL), streptomycin (100 µg/mL), and 2 mM L-Glutamate.

Hanks' Balanced Salt Solution 1x with $CaCl_2$ and $MgCl_2$ (1x HBSS): 1x HBSS was purchased from Life Technologies (Paisley, UK).

Chemotaxis buffer: 0.5% w/v Bovine Serum Albumin (BSA) in IMDM

Fluorescence activated cell sorting (FACS) buffer: 500 ml of 1x DPBS containing 4% v/v FCS, 2 mM EDTA and 0.09% w/v Sodium Azide.

Dulbecco's Phosphate Buffered Saline, 1x (1x DPBS) without $CaCl_2$ & $MgCl_2$: 1x DPBS was purchased from Life Technologies (Paisley, UK).

Modified HMI-9 for culturing Pleiomorphic *T. b. brucei*

ßBCPT comprises of the components below:

Bathocuproinedisulfonic acid disodium salt	14.1mg (5 mM) – final 0.5 mM
Distilled water (d.H_20)	5 ml
Thymidine	19.5 mg (16 mM) – final 0.16 mM
d.H_20	5 ml
Sodium Pyruvate	110 mg
d.H_20	5 ml
ß-mercaptoethanol	7ul (200 mM) – final 2 mM
d.H_20	5 ml

L-cysteine $C_3H_7NO_2S$	91.0 mg (100 mM) – final 1mM
d.H_20	5 ml

Filter sterilise and add to medium as directed below, or store at -20°C until needed.

For 500 ml HM19 add in the following order:

Iscoves modified Dulbecco's medium + glutamax	365 ml
Hypoxanthine (stored at 40 °C)	5 ml
Kanamycin (10mg/ml -20 °C)	1.5 ml
Pen/Strep (5000 Units each -20 °C) (or 2.5 ml of 10 000 U/ml)	5 ml
ßBCPT (5 ml of each component mixed together as above)	25 ml
Glucose	500 mg
Adenosine	67 mg
Guanosine	71 mg
Methyl cellulose	0.55 g

Leave overnight on stirrer in cold room

Add 133 ml Serum Plus (20%) + 133 ml PAA Gold FCS (20%) to 400 ml Mod-HMI-9

Filter sterilise and store at 4 °C

II List of antibodies

Antibody	Clone	Company
Ly6G	Gr1	BD
F4/80	BM8	eBioscience
CD45	30-F11	BD
CD11b	M1/70	BD
IA/IE (MHC II)	2G9	BD
Ly6C	RB-8C5	eBioscience
Viability		eBioscience
Ly6G	IA8	BioXcell

List of References

1. Turner, C.M., N. Aslam, and C. Dye, *Replication, differentiation, growth and the virulence of Trypanosoma brucei infections.* Parasitology, 1995. **111 (Pt 3)**: p. 289-300.
2. Vassella, E., et al., *Differentiation of African trypanosomes is controlled by a density sensing mechanism which signals cell cycle arrest via the cAMP pathway.* J Cell Sci, 1997. **110 (Pt 21)**: p. 2661-71.
3. Brun, R., et al., *Human African trypanosomiasis.* Lancet, 2010. **375**(9709): p. 148-59.
4. Burri, C., *Chemotherapy against human African trypanosomiasis: is there a road to success?* Parasitology, 2010. **137**(14): p. 1987-94.
5. Ilemobade, A.A., *Tsetse and trypanosomosis in Africa: the challenges, the opportunities.* Onderstepoort J Vet Res, 2009. **76**(1): p. 35-40.
6. Kuzoe, F.A., *Perspectives in research on and control of African trypanosomiasis.* Ann Trop Med Parasitol, 1991. **85**(1): p. 33-41.
7. Shaw, A.P., et al., *Mapping the economic benefits to livestock keepers from intervening against bovine trypanosomosis in Eastern Africa.* Prev Vet Med, 2014. **113**(2): p. 197-210.
8. Urbaniak, M.D., M.L. Guther, and M.A. Ferguson, *Comparative SILAC proteomic analysis of Trypanosoma brucei bloodstream and procyclic lifecycle stages.* PLoS One, 2012. **7**(5): p. e36619.
9. Barry, J.D. and R. McCulloch, *Antigenic variation in trypanosomes: enhanced phenotypic variation in a eukaryotic parasite.* Adv Parasitol, 2001. **49**: p. 1-70.
10. *Genome sequence of the tsetse fly (Glossina morsitans): vector of African trypanosomiasis.* Science, 2014. **344**(6182): p. 380-6.
11. Akol, G.W. and M. Murray, *Early events following challenge of cattle with tsetse infected with Trypanosoma congolense: development of the local skin reaction.* Vet Rec, 1982. **110**(13): p. 295-302.
12. Malvy, D., et al., *Guess what! Human West African trypanosomiasis with chancre presentation.* Eur J Dermatol, 2000. **10**(7): p. 561-2.
13. Taiwo, V.O., et al., *Role of the chancre in induction of immunity to tsetse-transmitted Trypanosoma (Nannomonas) congolense in goats.* Vet Immunol Immunopathol, 1990. **26**(1): p. 59-70.
14. Matthews, K.R., *The developmental cell biology of Trypanosoma brucei.* J Cell Sci, 2005. **118**(Pt 2): p. 283-90.
15. Pays, E., L. Vanhamme, and D. Perez-Morga, *Antigenic variation in Trypanosoma brucei: facts, challenges and mysteries.* Curr Opin Microbiol, 2004. **7**(4): p. 369-74.
16. McCulloch, R., *Antigenic variation in African trypanosomes: monitoring progress.* Trends Parasitol, 2004. **20**(3): p. 117-21.
17. Matthews, K.R., J.R. Ellis, and A. Paterou, *Molecular regulation of the life cycle of African trypanosomes.* Trends Parasitol, 2004. **20**(1): p. 40-7.
18. Vickerman, K., *Developmental cycles and biology of pathogenic trypanosomes.* Br Med Bull, 1985. **41**(2): p. 105-14.
19. Tyler, K.M., K.R. Matthews, and K. Gull, *The bloodstream differentiation-division of Trypanosoma brucei studied using mitochondrial markers.* Proc Biol Sci, 1997. **264**(1387): p. 1481-90.

20. Van Den Abbeele, J., et al., *Trypanosoma brucei spp. development in the tsetse fly: characterization of the post-mesocyclic stages in the foregut and proboscis.* Parasitology, 1999. **118 (Pt 5)**: p. 469-78.
21. Roditi, I. and M. Liniger, *Dressed for success: the surface coats of insect-borne protozoan parasites.* Trends Microbiol, 2002. **10**(3): p. 128-34.
22. Rotureau, B., et al., *A new asymmetric division contributes to the continuous production of infective trypanosomes in the tsetse fly.* Development, 2012. **139**(10): p. 1842-50.
23. Vickerman, K., et al., *Biology of African trypanosomes in the tsetse fly.* Biol Cell, 1988. **64**(2): p. 109-19.
24. Matthews, K.R. and K. Gull, *Commitment to differentiation and cell cycle re-entry are coincident but separable events in the transformation of African trypanosomes from their bloodstream to their insect form.* J Cell Sci, 1997. **110 (Pt 20)**: p. 2609-18.
25. Amole, B.O., A.B. Clarkson, Jr., and H.L. Shear, *Pathogenesis of anemia in Trypanosoma brucei-infected mice.* Infect Immun, 1982. **36**(3): p. 1060-8.
26. Connor, R.J., *The impact of nagana.* Onderstepoort J Vet Res, 1994. **61**(4): p. 379-83.
27. Woodruff, A.W., et al., *Anaemia in African trypanosomiasis and 'big spleen disease' in Uganda.* Trans R Soc Trop Med Hyg, 1973. **67**(3): p. 329-37.
28. Sadun, E.H., et al., *Experimental infections with African trypanosomes. V. Preliminary parasitological, clinical, hematological, serological, and pathological observations in rhesus monkeys infected with Trypanosoma rhodesiense.* Am J Trop Med Hyg, 1973. **22**(3): p. 323-30.
29. Masocha, W., M.E. Rottenberg, and K. Kristensson, *Migration of African trypanosomes across the blood-brain barrier.* Physiol Behav, 2007. **92**(1-2): p. 110-4.
30. Odiit, M., F. Kansiime, and J.C. Enyaru, *Duration of symptoms and case fatality of sleeping sickness caused by Trypanosoma brucei rhodesiense in Tororo, Uganda.* East Afr Med J, 1997. **74**(12): p. 792-5.
31. Duggan, A.J. and M.P. Hutchinson, *Sleeping sickness in Europeans: a review of 109 cases.* J Trop Med Hyg, 1966. **69**(6): p. 124-31.
32. Blum, J., C. Schmid, and C. Burri, *Clinical aspects of 2541 patients with second stage human African trypanosomiasis.* Acta Trop, 2006. **97**(1): p. 55-64.
33. Kennedy, P.G., *Human African trypanosomiasis-neurological aspects.* J Neurol, 2006. **253**(4): p. 411-6.
34. Buguet, A., et al., *[Sleeping sickness: major disorders of circadian rhythm].* Med Trop (Mars), 2001. **61**(4-5): p. 328-39.
35. Kennedy, P.G., *Human African trypanosomiasis of the CNS: current issues and challenges.* J Clin Invest, 2004. **113**(4): p. 496-504.
36. Chappuis, F., et al., *Field evaluation of the CATT/Trypanosoma brucei gambiense on blood-impregnated filter papers for diagnosis of human African trypanosomiasis in southern Sudan.* Trop Med Int Health, 2002. **7**(11): p. 942-8.
37. Noireau, F., P. Force-Barge, and P. Cattand, *Evaluation of Testryp CATT applied to samples of dried blood for the diagnosis of sleeping sickness.* Bull World Health Organ, 1991. **69**(5): p. 603-8.
38. Penchenier, L., et al., *Evaluation of LATEX/T.b.gambiense for mass screening of Trypanosoma brucei gambiense sleeping sickness in Central Africa.* Acta Trop, 2003. **85**(1): p. 31-7.

39. Noireau, F., et al., *Serodiagnosis of sleeping sickness in the Republic of the Congo: comparison of indirect immunofluorescent antibody test and card agglutination test.* Trans R Soc Trop Med Hyg, 1988. **82**(2): p. 237-40.
40. Lejon, V., et al., *A semi-quantitative ELISA for detection of Trypanosoma brucei gambiense specific antibodies in serum and cerebrospinal fluid of sleeping sickness patients.* Acta Trop, 1998. **69**(2): p. 151-64.
41. Knobloch, J., et al., *Evaluation of immunoassays for diagnosis and management of sleeping sickness in Liberia.* Tropenmed Parasitol, 1984. **35**(3): p. 137-40.
42. Lambert, P.H., M. Berney, and G. Kazyumba, *Immune complexes in serum and in cerebrospinal fluid in African trypanosomiasis. Correlation with polyclonal B cell activation and with intracerebral immunoglobulin synthesis.* J Clin Invest, 1981. **67**(1): p. 77-85.
43. Whittle, H.C., et al., *IgM and antibody measurement in the diagnosis and management of Gambian trypanosomiasis.* Am J Trop Med Hyg, 1977. **26**(6 Pt 1): p. 1129-34.
44. Van Meirvenne, N., E. Magnus, and P. Buscher, *Evaluation of variant specific trypanolysis tests for serodiagnosis of human infections with Trypanosoma brucei gambiense.* Acta Trop, 1995. **60**(3): p. 189-99.
45. Barry, J.D. and C.M. Turner, *The dynamics of antigenic variation and growth of African trypanosomes.* Parasitol Today, 1991. **7**(8): p. 207-11.
46. Lejon, V., et al., *Neuro-inflammatory risk factors for treatment failure in "early second stage" sleeping sickness patients treated with pentamidine.* J Neuroimmunol, 2003. **144**(1-2): p. 132-8.
47. Balasegaram, M., et al., *Treatment outcomes and risk factors for relapse in patients with early-stage human African trypanosomiasis (HAT) in the Republic of the Congo.* Bull World Health Organ, 2006. **84**(10): p. 777-82.
48. Kennedy, P.G., *Diagnostic and neuropathogenesis issues in human African trypanosomiasis.* Int J Parasitol, 2006. **36**(5): p. 505-12.
49. Sternberg, J.M., et al., *Evaluation of the diagnostic accuracy of prototype rapid tests for human African trypanosomiasis.* PLoS Negl Trop Dis, 2014. **8**(12): p. e3373.
50. Wastling, S.L., et al., *LAMP for human African trypanosomiasis: a comparative study of detection formats.* PLoS Negl Trop Dis, 2010. **4**(11): p. e865.
51. Naessens, J., A.J. Teale, and M. Sileghem, *Identification of mechanisms of natural resistance to African trypanosomiasis in cattle.* Vet Immunol Immunopathol, 2002. **87**(3-4): p. 187-94.
52. Anosa, V.O., L.L. Logan-Henfrey, and M.K. Shaw, *A light and electron microscopic study of changes in blood and bone marrow in acute hemorrhagic Trypanosoma vivax infection in calves.* Vet Pathol, 1992. **29**(1): p. 33-45.
53. Murray, M., et al., *Genetic resistance to African Trypanosomiasis.* J Infect Dis, 1984. **149**(3): p. 311-9.
54. Roelants, G.E., et al., *Identification and selection of cattle naturally resistant to African trypanosomiasis.* Acta Trop, 1987. **44**(1): p. 55-66.
55. Molina-Portela, M.P., M. Samanovic, and J. Raper, *Distinct roles of apolipoprotein components within the trypanosome lytic factor complex revealed in a novel transgenic mouse model.* J Exp Med, 2008. **205**(8): p. 1721-8.

56. Thomson, R., et al., *Hydrodynamic gene delivery of baboon trypanosome lytic factor eliminates both animal and human-infective African trypanosomes.* Proc Natl Acad Sci U S A, 2009. **106**(46): p. 19509-14.
57. Vreysen, M.J., et al., *Sterile insects to enhance agricultural development: the case of sustainable tsetse eradication on Unguja Island, Zanzibar, using an area-wide integrated pest management approach.* PLoS Negl Trop Dis, 2014. **8**(5): p. e2857.
58. Vreysen, M.J., *Principles of area-wide integrated tsetse fly control using the sterile insect technique.* Med Trop (Mars), 2001. **61**(4-5): p. 397-411.
59. Barrett, M.P., *Potential new drugs for human African trypanosomiasis: some progress at last.* Curr Opin Infect Dis, 2010. **23**(6): p. 603-8.
60. Barrett, M.P., et al., *The trypanosomiases.* Lancet, 2003. **362**(9394): p. 1469-80.
61. Paine, M.F., et al., *Diamidines for human African trypanosomiasis.* Curr Opin Investig Drugs, 2010. **11**(8): p. 876-83.
62. Barrett, M.P. and S.L. Croft, *Management of trypanosomiasis and leishmaniasis.* Br Med Bull, 2012. **104**: p. 175-96.
63. Yun, O., et al., *NECT is next: implementing the new drug combination therapy for Trypanosoma brucei gambiense sleeping sickness.* PLoS Negl Trop Dis, 2010. **4**(5): p. e720.
64. Babokhov, P., et al., *A current analysis of chemotherapy strategies for the treatment of human African trypanosomiasis.* Pathog Glob Health, 2013. **107**(5): p. 242-52.
65. Jacobs, R.T., et al., *Benzoxaboroles: a new class of potential drugs for human African trypanosomiasis.* Future Med Chem, 2011. **3**(10): p. 1259-78.
66. Bronner, U., et al., *Pentamidine concentrations in plasma, whole blood and cerebrospinal fluid during treatment of Trypanosoma gambiense infection in Cote d'Ivoire.* Trans R Soc Trop Med Hyg, 1991. **85**(5): p. 608-11.
67. Delespaux, V. and H.P. de Koning, *Drugs and drug resistance in African trypanosomiasis.* Drug Resist Updat, 2007. **10**(1-2): p. 30-50.
68. Vansterkenburg, E.L., et al., *The uptake of the trypanocidal drug suramin in combination with low-density lipoproteins by Trypanosoma brucei and its possible mode of action.* Acta Trop, 1993. **54**(3-4): p. 237-50.
69. Burri, C., et al., *Efficacy of new, concise schedule for melarsoprol in treatment of sleeping sickness caused by Trypanosoma brucei gambiense: a randomised trial.* Lancet, 2000. **355**(9213): p. 1419-25.
70. Matovu, E., et al., *Drug resistance in Trypanosoma brucei spp., the causative agents of sleeping sickness in man and nagana in cattle.* Microbes Infect, 2001. **3**(9): p. 763-70.
71. Brun, R., et al., *The phenomenon of treatment failures in Human African Trypanosomiasis.* Trop Med Int Health, 2001. **6**(11): p. 906-14.
72. Balasegaram, M., et al., *Melarsoprol versus eflornithine for treating late-stage Gambian trypanosomiasis in the Republic of the Congo.* Bull World Health Organ, 2006. **84**(10): p. 783-91.
73. Checchi, F., et al., *Nifurtimox plus Eflornithine for late-stage sleeping sickness in Uganda: a case series.* PLoS Negl Trop Dis, 2007. **1**(2): p. e64.
74. Chitambo, H. and A. Arakawa, *Trypanosoma congolense: manifestation of resistance to Berenil and Samorin in cloned trypanosomes isolated from Zambian cattle.* Zentralbl Bakteriol, 1992. **277**(3): p. 371-81.

75. Osman, A.S., F.W. Jennings, and P.H. Holmes, *The rapid development of drug-resistance by Trypanosoma evansi in immunosuppressed mice*. Acta Trop, 1992. **50**(3): p. 249-57.
76. Peregrine, A.S., et al., *Variation in resistance to isometamidium chloride and diminazene aceturate by clones derived from a stock of Trypanosoma congolense*. Parasitology, 1991. **102 Pt 1**: p. 93-100.
77. Roy Chowdhury, A., et al., *The killing of African trypanosomes by ethidium bromide*. PLoS Pathog, 2010. **6**(12): p. e1001226.
78. Baker, N., et al., *Drug resistance in African trypanosomiasis: the melarsoprol and pentamidine story*. Trends Parasitol, 2013. **29**(3): p. 110-8.
79. Barrett, M.P., et al., *Drug resistance in human African trypanosomiasis*. Future Microbiol, 2011. **6**(9): p. 1037-47.
80. Graf, F.E., et al., *Aquaporin 2 mutations in Trypanosoma brucei gambiense field isolates correlate with decreased susceptibility to pentamidine and melarsoprol*. PLoS Negl Trop Dis, 2013. **7**(10): p. e2475.
81. Alsford, S., et al., *High-throughput decoding of antitrypanosomal drug efficacy and resistance*. Nature, 2012. **482**(7384): p. 232-6.
82. Heath, W.R. and F.R. Carbone, *The skin-resident and migratory immune system in steady state and memory: innate lymphocytes, dendritic cells and T cells*. Nat Immunol, 2013. **14**(10): p. 978-85.
83. Farrar, C.A., J.W. Kupiec-Weglinski, and S.H. Sacks, *The innate immune system and transplantation*. Cold Spring Harb Perspect Med, 2013. **3**(10): p. a015479.
84. Takeuchi, O. and S. Akira, *Pattern recognition receptors and inflammation*. Cell, 2010. **140**(6): p. 805-20.
85. Walport, M.J., *Complement. First of two parts*. N Engl J Med, 2001. **344**(14): p. 1058-66.
86. Walport, M.J., *Complement. Second of two parts*. N Engl J Med, 2001. **344**(15): p. 1140-4.
87. Medzhitov, R., *Recognition of microorganisms and activation of the immune response*. Nature, 2007. **449**(7164): p. 819-26.
88. Dunkelberger, J.R. and W.C. Song, *Complement and its role in innate and adaptive immune responses*. Cell Res, 2010. **20**(1): p. 34-50.
89. Medzhitov, R. and C. Janeway, Jr., *Innate immunity*. N Engl J Med, 2000. **343**(5): p. 338-44.
90. Medzhitov, R. and C.A. Janeway, Jr., *Decoding the patterns of self and nonself by the innate immune system*. Science, 2002. **296**(5566): p. 298-300.
91. Sumikawa, Y., et al., *Induction of beta-defensin 3 in keratinocytes stimulated by bacterial lipopeptides through toll-like receptor 2*. Microbes Infect, 2006. **8**(6): p. 1513-21.
92. Akira, S. and K. Takeda, *Toll-like receptor signalling*. Nat Rev Immunol, 2004. **4**(7): p. 499-511.
93. Nestle, F.O., et al., *Skin immune sentinels in health and disease*. Nat Rev Immunol, 2009. **9**(10): p. 679-91.
94. Meephansan, J., et al., *Regulation of IL-33 expression by IFN-gamma and tumor necrosis factor-alpha in normal human epidermal keratinocytes*. J Invest Dermatol, 2012. **132**(11): p. 2593-600.
95. Borkowski, T.A., et al., *Expression of gp40, the murine homologue of human epithelial cell adhesion molecule (Ep-CAM), by murine dendritic cells*. Eur J Immunol, 1996. **26**(1): p. 110-4.

96. Igyarto, B.Z., et al., *Skin-resident murine dendritic cell subsets promote distinct and opposing antigen-specific T helper cell responses.* Immunity, 2011. **35**(2): p. 260-72.
97. Haley, K., et al., *Langerhans cells require MyD88-dependent signals for Candida albicans response but not for contact hypersensitivity or migration.* J Immunol, 2012. **188**(9): p. 4334-9.
98. Bursch, L.S., et al., *Identification of a novel population of Langerin+ dendritic cells.* J Exp Med, 2007. **204**(13): p. 3147-56.
99. Shklovskaya, E., et al., *Langerhans cells are precommitted to immune tolerance induction.* Proc Natl Acad Sci U S A, 2011. **108**(44): p. 18049-54.
100. Kautz-Neu, K., et al., *Langerhans cells are negative regulators of the anti-Leishmania response.* J Exp Med, 2011. **208**(5): p. 885-91.
101. Poulin, L.F., et al., *The dermis contains langerin+ dendritic cells that develop and function independently of epidermal Langerhans cells.* J Exp Med, 2007. **204**(13): p. 3119-31.
102. Ginhoux, F., et al., *Blood-derived dermal langerin+ dendritic cells survey the skin in the steady state.* J Exp Med, 2007. **204**(13): p. 3133-46.
103. Henri, S., et al., *CD207+ CD103+ dermal dendritic cells cross-present keratinocyte-derived antigens irrespective of the presence of Langerhans cells.* J Exp Med, 2010. **207**(1): p. 189-206.
104. Ritter, U., et al., *CD8 alpha- and Langerin-negative dendritic cells, but not Langerhans cells, act as principal antigen-presenting cells in leishmaniasis.* Eur J Immunol, 2004. **34**(6): p. 1542-50.
105. Martinez-Pomares, L. and S. Gordon, *Antigen presentation the macrophage way.* Cell, 2007. **131**(4): p. 641-3.
106. Davies, L.C., et al., *Tissue-resident macrophages.* Nat Immunol, 2013. **14**(10): p. 986-95.
107. MacDonald, K.P., et al., *An antibody against the colony-stimulating factor 1 receptor depletes the resident subset of monocytes and tissue- and tumor-associated macrophages but does not inhibit inflammation.* Blood, 2010. **116**(19): p. 3955-63.
108. Heredia, J.E., et al., *Type 2 innate signals stimulate fibro/adipogenic progenitors to facilitate muscle regeneration.* Cell, 2013. **153**(2): p. 376-88.
109. Henson, P.M. and D.A. Hume, *Apoptotic cell removal in development and tissue homeostasis.* Trends Immunol, 2006. **27**(5): p. 244-50.
110. Gautier, E.L., et al., *Systemic analysis of PPARgamma in mouse macrophage populations reveals marked diversity in expression with critical roles in resolution of inflammation and airway immunity.* J Immunol, 2012. **189**(5): p. 2614-24.
111. Lucas, T., et al., *Differential roles of macrophages in diverse phases of skin repair.* J Immunol, 2010. **184**(7): p. 3964-77.
112. Raes, G., et al., *Alternatively activated macrophages in protozoan infections.* Curr Opin Immunol, 2007. **19**(4): p. 454-9.
113. Mirza, R., L.A. DiPietro, and T.J. Koh, *Selective and specific macrophage ablation is detrimental to wound healing in mice.* Am J Pathol, 2009. **175**(6): p. 2454-62.
114. Cailhier, J.F., et al., *Conditional macrophage ablation demonstrates that resident macrophages initiate acute peritoneal inflammation.* J Immunol, 2005. **174**(4): p. 2336-42.
115. Maus, U.A., et al., *Role of resident alveolar macrophages in leukocyte traffic into the alveolar air space of intact mice.* Am J Physiol Lung Cell Mol Physiol, 2002. **282**(6): p. L1245-52.

116. Ajuebor, M.N., et al., *Role of resident peritoneal macrophages and mast cells in chemokine production and neutrophil migration in acute inflammation: evidence for an inhibitory loop involving endogenous IL-10.* J Immunol, 1999. **162**(3): p. 1685-91.
117. Kolaczkowska, E., et al., *Resident peritoneal leukocytes are important sources of MMP-9 during zymosan peritonitis: superior contribution of macrophages over mast cells.* Immunol Lett, 2007. **113**(2): p. 99-106.
118. Clark, R.A., et al., *The vast majority of CLA+ T cells are resident in normal skin.* J Immunol, 2006. **176**(7): p. 4431-9.
119. Kupper, T.S. and R.C. Fuhlbrigge, *Immune surveillance in the skin: mechanisms and clinical consequences.* Nat Rev Immunol, 2004. **4**(3): p. 211-22.
120. Hayday, A. and R. Tigelaar, *Immunoregulation in the tissues by gammadelta T cells.* Nat Rev Immunol, 2003. **3**(3): p. 233-42.
121. Kronenberg, M., *Toward an understanding of NKT cell biology: progress and paradoxes.* Annu Rev Immunol, 2005. **23**: p. 877-900.
122. Zhang, J.M. and J. An, *Cytokines, inflammation, and pain.* Int Anesthesiol Clin, 2007. **45**(2): p. 27-37.
123. Dinarello, C.A., *Proinflammatory cytokines.* Chest, 2000. **118**(2): p. 503-8.
124. Plata, F., et al., *Synergistic protection by specific antibodies and interferon against infection by Trypanosoma cruzi in vitro.* Eur J Immunol, 1984. **14**(10): p. 930-5.
125. Wirth, J.J., et al., *Enhancing effects of gamma interferon on phagocytic cell association with and killing of Trypanosoma cruzi.* Infect Immun, 1985. **49**(1): p. 61-6.
126. De Titto, E.H., J.R. Catterall, and J.S. Remington, *Activity of recombinant tumor necrosis factor on Toxoplasma gondii and Trypanosoma cruzi.* J Immunol, 1986. **137**(4): p. 1342-5.
127. Wirth, J.J. and F. Kierszenbaum, *Recombinant tumor necrosis factor enhances macrophage destruction of Trypanosoma cruzi in the presence of bacterial endotoxin.* J Immunol, 1988. **141**(1): p. 286-8.
128. Reed, S.G., *In vivo administration of recombinant IFN-gamma induces macrophage activation, and prevents acute disease, immune suppression, and death in experimental Trypanosoma cruzi infections.* J Immunol, 1988. **140**(12): p. 4342-7.
129. Looareesuwan, S., et al., *Polyclonal anti-tumor necrosis factor-alpha Fab used as an ancillary treatment for severe malaria.* Am J Trop Med Hyg, 1999. **61**(1): p. 26-33.
130. Favre, N., et al., *The course of Plasmodium chabaudi chabaudi infections in interferon-gamma receptor deficient mice.* Parasite Immunol, 1997. **19**(8): p. 375-83.
131. Magez, S., et al., *Tumor necrosis factor alpha is a key mediator in the regulation of experimental Trypanosoma brucei infections.* Infect Immun, 1999. **67**(6): p. 3128-32.
132. Magez, S. and G. Caljon, *Mouse models for pathogenic African trypanosomes: unravelling the immunology of host-parasite-vector interactions.* Parasite Immunol, 2011. **33**(8): p. 423-9.
133. Luster, A.D., *Chemokines--chemotactic cytokines that mediate inflammation.* N Engl J Med, 1998. **338**(7): p. 436-45.
134. Locati, M., R. Bonecchi, and M.M. Corsi, *Chemokines and their receptors: roles in specific clinical conditions and measurement in the clinical laboratory.* Am J Clin Pathol, 2005. **123 Suppl**: p. S82-95.

135. Moser, B., *Chemokines: role in immune cell traffic.* Eur Cytokine Netw, 2003. **14**(4): p. 204-10.
136. Zimmermann, N., et al., *Chemokines in asthma: cooperative interaction between chemokines and IL-13.* J Allergy Clin Immunol, 2003. **111**(2): p. 227-42; quiz 243.
137. Rot, A. and U.H. von Andrian, *Chemokines in innate and adaptive host defense: basic chemokinese grammar for immune cells.* Annu Rev Immunol, 2004. **22**: p. 891-928.
138. Charo, I.F. and R.M. Ransohoff, *The many roles of chemokines and chemokine receptors in inflammation.* N Engl J Med, 2006. **354**(6): p. 610-21.
139. MartIn-Fontecha, A., et al., *Regulation of dendritic cell migration to the draining lymph node: impact on T lymphocyte traffic and priming.* J Exp Med, 2003. **198**(4): p. 615-21.
140. Muller, G. and M. Lipp, *Concerted action of the chemokine and lymphotoxin system in secondary lymphoid-organ development.* Curr Opin Immunol, 2003. **15**(2): p. 217-24.
141. Forster, R., A.C. Davalos-Misslitz, and A. Rot, *CCR7 and its ligands: balancing immunity and tolerance.* Nat Rev Immunol, 2008. **8**(5): p. 362-71.
142. Ohl, L., et al., *Chemokines as organizers of primary and secondary lymphoid organs.* Semin Immunol, 2003. **15**(5): p. 249-55.
143. Kopp, E. and R. Medzhitov, *Recognition of microbial infection by Toll-like receptors.* Curr Opin Immunol, 2003. **15**(4): p. 396-401.
144. Esche, C., C. Stellato, and L.A. Beck, *Chemokines: key players in innate and adaptive immunity.* J Invest Dermatol, 2005. **125**(4): p. 615-28.
145. Zimmerman, G.A., T.M. McIntyre, and S.M. Prescott, *Adhesion and signaling in vascular cell--cell interactions.* J Clin Invest, 1996. **98**(8): p. 1699-702.
146. Ley, K., *Pathways and bottlenecks in the web of inflammatory adhesion molecules and chemoattractants.* Immunol Res, 2001. **24**(1): p. 87-95.
147. Springer, T.A., *Traffic signals on endothelium for lymphocyte recirculation and leukocyte emigration.* Annu Rev Physiol, 1995. **57**: p. 827-72.
148. McEver, R.P., et al., *GMP-140, a platelet alpha-granule membrane protein, is also synthesized by vascular endothelial cells and is localized in Weibel-Palade bodies.* J Clin Invest, 1989. **84**(1): p. 92-9.
149. Bevilacqua, M.P., *Endothelial-leukocyte adhesion molecules.* Annu Rev Immunol, 1993. **11**: p. 767-804.
150. Summers, C., et al., *Neutrophil kinetics in health and disease.* Trends Immunol, 2010. **31**(8): p. 318-24.
151. Amulic, B., et al., *Neutrophil function: from mechanisms to disease.* Annu Rev Immunol, 2012. **30**: p. 459-89.
152. Chtanova, T., et al., *Dynamics of neutrophil migration in lymph nodes during infection.* Immunity, 2008. **29**(3): p. 487-96.
153. Mantovani, A., et al., *Neutrophils in the activation and regulation of innate and adaptive immunity.* Nat Rev Immunol, 2011. **11**(8): p. 519-31.
154. Borregaard, N., *Neutrophils, from marrow to microbes.* Immunity, 2010. **33**(5): p. 657-70.
155. Hager, M., J.B. Cowland, and N. Borregaard, *Neutrophil granules in health and disease.* J Intern Med, 2010. **268**(1): p. 25-34.
156. Brinkmann, V., et al., *Neutrophil extracellular traps kill bacteria.* Science, 2004. **303**(5663): p. 1532-5.

157. Papayannopoulos, V. and A. Zychlinsky, *NETs: a new strategy for using old weapons.* Trends Immunol, 2009. **30**(11): p. 513-21.
158. Yipp, B.G., et al., *Infection-induced NETosis is a dynamic process involving neutrophil multitasking in vivo.* Nat Med, 2012. **18**(9): p. 1386-93.
159. Menegazzi, R., E. Decleva, and P. Dri, *Killing by neutrophil extracellular traps: fact or folklore?* Blood, 2012. **119**(5): p. 1214-6.
160. Guimaraes-Costa, A.B., et al., *Leishmania amazonensis promastigotes induce and are killed by neutrophil extracellular traps.* Proc Natl Acad Sci U S A, 2009. **106**(16): p. 6748-53.
161. Kuijpers, T.W., R.S. Weening, and D. Roos, *Clinical and laboratory work-up of patients with neutrophil shortage or dysfunction.* J Immunol Methods, 1999. **232**(1-2): p. 211-29.
162. Winkelstein, J.A., et al., *Chronic granulomatous disease. Report on a national registry of 368 patients.* Medicine (Baltimore), 2000. **79**(3): p. 155-69.
163. van den Berg, J.M., et al., *Chronic granulomatous disease: the European experience.* PLoS One, 2009. **4**(4): p. e5234.
164. Segal, B.H., et al., *NADPH oxidase limits innate immune responses in the lungs in mice.* PLoS One, 2010. **5**(3): p. e9631.
165. Peters, N.C., et al., *In vivo imaging reveals an essential role for neutrophils in leishmaniasis transmitted by sand flies.* Science, 2008. **321**(5891): p. 970-4.
166. Ribeiro-Gomes, F.L., et al., *Efficient capture of infected neutrophils by dendritic cells in the skin inhibits the early anti-leishmania response.* PLoS Pathog, 2012. **8**(2): p. e1002536.
167. Geissmann, F., S. Jung, and D.R. Littman, *Blood monocytes consist of two principal subsets with distinct migratory properties.* Immunity, 2003. **19**(1): p. 71-82.
168. van Furth, R. and Z.A. Cohn, *The origin and kinetics of mononuclear phagocytes.* J Exp Med, 1968. **128**(3): p. 415-35.
169. Geissmann, F., et al., *Unravelling mononuclear phagocyte heterogeneity.* Nat Rev Immunol, 2010. **10**(6): p. 453-60.
170. Randolph, G.J., C. Jakubzick, and C. Qu, *Antigen presentation by monocytes and monocyte-derived cells.* Curr Opin Immunol, 2008. **20**(1): p. 52-60.
171. Sheel, M. and C.R. Engwerda, *The diverse roles of monocytes in inflammation caused by protozoan parasitic diseases.* Trends Parasitol, 2012. **28**(10): p. 408-16.
172. Jakubzick, C., et al., *Minimal differentiation of classical monocytes as they survey steady-state tissues and transport antigen to lymph nodes.* Immunity, 2013. **39**(3): p. 599-610.
173. Auffray, C., et al., *Monitoring of blood vessels and tissues by a population of monocytes with patrolling behavior.* Science, 2007. **317**(5838): p. 666-70.
174. Dunay, I.R., et al., *Gr1(+) inflammatory monocytes are required for mucosal resistance to the pathogen Toxoplasma gondii.* Immunity, 2008. **29**(2): p. 306-17.
175. Bosschaerts, T., et al., *Tip-DC development during parasitic infection is regulated by IL-10 and requires CCL2/CCR2, IFN-gamma and MyD88 signaling.* PLoS Pathog, 2010. **6**(8): p. e1001045.
176. Stijlemans, B., et al., *The central role of macrophages in trypanosomiasis-associated anemia: rationale for therapeutical*

approaches. Endocr Metab Immune Disord Drug Targets, 2010. **10**(1): p. 71-82.
177. Sponaas, A.M., et al., *Migrating monocytes recruited to the spleen play an important role in control of blood stage malaria*. Blood, 2009. **114**(27): p. 5522-31.
178. De Trez, C., et al., *iNOS-producing inflammatory dendritic cells constitute the major infected cell type during the chronic Leishmania major infection phase of C57BL/6 resistant mice*. PLoS Pathog, 2009. **5**(6): p. e1000494.
179. Goldszmid, R.S. and G. Trinchieri, *The price of immunity*. Nat Immunol, 2012. **13**(10): p. 932-8.
180. Goldszmid, R.S., et al., *NK cell-derived interferon-gamma orchestrates cellular dynamics and the differentiation of monocytes into dendritic cells at the site of infection*. Immunity, 2012. **36**(6): p. 1047-59.
181. Guilliams, M., et al., *IL-10 dampens TNF/inducible nitric oxide synthase-producing dendritic cell-mediated pathogenicity during parasitic infection*. J Immunol, 2009. **182**(2): p. 1107-18.
182. Goncalves, R., et al., *Platelet activation attracts a subpopulation of effector monocytes to sites of Leishmania major infection*. J Exp Med, 2011. **208**(6): p. 1253-65.
183. Amino, R., et al., *Quantitative imaging of Plasmodium transmission from mosquito to mammal*. Nat Med, 2006. **12**(2): p. 220-4.
184. Yamauchi, L.M., et al., *Plasmodium sporozoites trickle out of the injection site*. Cell Microbiol, 2007. **9**(5): p. 1215-22.
185. Chakravarty, S., et al., *CD8+ T lymphocytes protective against malaria liver stages are primed in skin-draining lymph nodes*. Nat Med, 2007. **13**(9): p. 1035-41.
186. Caljon, G., et al., *Tsetse fly saliva accelerates the onset of Trypanosoma brucei infection in a mouse model associated with a reduced host inflammatory response*. Infect Immun, 2006. **74**(11): p. 6324-30.
187. Ribeiro, J.M. and I.M. Francischetti, *Role of arthropod saliva in blood feeding: sialome and post-sialome perspectives*. Annu Rev Entomol, 2003. **48**: p. 73-88.
188. Caljon, G., et al., *Tsetse fly saliva biases the immune response to Th2 and induces anti-vector antibodies that are a useful tool for exposure assessment*. Int J Parasitol, 2006. **36**(9): p. 1025-35.
189. Gray, A.R. and A.G. Luckins, *The initial stage of infection with cyclically-transmitted Trypanosoma congolense in rabbits, calves and sheep*. J Comp Pathol, 1980. **90**(4): p. 499-512.
190. Mwangi, D.M., J. Hopkins, and A.G. Luckins, *Cellular phenotypes in Trypanosoma congolense infected sheep: the local skin reaction*. Parasite Immunol, 1990. **12**(6): p. 647-58.
191. Barry, J.D. and D.L. Emergy, *Parasite development and host responses during the establishment of Trypanosoma brucei infection transmitted by tsetse fly*. Parasitology, 1984. **88 (Pt 1)**: p. 67-84.
192. Mwangi, D.M., J. Hopkins, and A.G. Luckins, *Immunohistology of lymph nodes draining local skin reactions (chancres) in sheep infected with Trypanosoma congolense*. J Comp Pathol, 1991. **105**(1): p. 27-35.
193. Forster, R., A. Braun, and T. Worbs, *Lymph node homing of T cells and dendritic cells via afferent lymphatics*. Trends Immunol, 2012. **33**(6): p. 271-80.
194. Pepper, M.S. and M. Skobe, *Lymphatic endothelium: morphological, molecular and functional properties*. J Cell Biol, 2003. **163**(2): p. 209-13.

195. Schmid-Schonbein, G.W., *Microlymphatics and lymph flow*. Physiol Rev, 1990. **70**(4): p. 987-1028.
196. Ikomi, F. and G.W. Schmid-Schonbein, *Lymph pump mechanics in the rabbit hind leg*. Am J Physiol, 1996. **271**(1 Pt 2): p. H173-83.
197. Drexhage, H.A., et al., *A study of cells present in peripheral lymph of pigs with special reference to a type of cell resembling the Langerhans cell*. Cell Tissue Res, 1979. **202**(3): p. 407-30.
198. Pugh, C.W., G.G. MacPherson, and H.W. Steer, *Characterization of nonlymphoid cells derived from rat peripheral lymph*. J Exp Med, 1983. **157**(6): p. 1758-79.
199. Mayrhofer, G., P.G. Holt, and J.M. Papadimitriou, *Functional characteristics of the veiled cells in afferent lymph from the rat intestine*. Immunology, 1986. **58**(3): p. 379-87.
200. Brenner, I.K., et al., *Immune changes in humans during cold exposure: effects of prior heating and exercise*. J Appl Physiol (1985), 1999. **87**(2): p. 699-710.
201. Kripke, M.L., et al., *Evidence that cutaneous antigen-presenting cells migrate to regional lymph nodes during contact sensitization*. J Immunol, 1990. **145**(9): p. 2833-8.
202. Johnson, L.A. and D.G. Jackson, *Inflammation-induced secretion of CCL21 in lymphatic endothelium is a key regulator of integrin-mediated dendritic cell transmigration*. Int Immunol, 2010. **22**(10): p. 839-49.
203. Tal, O., et al., *DC mobilization from the skin requires docking to immobilized CCL21 on lymphatic endothelium and intralymphatic crawling*. J Exp Med, 2011. **208**(10): p. 2141-53.
204. Pflicke, H. and M. Sixt, *Preformed portals facilitate dendritic cell entry into afferent lymphatic vessels*. J Exp Med, 2009. **206**(13): p. 2925-35.
205. Vanhamme, L., et al., *An update on antigenic variation in African trypanosomes*. Trends Parasitol, 2001. **17**(7): p. 338-43.
206. Raper, J., et al., *Trypanosome lytic factors: novel mediators of human innate immunity*. Curr Opin Microbiol, 2001. **4**(4): p. 402-8.
207. Vanhollebeke, B., et al., *A haptoglobin-hemoglobin receptor conveys innate immunity to Trypanosoma brucei in humans*. Science, 2008. **320**(5876): p. 677-81.
208. Bullard, W., et al., *Haptoglobin-hemoglobin receptor independent killing of African trypanosomes by human serum and trypanosome lytic factors*. Virulence, 2012. **3**(1): p. 72-6.
209. Capewell, P., et al., *The TgsGP gene is essential for resistance to human serum in Trypanosoma brucei gambiense*. PLoS Pathog, 2013. **9**(10): p. e1003686.
210. Turner, C.M., *Antigenic variation in Trypanosoma brucei infections: an holistic view*. J Cell Sci, 1999. **112 (Pt 19)**: p. 3187-92.
211. Pays, E., *Regulation of antigen gene expression in Trypanosoma brucei*. Trends Parasitol, 2005. **21**(11): p. 517-20.
212. Morrison, L.J., L. Marcello, and R. McCulloch, *Antigenic variation in the African trypanosome: molecular mechanisms and phenotypic complexity*. Cell Microbiol, 2009. **11**(12): p. 1724-34.
213. Turner, C.M. and J.D. Barry, *High frequency of antigenic variation in Trypanosoma brucei rhodesiense infections*. Parasitology, 1989. **99 Pt 1**: p. 67-75.
214. Sileghem, M., et al., *Dual role of macrophages in the suppression of interleukin 2 production and interleukin 2 receptor expression in trypanosome-infected mice*. Eur J Immunol, 1989. **19**(5): p. 829-35.

215. Sileghem, M., et al., *Different mechanisms account for the suppression of interleukin 2 production and the suppression of interleukin 2 receptor expression in Trypanosoma brucei-infected mice*. Eur J Immunol, 1989. **19**(1): p. 119-24.
216. Radwanska, M., et al., *Trypanosomiasis-induced B cell apoptosis results in loss of protective anti-parasite antibody responses and abolishment of vaccine-induced memory responses.* PLoS Pathog, 2008. **4**(5): p. e1000078.
217. Branche, C., et al., *Conserved and specific functions of axoneme components in trypanosome motility.* J Cell Sci, 2006. **119**(Pt 16): p. 3443-55.
218. Baron, D.M., Z.P. Kabututu, and K.L. Hill, *Stuck in reverse: loss of LC1 in Trypanosoma brucei disrupts outer dynein arms and leads to reverse flagellar beat and backward movement.* J Cell Sci, 2007. **120**(Pt 9): p. 1513-20.
219. Broadhead, R., et al., *Flagellar motility is required for the viability of the bloodstream trypanosome.* Nature, 2006. **440**(7081): p. 224-7.
220. Ralston, K.S., et al., *The Trypanosoma brucei flagellum: moving parasites in new directions.* Annu Rev Microbiol, 2009. **63**: p. 335-62.
221. Walker, P.J., *Organization of function in trypanosome flagella.* Nature, 1961. **189**: p. 1017-8.
222. Ralston, K.S. and K.L. Hill, *The flagellum of Trypanosoma brucei: new tricks from an old dog.* Int J Parasitol, 2008. **38**(8-9): p. 869-84.
223. Ginger, M.L., N. Portman, and P.G. McKean, *Swimming with protists: perception, motility and flagellum assembly.* Nat Rev Microbiol, 2008. **6**(11): p. 838-50.
224. Ralston, K.S. and K.L. Hill, *Trypanin, a component of the flagellar Dynein regulatory complex, is essential in bloodstream form African trypanosomes.* PLoS Pathog, 2006. **2**(9): p. e101.
225. Uppaluri, S., et al., *Impact of microscopic motility on the swimming behavior of parasites: straighter trypanosomes are more directional.* PLoS Comput Biol, 2011. **7**(6): p. e1002058.
226. Rodriguez, J.A., et al., *Propulsion of African trypanosomes is driven by bihelical waves with alternating chirality separated by kinks.* Proc Natl Acad Sci U S A, 2009. **106**(46): p. 19322-7.
227. Heddergott, N., et al., *Trypanosome motion represents an adaptation to the crowded environment of the vertebrate bloodstream.* PLoS Pathog, 2012. **8**(11): p. e1003023.
228. Wilson, L.G., L.M. Carter, and S.E. Reece, *High-speed holographic microscopy of malaria parasites reveals ambidextrous flagellar waveforms.* Proc Natl Acad Sci U S A, 2013. **110**(47): p. 18769-74.
229. Shaevitz, J.W., J.Y. Lee, and D.A. Fletcher, *Spiroplasma swim by a processive change in body helicity.* Cell, 2005. **122**(6): p. 941-5.
230. Rotureau, B., et al., *Forward motility is essential for trypanosome infection in the tsetse fly.* Cell Microbiol, 2014. **16**(3): p. 425-33.
231. Weisse, S., et al., *A quantitative 3D motility analysis of Trypanosoma brucei by use of digital in-line holographic microscopy.* PLoS One, 2012. **7**(5): p. e37296.
232. Kisalu, N.K., et al., *Mouse infection and pathogenesis by Trypanosoma brucei motility mutants.* Cell Microbiol, 2014. **16**(6): p. 912-24.
233. Hill, K.L., *Biology and mechanism of trypanosome cell motility.* Eukaryot Cell, 2003. **2**(2): p. 200-8.

234. Jennings, F.W., et al., *The brain as a source of relapsing Trypanosoma brucei infection in mice after chemotherapy.* Int J Parasitol, 1979. **9**(4): p. 381-4.
235. Mulenga, C., et al., *Trypanosoma brucei brucei crosses the blood-brain barrier while tight junction proteins are preserved in a rat chronic disease model.* Neuropathol Appl Neurobiol, 2001. **27**(1): p. 77-85.
236. Wolburg, H., et al., *Late stage infection in sleeping sickness.* PLoS One, 2012. **7**(3): p. e34304.
237. Frevert, U., et al., *Early invasion of brain parenchyma by African trypanosomes.* PLoS One, 2012. **7**(8): p. e43913.
238. Roditi, I. and M.J. Lehane, *Interactions between trypanosomes and tsetse flies.* Curr Opin Microbiol, 2008. **11**(4): p. 345-51.
239. Sharma, R., et al., *The heart of darkness: growth and form of Trypanosoma brucei in the tsetse fly.* Trends Parasitol, 2009. **25**(11): p. 517-24.
240. Engstler, M., et al., *Hydrodynamic flow-mediated protein sorting on the cell surface of trypanosomes.* Cell, 2007. **131**(3): p. 505-15.
241. Grunfelder, C.G., et al., *Endocytosis of a glycosylphosphatidylinositol-anchored protein via clathrin-coated vesicles, sorting by default in endosomes, and exocytosis via RAB11-positive carriers.* Mol Biol Cell, 2003. **14**(5): p. 2029-40.
242. Pal, A., et al., *Rab5 and Rab11 mediate transferrin and anti-variant surface glycoprotein antibody recycling in Trypanosoma brucei.* Biochem J, 2003. **374**(Pt 2): p. 443-51.
243. Engstler, M., et al., *Kinetics of endocytosis and recycling of the GPI-anchored variant surface glycoprotein in Trypanosoma brucei.* J Cell Sci, 2004. **117**(Pt 7): p. 1105-15.
244. Kieft, R., et al., *Mechanism of Trypanosoma brucei gambiense (group 1) resistance to human trypanosome lytic factor.* Proc Natl Acad Sci U S A, 2010. **107**(37): p. 16137-41.
245. Hager, K.M., et al., *Endocytosis of a cytotoxic human high density lipoprotein results in disruption of acidic intracellular vesicles and subsequent killing of African trypanosomes.* J Cell Biol, 1994. **126**(1): p. 155-67.
246. Webb, H., et al., *The GPI-phospholipase C of Trypanosoma brucei is nonessential but influences parasitemia in mice.* J Cell Biol, 1997. **139**(1): p. 103-14.
247. Grandgenett, P.M., et al., *A function for a specific zinc metalloprotease of African trypanosomes.* PLoS Pathog, 2007. **3**(10): p. 1432-45.
248. Paindavoine, P., et al., *A gene from the variant surface glycoprotein expression site encodes one of several transmembrane adenylate cyclases located on the flagellum of Trypanosoma brucei.* Mol Cell Biol, 1992. **12**(3): p. 1218-25.
249. Emmer, B.T., et al., *Identification of a palmitoyl acyltransferase required for protein sorting to the flagellar membrane.* J Cell Sci, 2009. **122**(Pt 6): p. 867-74.
250. Proto, W.R., et al., *Trypanosoma brucei metacaspase 4 is a pseudopeptidase and a virulence factor.* J Biol Chem, 2011. **286**(46): p. 39914-25.
251. Millington, O.R., et al., *Imaging of the host/parasite interplay in cutaneous leishmaniasis.* Exp Parasitol, 2010. **126**(3): p. 310-7.

252. Myburgh, E., et al., *In vivo imaging of trypanosome-brain interactions and development of a rapid screening test for drugs against CNS stage trypanosomiasis.* PLoS Negl Trop Dis, 2013. **7**(8): p. e2384.
253. Claes, F., et al., *Bioluminescent imaging of Trypanosoma brucei shows preferential testis dissemination which may hamper drug efficacy in sleeping sickness.* PLoS Negl Trop Dis, 2009. **3**(7): p. e486.
254. Okuno, T., et al., *Applications of recombinant Leishmania amazonensis expressing egfp or the beta-galactosidase gene for drug screening and histopathological analysis.* Exp Anim, 2003. **52**(2): p. 109-18.
255. Lang, T., et al., *Bioluminescent Leishmania expressing luciferase for rapid and high throughput screening of drugs acting on amastigote-harbouring macrophages and for quantitative real-time monitoring of parasitism features in living mice.* Cell Microbiol, 2005. **7**(3): p. 383-92.
256. Akopyants, N.S., et al., *Demonstration of genetic exchange during cyclical development of Leishmania in the sand fly vector.* Science, 2009. **324**(5924): p. 265-8.
257. Kimblin, N., et al., *Quantification of the infectious dose of Leishmania major transmitted to the skin by single sand flies.* Proc Natl Acad Sci U S A, 2008. **105**(29): p. 10125-30.
258. Shapiro, E., C. Lu, and F. Baneyx, *A set of multicolored Photinus pyralis luciferase mutants for in vivo bioluminescence applications.* Protein Eng Des Sel, 2005. **18**(12): p. 581-7.
259. Loening, A.M., A.M. Wu, and S.S. Gambhir, *Red-shifted Renilla reniformis luciferase variants for imaging in living subjects.* Nat Methods, 2007. **4**(8): p. 641-3.
260. Kupfer, A., et al., *The specific direct interaction of helper T cells and antigen-presenting B cells.* Proc Natl Acad Sci U S A, 1986. **83**(16): p. 6080-3.
261. Monks, C.R., et al., *Three-dimensional segregation of supramolecular activation clusters in T cells.* Nature, 1998. **395**(6697): p. 82-6.
262. Dunbar, K.B. and M.I. Canto, *Confocal laser endomicroscopy in Barrett's esophagus and endoscopically inapparent Barrett's neoplasia: a prospective, randomized, double-blind, controlled, crossover trial.* Gastrointest Endosc, 2010. **72**(3): p. 668.
263. Squirrell, J.M., et al., *Long-term two-photon fluorescence imaging of mammalian embryos without compromising viability.* Nat Biotechnol, 1999. **17**(8): p. 763-7.
264. Cahalan, M.D., et al., *Two-photon tissue imaging: seeing the immune system in a fresh light.* Nat Rev Immunol, 2002. **2**(11): p. 872-80.
265. Andrade, B.B., et al., *Role of sand fly saliva in human and experimental leishmaniasis: current insights.* Scand J Immunol, 2007. **66**(2-3): p. 122-7.
266. Ng, L.G., et al., *Migratory dermal dendritic cells act as rapid sensors of protozoan parasites.* PLoS Pathog, 2008. **4**(11): p. e1000222.
267. Faust, N., et al., *Insertion of enhanced green fluorescent protein into the lysozyme gene creates mice with green fluorescent granulocytes and macrophages.* Blood, 2000. **96**(2): p. 719-26.
268. Hong, Y.K., et al., *Prox1 is a master control gene in the program specifying lymphatic endothelial cell fate.* Dev Dyn, 2002. **225**(3): p. 351-7.
269. Hagerling, R., et al., *Intravital two-photon microscopy of lymphatic vessel development and function using a transgenic Prox1 promoter-directed mOrange2 reporter mouse.* Biochem Soc Trans, 2011. **39**(6): p. 1674-81.

270. Kilkenny, C., et al., *Improving bioscience research reporting: the ARRIVE guidelines for reporting animal research.* PLoS Biol, 2010. **8**(6): p. e1000412.
271. Jenni, L., et al., *Hybrid formation between African trypanosomes during cyclical transmission.* Nature, 1986. **322**(6075): p. 173-5.
272. Jennings, F.W. and G.D. Gray, *Relapsed parasitaemia following chemotherapy of chronic T. brucei infections in mice and its relation to cerebral trypanosomes.* Contrib Microbiol Immunol, 1983. **7**: p. 147-54.
273. Jennings, F.W., *Chemotherapy of CNS-trypanosomiasis: combination chemotherapy with a 5-nitroimidazole (MK 436), an arsenical (Cymelarsan) and suramin.* Trop Med Parasitol, 1991. **42**(3): p. 157-60.
274. Hirumi, H. and K. Hirumi, *Continuous cultivation of Trypanosoma brucei blood stream forms in a medium containing a low concentration of serum protein without feeder cell layers.* J Parasitol, 1989. **75**(6): p. 985-9.
275. Wetzel, H. and G. Thiemann, *[Effect of bacterial infections and antibiotics on tsetse flies (Diptera, Glossinidae) (author's transl)].* Zentralbl Bakteriol Orig A, 1979. **245**(4): p. 534-43.
276. Herbert, W.J. and W.H. Lumsden, *Trypanosoma brucei: a rapid "matching" method for estimating the host's parasitemia.* Exp Parasitol, 1976. **40**(3): p. 427-31.
277. Schroeder, A., et al., *The RIN: an RNA integrity number for assigning integrity values to RNA measurements.* BMC Mol Biol, 2006. **7**: p. 3.
278. Weber, C., et al., *Role of alpha L beta 2 integrin avidity in transendothelial chemotaxis of mononuclear cells.* J Immunol, 1997. **159**(8): p. 3968-75.
279. Peacock, L., et al., *The influence of sex and fly species on the development of trypanosomes in tsetse flies.* PLoS Negl Trop Dis, 2012. **6**(2): p. e1515.
280. Dyer, N.A., et al., *Flying tryps: survival and maturation of trypanosomes in tsetse flies.* Trends Parasitol, 2013. **29**(4): p. 188-96.
281. Aksoy, S., W.C. Gibson, and M.J. Lehane, *Interactions between tsetse and trypanosomes with implications for the control of trypanosomiasis.* Adv Parasitol, 2003. **53**: p. 1-83.
282. van Grinsven, K.W., et al., *Adaptations in the glucose metabolism of procyclic Trypanosoma brucei isolates from tsetse flies and during differentiation of bloodstream forms.* Eukaryot Cell, 2009. **8**(8): p. 1307-11.
283. Rotureau, B., I. Subota, and P. Bastin, *Molecular bases of cytoskeleton plasticity during the Trypanosoma brucei parasite cycle.* Cell Microbiol, 2011. **13**(5): p. 705-16.
284. Gibson, W., et al., *The use of yellow fluorescent hybrids to indicate mating in Trypanosoma brucei.* Parasit Vectors, 2008. **1**(1): p. 4.
285. Otieno, L.H. and N. Darji, *Abundance of Pathogenic African Trypanosomes in the Salivary Secretions of Wild Glossina-Pallidipes.* Ann Trop Med Parasitol, 1979. **73**(6): p. 583-588.
286. Maudlin, I. and S.C. Welburn, *The role of lectins and trypanosome genotype in the maturation of midgut infections in Glossina morsitans.* Trop Med Parasitol, 1988. **39**(1): p. 56-8.
287. Dale, C., et al., *The kinetics of maturation of trypanosome infections in tsetse.* Parasitology, 1995. **111 (Pt 2)**: p. 187-91.
288. Maudlin, I., S.C. Welburn, and P. Milligan, *Salivary gland infection: a sex-linked recessive character in tsetse?* Acta Trop, 1990. **48**(1): p. 9-15.

289. Moloo, S.K., C.L. Sabwa, and J.M. Kabata, *Vector competence of Glossina pallidipes and G. morsitans centralis for Trypanosoma vivax, T. congolense and T. b. brucei.* Acta Trop, 1992. **51**(3-4): p. 271-80.
290. Rico, E., et al., *Bloodstream form pre-adaptation to the tsetse fly in Trypanosoma brucei.* Front Cell Infect Microbiol, 2013. **3**: p. 78.
291. MacGregor, P. and K.R. Matthews, *New discoveries in the transmission biology of sleeping sickness parasites: applying the basics.* J Mol Med (Berl), 2010. **88**(9): p. 865-71.
292. Walshe, D.P., M.J. Lehane, and L.R. Haines, *Post eclosion age predicts the prevalence of midgut trypanosome infections in Glossina.* PLoS One, 2011. **6**(11): p. e26984.
293. Welburn, S.C. and I. Maudlin, *The nature of the teneral state in Glossina and its role in the acquisition of trypanosome infection in tsetse.* Ann Trop Med Parasitol, 1992. **86**(5): p. 529-36.
294. Walshe, D.P., et al., *Prolonged gene knockdown in the tsetse fly Glossina by feeding double stranded RNA.* Insect Mol Biol, 2009. **18**(1): p. 11-9.
295. Kubi, C., et al., *The effect of starvation on the susceptibility of teneral and non-teneral tsetse flies to trypanosome infection.* Med Vet Entomol, 2006. **20**(4): p. 388-92.
296. Otieno, L.H., et al., *Some observations on factors associated with the development of Trypanosoma brucei brucei infections in Glossina morsitans morsitans.* Acta Trop, 1983. **40**(2): p. 113-20.
297. Dipeolu, O.O. and K.M. Adam, *On the use of membrane feeding to study the development of Trypanosoma brucei in Glossina.* Acta Trop, 1974. **32**(3): p. 185-201.
298. Olubayo, R.O., et al., *Dynamics of host blood effects in Glossina morsitans sspp. infected with Trypanosoma congolense and T. brucei.* Parasitol Res, 1994. **80**(3): p. 177-81.
299. Mihok, S., et al., *The influence of host blood on infection rates in Glossina morsitans sspp. infected with Trypanosoma congolense, T. brucei and T. simiae.* Parasitology, 1993. **107 (Pt 1)**: p. 41-8.
300. Mihok, S., et al., *Influence of D(+)-glucosamine on infection rates and parasite loads in tsetse flies (Glossina spp.) infected with Trypanosoma brucei.* Acta Trop, 1992. **51**(3-4): p. 217-28.
301. Maudlin, I. and S.C. Welburn, *Lectin mediated establishment of midgut infections of Trypanosoma congolense and Trypanosoma brucei in Glossina morsitans.* Trop Med Parasitol, 1987. **38**(3): p. 167-70.
302. Okoth, J.O. and R. Kapaata, *Trypanosome infection rates in Glossina fuscipes fuscipes Newst. in the Busoga sleeping sickness focus, Uganda.* Ann Trop Med Parasitol, 1986. **80**(4): p. 459-61.
303. Maudlin, I. and S.C. Welburn, *Maturation of trypanosome infections in tsetse.* Exp Parasitol, 1994. **79**(2): p. 202-5.
304. Welburn, S.C., I. Maudlin, and P.J. Milligan, *Trypanozoon: infectivity to humans is linked to reduced transmissibility in tsetse. I. Comparison of human serum-resistant and human serum-sensitive field isolates.* Exp Parasitol, 1995. **81**(3): p. 404-8.
305. Gibson, W. and M. Bailey, *The development of Trypanosoma brucei within the tsetse fly midgut observed using green fluorescent trypanosomes.* Kinetoplastid Biol Dis, 2003. **2**(1): p. 1.
306. Welburn, S.C. and I. Maudlin, *Lectin signalling of maturation of T. congolense infections in tsetse.* Med Vet Entomol, 1989. **3**(2): p. 141-5.
307. Gingrich, J.B., et al., *Trypanosoma brucei rhodesiense (Trypanosomatidae): factors influencing infection rates of a recent*

human isolate in the tsetse Glossina morsitans (Diptera: Glossinidae). J Med Entomol, 1982. **19**(3): p. 268-74.
308. Distelmans, W., et al., *The susceptibility of Glossina palpalis palpalis at different ages to infection with Trypanosoma congolense.* Ann Soc Belg Med Trop, 1982. **62**(1): p. 41-7.
309. Macleod, E.T., et al., *Factors affecting trypanosome maturation in tsetse flies.* PLoS One, 2007. **2**(2): p. e239.
310. Mews, A.R., *In vitro feeding of tsetse flies [proceedings].* Trans R Soc Trop Med Hyg, 1980. **74**(2): p. 276-7.
311. Welburn, S.C., I. Maudlin, and D.H. Molyneux, *Midgut lectin activity and sugar specificity in teneral and fed tsetse.* Med Vet Entomol, 1994. **8**(1): p. 81-7.
312. Harley, J.M.B., *Comparison of Susceptibility to Infection with Trypanosoma-Rhodesiense of Glossina-Pallidipes, G-Morsitans, G-Fuscipes and G-Brevipalpis.* Ann Trop Med Parasitol, 1971. **65**(2): p. 185-&.
313. Shapiro, S.Z., et al., *Analysis by flow cytometry of DNA synthesis during the life cycle of African trypanosomes.* Acta Trop, 1984. **41**(4): p. 313-23.
314. Nolan, D.P., et al., *Slender and stumpy bloodstream forms of Trypanosoma brucei display a differential response to extracellular acidic and proteolytic stress.* Eur J Biochem, 2000. **267**(1): p. 18-27.
315. Robertson, M., *Notes on the polymorphism of Trypanosoma gambiense in the blood and its relation to the exogenous cycle in Glossina palpalis.* Proceedings of the Royal Society of London Series B-Containing Papers of a Biological Character, 1912. **85**(582): p. 527-539.
316. Vickerman, K., *Polymorphism and mitochondrial activity in sleeping sickness trypanosomes.* Nature, 1965. **208**(5012): p. 762-6.
317. Bass, K.E. and C.C. Wang, *The in vitro differentiation of pleomorphic Trypanosoma brucei from bloodstream into procyclic form requires neither intermediary nor short-stumpy stage.* Mol Biochem Parasitol, 1991. **44**(2): p. 261-70.
318. Oberle, M., et al., *Bottlenecks and the maintenance of minor genotypes during the life cycle of Trypanosoma brucei.* PLoS Pathog, 2010. **6**(7): p. e1001023.
319. Peacock, L., et al., *Intraclonal mating occurs during tsetse transmission of Trypanosoma brucei.* Parasit Vectors, 2009. **2**(1): p. 43.
320. Maudlin, I. and P. Dukes, *Extrachromosomal inheritance of susceptibility to trypanosome infection in tsetse flies. I. Selection of susceptible and refractory lines of Glossina morsitans morsitans.* Ann Trop Med Parasitol, 1985. **79**(3): p. 317-24.
321. Amino, R., et al., *Quantitative imaging of Plasmodium sporozoites in the mammalian host.* C R Biol, 2006. **329**(11): p. 858-62.
322. Amino, R., R. Menard, and F. Frischknecht, *In vivo imaging of malaria parasites--recent advances and future directions.* Curr Opin Microbiol, 2005. **8**(4): p. 407-14.
323. Tavares, J., et al., *Role of host cell traversal by the malaria sporozoite during liver infection.* J Exp Med, 2013. **210**(5): p. 905-15.
324. Shannon, J.G., C.F. Bosio, and B.J. Hinnebusch, *Dermal Neutrophil, Macrophage and Dendritic Cell Responses to Yersinia pestis Transmitted by Fleas.* PLoS Pathog, 2015. **11**(3): p. e1004734.
325. Gibson, V.B., et al., *A novel method to allow noninvasive, longitudinal imaging of the murine immune system in vivo.* Blood, 2012. **119**(11): p. 2545-51.

326. Peters, N.C., et al., *In vivo imaging reveals an essential role for neutrophils in leishmaniasis transmitted by sand flies.* Science, 2008. **321**(5891): p. 970-974.
327. Wei, G., et al., *Intradermal infections of mice by low numbers of african trypanosomes are controlled by innate resistance but enhance susceptibility to reinfection.* J Infect Dis, 2011. **203**(3): p. 418-29.
328. Van Den Abbeele, J., et al., *The Glossina morsitans tsetse fly saliva: general characteristics and identification of novel salivary proteins.* Insect Biochem Mol Biol, 2007. **37**(10): p. 1075-85.
329. Caljon, G., et al., *Identification of a tsetse fly salivary protein with dual inhibitory action on human platelet aggregation.* PLoS One, 2010. **5**(3): p. e9671.
330. Van Den Abbeele, J., et al., *Trypanosoma brucei modifies the tsetse salivary composition, altering the fly feeding behavior that favors parasite transmission.* PLoS Pathog, 2010. **6**(6): p. e1000926.
331. Belkaid, Y., et al., *Development of a natural model of cutaneous leishmaniasis: powerful effects of vector saliva and saliva preexposure on the long-term outcome of Leishmania major infection in the mouse ear dermis.* J Exp Med, 1998. **188**(10): p. 1941-53.
332. Titus, R.G. and J.M. Ribeiro, *Salivary gland lysates from the sand fly Lutzomyia longipalpis enhance Leishmania infectivity.* Science, 1988. **239**(4845): p. 1306-8.
333. Emery, D.L. and S.K. Moloo, *The Sequential Cellular-Changes in the Local Skin Reaction Produced in Goats by Glossina-Morsitans-Morsitans Infected with Trypanosoma-(Trypanozoon)-Brucei.* Acta Trop, 1980. **37**(2): p. 137-149.
334. Emery, D.L., J.D. Barry, and S.K. Moloo, *The Appearance of Trypanosoma (Duttonella) Vivax in Lymph Following Challenge of Goats with Infected Glossina-Morsitans-Morsitans - Short Communication.* Acta Trop, 1980. **37**(4): p. 375-379.
335. Maudlin, I. and S.C. Welburn, *A single trypanosome is sufficient to infect a tsetse fly.* Ann Trop Med Parasitol, 1989. **83**(4): p. 431-3.
336. Deflorin, J., M. Rudolf, and T. Seebeck, *The major components of the paraflagellar rod of Trypanosoma brucei are two similar, but distinct proteins which are encoded by two different gene loci.* J Biol Chem, 1994. **269**(46): p. 28745-51.
337. Gueirard, P., et al., *Development of the malaria parasite in the skin of the mammalian host.* Proc Natl Acad Sci U S A, 2010. **107**(43): p. 18640-5.
338. Titus, R.G., J.V. Bishop, and J.S. Mejia, *The immunomodulatory factors of arthropod saliva and the potential for these factors to serve as vaccine targets to prevent pathogen transmission.* Parasite Immunol, 2006. **28**(4): p. 131-41.
339. Peters, N.C., et al., *Vector transmission of leishmania abrogates vaccine-induced protective immunity.* PLoS Pathog, 2009. **5**(6): p. e1000484.
340. Donovan, M.J., et al., *Uninfected mosquito bites confer protection against infection with malaria parasites.* Infect Immun, 2007. **75**(5): p. 2523-30.
341. Vaughan, J.A., et al., *Infectivity of Plasmodium berghei sporozoites delivered by intravenous inoculation versus mosquito bite: implications for sporozoite vaccine trials.* Infect Immun, 1999. **67**(8): p. 4285-9.
342. Kovar, L., *Tick saliva in anti-tick immunity and pathogen transmission.* Folia Microbiol (Praha), 2004. **49**(3): p. 327-36.

343. Nuttall, P.A., et al., *Vector-host interactions in disease transmission.* J Mol Microbiol Biotechnol, 2000. **2**(4): p. 381-6.
344. Schoeler, G.B. and S.K. Wikel, *Modulation of host immunity by haematophagous arthropods.* Ann Trop Med Parasitol, 2001. **95**(8): p. 755-71.
345. Wikel, S.K. and D. Bergman, *Tick-host immunology: Significant advances and challenging opportunities.* Parasitol Today, 1997. **13**(10): p. 383-9.
346. Brossard, M. and S.K. Wikel, *Immunology of interactions between ticks and hosts.* Med Vet Entomol, 1997. **11**(3): p. 270-6.
347. Wikel, S.K., et al., *Infestation with pathogen-free nymphs of the tick Ixodes scapularis induces host resistance to transmission of Borrelia burgdorferi by ticks.* Infect Immun, 1997. **65**(1): p. 335-8.
348. Champagne, D.E., *Antihemostatic strategies of blood-feeding arthropods.* Curr Drug Targets Cardiovasc Haematol Disord, 2004. **4**(4): p. 375-96.
349. Desbarats, J., et al., *Rapid early onset lymphocyte cell death in mice resistant, but not susceptible to Leishmania major infection.* Apoptosis, 2000. **5**(2): p. 189-96.
350. Gillespie, R.D., M.L. Mbow, and R.G. Titus, *The immunomodulatory factors of bloodfeeding arthropod saliva.* Parasite Immunol, 2000. **22**(7): p. 319-31.
351. Bowman, A.S., et al., *Tick saliva: recent advances and implications for vector competence.* Med Vet Entomol, 1997. **11**(3): p. 277-85.
352. Teixeira, C., et al., *Characterization of the early inflammatory infiltrate at the feeding site of infected sand flies in mice protected from vector-transmitted Leishmania major by exposure to uninfected bites.* PLoS Negl Trop Dis, 2014. **8**(4): p. e2781.
353. Soares, M.B., et al., *The vasoactive peptide maxadilan from sand fly saliva inhibits TNF-alpha and induces IL-6 by mouse macrophages through interaction with the pituitary adenylate cyclase-activating polypeptide (PACAP) receptor.* J Immunol, 1998. **160**(4): p. 1811-6.
354. Morris, R.V., et al., *Sandfly maxadilan exacerbates infection with Leishmania major and vaccinating against it protects against L. major infection.* J Immunol, 2001. **167**(9): p. 5226-30.
355. Hall, L.R. and R.G. Titus, *Sand fly vector saliva selectively modulates macrophage functions that inhibit killing of Leishmania major and nitric oxide production.* J Immunol, 1995. **155**(7): p. 3501-6.
356. Thangamani, S., et al., *Host immune response to mosquito-transmitted chikungunya virus differs from that elicited by needle inoculated virus.* PLoS One, 2010. **5**(8): p. e12137.
357. Chen, G.Y. and G. Nunez, *Sterile inflammation: sensing and reacting to damage.* Nat Rev Immunol, 2010. **10**(12): p. 826-37.
358. Mansfield, J.M. and D.M. Paulnock, *Regulation of innate and acquired immunity in African trypanosomiasis.* Parasite Immunol, 2005. **27**(10-11): p. 361-71.
359. Beschin, A., et al., *Trypanosoma brucei infection elicits nitric oxide-dependent and nitric oxide-independent suppressive mechanisms.* J Leukoc Biol, 1998. **63**(4): p. 429-39.
360. Roelants, G.E. and M. Pinder, *Immunobiology of African trypanosomiasis.* Contemp Top Immunobiol, 1984. **12**: p. 225-74.
361. Askonas, B.A., *Macrophages as mediators of immunosuppression in murine African trypanosomiasis.* Curr Top Microbiol Immunol, 1985. **117**: p. 119-27.

362. Tabel, H., R.S. Kaushik, and J.E. Uzonna, *Susceptibility and resistance to Trypanosoma congolense infections.* Microbes Infect, 2000. **2**(13): p. 1619-29.
363. Germena, G., et al., *Mutation in the CD45 inhibitory wedge modulates integrin activation and leukocyte recruitment during inflammation.* J Immunol, 2015. **194**(2): p. 728-38.
364. Craig, A., et al., *Neutrophil recruitment to the lungs during bacterial pneumonia.* Infect Immun, 2009. **77**(2): p. 568-75.
365. Mantovani, B., M. Rabinovitch, and V. Nussenzweig, *Phagocytosis of immune complexes by macrophages. Different roles of the macrophage receptor sites for complement (C3) and for immunoglobulin (IgG).* J Exp Med, 1972. **135**(4): p. 780-92.
366. Murray, P.J. and T.A. Wynn, *Protective and pathogenic functions of macrophage subsets.* Nat Rev Immunol, 2011. **11**(11): p. 723-37.
367. Baetselier, P.D., et al., *Alternative versus classical macrophage activation during experimental African trypanosomosis.* Int J Parasitol, 2001. **31**(5-6): p. 575-87.
368. Schleifer, K.W. and J.M. Mansfield, *Suppressor macrophages in African trypanosomiasis inhibit T cell proliferative responses by nitric oxide and prostaglandins.* J Immunol, 1993. **151**(10): p. 5492-503.
369. Schleifer, K.W., et al., *Characterization of T helper cell responses to the trypanosome variant surface glycoprotein.* J Immunol, 1993. **150**(7): p. 2910-9.
370. Hertz, C.J., H. Filutowicz, and J.M. Mansfield, *Resistance to the African trypanosomes is IFN-gamma dependent.* J Immunol, 1998. **161**(12): p. 6775-83.
371. Hertz, C.J. and J.M. Mansfield, *IFN-gamma-dependent nitric oxide production is not linked to resistance in experimental African trypanosomiasis.* Cell Immunol, 1999. **192**(1): p. 24-32.
372. Nathan, C., *Mechanisms and modulation of macrophage activation.* Behring Inst Mitt, 1991(88): p. 200-7.
373. Mosser, D.M., *The many faces of macrophage activation.* J Leukoc Biol, 2003. **73**(2): p. 209-12.
374. Landsverk, O.J., O. Bakke, and T.F. Gregers, *MHC II and the endocytic pathway: regulation by invariant chain.* Scand J Immunol, 2009. **70**(3): p. 184-93.
375. White, G.E., A.J. Iqbal, and D.R. Greaves, *CC chemokine receptors and chronic inflammation--therapeutic opportunities and pharmacological challenges.* Pharmacol Rev, 2013. **65**(1): p. 47-89.
376. Loetscher, P., et al., *The ligands of CXC chemokine receptor 3, I-TAC, Mig, and IP10, are natural antagonists for CCR3.* J Biol Chem, 2001. **276**(5): p. 2986-91.
377. Nouailles, G., et al., *CXCL5-secreting pulmonary epithelial cells drive destructive neutrophilic inflammation in tuberculosis.* J Clin Invest, 2014. **124**(3): p. 1268-82.
378. Daley, J.M., et al., *Use of Ly6G-specific monoclonal antibody to deplete neutrophils in mice.* J Leukoc Biol, 2008. **83**(1): p. 64-70.
379. Mac-Daniel, L., et al., *Local immune response to injection of Plasmodium sporozoites into the skin.* J Immunol, 2014. **193**(3): p. 1246-57.
380. Ganz, M., et al., *Lipopolysaccharide induces and activates the Nalp3 inflammasome in the liver.* World J Gastroenterol, 2011. **17**(43): p. 4772-8.

381. Pawlinski, R., et al., *Regulation of tissue factor and inflammatory mediators by Egr-1 in a mouse endotoxemia model.* Blood, 2003. **101**(10): p. 3940-7.
382. Ishikawa, Y., et al., *Local skin response in mice induced by a single intradermal injection of bacterial lipopolysaccharide and lipid A.* Infect Immun, 1991. **59**(6): p. 1954-60.
383. Magez, S., et al., *Interferon-gamma and nitric oxide in combination with antibodies are key protective host immune factors during trypanosoma congolense Tc13 Infections.* J Infect Dis, 2006. **193**(11): p. 1575-83.
384. Dagenais, T.R., et al., *Processing and presentation of variant surface glycoprotein molecules to T cells in African trypanosomiasis.* J Immunol, 2009. **183**(5): p. 3344-55.
385. Bafort, J.M., H. Schmidt, and D.H. Molyneux, *Development of Trypanosoma brucei in suckling mouse brain following intracerebral injection.* Trans R Soc Trop Med Hyg, 1987. **81**(3): p. 487-90.
386. Mogk, S., et al., *The lane to the brain: how African trypanosomes invade the CNS.* Trends Parasitol, 2014. **30**(10): p. 470-7.
387. Mogk, S., et al., *Cyclical appearance of African trypanosomes in the cerebrospinal fluid: new insights in how trypanosomes enter the CNS.* PLoS One, 2014. **9**(3): p. e91372.
388. Peters, N.C. and D.L. Sacks, *The impact of vector-mediated neutrophil recruitment on cutaneous leishmaniasis.* Cell Microbiol, 2009. **11**(9): p. 1290-6.
389. Nathan, C., *Neutrophils and immunity: challenges and opportunities.* Nat Rev Immunol, 2006. **6**(3): p. 173-82.
390. Tateda, K., et al., *Early recruitment of neutrophils determines subsequent T1/T2 host responses in a murine model of Legionella pneumophila pneumonia.* J Immunol, 2001. **166**(5): p. 3355-61.
391. Romani, L., et al., *An immunoregulatory role for neutrophils in CD4+ T helper subset selection in mice with candidiasis.* J Immunol, 1997. **158**(5): p. 2356-62.
392. Mocsai, A., *Diverse novel functions of neutrophils in immunity, inflammation, and beyond.* J Exp Med, 2013. **210**(7): p. 1283-99.
393. Kim, J.V. and M.L. Dustin, *Innate response to focal necrotic injury inside the blood-brain barrier.* J Immunol, 2006. **177**(8): p. 5269-77.
394. Teixeira, C.R., et al., *Saliva from Lutzomyia longipalpis induces CC chemokine ligand 2/monocyte chemoattractant protein-1 expression and macrophage recruitment.* J Immunol, 2005. **175**(12): p. 8346-53.
395. van Zandbergen, G., et al., *Cutting edge: neutrophil granulocyte serves as a vector for Leishmania entry into macrophages.* J Immunol, 2004. **173**(11): p. 6521-5.
396. McFarlane, E., et al., *Neutrophils contribute to development of a protective immune response during onset of infection with Leishmania donovani.* Infect Immun, 2008. **76**(2): p. 532-41.
397. Tacchini-Cottier, F., et al., *An immunomodulatory function for neutrophils during the induction of a CD4+ Th2 response in BALB/c mice infected with Leishmania major.* J Immunol, 2000. **165**(5): p. 2628-36.
398. Ribeiro-Gomes, F.L., et al., *Macrophage interactions with neutrophils regulate Leishmania major infection.* J Immunol, 2004. **172**(7): p. 4454-62.
399. Ribeiro-Gomes, F.L., M.T. Silva, and G.A. Dosreis, *Neutrophils, apoptosis and phagocytic clearance: an innate sequence of cellular responses*

regulating intramacrophagic parasite infections. Parasitology, 2006. **132 Suppl**: p. S61-8.
400. Laskay, T., G. van Zandbergen, and W. Solbach, *Neutrophil granulocytes as host cells and transport vehicles for intracellular pathogens: apoptosis as infection-promoting factor*. Immunobiology, 2008. **213**(3-4): p. 183-91.
401. Cappello, M., et al., *Tsetse thrombin inhibitor: bloodmeal-induced expression of an anticoagulant in salivary glands and gut tissue of Glossina morsitans morsitans*. Proc Natl Acad Sci U S A, 1998. **95**(24): p. 14290-5.
402. Caljon, G., et al., *Tsetse salivary gland proteins 1 and 2 are high affinity nucleic acid binding proteins with residual nuclease activity*. PLoS One, 2012. **7**(10): p. e47233.
403. Caljon, G., et al., *Identification of a functional Antigen5-related allergen in the saliva of a blood feeding insect, the tsetse fly*. Insect Biochem Mol Biol, 2009. **39**(5-6): p. 332-41.
404. Cappello, M., et al., *Isolation and characterization of the tsetse thrombin inhibitor: a potent antithrombotic peptide from the saliva of Glossina morsitans morsitans*. Am J Trop Med Hyg, 1996. **54**(5): p. 475-80.
405. Kopecky, J., M. Kuthejlova, and J. Pechova, *Salivary gland extract from Ixodes ricinus ticks inhibits production of interferon-gamma by the upregulation of interleukin-10*. Parasite Immunol, 1999. **21**(7): p. 351-6.
406. Kovar, L., J. Kopecky, and B. Rihova, *Salivary gland extract from Ixodes ricinus tick polarizes the cytokine profile toward Th2 and suppresses proliferation of T lymphocytes in human PBMC culture*. J Parasitol, 2001. **87**(6): p. 1342-8.
407. Zer, R., et al., *Effect of sand fly saliva on Leishmania uptake by murine macrophages*. Int J Parasitol, 2001. **31**(8): p. 810-4.
408. Peters, N.C., *In vivo imaging reveals an essential role for neutrophils in leishmaniasis transmitted by sand flies (vol 321, pg 970, 2008)*. Science, 2008. **322**(5908): p. 1634-1634.
409. Cassatella, M.A., *The production of cytokines by polymorphonuclear neutrophils*. Immunol Today, 1995. **16**(1): p. 21-6.
410. Galligan, C. and T. Yoshimura, *Phenotypic and functional changes of cytokine-activated neutrophils*. Chem Immunol Allergy, 2003. **83**: p. 24-44.
411. Allen, L.A. and R.L. McCaffrey, *To activate or not to activate: distinct strategies used by Helicobacter pylori and Francisella tularensis to modulate the NADPH oxidase and survive in human neutrophils*. Immunol Rev, 2007. **219**: p. 103-17.
412. Carlyon, J.A. and E. Fikrig, *Mechanisms of evasion of neutrophil killing by Anaplasma phagocytophilum*. Curr Opin Hematol, 2006. **13**(1): p. 28-33.
413. El-Sayed, N.M. and J.E. Donelson, *African trypanosomes have differentially expressed genes encoding homologues of the Leishmania GP63 surface protease*. J Biol Chem, 1997. **272**(42): p. 26742-8.
414. Langousis, G. and K.L. Hill, *Motility and more: the flagellum of Trypanosoma brucei*. Nat Rev Microbiol, 2014. **12**(7): p. 505-18.
415. Brittingham, A., et al., *Role of the Leishmania surface protease gp63 in complement fixation, cell adhesion, and resistance to complement-mediated lysis*. J Immunol, 1995. **155**(6): p. 3102-11.
416. Campbell, D.A., U. Kurath, and J. Fleischmann, *Identification of a gp63 surface glycoprotein in Leishmania tarentolae*. FEMS Microbiol Lett, 1992. **75**(1): p. 89-92.

417. d'Avila-Levy, C.M., et al., *Crithidia deanei: influence of parasite gp63 homologue on the interaction of endosymbiont-harboring and aposymbiotic strains with Aedes aegypti midgut.* Exp Parasitol, 2008. **118**(3): p. 345-53.
418. LaCount, D.J., et al., *Expression and function of the Trypanosoma brucei major surface protease (GP63) genes.* J Biol Chem, 2003. **278**(27): p. 24658-64.
419. Amino, R., et al., *Host cell traversal is important for progression of the malaria parasite through the dermis to the liver.* Cell Host Microbe, 2008. **3**(2): p. 88-96.
420. Lukacs, N.W., et al., *Chemokines: function, regulation and alteration of inflammatory responses.* Chem Immunol, 1999. **72**: p. 102-20.
421. Baggiolini, M., *Chemokines and leukocyte traffic.* Nature, 1998. **392**(6676): p. 565-8.
422. Bozic, C.R., et al., *The murine interleukin 8 type B receptor homologue and its ligands. Expression and biological characterization.* J Biol Chem, 1994. **269**(47): p. 29355-8.
423. Faunce, D.E., K.H. Sonoda, and J. Stein-Streilein, *MIP-2 recruits NKT cells to the spleen during tolerance induction.* J Immunol, 2001. **166**(1): p. 313-21.
424. Zhao, M.Q., et al., *Alveolar epithelial cell chemokine expression triggered by antigen-specific cytolytic CD8(+) T cell recognition.* J Clin Invest, 2000. **106**(6): p. R49-58.
425. Mancardi, S., et al., *Evidence of CXC, CC and C chemokine production by lymphatic endothelial cells.* Immunology, 2003. **108**(4): p. 523-30.
426. Liu, Q., Y. Wang, and H. Thorlacius, *Dexamethasone inhibits tumor necrosis factor-alpha-induced expression of macrophage inflammatory protein-2 and adhesion of neutrophils to endothelial cells.* Biochem Biophys Res Commun, 2000. **271**(2): p. 364-7.
427. Kato, A., et al., *Specific role of interleukin-1 in hepatic neutrophil recruitment after ischemia/reperfusion.* Am J Pathol, 2002. **161**(5): p. 1797-803.
428. Craciun, F.L., E.R. Schuller, and D.G. Remick, *Early enhanced local neutrophil recruitment in peritonitis-induced sepsis improves bacterial clearance and survival.* J Immunol, 2010. **185**(11): p. 6930-8.
429. Chong, S.Z., M. Evrard, and L.G. Ng, *Lights, camera, and action: vertebrate skin sets the stage for immune cell interaction with arthropod-vectored pathogens.* Front Immunol, 2013. **4**: p. 286.
430. Roediger, B., et al., *Visualizing dendritic cell migration within the skin.* Histochem Cell Biol, 2008. **130**(6): p. 1131-46.
431. Ng, L.G., et al., *Visualizing the neutrophil response to sterile tissue injury in mouse dermis reveals a three-phase cascade of events.* J Invest Dermatol, 2011. **131**(10): p. 2058-68.
432. Ariotti, S., et al., *Tissue-resident memory CD8+ T cells continuously patrol skin epithelia to quickly recognize local antigen.* Proc Natl Acad Sci U S A, 2012. **109**(48): p. 19739-44.
433. Frevert, U., et al., *Intravital observation of Plasmodium berghei sporozoite infection of the liver.* PLoS Biol, 2005. **3**(6): p. e192.
434. Vanderberg, J.P. and U. Frevert, *Intravital microscopy demonstrating antibody-mediated immobilisation of Plasmodium berghei sporozoites injected into skin by mosquitoes.* Int J Parasitol, 2004. **34**(9): p. 991-6.

435. Frischknecht, F., et al., *Imaging movement of malaria parasites during transmission by Anopheles mosquitoes.* Cell Microbiol, 2004. **6**(7): p. 687-94.
436. Baldacci, P. and R. Menard, *The elusive malaria sporozoite in the mammalian host.* Mol Microbiol, 2004. **54**(2): p. 298-306.
437. Peters, N. and D. Sacks, *Immune privilege in sites of chronic infection: Leishmania and regulatory T cells.* Immunol Rev, 2006. **213**: p. 159-79.
438. Coombes, J.L. and E.A. Robey, *Dynamic imaging of host-pathogen interactions in vivo.* Nat Rev Immunol, 2010. **10**(5): p. 353-64.
439. Filipe-Santos, O., et al., *A dynamic map of antigen recognition by CD4 T cells at the site of Leishmania major infection.* Cell Host Microbe, 2009. **6**(1): p. 23-33.
440. Schaeffer, M., et al., *Dynamic imaging of T cell-parasite interactions in the brains of mice chronically infected with Toxoplasma gondii.* J Immunol, 2009. **182**(10): p. 6379-93.
441. Wilson, E.H., et al., *Behavior of parasite-specific effector CD8+ T cells in the brain and visualization of a kinesis-associated system of reticular fibers.* Immunity, 2009. **30**(2): p. 300-11.
442. Morrison, W.I. and M. Murray, *Trypanosoma congolense: inheritance of susceptibility to infection in inbred strains of mice.* Exp Parasitol, 1979. **48**(3): p. 364-74.
443. Kolaczkowska, E. and P. Kubes, *Neutrophil recruitment and function in health and inflammation.* Nat Rev Immunol, 2013. **13**(3): p. 159-75.
444. Stutzmann, G.E. and I. Parker, *Dynamic multiphoton imaging: a live view from cells to systems.* Physiology (Bethesda), 2005. **20**: p. 15-21.
445. Sumen, C., et al., *Intravital microscopy: visualizing immunity in context.* Immunity, 2004. **21**(3): p. 315-29.
446. Garbow, J.R., Z. Zhang, and M. You, *Detection of primary lung tumors in rodents by magnetic resonance imaging.* Cancer Res, 2004. **64**(8): p. 2740-2.
447. Hutchings, N.R., J.E. Donelson, and K.L. Hill, *Trypanin is a cytoskeletal linker protein and is required for cell motility in African trypanosomes.* J Cell Biol, 2002. **156**(5): p. 867-77.
448. Li, W., et al., *Wound-healing perspectives.* Dermatol Clin, 2005. **23**(2): p. 181-92.
449. Cross, M., et al., *Mouse lysozyme M gene: isolation, characterization, and expression studies.* Proc Natl Acad Sci U S A, 1988. **85**(17): p. 6232-6.
450. Chtanova, T., et al., *Dynamics of neutrophil migration in lymph nodes during infection.* Immunity, 2008. **29**(3): p. 487-496.
451. Kreisel, D., et al., *In vivo two-photon imaging reveals monocyte-dependent neutrophil extravasation during pulmonary inflammation.* Proc Natl Acad Sci U S A, 2010. **107**(42): p. 18073-18078.
452. Coombes, J.L., et al., *Motile invaded neutrophils in the small intestine of Toxoplasma gondii-infected mice reveal a potential mechanism for parasite spread.* Proc Natl Acad Sci U S A, 2013. **110**(21): p. E1913-22.
453. Wigle, J.T. and G. Oliver, *Prox1 function is required for the development of the murine lymphatic system.* Cell, 1999. **98**(6): p. 769-78.
454. Bianchi, R., et al., *A transgenic Prox1-Cre-tdTomato reporter mouse for lymphatic vessel research.* PLoS One, 2015. **10**(4): p. e0122976.
455. Worbs, T., et al., *CCR7 ligands stimulate the intranodal motility of T lymphocytes in vivo.* J Exp Med, 2007. **204**(3): p. 489-95.

456. Gunn, M.D., et al., *A chemokine expressed in lymphoid high endothelial venules promotes the adhesion and chemotaxis of naive T lymphocytes.* Proc Natl Acad Sci U S A, 1998. **95**(1): p. 258-63.
457. Kohl, L., D. Robinson, and P. Bastin, *Novel roles for the flagellum in cell morphogenesis and cytokinesis of trypanosomes.* EMBO J, 2003. **22**(20): p. 5336-46.
458. Sun, S.Y., et al., *An intracellular membrane junction consisting of flagellum adhesion glycoproteins links flagellum biogenesis to cell morphogenesis in Trypanosoma brucei.* J Cell Sci, 2013. **126**(Pt 2): p. 520-31.
459. Roberts, C.J., M.A. Gray, and A.R. Gray, *Local Skin Reactions in Cattle at Site on Infection with Trypanosoma Congolense by Glossina Morsitans and G Tachinoides.* Trans R Soc Trop Med Hyg, 1969. **63**(5): p. 620-&.
460. Nathan, C., *Points of control in inflammation.* Nature, 2002. **420**(6917): p. 846-852.
461. Ley, K., et al., *Getting to the site of inflammation: the leukocyte adhesion cascade updated.* Nature Reviews Immunology, 2007. **7**(9): p. 678-689.
462. Ng, L.G., et al., *Visualizing the Neutrophil Response to Sterile Tissue Injury in Mouse Dermis Reveals a Three-Phase Cascade of Events.* Journal of Investigative Dermatology, 2011. **131**(10): p. 2058-2068.
463. Bruns, S., et al., *Production of Extracellular Traps against Aspergillus fumigatus In Vitro and in Infected Lung Tissue Is Dependent on Invading Neutrophils and Influenced by Hydrophobin RodA.* PLoS Pathog, 2010. **6**(4).
464. Yipp, B.G., et al., *Infection-induced NETosis is a dynamic process involving neutrophil multitasking in vivo.* Nat Med, 2012. **18**(9): p. 1386-+.
465. Liese, J., et al., *Intravital two-photon microscopy of host-pathogen interactions in a mouse model of Staphylococcus aureus skin abscess formation.* Cell Microbiol, 2013. **15**(6): p. 891-909.
466. Harvie, E.A., et al., *Innate Immune Response to Streptococcus iniae Infection in Zebrafish Larvae.* Infect Immun, 2013. **81**(1): p. 110-121.
467. McDonald, B., *Intravascular danger signals guide neutrophils to sites of sterile inflammation (October, pg 362, 2010).* Science, 2011. **331**(6024): p. 1517-1517.
468. McDonald, B., et al., *Intravascular Danger Signals Guide Neutrophils to Sites of Sterile Inflammation.* Science, 2010. **330**(6002): p. 362-366.
469. Lammermann, T., et al., *Rapid leukocyte migration by integrin-independent flowing and squeezing.* Nature, 2008. **453**(7191): p. 51-+.
470. Lammermann, T., et al., *Neutrophil swarms require LTB4 and integrins at sites of cell death in vivo.* Nature, 2013. **498**(7454): p. 371-+.
471. Chtanova, T., et al., *Dynamics of T Cell, Antigen-Presenting Cell, and Pathogen Interactions during Recall Responses in the Lymph Node.* Immunity, 2009. **31**(2): p. 342-355.
472. McDonald, B., et al., *Intravascular danger signals guide neutrophils to sites of sterile inflammation.* Science, 2010. **330**(6002): p. 362-6.
473. Abadie, V., et al., *Neutrophils rapidly migrate via lymphatics after Mycobacterium bovis BCG intradermal vaccination and shuttle live bacilli to the draining lymph nodes.* Blood, 2005. **106**(5): p. 1843-50.
474. Ryan, T.J., *Structure and function of lymphatics.* J Invest Dermatol, 1989. **93**(2 Suppl): p. 18S-24S.

475. Muller, W.A., *Mechanisms of transendothelial migration of leukocytes.* Circ Res, 2009. **105**(3): p. 223-30.
476. Petri, B. and M.G. Bixel, *Molecular events during leukocyte diapedesis.* FEBS J, 2006. **273**(19): p. 4399-407.
477. Sage, P.T. and C.V. Carman, *Settings and mechanisms for trans-cellular diapedesis.* Front Biosci (Landmark Ed), 2009. **14**: p. 5066-83.
478. Lammermann, T., et al., *Rapid leukocyte migration by integrin-independent flowing and squeezing.* Nature, 2008. **453**(7191): p. 51-5.
479. Randolph, G.J., *Dendritic cell migration to lymph nodes: cytokines, chemokines, and lipid mediators.* Semin Immunol, 2001. **13**(5): p. 267-74.
480. Dieu, M.C., et al., *Selective recruitment of immature and mature dendritic cells by distinct chemokines expressed in different anatomic sites.* J Exp Med, 1998. **188**(2): p. 373-86.
481. Saeki, H., et al., *Cutting edge: secondary lymphoid-tissue chemokine (SLC) and CC chemokine receptor 7 (CCR7) participate in the emigration pathway of mature dendritic cells from the skin to regional lymph nodes.* J Immunol, 1999. **162**(5): p. 2472-5.
482. Weber, M., et al., *Interstitial dendritic cell guidance by haptotactic chemokine gradients.* Science, 2013. **339**(6117): p. 328-32.
483. Murphy, P.M., *Double duty for CCL21 in dendritic cell trafficking.* Immunity, 2010. **32**(5): p. 590-2.
484. Chen, S.C., et al., *Ectopic expression of the murine chemokines CCL21a and CCL21b induces the formation of lymph node-like structures in pancreas, but not skin, of transgenic mice.* J Immunol, 2002. **168**(3): p. 1001-8.
485. Baluk, P., et al., *Functionally specialized junctions between endothelial cells of lymphatic vessels.* J Exp Med, 2007. **204**(10): p. 2349-62.
486. Randolph, G.J., V. Angeli, and M.A. Swartz, *Dendritic-cell trafficking to lymph nodes through lymphatic vessels.* Nat Rev Immunol, 2005. **5**(8): p. 617-28.
487. Randolph, G.J., G. Sanchez-Schmitz, and V. Angeli, *Factors and signals that govern the migration of dendritic cells via lymphatics: recent advances.* Springer Semin Immunopathol, 2005. **26**(3): p. 273-87.
488. Swartz, M.A., J.A. Hubbell, and S.T. Reddy, *Lymphatic drainage function and its immunological implications: from dendritic cell homing to vaccine design.* Semin Immunol, 2008. **20**(2): p. 147-56.
489. Yamauchi, L.M., et al., *The binding of CCL2 to the surface of Trypanosoma cruzi induces chemo-attraction and morphogenesis.* Microbes Infect, 2007. **9**(1): p. 111-8.
490. Turner, L., W.S. Ryu, and H.C. Berg, *Real-time imaging of fluorescent flagellar filaments.* J Bacteriol, 2000. **182**(10): p. 2793-801.
491. Wadhams, G.H. and J.P. Armitage, *Making sense of it all: bacterial chemotaxis.* Nat Rev Mol Cell Biol, 2004. **5**(12): p. 1024-37.
492. Sinnis, P. and F. Zavala, *The skin: where malaria infection and the host immune response begin.* Semin Immunopathol, 2012. **34**(6): p. 787-92.
493. Welburn, S.C. and I. Maudlin, *A simple in vitro method for infecting tsetse with trypanosomes.* Ann Trop Med Parasitol, 1987. **81**(4): p. 453-5.
494. Akol, G.W. and M. Murray, *Parasite kinetics and immune responses in efferent prefemoral lymph draining skin reactions induced by tsetse-transmitted Trypanosoma congolense.* Vet Parasitol, 1986. **19**(3-4): p. 281-93.
495. Kennedy, A.D. and F.R. DeLeo, *Neutrophil apoptosis and the resolution of infection.* Immunol Res, 2009. **43**(1-3): p. 25-61.

496. Wright, H.L., et al., *Neutrophil function in inflammation and inflammatory diseases.* Rheumatology (Oxford), 2010. **49**(9): p. 1618-31.
497. Baici, A., et al., *Action of collagenase and elastase from human polymorphonuclear leukocytes on human articular cartilage.* Rheumatol Int, 1982. **2**(1): p. 11-6.
498. Scapini, P., et al., *The neutrophil as a cellular source of chemokines.* Immunol Rev, 2000. **177**: p. 195-203.
499. Lee, J., et al., *Chemokine binding and activities mediated by the mouse IL-8 receptor.* J Immunol, 1995. **155**(4): p. 2158-64.
500. Owhashi, M., et al., *The role of saliva of Anopheles stephensi in inflammatory response: identification of a high molecular weight neutrophil chemotactic factor.* Parasitol Res, 2001. **87**(5): p. 376-82.
501. Haddow, J.D., et al., *Identification of major soluble salivary gland proteins in teneral Glossina morsitans morsitans.* Insect Biochem Mol Biol, 2002. **32**(9): p. 1045-53.
502. Fontaine, A., et al., *Implication of haematophagous arthropod salivary proteins in host-vector interactions.* Parasit Vectors, 2011. **4**: p. 187.
503. Taiwo, V.O., J.O. Adejinmi, and J.O. Oluwaniyi, *Non-immune control of trypanosomosis: in vitro oxidative burst of PMA- and trypanosome-stimulated neutrophils of Boran and N'Dama cattle.* Onderstepoort J Vet Res, 2002. **69**(2): p. 155-61.
504. Schumann, K., et al., *Immobilized chemokine fields and soluble chemokine gradients cooperatively shape migration patterns of dendritic cells.* Immunity, 2010. **32**(5): p. 703-13.
505. Kabashima, K., et al., *CXCL12-CXCR4 engagement is required for migration of cutaneous dendritic cells.* Am J Pathol, 2007. **171**(4): p. 1249-57.
506. Qu, C., et al., *Role of CCR8 and other chemokine pathways in the migration of monocyte-derived dendritic cells to lymph nodes.* J Exp Med, 2004. **200**(10): p. 1231-41.
507. Tan, T.H., et al., *Macrophage migration inhibitory factor of the parasitic nematode Trichinella spiralis.* Biochem J, 2001. **357**(Pt 2): p. 373-83.
508. Pennock, J.L., et al., *Rapid purification and characterization of L-dopachrome-methyl ester tautomerase (macrophage-migration-inhibitory factor) from Trichinella spiralis, Trichuris muris and Brugia pahangi.* Biochem J, 1998. **335 (Pt 3)**: p. 495-8.
509. Han, Z.F., D.D. Shao, and H. Wang, *[Cloning and expression of a homologue of human macrophage migration inhibitory factor from P. falciparum 3D7].* Zhongguo Yi Xue Ke Xue Yuan Xue Bao, 2004. **26**(5): p. 515-8.
510. Sommerville, C., et al., *Biochemical and immunological characterization of Toxoplasma gondii macrophage migration inhibitory factor.* J Biol Chem, 2013. **288**(18): p. 12733-41.
511. Stein, L.H., et al., *Eosinophils utilize multiple chemokine receptors for chemotaxis to the parasitic nematode Strongyloides stercoralis.* J Innate Immun, 2009. **1**(6): p. 618-30.
512. Dadiani, M., et al., *Real-time imaging of lymphogenic metastasis in orthotopic human breast cancer.* Cancer Res, 2006. **66**(16): p. 8037-41.
513. Hayashi, K., et al., *Real-time imaging of tumor-cell shedding and trafficking in lymphatic channels.* Cancer Res, 2007. **67**(17): p. 8223-8.